# COMPUTER SIMULATION

# OF DINOSAUR TRACKS.

A thesis submitted to The University of Manchester for the degree of Ph.D in the

Faculty of Engineering and Physical Sciences

**2010**

***PETER L. FALKINGHAM***

**School of Earth Atmospheric and Environmental Sciences.**

# Contents

# List of figures

## List of tables

# Abstract

Fossil tracks represent the only direct record of behaviour and locomotion of extinct animals. A computer model using finite element analysis (FEA) has been developed to simulate vertebrate track formation in cohesive substrates. This model has been designed for, and successfully run on, high performance computing (HPC) resources. A number of individual studies were carried out using the computer model to simulate both abstract indenters and virtual dinosaur autopodia. In addition to the simulation studies, two fossil tracks were described, including the first report of bird tracks at the Mammoth Site of Hot Springs, South Dakota (USA) and a re-description of a 'dinosaur tail drag' as the trace of a crocodilian.

Using the computer model, it has been shown that in a wet, soft mud the indentation of a non-webbed virtual tridactyl foot created a resultant track with features analogous to 'webbing' between digits. This 'webbing' was a function of sediment deformation and subsequent failure in 3D, specific to rheology. Apparent webbing impressions were clearly developed only within a limited range of sediment conditions and pedal geometry.

Indenter (pedal) geometry and morphology affect track depth independently of substrate and loading parameters. More complex morphologies interact with the cohesive substrate creating a lower effective load than that applied. In non-cohesive substrates such as sand, this effect is reversed, and it is the more compact morphologies that indent to a lesser degree.

Virtual sauropod tracks were modelled, based on published soft tissue reconstructions of autopodia anatomy, and published mass/centre of mass estimates. It was shown that foot morphology and differential loading between fore- and hind- limbs leads to a range of substrates in which only the manus or pes are able to generate tracks. This offers a new mechanism for the formation of manus-only sauropod trackways, previously interpreted as having been made by swimming dinosaurs.

A series of tracks were simulated using input data (loads, pedal morphologies) from four different dinosaurs (*Brachiosaurus, Tyrannosaurus, Struthiomimus*, and *Edmontosaurus*). The cohesive substrates used displayed a 'Goldilocks' effect, allowing the formation oftracks only for a very limited range of loads for any given foot. In addition, there was a strong bias toward larger animals, both in homogeneous and theoretically heterogeneous substrates. These findings imply that interpretations from track assemblages must consider that only a small proportion of the total fauna present may be recorded as a track assemblage due to substrate properties.

The use of FEA to simulate dinosaur track formation has been shown to be successful, and offers a number of advantages over physical modelling including; consistency between experiments, specific control over input variables, rapid undertaking of repeatable experiments, and the ability to view subsurface deformation non-destructively. It is hoped that this work will lead to an increased interest in modelling tracks, and offer a quantitative method for studying fossil tracks.

# Lay abstract

Fossil tracks are important sources of information about aspects such as behaviour that would otherwise be unavailable from the body fossil record. A track is formed by the interaction of an animal's foot and the sediment upon which it walks. A computer program has been developed to simulate the formation of tracks in mud-like sediments, so that fossil tracks may be 'reverse engineered' in order to better understand these extinct animals. This program was used in a number of individual studies. In addition to the computer simulation work, two fossil tracks were described.

The first of the computer simulation studies showed that in certain conditions (wet, soft mud), a non-webbed foot could produce what appeared to be webbed tracks. Such an artefact of track formation has large implications for interpreting 'webbed' tracks in the fossil record. Indenting a series of different shapes into a mud produced tracks of different depth. More complex shapes were shown to indent to a greater degree than compact shapes (e.g. a square) in muds, whilst the reverse was shown to be the case in sand. Attempting to use fossil tracks to interpret the conditions of the sediment at the time of track formation must therefore take account of track shape as well as track size.

Simulating tracks made by sauropod dinosaurs, using published reconstructions of mass and foot anatomy, showed that the distribution of weight along with the size and shape of the feet meant that different pressures were created under the front or hind feet. This lead to a range of sediment types in which only front or hind feet could leave tracks, providing a mechanism for so called 'manus-only' trackways of sauropods (in which only tracks made by the front feet are recorded) far simpler than current theories involving swimming or 'punting' dinosaurs. Finally, a number of dinosaurs were simulated, ranging from 400 to 25,000 kg. Results showed a strong bias towards larger animals, indicating that interpretations based on track assemblages may not be representative of the full range of animals living in the area when the tracks were made.

By using computer simulation, rather than physically modelling the tracks, a range of conditions became possible (e.g. simulating tracks made by a 25,000 kg animal). The computer model allowed for rapid completion of repeatable experiments, and the digital data could be cut and viewed from any angle to see beneath the surface, whilst retaining the original sample. This work opens up multiple possibilities for the study of fossil tracks in the future.

## Declaration

No portion of the work referred to in this thesis has been submitted in support of an application for another degree or qualification of this or any other university or other institute of learning.

# Copyright

## About the author

Peter Falkingham has had a passion for dinosaurs, palaeontology, and earth history throughout his life. The author graduated from the University of Bristol, U.K. with a BSc in Biology and Geology (Joint honours) in 2003, and the following year with an MSc in Computer Science, feeling that there was an under exploited niche in palaeontology for advanced computational methods. Peter spent a year at the Yorkshire Museum as a documentation assistant before undertaking a PhD at the University of Manchester, U.K. His academic career then, has always been focused on palaeobiology, and particularly on the application of modern techniques in studying locomotion and biomechanics in extinct animals.

## Acknowledgements

This PhD may never have been undertaken by me had it not been for Dr Phil Manning. Dr Manning saw in me exactly the potential I had hoped to achieve through my BSc and MSc. He provided encouragement and advice even before the Ph.D began, and continued this throughout the course of this research, providing just enough 'hands on' assistance, whilst letting me carry on in whichever directions I saw fit.

The computational side of this Ph.D was initially built almost entirely upon the work by Dr Lee Margetts. Dr Margetts never ceased to be anything but most helpful and pleasant, allowing me to guide the development of the software, and being immensely patient as I asked again and again what must have been to him the simplest of questions. Being a non-palaeontologist by training, Lee provided a grounding for my research, teaching me to always focus on the question to be answered.

I wish to acknowledge the staff at the Yorkshire Museum in 2006 (That is: Camilla Nichols, Stuart Ogilvy, Martin Lund, and Dr David Gelsthorpe). The opportunity they gave me for experience was immensely useful for the initial PhD application. The help from the YM staff has never ceased – those that remain at York have continued to provide access to any specimen, and have invited me to give talks presenting my research and my love of palaeontology to the public. Dr Gelsthorpe continued to be of great assistance with his move to the Manchester Museum as I started this Ph.D.

The Palaeontology Research Group, particularly Karl Bates and James Jepson who undertook Ph.Ds concurrently with my own, were always a source of discussion, advice, and abuse! Karl, whose research so neatly complimented my own, proved to be an ideal working partner, unafraid to tell me when I was talking/writing rubbish, and strengthening my weaknesses in doing so, and James, who was ever ready to head for a coffee or beer without hesitation, and had a knack of keeping things in perspective ("it could be worse").

Dr Nic Minter (University of Bristol) and Dr Jesper Milán (Østsjællands Museum, Denmark) both provided many enlightening conversations about ichnology and careers therein.

In addition to the above, the following persons provided access to field sites and collections:

- The Larson's, Peter and Neal, from the Black Hill's Institute, are acknowledged if not for the unrestricted access to their museum and the fantastic collections therein, then for the wonderful meals they both cooked for me.
- Whitey Hagedorn and Kate Wellspring from the Amherst College Museum of Natural History, for access to the amazing and important 'track books' early during my research.
- Kris Thompson and Dr Larry Agenbroad, from the Mammoth Site of Hot Springs, who were more than happy to let me run amok in front of their visitors.
- Ken Carpenter from the Denver Museum.

- Jim Farlow and Mike O'Brian at the Glen Rose Paluxy River track site, for introducing me to some amazing and world famous tracks.
- Brent Breithaupt and Neffra Mathews (Bureau of Land Management, USA), who both acted to welcome me to the world of ichnology, and proved to be most generous and hospitable during fieldwork, and at conferences.
- And Arlene Zerbst, who provided access to the Zerbst ranch, and the tracks within.

Finally, thanks to my family who, whilst perhaps difficult to convince that the intricacies of computer simulated dinosaur tracks are in fact interesting, were nevertheless always encouraging me in my childhood goal to study dinosaurs, and more importantly than anything, helping me to get to the position, via undergraduate and postgraduate degrees, where I could accomplish my greatest goals in life.

This work was funded primarily by a doctoral dissertation grant from the National Environmental Research Council.

"*Slowly but surely and ever faster now, we draw close to the birds and animals we shall find at the end of the trail.*

*We have found their footprints, sure sign of their recent presence. We must learn to recognise them and know something of how to read them.*

*But you will not find here a description of all that you may find; that is the work that you will do for yourself. I want you to use your eyes, and to think for yourself. The more you use your eyes, the keener and the more alert they will become. Footprints are everywhere, but few are the eyes that read them…*

*…But how shall you read these tales so lightly written in the shifting dust, the mud that a single shower may smooth again? They are not always easily read; but the things most worth-while are not always the easiest to do*."

*Fred J. Speakman, from*

Tracks, Trails and Signs, *1958*

# Chapter 1 - Account of work undertaken

## *1.1 Introduction*

Vertebrate tracks are complex sedimentary structures, where the mechanics of formation has often been overlooked in favour of identifying the track maker (Manning, 2004). The identification of tracks can be further hampered by the assumption that the feature represents the original surface on which the animal walked, thus closely resembling the track maker's foot. However, tracks are inherently three-dimensional structures extending beneath (and sometimes above) the original surface upon which the animal once walked, implying that in many cases the visible track may not be an accurate representation of the track maker's foot (Allen, 1989, 1997; Hitchcock, 1858; Manning, 1999, 2004, 2008; Milàn and Bromley, 2006). This project has investigated the mechanics of soils and limb kinematics through computer modelling, facilitating a highly quantitative and versatile approach to the study of track formation.

The Dinosauria comprise one of the most morphologically diverse groups of terrestrial vertebrates in life history (Alexander, 1989). As a group (including modern birds), dinosaurs range in size from a few grams to many tens of tons including some of the largest terrestrial vertebrates ever to have existed (Henderson, 2006a). Dinosaurs represent a group for which track simulations can be made for a diverse range of animals, enabling the investigations of track formation in relation to size.

Dinosaurs also present an ideal group for the study of tracks in that they can be simultaneously both diverse and relatively conservative in foot

morphology – the group as a whole vary considerably in size and shape, whilst clades within the dinosauria, such as the Theropoda, remain highly conservative in their pedal morphology. Dinosaurs as a group include an array of pedal forms from the round, plate like feet of sauropods to the small, narrow, functionally two-toed feet of dromaeosaurs (Thulborn, 1990). Theropods however (a group arising in the Triassic and continuing to the present day as birds) are for the most part highly conservative in foot morphology, remaining bipedal and predominantly tridactyl (three toed) throughout their long evolutionary history. This source of 'input feet' for the simulations undertaken in this work has provided the ability to explore the effects of size and shape on resultant track morphology independently.

## *1.2 Work undertaken*

This thesis takes the alternative format for a Ph.D thesis as outlined by the regulations of the University of Manchester. Background and methods sections are followed by a series of original papers accepted, submitted, or to be submitted for peer-review in academic journals. These papers are then followed by a discussion and conclusion. The nature of the Ph.D, involving the development of software and subsequent application of this software to various problems lends itself well to this format.

During the first two years of the project, time was split between reviewing the literature, fieldwork and developing the computer model. The literature review was a particularly time consuming and important part of the project as a whole, because it involved bringing together the literature from three disparate fields; vertebrate ichnology, soil mechanics, and finite element

analysis. Ichnology is a particularly difficult field to consider. Given that the subject has existed for over 200 years, there has been considerable time for terminology to become rather complex and contradictory, to the point where even measuring the length of a track requires selecting from a range of methods from a number of references (e.g. Leonardi, 1987; Lockley, 1991; Manning, 2004; Thulborn, 1990). Compounding this was the introduction of soil mechanics terminology, which had meanings distinctly opposite to the geological terms this author was familiar with (the word 'soil' being a prime example, meaning any loose deposit in geotechnical terms, but implying an organic weathered layer in geology). Finally, on top of this was the computational literature, which at first was considerably distant from the ichnology. Understanding all three topics to a high enough level therefore represented a considerable amount of time and effort, and this is reflected in the background/literature review herein.

Fieldwork was undertaken in the USA and Europe over three seasons (2007-2009) in order to visit track collections in museums and track sites in the field. Such work presented the opportunity to examine a vast range of tracks and preservational features that simply are not present in the literature. Reports of tracks and track sites generally figure and describe only the most pristine and well preserved tracks as representative, but to understand track formation, it is often the more complicated and messy tracks that provide insight (e.g. Gatesy *et al.*, 1999). Aside from the opportunity to see a large range of tracks in various modes of preservation, the fieldwork would later provide the means for publications describing, for the first time, small bird tracks at the Mammoth site of Hot springs, South Dakota (Chapter 4) and reinterpreting a dinosaur tail drag trace as the mark left by a crocodilian (Chapter 5Chapter 5 -).

Whilst not in the field, a large portion of time was devoted to the development of the FEA software – PalaeoFEM. Development of the core code was collaboratively undertaken with Dr Lee Margetts (University of Manchester), bug finding, testing, validation, implementation, and development of pre- and post-processing software were undertaken as part of the work herein. It is difficult to convey the amount of work that went into these stages, because weeks could pass whilst trying to iron out the bugs of the most recent version. After each bug was found, testing and validation had to be carried out once more. Preliminary analyses could be undertaken which encouraged the implementation of new features, which would subsequently have to be tested and validated once more.

Development has been ongoing, and continued until the final months of the PhD. Included in this development was the creation of a mesh generation program, which could create a soil volume, convert this volume to elements, and then apply specific loads to the surface. Later this program would create a mesh from higher order elements, which involved completely re-writing the software. It would also see the implementation of foot generation, whereby a basic foot could be meshed onto the surface of the soil to provide a rigid indenter to load.

As development proceeded, studies were undertaken and completed as papers submitted for peer review. The first of these showed that webbed tracks could form in wet substrates, even when the foot itself was not webbed. This work had implications not only for ichnology, but for the evolutionary history of animals with webbed feet. Given that interdigital webbing is composed of soft tissue, it is rarely directly preserved in the fossil record (though see for example You *et al.*, 2006), instead being known almost exclusively from fossil tracks.

The importance of the paper then was to highlight the need for caution when describing apparent webbing in fossil tracks.

The second FEA paper explored the effects of foot morphology on track depth. The ability to mesh a foot and apply a force had been implemented in PalaeoFEM and the mesh generation program. As such, a series of abstract shapes were generated and loaded with force to create a number of individual tracks. A metric was determined to describe shape, and this was correlated with track depth. The paper showed that even when loaded equally, tracks of differing morphology would indent to different depths. Track depth, then, was shown to be not only a function of force, but of pedal morphology too.

The phenomenon of manus-only sauropod trackways was revised using FEA. The work allowed collaboration with another researcher working on dinosaur body mass, as it became apparent that distribution of body mass in a quadrupedal animal combined with a sensitive point of failure in the soil would result in only the fore- or hind-feet making a significant impression. These trackways could therefore be explained through relatively straightforward soil mechanics, without invoking explanations relying upon undertracks or even swimming (or at least punting) sauropods.

The final paper simulated a number of dinosaur tracks (covering multiple foot morphologies and masses) in a range of substrates. It was found that homogenous, cohesive substrates, particularly if considered as semi-infinite (Allen, 1997), are poor track bearing media, requiring a very specific range of loads in order to make a track. Loading below or above this small range results either in no track being formed, or the substrate being unable to support the animal. In addition, simulated tracks and undertracks were examined. A number

of features were observed that appeared superficially similar to features noted in fossil tracks attributed to complex limb kinematics (most specifically features such as ridges in track interiors attributed to limb kinematics, Thulborn and Wade, 1989). In this final paper, all three factors determining track formation; force, foot anatomy, and substrate, were considered as a whole system.

## *1.3 Co-author contributions to papers included in this work.*

Each of the papers included in this thesis were written with co-authors. Their contributions to each paper are detailed below. Descriptive papers and simulation papers are considered separately due to the very different nature of collaborative work involved. The contributions are summarised in Table 1.1 and Table 1.2. Where papers have been through the process of peer review, it is noted that reviewers may have made additional contributions through editorial suggestions. In such cases, reviewers are acknowledged separately in each Chapter.

### 1.3.1 Descriptive papers

#### *1.3.1.1 Co-author contributions to Chapter 4*

The bird tracks at the Mammoth Site of Hot Springs were discovered by the author of this thesis in the field season of 2007. The first draft of the paper was written by this author, including most figures, and editorial comments and additions were contributed by supervisor Dr Phil Manning (University of Manchester), and curators of the Mammoth Site Dr Larry Agenbroad and Kristine Thompson (including a map of the site). The text was further improved by suggestions from reviewers when submitted to the journal Ichnos.

#### *1.3.1.2 Co-author contributions to Chapter 5*

The Zerbst Ranch, Wyoming, USA was visited in the field season of 2007 by this author and Dr Phil Manning. Though the site had previously been described (Lockley *et al.*, 2004), it was through discussions between the author of this

thesis and Dr Jesper Milán (Østsjællands Museum, Denmark) that the crocodilian origin of the trace became apparant. The paper was written by this author, who also created the figures with additional data from Dr Milán, who carried out the experimental work with extant crocodiles. Editorial contributions were given to the text by both co-authors and reviewers.

### 1.3.2 Simulation papers

#### *1.3.2.1 Co-author contributions to Chapter 7*

The experiments in this work were designed and carried out entirely by the author of this thesis using software co-developed with Dr Lee Margetts (University of Manchester). This author wrote the paper and made the figures, and this paper was then contributed to editorially by the three co-authors, Dr Lee Margetts, Dr Phil Manning, and by Prof. Ian Smith (University of Manchester). Dr Ian Smith had developed the code upon which PalaeoFEM was based (Smith and Griffiths, 2004), and was consulted to ensure the simulations were correct, and that the geotechnical theory was sound. Once again, reviewers comments improved the content of the work when submitted for peer-review.

#### *1.3.2.2 Co author contributions to Chapter 8*

This study was designed and carried out, then subsequently written, by the author of this thesis, using software co-developed with Dr Lee Margetts. The manuscript was improved by editorial comments from both co-authors, and from reviewers when submitted for peer-review.

#### *1.3.2.3 Co-author contributions to Chapter 9*

The initial question relating to differential underfoot pressures according to centre of mass arose during discussion between this author and Karl Bates (University of Manchester), who was working on dinosaur mass reconstructions. Experiments were then designed and carried out by the author of this thesis, who subsequently wrote the manuscript. This manuscript was edited by the three co-authors.

#### *1.3.2.4 Co-author contributions to Chapter 10*

Co-author contributions to the work were as for Chapter 9.

| | *Discovered the trace* | *Interpreted the trace* | *Contributed additional data* | *Wrote the manuscript* | *Figures* | *Contributed editorial changes or provided resources* |
|---|---|---|---|---|---|---|
| ***Chapter 4*** | **PLF** | **PLF** | KT + LDA | **PLF** | **PLF** + KT + LDA | PLM + KT + LDA (*) |
| ***Chapter 5*** | N/A | **PLF** + JM | JM | **PLF** | **PLF** + JM | PLM + JM (*) |

**Table 1.1 - Co-author contributions to descriptive work (Chapters 4 & 5). *Also reviewer comments.**

| | *Conceived of Original Idea* | *Developed necessary software* | *Designed experiments* | *Carried out experiments* |
|---|---|---|---|---|
| ***Chapter 7*** | **PLF** | **PLF** + LM | **PLF** | **PLF** |
| ***Chapter 8*** | **PLF** | **PLF** + LM | **PLF** | **PLF** |
| ***Chapter 9*** | **PLF** + KTB | **PLF** + LM | **PLF** | **PLF** |
| ***Chapter 10*** | **PLF** + KTB | **PLF** + LM | **PLF** | **PLF** |
| | ***Analysed the data*** | ***Wrote the Manuscript*** | ***Figures*** | ***Contributed editorial changes or provided resources*** |
| ***Chapter 7*** | **PLF** | **PLF** | **PLF** | LM + IMS + PLM (*) |
| ***Chapter 8*** | **PLF** | **PLF** | **PLF** | LM + PLM (*) |
| ***Chapter 9*** | **PLF** | **PLF** | **PLF** | KTB + PLM + LM |
| ***Chapter 10*** | **PLF** | **PLF** | **PLF** | KTB + PLM + LM |

**Table 1.2 - Co-author contributions to simulation work (Chapter 7-10). *Also reviewer comments.**

Abbreviations of co-authors:

JM: Dr Jesper Milán (Østsjællands Museum, Denmark)

PLM: Dr Phil L. Manning (University of Manchester)

LM: Dr Lee Margetts (University of Manchester)

KT: Kristina Thompson (Mammoth site of Hot Springs, SD, USA)

KTB: Karl Thomas Bates (University of Manchester)

LDA: Dr Larry D. Agenbroad (Mammoth site of Hot Springs, SD, USA)

IMS: Prof. Ian M. Smith. (University of Manchester)

# Chapter 2 - Background

## *2.1 Introduction.*

The first recorded observation of fossil vertebrate trackways dates to 1802, when a young boy (Pliny Moody Esq.) discovered bird-like tracks in the sandstone of the Connecticut valley (Sarjeant, 1974). However, the tracks were not published on until 1836 (Hitchcock, 1836). The first scientific report of fossil trackways then, belongs to the Reverend Henry Duncan, who described trackways from Corncockle Muir in Annandale, Scotland, in 1828 (read to the Royal society of Edinburgh, it would be 1831 before the descriptions were published by the society) (Pemberton and Gingras, 2003; Sarjeant, 1974). When first working on the rock slabs containing the trackways from Corncockle Muir, Duncan involved the Reverend William Buckland, who took it upon himself to conduct experiments in trackway formation by persuading a crocodile and then a tortoise to walk across substrates composed of a soft pie crust, wet sand, and clay (Sarjeant, 1974).

**The importance of fossil tracks**

The fossil tracks of vertebrates have the potential to yield considerable information concerning palaeobiology and palaeoecology, as well as providing sedimentological evidence to aid in palaeoenvironmental and palaeogeographic interpretations. In many cases, tracks may occur in environments of deposition devoid of bones, and thus provide an otherwise lacking evidence of dinosaur presence in the facies (Padian and Olsen, 1984).

Potentially, tracks can provide us with the opportunity to learn almost as much about how the animal lived as from the osteological record. A track can reveal information on the maker's size (Thulborn, 1990), gait (Day *et al.*, 2002; Gatesy *et al.*, 1999), speed (Alexander, 1976), and even behaviour (Milner *et al.*, 2009; Thomas and Farlow, 1997). A track can preserve data on the limb motion – the kinematics of the leg, which means that examining tracks through time may shed light on locomotor evolution (e.g. the transition from hip based movement to the more bird like knee based flexion (Gatesy, 1995), or changes in pressure distribution). Trackway assemblages offer us potential glimpses of herd behaviour (Ostrom, 1972), or species composition of the palaeoecology (Lockley *et al.*, 2004), though the effects of time averaging (that the tracks need not be contemporary to each other) means caution should be taken when making such interpretations (Thulborn, 1990).

It is not just information about the track maker that tracks offer us. A track is a biogenic sedimentary feature, and as such can be used to provide sedimentological interpretations (Nadon, 2001; Nadon and Issler, 1997). Shorelines, for instance, can be interpreted from the direction of travel by a dinosaur (assuming that the dinosaurs walked parallel to the shore) (Lockley, 1991). Current strength and direction may be inferred by the 'veering' of an animal from its intended direction of travel (Benton, 1986; Coombs, 1980). In a similar manner, the palaeoslope of terrestrial sediments can also be inferred by a sideways gait, or asymmetrical displacements (Milàn and Loope, 2007; Wilson *et al.*, 2009). Indeed, there are cases where the sediment would be considered deep marine were it not for the presence of dinosaur tracks (Conti *et al.*, 2005; Lockley, 1986). Smaller scale sedimentary information can also be inferred from

a track, that otherwise might not be available – the moisture content of the sediment for instance (Manning, 2004). Given that sediment water content is controlled by environmental and climatic factors, tracks may indirectly aid interpretations of palaeoenvironment and palaeoclimate (Lockley, 1991; Thulborn, 1990).

**Difficulties in interpreting tracks**

Many of the interpretations that can be inferred from trackways rely strongly on the relationship between the track maker and the track. In calculating speed (Alexander, 1976) for example, it is assumed that by measuring the track one is measuring the track maker's foot . However, this assumption is not necessarily correct – indeed, it is in fact unlikely. In over 200 years of study since the first dinosaur footprints were recorded in 1802 (albeit described as large bird tracks) (Lockley, 2006; Sarjeant, 1974), the unwritten assumption in the interpretation of many large vertebrate tracks has been that what is seen is the original footprint left by direct interaction between the foot and the substrate (Manning, 2004, 2008). This is despite work as early as 1858 (Hitchcock, 1858) showing that tracks can be transmitted through the sediment. More recent work (Allen, 1989, 1997; Manning, 2004, 2008; Margetts *et al.*, 2005; Margetts *et al.*, 2006; Milàn and Bromley, 2006; Milàn *et al.*, 2004) has shown tracks to be complex three dimensional structures extending around and below the true track, and altering in their dimensions with depth. This being the case, it is reasonable to assume that what is exposed and observed in the fossil record will not always be a surface track. Indeed, in terms of number of sedimentary layers affected with each track made, undertracks should (assuming sedimentary layers can be

exposed with equal likelihood) statistically be considerably more prevalent in the fossil record.

The effects of such a realisation are far reaching – many interpretations made from vertebrate tracks, without this consideration, may need to be reconsidered; estimates of speed could be out by an order of magnitude (Manning, 2008), tracks made by 'swimming' dinosaurs (Coombs, 1980; Currie, 1983; Thulborn and Wade, 1989) may in fact be nothing more exotic than undertracks. The field of dinosaur ichnotaxonomy, to which the "*palaeontological community*[…] *is understandably bewildered by the confusion and complexity which surrounds* [it]" (Lockley, 1987, p247), may need substantial revision if numerous ichnotaxa are found to be parts of a continuum created by a single track and it's variation with depth, or conversely if a single ichnotaxon can be found in numerous distinct tracks at varying depths (Manning, 1999).

As such, what is required is a detailed understanding of how the track morphology is affected according to variation within the substrate, foot-sediment interaction (limb kinematics), and size (weight) of the track maker etc., not just during, but before and after a track is formed. Rather than approaching the problem of understanding fossil tracks from the viewpoint that they are of biological origin, an approach based on soil mechanics, and the treating of tracks as sedimentary structures, may help alleviate many of the assumptions made when studying fossil vertebrate tracks.

In order to fully understand track formation and preservation, computer modelling can be used to run many experiments with fine control over individual variables within the substrate and within the track maker's limbs. Margetts *et al.*

(2006), and earlier Manning (2004) and Allen (1989, 1997), have shown the potential in using techniques from both the geo-engineering and computational disciplines applied to the study of fossil vertebrate tracks. This work shall be discussed later.

The following sections aim to bring together the literature on current interpretations of dinosaur footprints, limb kinematics, sediment mechanics, and the computational methods that can be used to increase our understanding of dinosaur tracks. Due to the interdisciplinary nature of the project and the subject area, there are times when terminology may conflict. For instance, the term 'soil' has very different meanings in the fields of Geology and of Engineering; the former referring to a weathered layer of organic material, the latter referring to a loose sedimentary deposit (see below). Where this is the case, efforts have been made to clarify which definition is being used.

## *2.2 Dinosaur tracks.*

In studying fossil vertebrate tracks, dinosaurs represent an ideal group. They range in size from a few kilograms to several tons (Alexander, 1989), which can lead to some very large tracks, in which features associated with track formation can be readily seen. As stated at the start of this chapter, there is a record of over 200 years of research on dinosaur tracks, providing a wealth of comparative work. Theropod dinosaurs have ideal modern analogues in extant birds, whose tracks can be used for comparison with those made by their ancestors. A side effect of this is that evolutionary trends can be studied; the evolution of birds from dinosaurs is among the most famous examples of evolution, and an area of intense research – research that includes studies of limb kinematics through time. Finally, dinosaurs include large numbers of differing taxa that were bipedal, a relatively rare condition in extant taxa (only birds and humans are obligate bipeds today). This means that studies on tracks can be undertaken without worrying about confounding effects of quadrupedalism such as overprinting or shifts in centre of mass.

### 2.2.1 Recording Dinosaur tracks

The traditional method of recording data from dinosaur tracks has historically been a two dimensional approach. The original diagrams by Hitchcock (1836, 1858) of tracks and trackways are in many ways almost indistinguishable from those describing tracks some 150 years later, as shown in Figure 2.1.

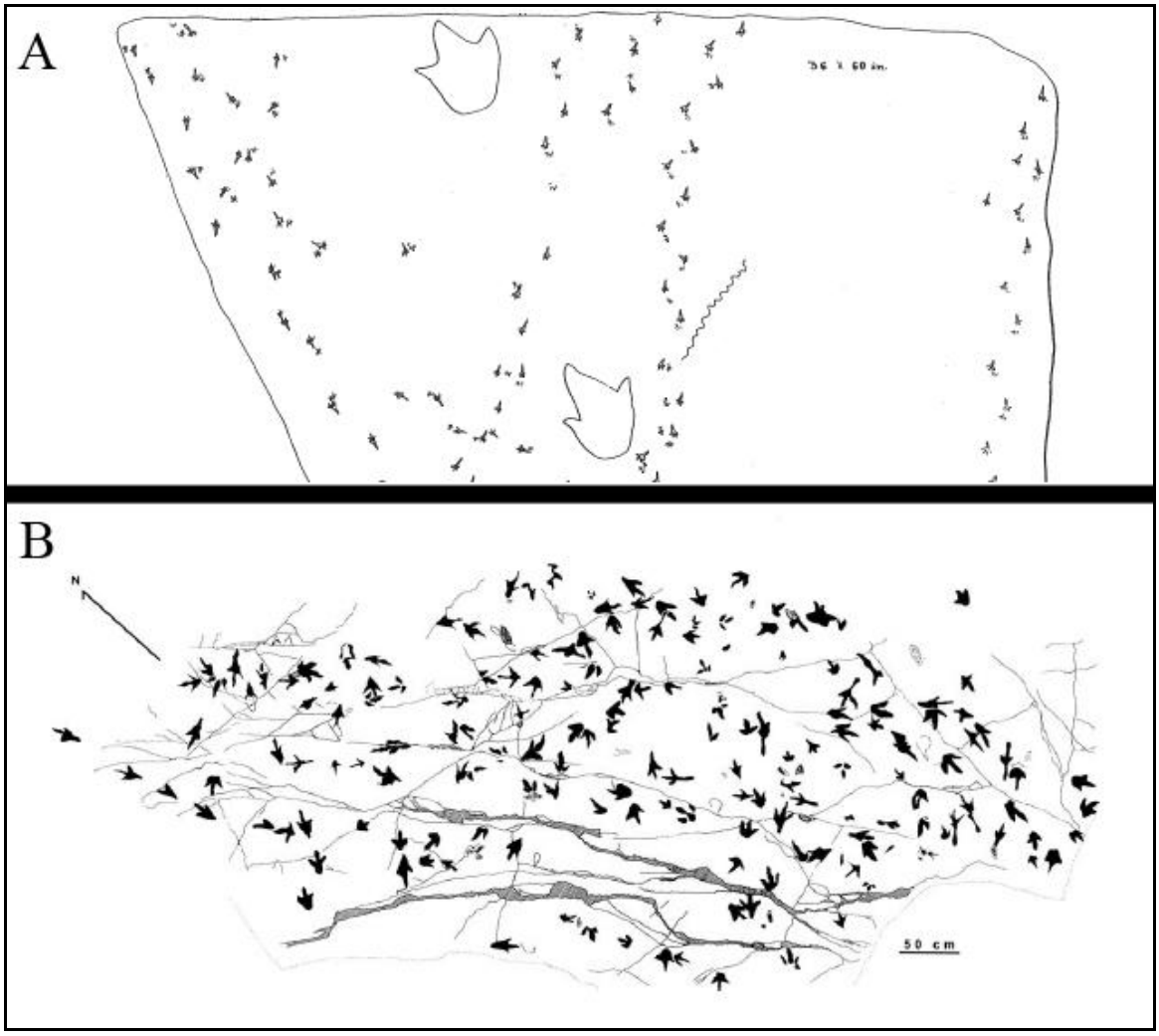


**Figure 2.1 – Comparison of trackway recordings by (A) Hitchcock (1858) and (B) Nicosia *et al.* (2007)**

Indeed, Thulborn in his chapter on track site documentation stated that:

> *"This documentation is a straightforward procedure, which does not require any special expertise, and it can be undertaken with a minimum of equipment. The basic equipment comprises: notebook, graph paper, pens or pencils, compass, clinometer, camera with tripod and plenty of film, a stiff brush, hammer and cold chisels, tape measure, ruler and chalk. Personal preferences will dictate the exact choice of equipment."*

*(Thulborn, 1990, p 67)*

Three dimensional (surface) data is traditionally recorded (if at all) either as shaded images or sometimes as photographs in low angle light, or as measurements of maximum depth and displacement height taken directly from the specimen (Thulborn, 1990).

Terminology for the recording of tracks was outlined comprehensively by Leonardi (1987) and by Thulborn (1990), including such parameters as track length, digit length, interdigital angle etc. (see section 3.1 for detail). Manning (2004) specified further terms for features found in transmitted tracks (see section 2.2.2) such as interdigital shear zone, and multiple digital transmissions. Graverson *et al.* (2007) applied crustal tectonic terms including fault systems and thrust complexes to theropod tracks. Many of the terms in this growing terminology apply to two dimensional descriptions, owing to the nature in which tracks are traditionally recorded. Recent technological advances, however, have allowed workers to begin using more advanced methods of track documentation, not only to capture more accurate two dimensional positional data, but also three dimensional surface data.

Photogrammetry is the use of correctly calibrated photographs to map an area. Advanced photogrammetry can be used to create three dimensional models from 2D images, and this process has successfully been applied to dinosaur tracks (Breithaupt *et al.*, 2004; Breithaupt and Matthews, 2001; Breithaupt *et al.*, 2001; Breithaupt *et al.*, 2006; Matthews *et al.*, 2005; Matthews *et al.*, 2006).

A more advanced, but also more expensive method of recording the three dimensional surface of a dinosaur track site is using laser scanning, in which a laser is used to scan the track surface to sub-centimetre accuracy. Calibrated

photographs can then be overlaid to produce a fully textured 3D model with georeferenced coordinates (Bates *et al.*, 2009b; Bates *et al.*, 2008a; Bates *et al.*, 2008b; Breithaupt *et al.*, 2004; Matthews *et al.*, 2006). That these techniques are only recently being employed means that their full potential has only begun to be uncovered. A move away from traditional drawings and their inherent subjectivity can only be a good thing, because as Thulborn notes:

> *"An outline drawing of a footprint should always be viewed with some reservation: it represents one person's interpretation of a complex three-dimensional object, and someone else's interpretation might differ considerably."*
>
> *(Thulborn, 1990, p91)*

### 2.2.2 True tracks and undertracks

Hitchcock (1858) recognised transmitted tracks (Figure 2.2) – the resultant deformation resulting from transmission of force into a layered substrate. For the most part however, until recently (Allen, 1989, 1997; Manning, 2004; Milàn and Bromley, 2006; Milàn *et al.*, 2004; Thulborn, 1990) it seems little consideration has been given to whether a track is a true surface track, formed in the layer of sediment upon which the animal walked, or whether it is a transmitted track exposed through upper layers being eroded, or planes of weakness between beds occurring below the original surface.

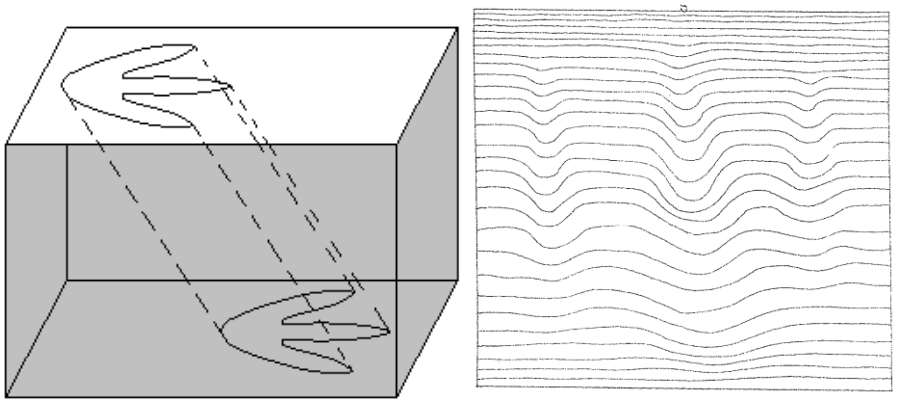

**Figure 2.2 - The 'Stacked Tracks' recognised by Hitchcock (from Hitchcock, 1858; Manning, 2004). Left, force is transmitted into the substrate volume. Right, laminations in the sediment are deformed by the transmitted force, causing sub-surface deformation.**

Allen's work on indenting a substrate to help explain fossil vertebrate tracks (Allen, 1989), specifically mammalian tracks from the Severn estuary (Allen, 1997), provided clear examples of how tracks may be transmitted through sedimentary layers. Figure 2.3 was created by Allen, and shows the results of indenting layered plasticine. The image shows a number of features related to soil mechanics (see next section):

- The displacement rim caused by the substrate flowing up and away from the load.
- The area directly below the indenter remains less deformed than around it (this also applies to each lobe of the indenter). This is the 'dead zone' beneath the load.
- By tracing the peaks of each layer (essentially the transmitted displacement rims), an outward direction can be seen. This is particularly important as it means that a track would appear to be a different size and shape depending on which sedimentary layer was exposed (see section 2.5).

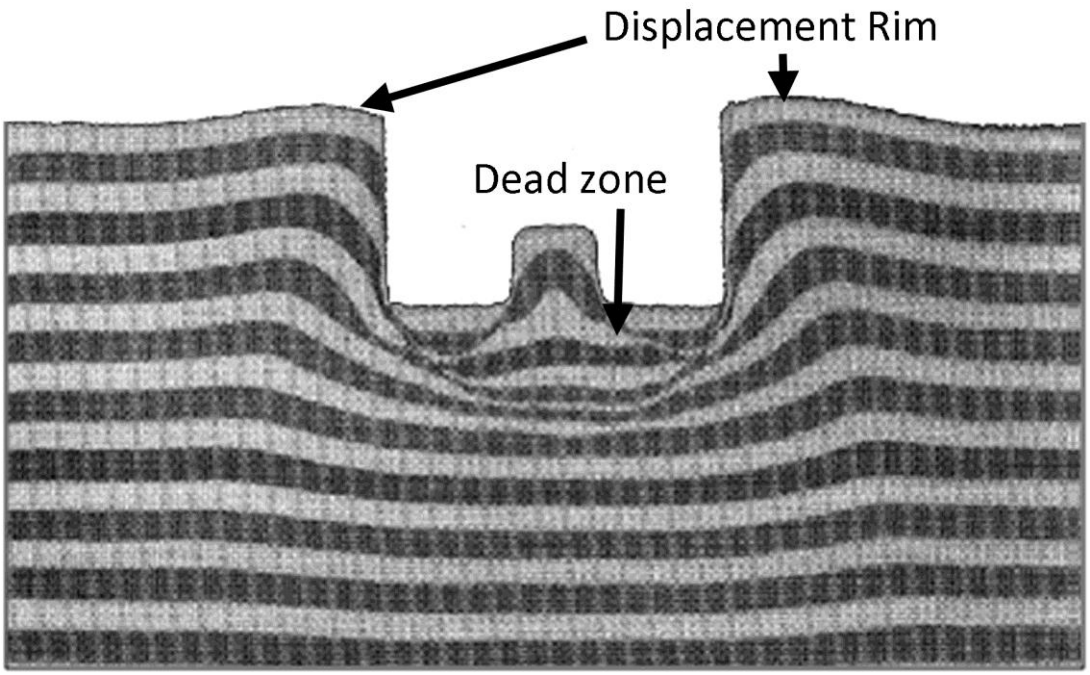


**Figure 2.3 - Layered plasticine after being indented (from Allen, 1997). Note the dead zone directly beneath the indenter and the raised displacement rims at the edges of the indenter.**

When a track is infilled with sediment, that sediment may have laminations which follow the contours of the track surface. When viewed in cross-section, the deformation appears to extend upwards from the original track surface. Such deformations are termed 'over-tracks' (Thulborn, 1990).

Specimens from the collections of the Amherst College Museum of Natural History, Massachusetts, U.S.A. (section 3.2.1) illustrate subsurface deformation in fossilised tracks. Margetts *et al.* (2006) presented images of a series of undertracks beneath a single surface track, and showed that the size and interdigital angle of the resultant outline altered with depth. These images are shown in Figure 2.4. Of particular note is the size difference in the track between the upper surface (Figure 2.4a) and the bottom surface (Figure 2.4b),

just a small increase in depth can lead to an appreciable change in size and shape of the track.

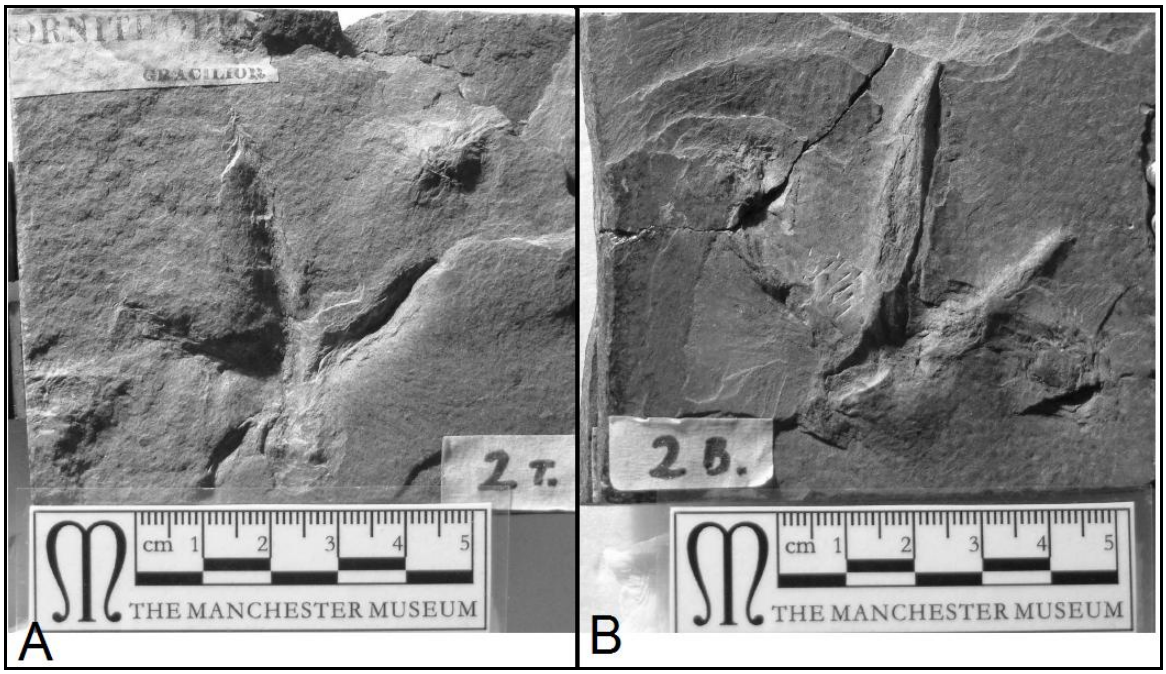


**Figure 2.4 - Top (a) and bottom (b) of a slab containing a dinosaur track. Notice how the track is much larger on the bottom of the layer (deeper) (from Margetts *et al.*, 2006)**

The matter of surface tracks and undertracks is further complicated if the case is considered in which a part of the trackmaker's foot punctures the surface layers of sediment, but the remainder of the foot does not. This could happen if the sediment is particularly firm, supporting the foot until the load passes over the toes and claws in the kick off phase (see Section 2.2.4 below), causing deformation or puncture (Thulborn and Wade, 1989).

Gatesy (2003) looked at this problem, and noted that defining surface tracks as the surface layer of sediment on which the dinosaur walked is not always applicable, particularly in reference to the Greenland tracks made in very soft mud (Gatesy *et al.*, 1999). In these cases, the toes cut through upper layers of sediment, creating a 'surface track' on multiple surfaces. Yet one would have

trouble defining the tracks as anything but true tracks. Gatesy's argument was for the tracking surface to be considered as two separate surfaces – the pre and post track surfaces, determined as the grains exposed before and after the animal interacts with the sediment. This allows the definition of 'Direct features' - those features composed of grains that were in contact with the foot, and 'indirect features' – those features formed by displaced grains that did not participate in the skin-substrate interaction. Indirect features are not necessarily less useful than direct features, with deflected laminations indicating shearing during entrance or exit of the foot, and pressure pads (Fornos *et al.*, 2002) revealing movement direction. Gatesy (2003) stated that displacement ridges and marginal upfolds are therefore poor indicators of foot motion as they move in the opposite direction to the foot. However, if the mechanisms are fully understood (with the application of soil mechanics, section 2.5), there is little reason why such indirect features cannot be interpreted to provide accurate track formation information.

### 2.2.3 Speed

Dinosaur tracks can provide vast amounts of information about the animals that created them. One of the most common interpretations of dinosaur trackways is regarding the speed at which the animal was travelling (Thulborn, 1990). Even when Buckland was conducting his trackway experiments with tortoises and crocodiles, he noted in a letter to Duncan that he "*found considerable variety in these positions* [of footprints] *as tortoises moved more or less rapidly and* [that] *most animals have three distinct kinds of impressions for their three paces of walk, trot, and gallop*." (Duncan, 1831, p202-203 as referenced in; Sarjeant, 1974) From this, Buckland interpreted Duncan's fossil tracks as being made by faster moving animals than he had used in his experiments (Sarjeant, 1974).

Alexander (1976) elaborated on this, formalising the relationship between speed (or rather, Froude number) and trackways with the following dimensionless speed formula:

$$\mathbf{u = 0.25g^{0.5}\lambda^{1.67}h^{-1.17}}$$

Where u = velocity, g = gravity, λ = stride length (distance from one track to the next made by the same foot), and h = hip height.

Of course, hip height is not a variable that can be directly measured from a trackway. Instead, Alexander used the length of footprint as an indicator of hip height, stating that if the metatarsophalangeal joint rested on the ground, but the tarsometatarsal joint did not, the length of hind footprint would be 0.23-0.28 times the hip height. He therefore went on to approximate that the hind footprint length is 0.25h in all cases (Alexander, 1976). With the equation alone, there is a large variation in hip height to foot length ratio (0.23-0.28), and hence room for error. This is compounded by the hip height to foot length ratio changing with growth, a function of allometry (Manning, 2008; Thulborn, 1990). Indeed, Alexander himself admitted that the method depends on "*doubtful estimates of leg length, usually based on footprint size, which may be misleading if erosion has removed the original surface of the substrate (Allen, 1997) or if the substrate was very soft (Gatesy et al., 1999).*" (Alexander, 2006, p 1850).

A number of attempts have been made to refine the speed estimating technique (Alexander, 1991; Henderson, 2003; Thulborn, 1990), but despite this, Alexander's method has been widely adopted by many (Farlow *et al.*, 2000; Irby, 1995; Manning, 2008). The errors inherent within the equation itself are

manifest even in the best case scenario; that an accurate surface track closely matching the shape of the track maker's foot is used. Manning (2008) showed that the estimation of speed using Alexander's equation, when applied to a series of undertracks produced experimentally (Manning, 1999) could cause the estimation of hip height to vary from 30 – 86cm, resulting in speed estimates from 2.65m/s to 10.29m/s – a massive difference, rendering any estimation of speed based on foot size of severely limited use without a full understanding of the conditions in which the track was formed, and an appreciation of what is a surface track and what is a transmitted track.

### 2.2.4 Limb kinematics

If the affected sediment in a track can be seen as a record of the motion of the foot, any variation in that movement has the potential to be be recorded in the track/trackway. This means that an animal's gait and limb kinematics can potentially be inferred from a trackway, much as Buckland attempted with Duncan's tracks (Sarjeant, 1974). At a basic level, this can be as simple as determining when the foot touches the substrate, when the load from the weight of the animal passes over, and when the foot is removed. Thulborn and Wade (1989) defined this as the touch down phase (T), the weight bearing phase (W) and the kick off phase (K). Thulborn and Wade (1989) provided examples from a rich dinosaur track site in Australia of tracks recording various phases, and showed how a firmer substrate would be more likely only to preserve the kick off phase, in which greater pressure is applied to the sediment due to the lower surface area of the foot in contact with the surface (i.e. just the toes and claws rather than the entire sole of the foot). Manning (2004) discussed a number of fossil and experimentally made tracks that displayed the three phases of foot-

sediment interaction, with an undulating form to the base of the track, the deepest area at the anterior end produced during the kick-off phase.

Padian and Olsen (1984) conducted comprehensive neoichnological experiments with a komodo monitor, and importantly not only reported on the tracks created by the animal, but also on the motion of the animal and its foot at the time. Comparison of komodo and caiman matched differences in step cycle of the forelimb to differences in the tracks, overstepping (where the hind foot is laid down in front of the preceding forefoot) was noticed to be exaggerated at increased speeds, and from the observation that the hind limbs become shorter and stouter with age, the implication was made that the relationship between manus and pes prints would alter between juvenile and adult forms. The most important part of Padian and Olsen's work was the message that many trackway interpretations were hampered by an inadequate understanding of the track-making processes, stating that to fully understand tracks one must consider the anatomy of the foot (the skeletal outline is not the true outline of the surface presented to the sediment (Duncan and Holdaway, 1989)), the kinematics of the step cycle, and the mechanics of the substrate.

The surface of the foot that interacts with the sediment may alter considerably with the depth that the foot sinks to in the substrate. Deeper impressions are more likely to preserve features such as the metatarsals or halux (Gatesy *et al.*, 1999), meaning that in some cases a tridactyl track maker can leave a four toed track (Harris *et al.*, 1996). Conversely, a very shallow track may preserve only small parts of the phalangeal pads and/or claw marks (Thulborn and Wade, 1989).

This kinematic information that may be found in tracks has the potential to provide clues as to locomotor evolution. Farlow *et al.* (2000) touched on this, looking at stride lengths in theropods over time, but found no indication that stride length changed between early and later non-avian theropods, despite the skeleton remains indicating the development of hind limb proportions that suggest a greater degree of cursoriality with time (Farlow *et al.*, 2000).

### 2.2.5 Inferring behaviour from tracks

Because tracks are made by living animals, they represent one of the best sources of evidence regarding the behaviour of an extinct animal. Minter *et al.* (2007) inferred behaviour as one of the three primary factors determining track morphology (the other two being producer and substrate).

One interpretation of behaviour from trackways seen in the literature is that of apparently 'swimming' dinosaurs (Coombs, 1980; Currie, 1983; Ezquerra *et al.*, 2007; Thulborn and Wade, 1989). These are reported from tracks consisting of parallel claw scratches, often found not in trackways but randomly orientated isolated tracks on a bedding surface. There is large potential that many tracks interpreted as 'swimming dinosaurs' may in fact be the result of track making conditions, perhaps being undertracks, or surface tracks made on firm sediment in which only the claws leave traces during the kick off phase (Thulborn and Wade, 1989).

Gregarious behaviour can also be cited as evident from trackways (Lockley *et al.*, 2002; Myers and Fiorillo, 2009; Ostrom, 1972), but the effects of time averaging make this extremely difficult to argue. The passing of two or more animals may occur contemporaneously or over days, weeks or longer to produce a single tracksite. Furthermore, a single animal may cross an area

multiple times, leaving numerous trackways. Measuring the proportion of trackways in given directions can shed some light on such situations, as a single animal will leave trackways in all directions randomly, whilst a passing group of animals will be more likely to leave trackways in predominantly one direction (Thulborn, 1990)

Tracks can vary immensely according to the sediment and the track maker. Hence a full understanding of how the track is formed including the motion of the foot, the soil mechanics and the interaction between the two is required in order to make more accurate and more confident interpretations. Most importantly it is unwise to assume that all the information present in a trackway is contained in its two dimensional outline, the primary means of reporting tracks in the literature, in doing so one ignores an entire extra dimension of information.

## *2.3 Neoichnology and extant analogues*

### 2.3.1 Extant bird tracks

From the first discovery of Archaeopteryx (a wonderful coincidence of science, occurring just two years after the publication of On The Origin of Species (Darwin, 1859)), to the 'Dino-birds' of China discovered from 1996 onwards (Chen *et al.*, 1998; Xu *et al.*, 2003), evidence supporting the theropod-bird lineage is in abundance, and is supported by modern cladistic analyses (Gauthier, 1986).

As the closest living relatives of dinosaurs, it is perhaps pertinent then, to take note of the tracks left by modern birds. Despite many birds being small and spending relatively little time on the ground, bird tracks are nevertheless numerous and diverse (Brown *et al.*, 1987). The foot morphology of birds varies in the orientation of the toes and the presence/absence of a first digit (the halux). The variation in avian pedal morphology is classified in Figure 2.5, and examples of bird tracks are shown in Figure 2.6. It should be noted that theropod feet were apparently more conservative in their morphology than modern birds, being almost exclusively tridactyl with a raised first digit (halux), following the phalangeal formula of 2:3:4:5:0 (Thulborn, 1990). Occasionally, the halux impression is preserved (Lockley *et al.*, 2004; Thulborn, 1990), or tracks appear didactyl (Xing *et al.*, 2009a), but for the majority of theropod tracks, a tridactyl form is observed.

Milàn (2006) used living Emus (*Dromaius novaehollandidiae*) to generate a variety of tracks in differing substrates, in order to show that

considerable variation in track morphology could result from sediment properties rather than pedal morphology or limb kinematics. Of particular note were the plantigrade impressions made by the Emus when feeding, and comparisons were drawn with fossilised tracks such as *Anomoepus*, interpreted as resting traces of theropod dinosaurs.

Milàn and Bromley (2006, 2008) used the severed foot of an Emu to explore true track and undertrack formation, impressing the severed foot into a mixture of sand and coloured cement. The experimental tracks were then sectioned horizontally and vertically. Aside from showing that the tracks increased in horizontal dimensions with depth (whilst simultaneously decreasing in vertical dimensions), the authors also demonstrated that in particularly wet substrate, the greatest preservation of detail was found in undertracks rather than surface tracks.

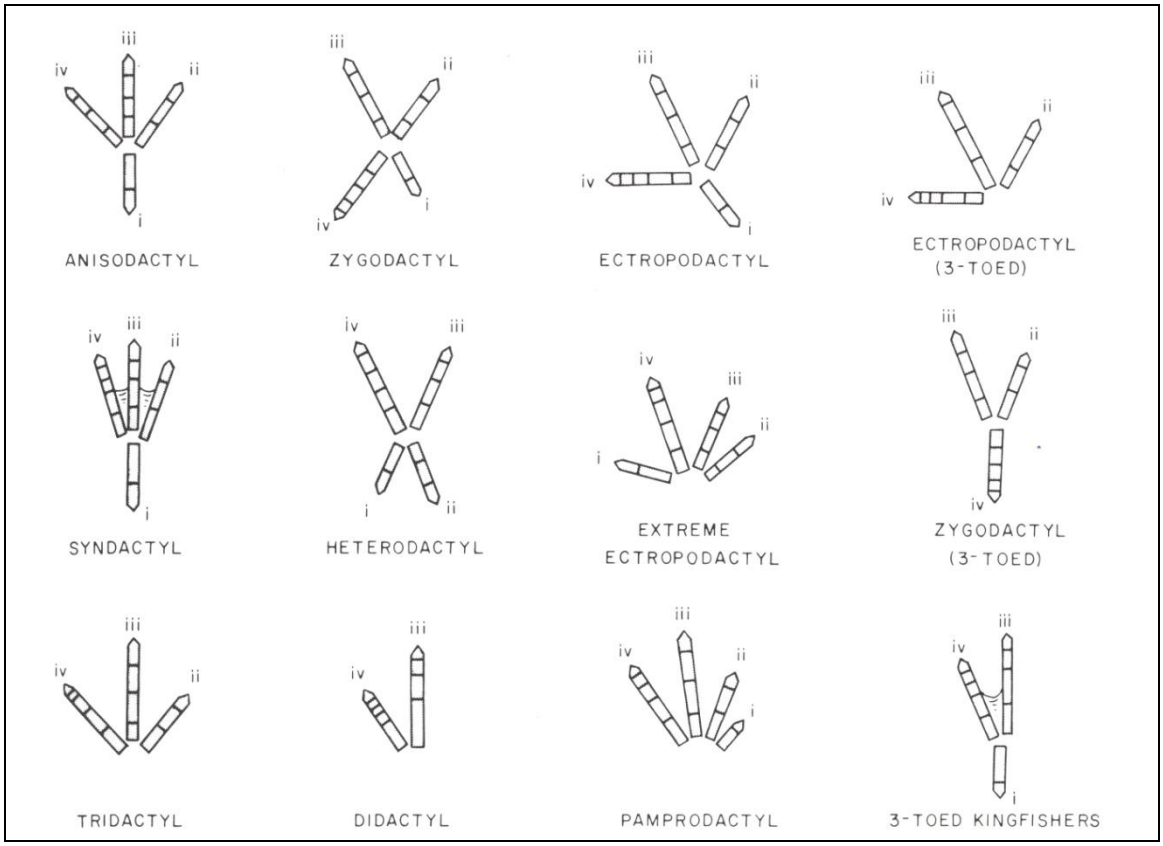


**Figure 2.5 - Representations of bird foot classification (from Raikow, 1985). Sections of each digit represent phalanges (including terminal ungul phalanx).**

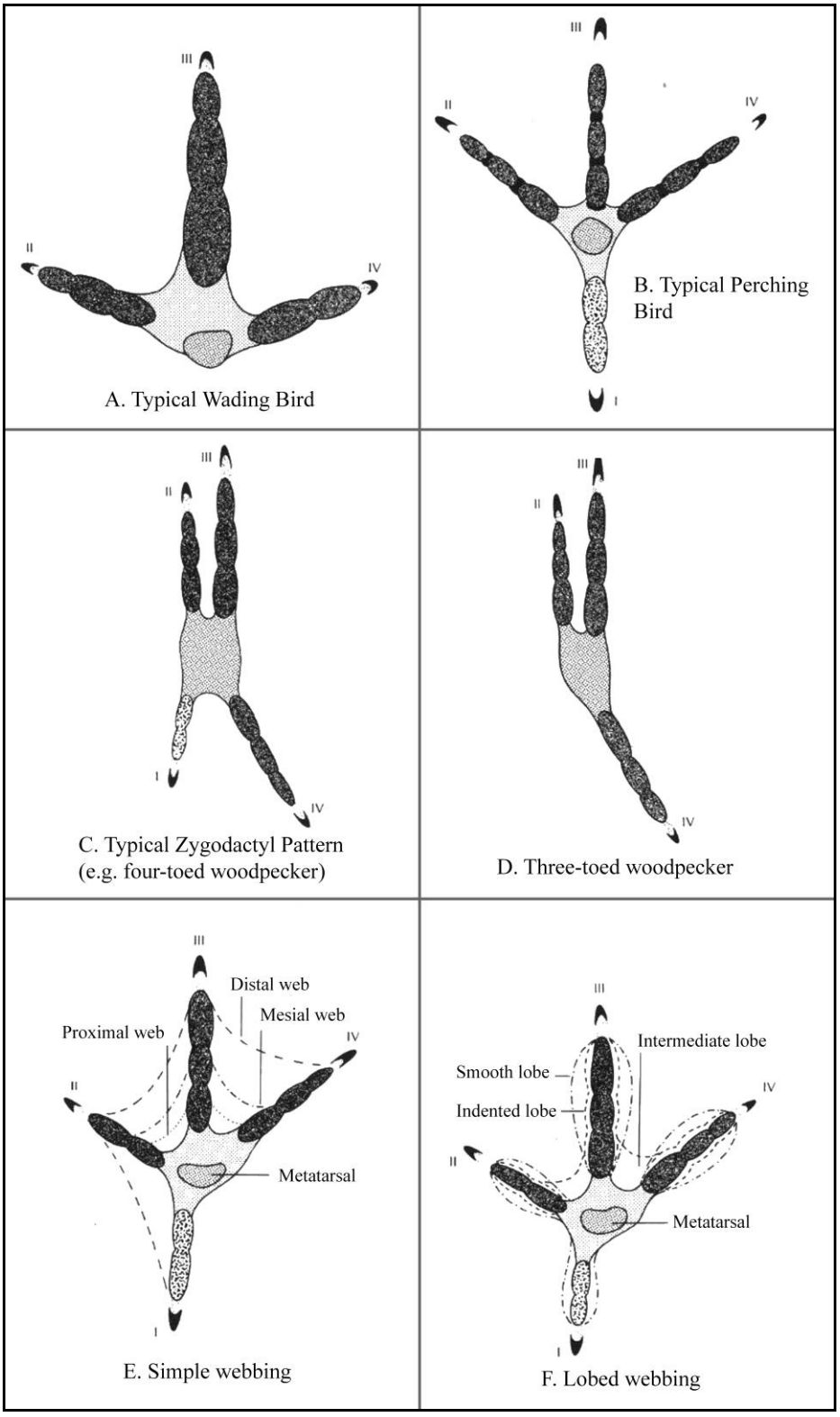


**Figure 2.6 - Example bird tracks. After Brown *et al.*(1987)**

## *2.4 Ichnotaxonomy and vertebrate vs. invertebrate ichnology*

Some of the tracks Duncan described were mentioned in the proceedings of the Geological Society of London for 1839 (vol. 3, p31), and in 1841 Richard Owen named them *Testudo duncani*, "*thus (rather oddly) treating the tracks as a living species of turtle!*" (Sarjeant, 1974, p 271). This was perhaps the beginning of vertebrate ichnotaxonomy, and the widespread use of the binomial Linnaean naming system to formally describe what are in essence sedimentary features. Hitchcock, in his Ichnology of New England (1858) stated:

> *"I ought to say, that for several years, I merely gave names to these tracks with reference to their supposed affinities; such as* Ornithicnites, *or stoney bird-tracks;* Sauroidichnites, *or like the tracks of Saurians, &c. But more recently, I have named the animals that made the tracks, as* Brontozoum giganteum, *or the huge animal giant:* Polemarchus giga *..."*
>
> (Hitchcock, 1858, p4).

Hitchcock therefore indicated a shift from naming the tracks themselves (after the assumed producers), to naming the producers. Hitchcock's reasoning for such naming was that:

> *"Without some such designations, it is nearly impossible, since they have become so numerous, to describe the different sorts of tracks; and if, as the tracks show, these animals once had a real existence, why is there not as much propriety in giving them names from their tracks, as from bones in other cases?"*
>
> (Hitchcock, 1858, p4).

The idea of naming animals solely from tracks seems perhaps a little too presumptuous, especially given the complexities in track formation outlined in section 2.2.2. However, given that Hitchcock's contemporaries were Owen, Mantell and Cuvier; his assertions do not seem so wild. If the anatomists of the time could identify an animal from a single bone, why then, reasoned Hitchcock, could the same not be done for an entire foot, preserved as a track? Regardless, in modern literature the names given are applied to the tracks themselves, rather than the animals. Nevertheless this has still resulted in the binomial naming of vertebrate tracks with an almost complete emphasis on the assumed producer (Lockley, 1991, 2007; Minter *et al.*, 2007). Even the more quantitative studies have, for the most part, used the quantitative data to assign a producer, rather than as a descriptor of the track itself (see re: *Tyrannosauropus below*). This was highlighted when Lockley (1998) pointed out that the analytical techniques used in the quantitative study of tracks were far from standardised, and that in some cases study was dealt with not through the track but the morphology of foot bones and potential track makers, summed up perfectly in one short statement:

*"Track morphology should first be described for what it is, then later interpreted for what it represents."*

(Lockley, 1998, p284)

This emphasis on naming tracks in such a manner as to create a link with assumed producer has resulted in ichnotaxa such as *Tyrannosauropus* (Haubold, 1971), a large tridactyl track believed to have been associated with the animal *Tyrannosaurus*. Unfortunately *Tyrannosauropus* was shown not to have been produced by the animal from which the track was given its name; instead the more likely track maker was a hadrosaur (Lockley and Hunt, 1994). Another example is of *Gigantosauropus*, a track originally named through the assumed producer – the theropod *Giganotosaurus*, but later shown to be a sauropod track (Lockley *et al.*, 2007). Table 2.1 is from Lockley *et al.* (2004) and lists a number of ichnogenera originally described as having ornithopod affinity. Of nine ichnotaxa, all of which are named after assumed producer, only 3 are considered by Lockley *et al.* (2004) to be of ornithopod origin.

| Ichnogenus and author(s) | Probable Trackmaker |
|---|---|
| *Camptosauruichnis* (Casamiquela, 1968) | Theropod |
| *Iguanodonichnus* (Casamiquela, 1968) | Sauropod |
| ***Amblydactylus*** (Sternberg, 1926) | **Ornithopod** |
| *Hadrosaurichnus* (Alonso, 1980) | Theropod |
| *Ornithopodichnites* (Llompart, 1984) | Theropod |
| *Orcauichnites* (Llompart, 1984) | Theropod |
| ***Caririchnium*** (Leonardi, 1984) | **Ornithopod** |
| *Hadrosaurichnoides* (Casanovas *et al.*, 1993) | Theropod |
| ***Iguanodontipus*** (Sarjeant *et al.*, 1998) | **Iguanodontid** |

**Table 2.1 - Named ichnogenera of purported hadrosaur or other large Ornithopod origin. Only those tracks in bold are considered of ornithopod affinity by Lockley et al (2004). Table from Lockley *et al.* (2004)**

With such potential for interpretations of tracks to change, the application of the binomial naming system - with genus and species for differing tracks, and an emphasis on assumed producer - has large scope for becoming confusing and misleading. Of even more worry with such a system is that with changing size and shape of tracks with depth in any given track volume, as well as potential for variation of shape according to substrate consistency, there is massive potential for differing species and genera of tracks to be found within a single track depending on depth, and the opposite effect of a single species being found in wildly differing tracks at different depths (Manning, 2004). Bertling *et al.* (2006) have considered this, and recommend that separate names for

"undertracks and other poorly preserved material" should be replaced by ichnotaxa based on well preserved specimens. Unfortunately, this relies on the assumption that undertracks will always display a loss of definition with depth, as stated by Nadon (2001), though as shown by Hitchcock (1858) and by Milàn *et al.* (2004), this may not always be the case. Such a recommendation also relies on correctly idententifying the track as surface or subsurface, which as will be seen in Chapter 3, is not always a mean feat. Bertling *et al.* (2006) also view size and producer as unsuitable ichnotaxobases, two features often used in naming dinosaur tracks (for instance *Tyrannosauropus*, named after an assumed producer, or *Grallator* and *Anchisauripus* that differ only in size).

Minter *et al.* (2007), have made an attempt to address this problem in ichnotaxonomy, advocating a descriptive name based on behaviour, producer, and morphology, stating that the result of all three factors interacting produces the trace. However, much of this focuses on arthropod trackways, and becomes less apparent and consistent with the move to larger vertebrate trace fossils. Almost all large vertebrate tracks are generated through walking or running behaviour, making their primary descriptor insufficient. This is coupled with the size difference of biotomes between invertebrates and vertebrates. A vertebrate may easily and rapidly pass through multiple sedimentary environments, leaving a multitude of different track morphologies.

However, the problems with Ichnotaxonomy mainly apply to the continuous nature of track morphologies within a track volume, the cynic may argue that such matters may be equally well applied to the taxonomy of biological organisms. Evolution produces a myriad of forms, all of which are ultimately part of a continuum. However, biological species, and even

morphospecies as defined from the fossil record have strict definitions; ichnospecies are often based on non-discrete characters.

## *2.5 Soil mechanics*

This section aims to present a number of concepts from the geotechnical literature regarding soil mechanics, specifically the deformation of a soil beneath a load. This begins with a discussion on characterising soil in an engineering context as opposed to a geological one. Following on from this is a discussion of the response of soils to stress, the stress strain relationship, along with failure mechanisms (the way in which the soil fails under load depending upon moisture content). Finally, various numerical models are presented for differing soil types and for solving different problems. The selection of a specific numerical model for use in the computer modelling carried out as part of this thesis is justified. The variables and symbols used throughout this section are summarised below (Table 2.2).

| Symbol | Meaning |
|---|---|
| $\tau$ | Shear stress |
| $\sigma$ | Compressive stress |
| $\bar{\sigma}$ | Effective stress |
| c | Apparent cohesion |
| *Cu* | Shear strength |
| *v* | Poisson ratio |
| *E* | Young's modulus |
| $\varphi$ | Angle of shearing resistance (or internal friction) |

**Table 2.2 - Symbols and meanings used in this section.**

### 2.5.1 Characterising soil

The term ‘soil’ has several meanings. In a geological sense, it is the weathered layer of organic material on the surface, or top soil (Smith, 1981). However, this section details the mechanics of loose sediment from a geotechnical standpoint, and as such it seems apt to use the engineering definition of ‘soil’; a loose sedimentary deposit, such as gravel, sand, clay or a mixture of these materials (Smith, 1981). It is important not to confuse the term ‘loose’ with ‘non-cohesive.’ In this context, a firm mud or clay is still classed as a loose sedimentary deposit, and consequently the term ‘soil’ still applies (Smith, 1981).

A soil can be classified on a number of characteristics such as geological origin, mineralogical make-up, grain size, and plasticity. In terms of fossil tracks, the former three allow palaeoenvironmental interpretation, which may provide information on the environment and thus the moisture present at the time of track formation and the potential track makers that may have been present in such an environment. Plasticity however, is not preserved in the rock record and can only be interpolated from sedimentary structures, including tracks. When classifying the soil, of primary importance is the grain size, shape and distribution. Analysing the size of the particles within a soil is done with one of two methods, depending on if the soil is coarse or fine. A coarser soil can be analysed with regards to size by sieving an oven dried sample (Smith, 1981). For fine grained soils, analysis of particle size is achieved through the application of Stoke’s law to settlement rates in water – that small spheres of different size settle at different rates (Craig, 2004).

A soil is composed of solid particles and voids containing air and/or water. The relative proportions of these particles and voids (and the contents of

the voids) are a major factor in determining the mechanics of the soil. Figure 2.7 displays diagrammatically the relationships the solids and voids create.

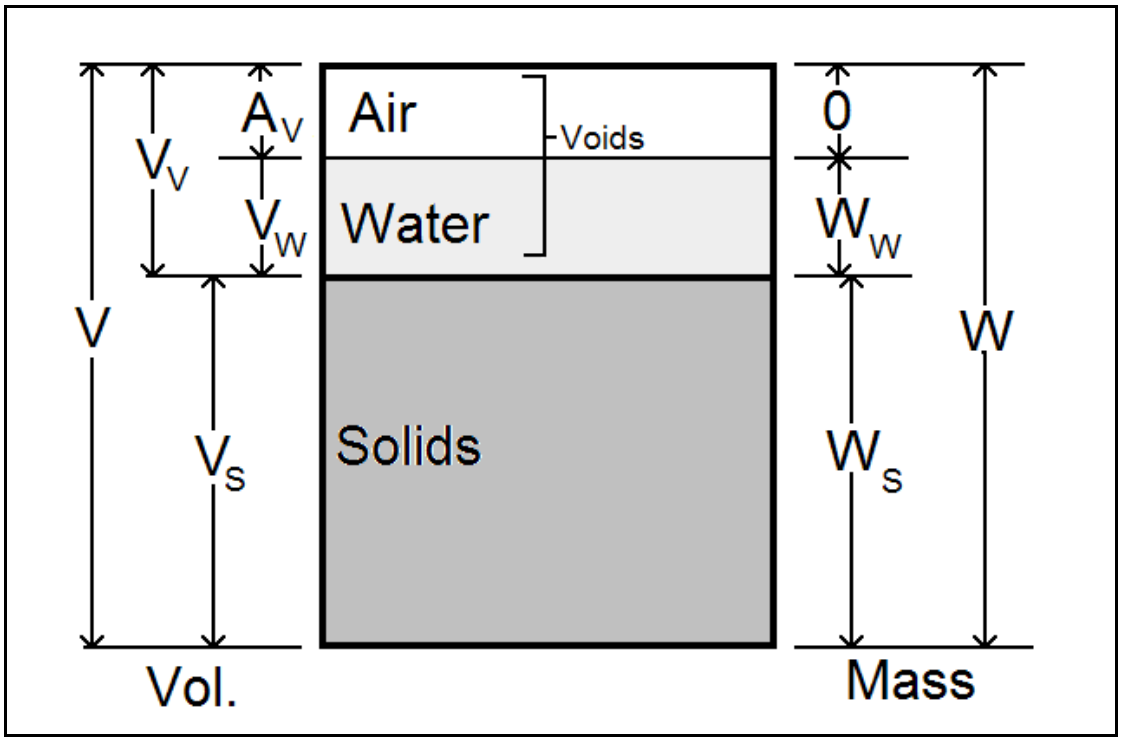


**Figure 2.7 - Block diagram of soil composition. V = total volume, $V_V$ = Volume of voids, $V_S$ = Volume of solids, $A_V$ = Volume of Air, $V_W$ = Volume of water, W = Total weight, $W_s$ = Weight of solids, $W_W$ = Weight of water (note that this is also the total weight of the voids, as air is considered to have no weight) (from Smith 1981).**

Differences in grain size, shape, and sorting, can alter the proportions of voids and solids. A poorly sorted soil may have considerably less voids as voids between large particles are filled with smaller particles. More angular grains may tend to interlock better, reducing void space. And of course, larger grains (in a well sorted soil) will leave larger voids. For characterising a soil with regards to its solid and void proportions, it can be assumed that the solids, if theoretically compressed together, provide one unit of volume (i.e. V = 1). (Smith, 1981)

The relationships between the voids and solids can define a number of mechanical properties. The porosity for instance is defined as the ratio of void

volume to total volume, or $V_V/V$, whilst the percentage of the sample that is air voids is calculated as $(A_V/V) \times 100$. The degree of saturation is the ratio of water volume within the total volume of voids, or $V_W/V_v$ (multiply by 100 for percentage saturation) (Smith, 1981).

The moisture content of a soil is one of the most important factors affecting the mechanics of the soil, determining the level of cohesion between solid particles (and thus the consistency – see below). Not to be confused with the degree of saturation, the moisture content is concerned with the ratio between weight of solids and weight of water - $W_W/W_S$ (again, multiply by 100 for percentage moisture content). The moisture content of a given sample of soil is determined by weighing the sample before and after drying in an oven. The difference in weight is the weight of water, the weight after drying is the weight of the solids only (Smith, 1981).

### 2.5.2 Plasticity

Moisture content directly influences the behaviour of the soil. The removal of water from a soil causes it to pass through a number of states, from liquid, through plastic, finally to solid. The points at which the states change are known as the consistency limits (Smith, 1981):

- Liquid limit - minimum moisture content at which the soil can flow under its own weight.
- Plastic limit – minimum moisture content at which the soil can be rolled into a thread 3mm in diameter without breaking up.
- Shrinkage limit – maximum moisture content at which further removal of water does not decrease the sample size.

The range between the plastic limit and the liquid limit is known as the plasticity index, and this is where the soil behaves in a plastic manner (Smith, 1981). Figure 2.8 shows this diagrammatically.

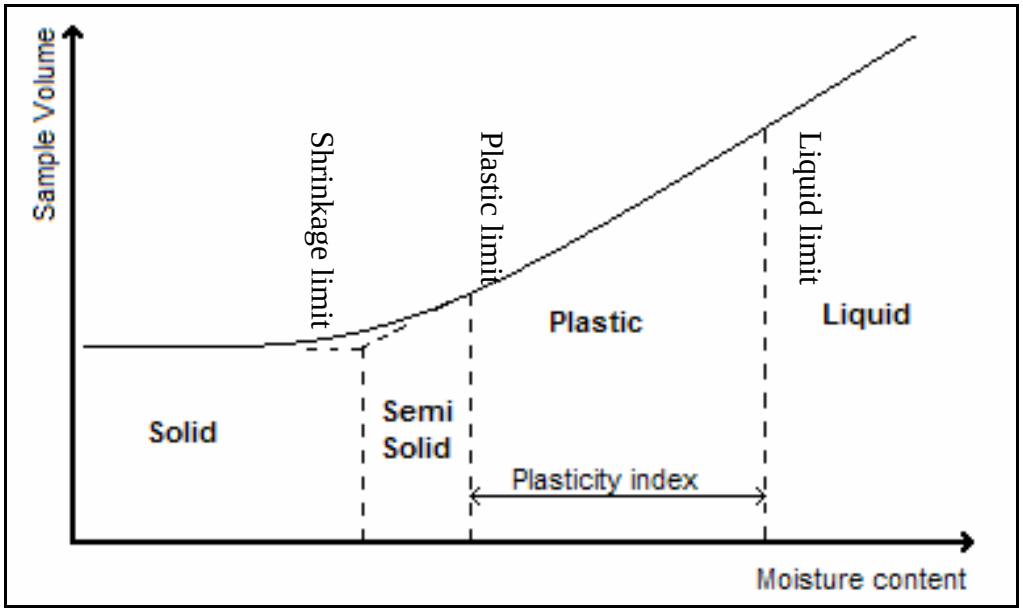


**Figure 2.8 - Graph showing consistency limits (from Smith, 1981).**

Plastic deformation is "*the ability of a soil to undergo unrecoverable deformation at a constant volume without cracking or crumbling*." (Craig, 1997, p7) This means that an animal can leave a track by deforming the soil around the foot (thus leaving a recognisable impression). At a liquid consistency, a soil cannot support an animal, nor will it retain track features. In a solid state, a soil will not be deformed easily, and if it is, any deformation will result in cracking and breaking.

### 2.5.3 Distribution of stress

An important aspect of soil mechanics with regards to undertrack formation is in understanding the distribution of load vertically into the soil.

Boussinesq's theory for elastic analysis (Boussinesq, 1883) allows the calculation of force exerted at any point beneath the application of force. Whilst loading from a single point is unlikely, understanding this simple case provides the framework for calculating pressure beneath more distributed loads. Figure 2.9 shows a basic point load.

Boussinesq's elastic analysis provides the following equation for finding $\sigma_v$ (the vertical stress at a given point beneath a load):

$$\sigma_v = \left(\frac{3P}{2\pi z^2}\right)\left(\frac{1}{(1+(r/z)^2)^{\frac{5}{2}}}\right)$$

By taking r/z as tan $\psi$, the equation can be re-written as:

$$\sigma_v = \left(\frac{3P}{2\pi z^2}\right)cos^5\,\psi$$

These equations provide a simple way of calculating the distribution of stress at any point beneath the load (Smith, 1981). Figure 2.10 shows a theoretical distribution of pressure below a 700kN point load. If the soil has a bearing capacity (see section 2.5.4 below) of 25kN/m$^2$, a 'pressure bulb' can be drawn (as in Figure 2.10) that delineates the failure envelope (Manning, 2004; Smith, 1981).

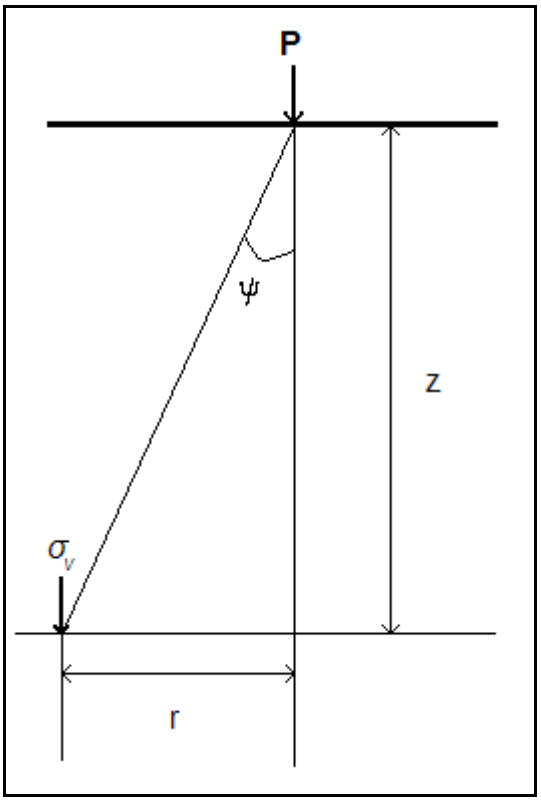


**Figure 2.9 - Point load acting on a soil mass, producing force $\sigma_v$ at z depth and r horizontal distance (from Smith, 1981).**

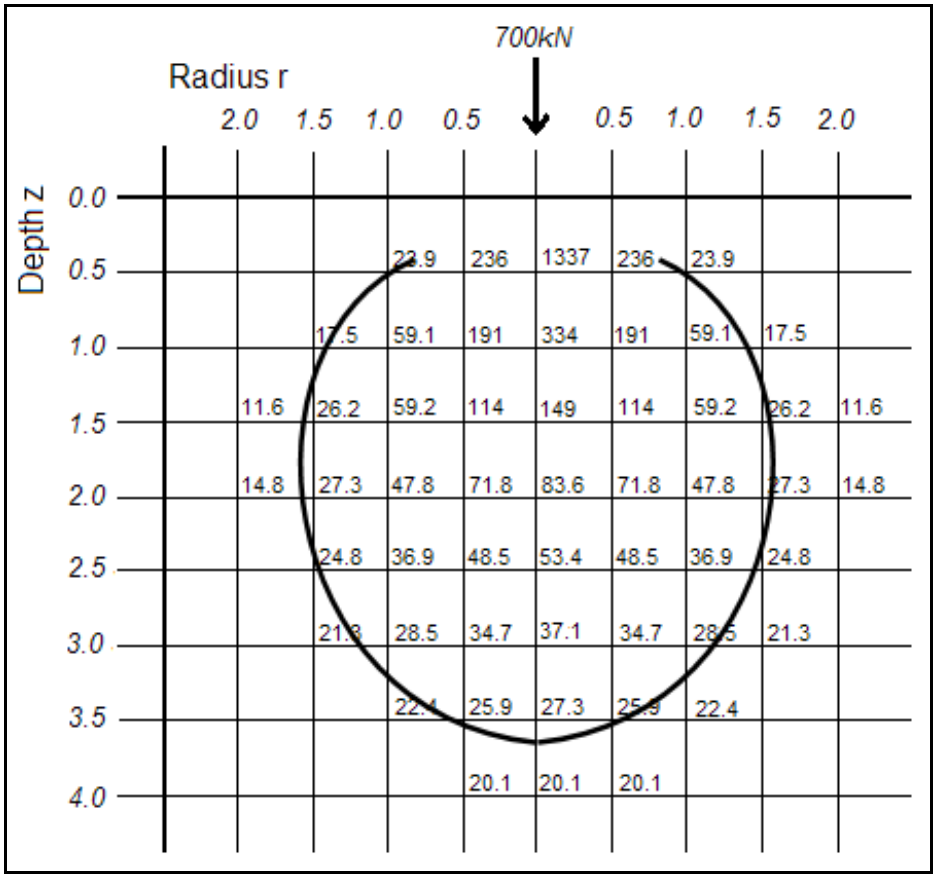


**Figure 2.10 - Distribution of pressure in a hypothetical homogenous soil under 700kN point load. Outline indicates 'pressure bulb' or failure envelope assuming bearing capacity of the soil is 25kN/m$^2$ (from Smith, 1981)**

### 2.5.4 Shear strength and failure

The shear strength of a soil is a measure of its maximum ability to resist stresses parallel to the face (shear stress) under any given conditions (Smith, 1981). This resistance comes from two sources: cohesive forces between particles (particularly fine grained particles), and friction caused by contact between particles.

The simplest test for finding the shear strength of soil is the shear-box test, or direct shear test, in which a shearing force is applied to the soil and the resistance measured on a proving ring (Smith, 1981). By undertaking this

procedure with the soil under varying compressive loads, a graph such as that represented in Figure 2.11 is created.

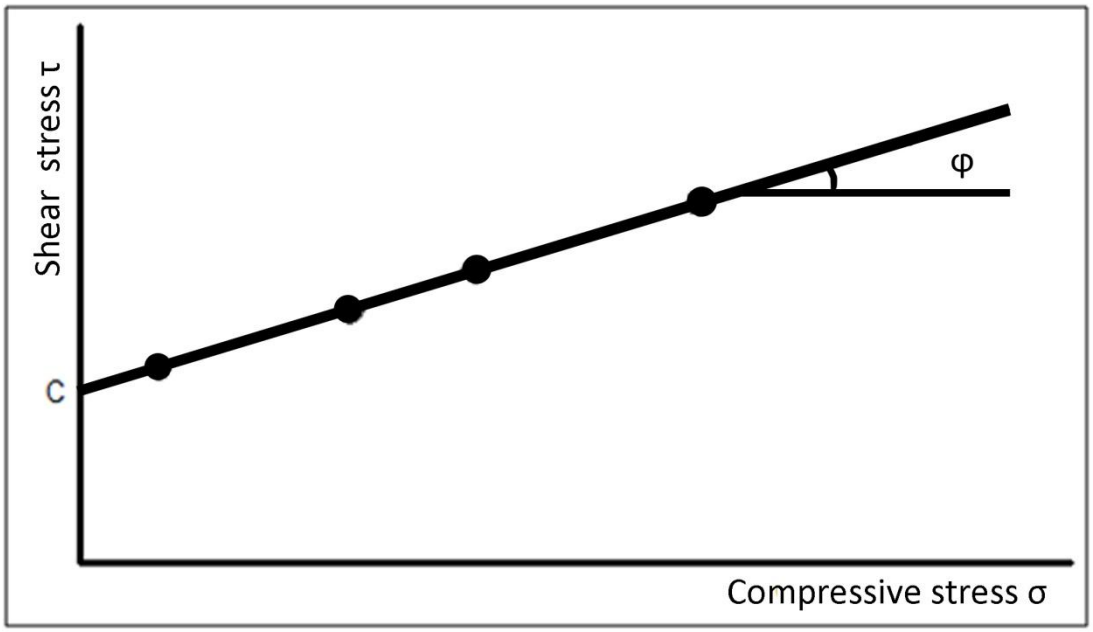


**Figure 2.11 - Plot of shear stress against compressive stress from shear box test (from Smith, 1981)**

The line in Figure 2.11 is defined by the equation $\boldsymbol{\tau = c + \sigma \tan \varphi}$ where:

$\tau$ = shear stress;

$\sigma$ = total compressive stress;

c = apparent cohesion (or shear strength); and

$\varphi$ = angle of shearing resistance (or internal friction).

This equation is known as Coulomb's law (Smith, 1981), and the line itself as the failure envelope. A state of stress above the line is not possible; the soil fails (Craig, 2004).

The shear box test is generally not used because it is difficult to apply to an undisturbed sample, and the distribution of stress is uncertain (Smith, 1981). A more popular test of shear strength is the tri-axial compression test, in which a

sample of soil is covered with a rubber membrane and placed within a cylinder filled with water. This provides lateral pressure that would come from the surrounding soil in the field. A load is then applied vertically until failure in the soil. By taking the cell pressure (the lateral pressure applied by the water) and the maximum principal stress (the pressure at failure + the cell pressure), a Mohr circle can be drawn. By running the test at numerous cell pressures, multiple Mohr circles can be drawn, the common tangent to which, the 'Mohr Envelope,' is the same as the line derived from Coulomb's law (see Figure 2.12) (Smith, 1981).

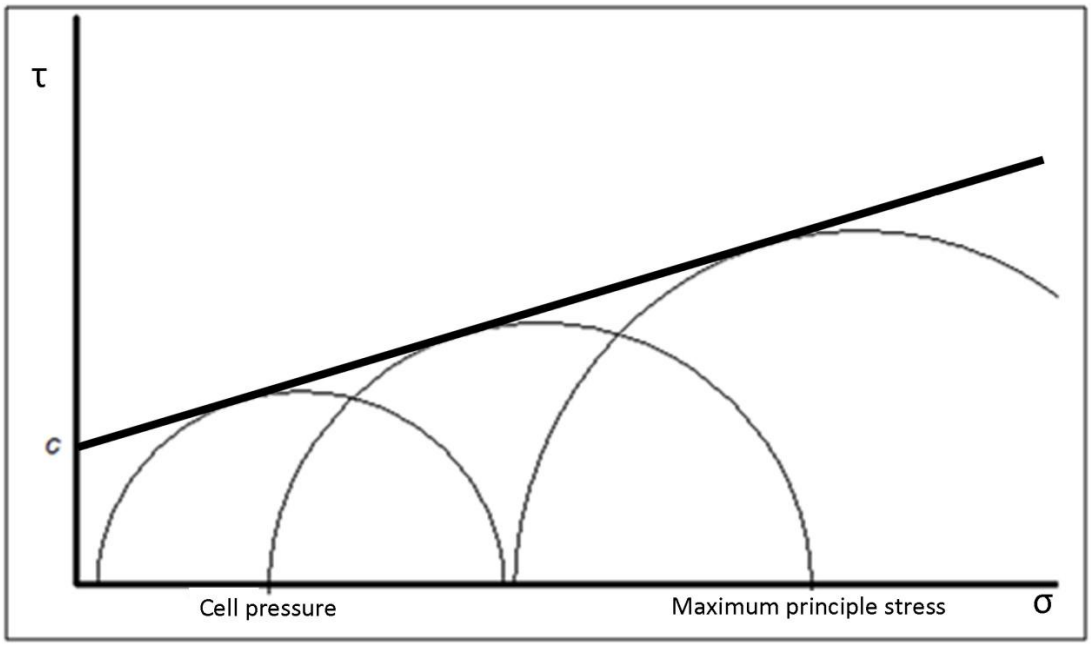


**Figure 2.12 - Mohr circles and the Mohr envelope (from Smith, 1981)**

From Figure 2.12 it can be seen that as the soil is put under more pressure, compressed more, the soil shear strength increases. As such, the denser a soil, the greater its shear strength (Karafiath and Nowatzki, 1978). In an *unconsolidated-undrained* test on saturated clays, in which there is no lateral support, only a single Mohr circle is drawn touching the origin. The undrained

shear strength (*Cu*) is given by the intercept of the horizontal tangent with the y axis. Internal friction (φ) is therefore zero, and *Cu* = c.

Field tests of shear strength can be undertaken using either a penetrometer, or a shear vane. The penetrometer is a circular punch, pressed into the soil at a slow, constant rate to a given depth. The force required to indent the penetrometer to the given depth is used to read off the shear strength of the soil. A hand shear vane is a long (> 0.3 m) pole with four blades at the base. At the top of the pole is a tension spring. The shear vane is pushed into the soil, and then turned using the tension spring at the top (again, a slow constant rate is required). When the soil shears, the blades rotate freely, and the tension spring relaxes. The maximum force required before shear is recorded. Values of undrained shear strength for clays are shown in Table 2.3.

| Stiffness state | Undrained shear strength ($kN/m^2$) | Test |
|---|---|---|
| Hard | >300 | Can be scratched by thumb nail |
| Very Stiff | 150-300 | Can be indented by thumb nail |
| Stiff | 75-150 | Can be indented slightly by thumb |
| Firm | 40-75 | Thumb makes impression easily |
| Soft | 20-40 | Finger pushed in up to 10 mm |
| Very soft | <20 | Finger easily pushed in up to 25 mm |

**Table 2.3 - Undrained strength classification of clays according to BS 5930:1999 (edited from Craig, 2004)**

The compressibility of a soil (or any other material) is given by the Poisson ratio, *v*. Poisson's ratio is the ratio of transverse contraction strain to longitudinal extension strain in the direction of a stretching force, that is, the amount of shrinking in cross section when stretched. Most common materials become narrower in cross section when stretched, which gives a possible Poisson's ratio of between 0 and 0.5. A material that is wholly incompressible

will, under vertical compression, extend laterally to an equal extent as it is compressed vertically, showing no volume change. This produces a Poisson ratio of 0.5. As a material becomes more compressible, *v* decreases. Typical values of *v* for geological materials are shown in Table 2.4.

| Material | Typical values for Poisson's Ratio |
|---|---|
| Saturated clay | 0.4 - 0.5 |
| Rock | 0.1 - 0.4 |
| Sand, gravely sand | 0.3 – 0.4 |
| Silt | 0.3 – 0.35 |
| Sandy clay | 0.2 – 0.3 |
| Loess | 0.1 – 0.3 |

**Table 2.4 - Typical values for Poisson's ratio (from Bowles, 1968)**

At low values of stress, a soil will behave elastically (Smith and Griffiths, 2004). That is to say, deformation is recoverable. The total response of a soil to load can therefore be considered to be elastic-plastic. The elastic part of the relationship is directly determined by the Young's modulus of the soil (*E*). The Young's modulus describes the modulus of elasticity of the soil - essentially its stiffness. In soils, particularly cohesive soils, *E* is approximately 1000 x *Cu* (Leach, 1994), as shown in Figure 2.13.

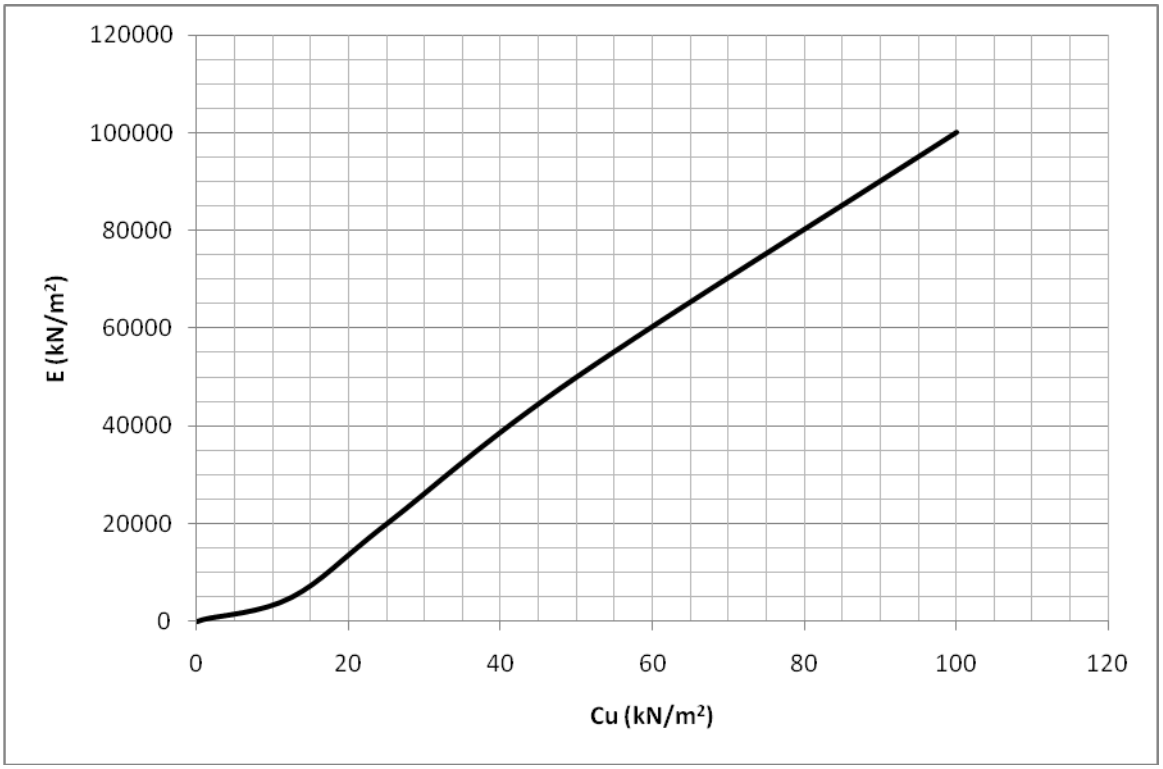


**Figure 2.13 - Relationship between Young's modulus (*E*) and undrained shear strength (*Cu*) (data from Leach, 1994)**

Figure 2.14 shows an elastic-plastic relationship for a saturated clay. In this scenario, once the ultimate bearing capacity ($q_u$) is reached or exceeded, the soil fails, and can no longer support the load, thus displacement increases with no further increase in load. First local yield ($q_y$) is the point at which some parts of the soil start to fail, but the soil as a whole remains able to support the load. If at any point the load is removed, recovery occurs along a line parallel to the elastic part of the curve. The curve above $q_u$ may be sloped either up or down in the cases of strain hardening or strain softening respectively (Craig, 2004).

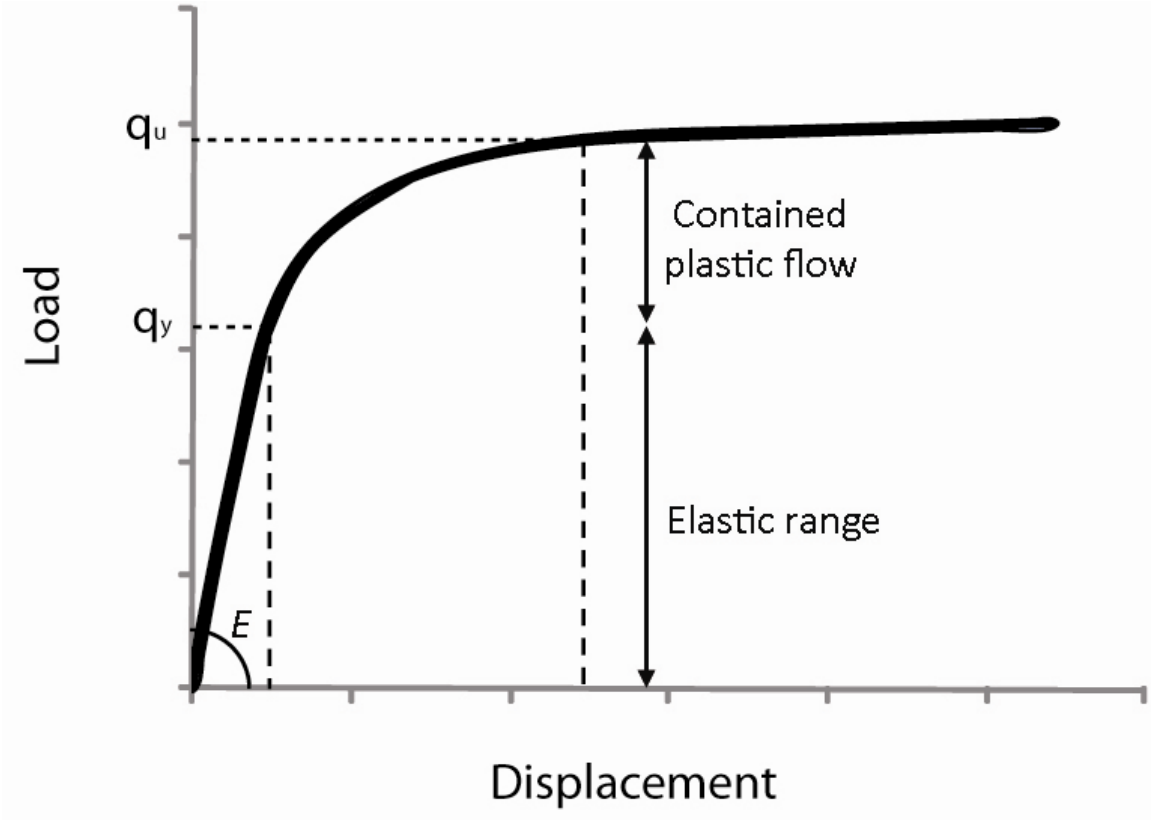


**Figure 2.14 – The relationship between load (stress) and displacement (strain) in an elastic-plastic behaving soil. The ultimate bearing capacity ($q_u$) represents the point of stress at which the soil fails, The point of first local yield ($q_y$) is where plastic deformation first occurs within the soil, causing the load-displacement curve to deviate away from a linear elastic relationship. The elasticity of the soil, as determined by the Young's Modulus (*E*) dictates the slope of the initial elastic deformation. Removal of the load at any point causes the curve to return to zero stress along a line with the same slope as the elastic region (adapted from Craig, 2004; D'Appolonia *et al.*, 1971; Smith, 1981)**

The ultimate bearing capacity of a soil beneath a strip footing (a load in the form of a strip, with limited width and up to infinite length) can be calculated according to Prandtl's equation:

$$q_u = Cu\,(\pi + 2)$$

Hence for a soil with shear strength of 100 kN/m$^2$, failure would occur at 514 kN/m$^2$. This however, considers the indenter to be a strip footing of infinite length. In order to calculate the bearing capacity of a soil beneath a finite footing, such as a square or circle, Skempton's equations are widely used (Skempton, 1951). For a footing on the surface of an undrained, cohesive soil, the ultimate bearing capacity is defined as:

$$q_u = Cu\, N_{cu}$$

Where $N_{cu}$ is a bearing capacity factor defined by:

$$N_{cu} = N_c\, S_c$$

Where $N_c$ = 5.14, and $S_c$ = 1 + 0.2 x (Breadth/Length).

A square footing at the surface of a soil where $Cu$ = 100 kN/m$^2$ would cause failure when loaded with 616.8 kN/m$^2$. A depth factor may also be included in the calculation of $N_{cu}$ for situations in which foundations are placed below the surface, but is removed here as tracks are made only on the soil surface.

When a soil fails through shear, Rankine's theory predicts that shear failure will occur along a plane at an angle of (45˚ + φ/2) from the plane of principal stress, where φ is the angle of the mohr envelope (Smith, 1981). Figure 2.15 shows the relationship between shear failure planes and the Mohr circle. In a saturated clay, shear will always occur along a plane at an angle of 45˚, as φ = 0.

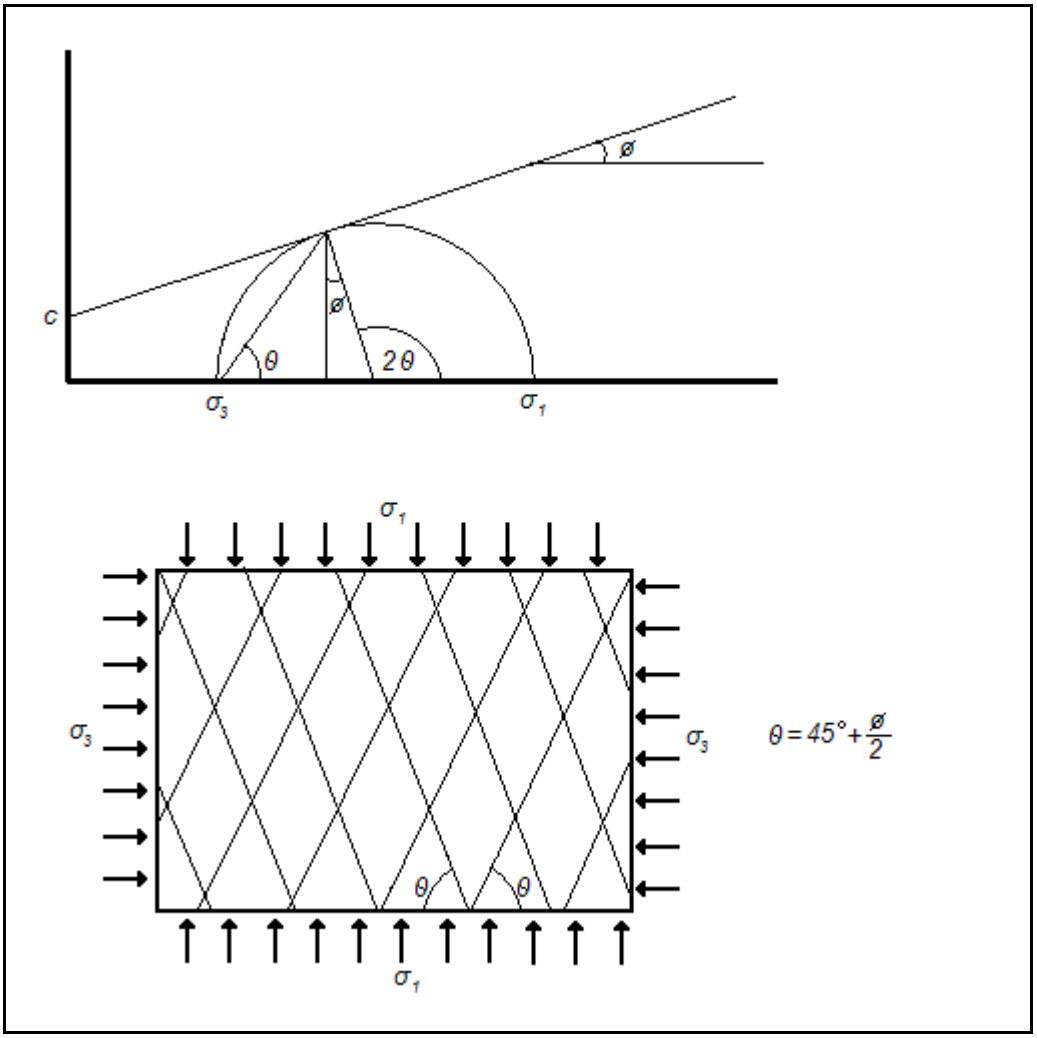


**Figure 2.15 - Rankine shear zones (from Smith 1981)**

There are 4 types of failure (Craig, 1997; Manning, 2004):

- General shear failure, whereby continuous failure surfaces develop between the indenter and the soil surface. The pressure is transmitted down and out through the shear surfaces, pushing up the surrounding soil surface, and creating a displacement rim (Figure 2.16a).
- Local shear, where there is significant compression of the soil beneath the load. Failure surfaces fail to reach the soil surface, and as such only a very slight displacement rim is created (Figure 2.16b).

- Punching shear occurs when a relatively high compression beneath the load is present, and shearing is vertical, producing a shaft with no displacement rim (Figure 2.16c).
- Liquefaction failure is a special state in which the pressure is created quickly, causing the soil to reach its liquid limit and flow into the depression (Figure 2.16d).

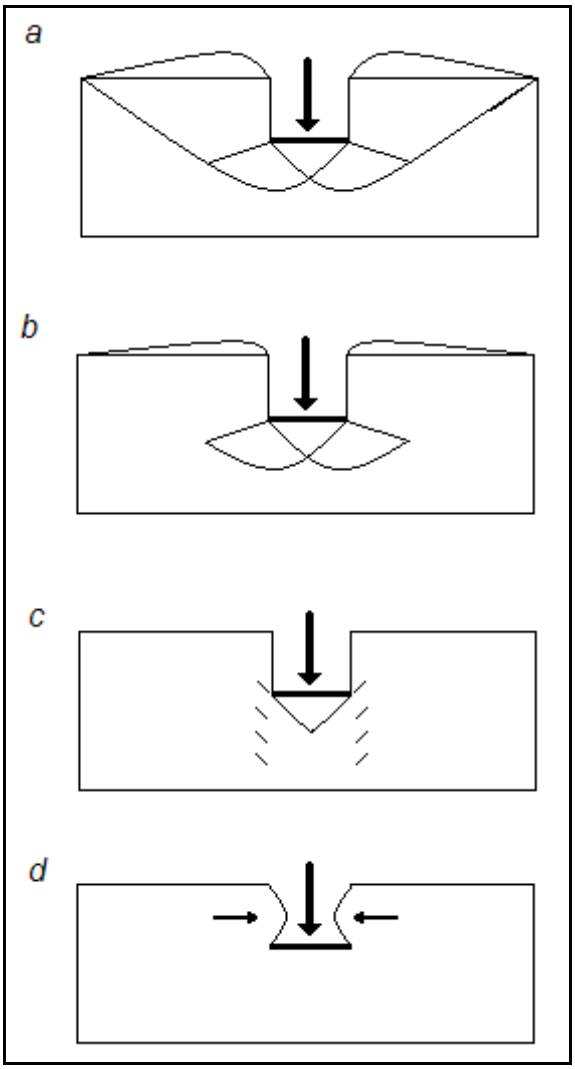


**Figure 2.16 - Failure modes - a) General shear, b) local shear, c) puncture shear, d) liquefaction failure (from Manning, 2004; Craig, 2004).**

The first three types of failure (general, local, and punching), are linked to the compressibility of the substrate. General shear is typical of sediments with

a low compressibility, resulting in the heaving around the load (the displacement rims). Slip will generally occur on one side, tilting the footing. Local shear occurs in substrates of high compressibility. This compressibility prevents the large heaving seen in general shear. Punching shear is associated with high compressibility and low shear strength (Craig, 2004). If a load-displacement curve is plotted for each mode of failure (Figure 2.17), it can be seen that general shear has a more abrupt bearing capacity, local shear a less defined bearing capacity, and puncture shear a poorly defined bearing capacity. It is also shown that higher compressibility results in greater displacements at lower loads.

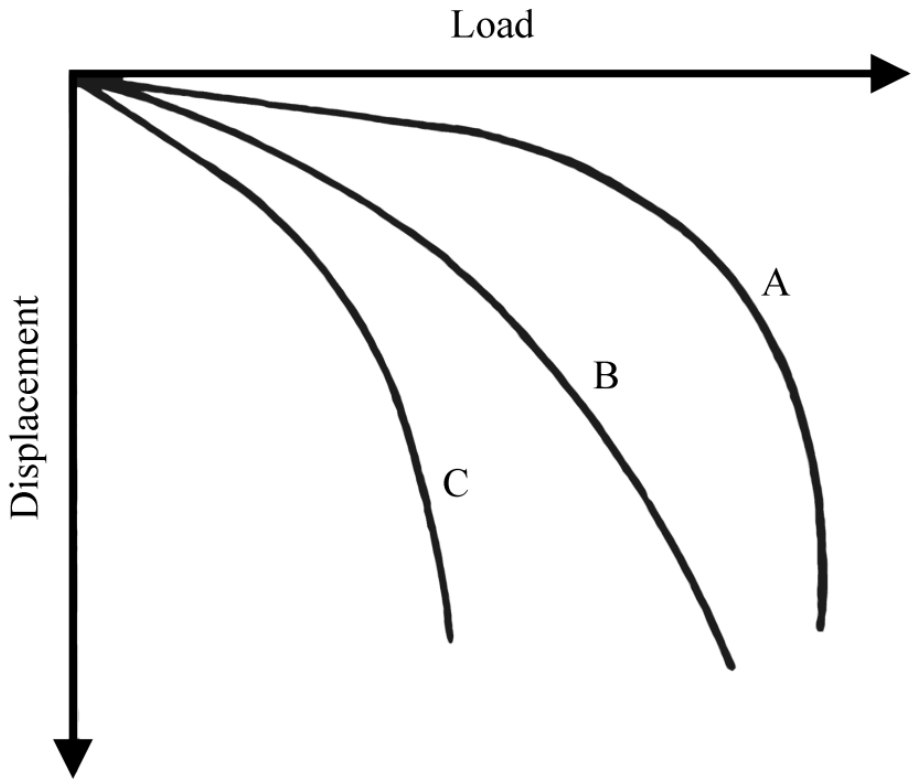


**Figure 2.17 - Load-displacement curve for 3 types of failure: (A) general shear, (B) local shear, and (C) puncture shear. Note that the curve is rather abrupt for (A), and less so for (B) and only gently sloping for (C) (from Craig, 2004).**

Figure 2.18 shows the mechanism that occurs during failure under general shear (found in soils of low compressibility), and the Rankine zones associated with this failure. The downward movement of the wedge ABC (and active Rankine zone) in Figure 2.18 is what produces the outward lateral forces. The transition from downward to outward movement occurs in areas ACD and BCG – zones of radial shear.

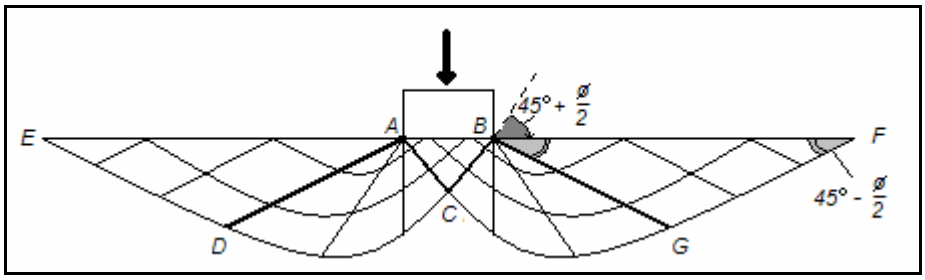


**Figure 2.18 - Failure zones in general shear (from Smith 1981).**

### 2.5.5 Modelling Failure

There have been several criteria proposed for representing the strength of a soil as an engineering material. Four of the most common are listed below. These can be divided into those suitable for frictionless, undrained clays (Tresca and von Mises) and those suitable for soils with a friction angle such as sand (Mour-Coulomb and Drucker-Prager), and also into those with a smooth failure surface (von Mises and Drucker-Prager) or those containing singularities (Tresca and Mohr Coulomb).

*Tresca Yield Criterion.*

The Tresca yield criterion defines a yield surface within three dimensional principal stress space (Figure 2.19). This surface takes the form of a hexagonal

prism with infinite length passing through the origin (Figure 2.19 A). When all three stress invariants are approximately equal, the soil remains in an elastic state (within the failure surface). As one or more stress invariants increase relative to the remainder, failure occurs. The equation defining the Tresca yield criterion is given by (Smith and Griffiths, 2004):

$$F_t = \frac{\bar{\sigma} cos\theta}{\sqrt{3}} - C_u$$

*Mohr-Coulomb Yield Criterion.*

If a friction angle is incorporated, the resultant yield surface becomes an irregular hexagonal cone (Figure 2.19 C). As the yield surface is derived from the geometry of Mohr's circles (Figure 2.12), we can see that the cone is formed from Mohr's circles of differing sizes. A friction angle of 0 implies all Mohr's circles are of the same size, hence the linear, infinite Tresca yield surface. The Mohr-Coulomb criterion is often used for concrete or granular soils such as sand (Smith and Griffiths, 2004), and is defined as such:

$$F_{mc} = \frac{\sigma_1 + \sigma_3}{2} \sin\varphi - \frac{\sigma_1 - \sigma_3}{2} \cos\varphi$$

*von MisesYield Criterion.*

Unfortunately, the corners inherent in the Tresca and Mohr-Coulomb yield surfaces present singularities. These singularities have in the past caused difficulties in computational techniques achieving a solution (Potts and Zdravković, 1999). As such, a yield criterion with a smooth surface is desirable. Taking the Tresca yield surface and inscribing or circumscribing it defines the

von Mises yield criterion (Figure 2.19 B, E). Under plane-strain conditions (where $\sigma_3$ is considered to be zero), the von Mises surface inscribes the Tresca surface and is defined as:

$$F_{vm} = \bar{\sigma} - \sqrt{3}C_u$$

Under triaxial conditions, where $\sigma_2 = \sigma_3$, the von Mises surface circumscribes the Tresca surface:

$$F_{vm} = \bar{\sigma} - 2C_u$$

The von Mises yield criterion is commonly used to define the behaviour of metals and frictionless, undrained clays (Smith and Griffiths, 2004).

*Drucker-Prager Yield Criterion.*

In the same way that the von Mises criterion is a 'smoothed' definition of the Tresca, so the Drucker-Prager yield criterion is a smoothed version of the Mohr-Coulomb. Again, the Drucker-Prager criterion may inscribe or circumscribe the Mohr Coulomb criterion (Figure 2.19 F). The Drucker-Prager is often used in the simulation of granular materials such as sand and concrete (Karthigeyan *et al.*, 2006; Tekeste *et al.*, In Press). The equation for the Drucker-Prager yield criterion is:

$$F_{dp} = 3\alpha\sigma_m + \bar{\sigma} - k$$

Where $\sigma_m$ is the mean stress, and α and *k* are material constants, functions of $\varphi$ and *c*.

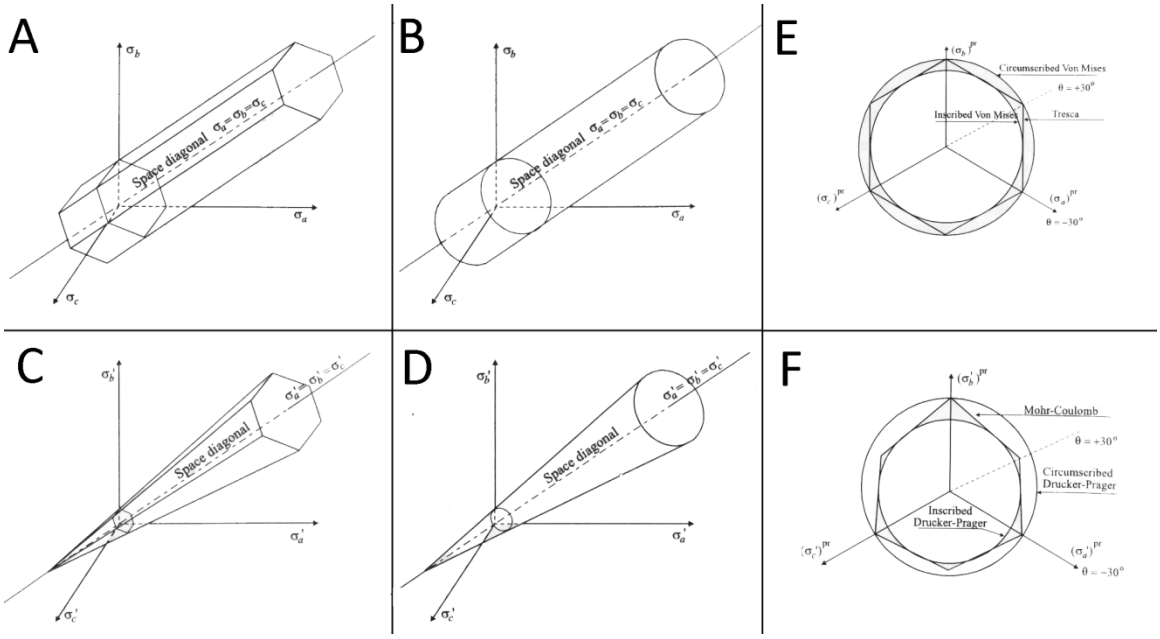


**Figure 2.19 - Yield surfaces in 3D stress space. A) Tresca yield surface, B) von Mises yield surface, C) Mohr Coulomb yield surface, D) Drucker-Prager yield surface, E) comparison between Tresca and von Mises surfaces in a diaviatoric plane (a plane normal to the space diagonal), and F) comparison between Mohr Coulomb and Drucker-Prager surfaces in a deviatoric plane. Adapted from Potts and Zdravković (1999).**

For the purposes of this thesis, the von Mises model has been used in the finite element analysis software (see Chapter 6 -). Many of the best preserved tracks are formed and subsequently preserved in fine, plastically behaving muds. It is therefore logical to use the numerical model most closely matching the formational conditions of such well preserved tracks. The lack of a friction angle (necessary for modelling sand) makes the model less computationally expensive than the Mohr Coulomb or Drucker-Prager criteria, while the curved surface of the von Mises model prevents numerical instabilities associated with the singularities present in the surface of the Tresca criterion.

The above sections detail the mechanics of soils in a simple case – that of static loading and uniform homogeneous substrate. However, the mechanics become more complex when considering a soil made up of numerous layers. For instance, the layering of a soil means that it's permeability may be much greater laterally as compared to vertically (Craig, 1997; Smith, 1981). Firm and soft interbedded layers will result in non- uniform pressure bulbs as the bearing capacity changes with depth. In a similar manner, a thin, firm substrate underlain by a weaker one will show preferential development of local shear zones in the weaker sediment (Manning, 2004), as the forces are transmitted through the firm substrate.

Dynamic forces compound the problems of pressure distribution and simple soil failure. A moving animal of given weight will apply differing amounts of pressure as the area of foot in contact with the soil alters, causing the soil to fail beneath the heel, for instance, but not beneath the fully planted foot. Also, the force vector will vary in direction according to the direction of movement of the foot.

## *2.6 Computer modelling*

### 2.6.1 Reasons for computational modelling.

Many previous neoichnological experiments have been carried out with physical modelling, using indenters on actual substrates (Allen, 1989, 1997; Manning, 1999, 2004; Milàn and Bromley, 2006), or the use of live animals moving over prepared areas (Milàn, 2006; Padian and Olsen, 1984).

Recent advances in computational power and advanced modelling software mean that numerical modelling can be used to investigate vertebrate track formation. Current uses of computational techniques in the study of fossilised tracks have not extended far beyond aiding in visualisation (Bimber *et al.*, 2002; Gatesy *et al.*, 2005; Manning, 2008; Padian, 1999), a useful endeavour, but only hinting at the potential. Henderson (2006b) used computer simulations to investigate weathering of dinosaur tracks, and to compare this to simulated undertracks. However, these tracks were artificially created (undertracks were generated according to what was expected) before being subjected to an arbitrary weathering algorithm (where raised areas were eroded faster).

Numerical modelling allows many experiments to be run repeatedly with consistent and accurate control over individual variables. Not only is data produced at the end of the experiment, but at any stage all information is available for study, allowing an accurate description of the end product, and also a detailed account of the track's formation at every stage. Numerical modelling also allows for experimentation that would be difficult to carry out physically, as in the case of modelling very large loads on a substrate.

A major consideration with computational modelling is in ensuring the model is accurate. The model must be able to make accurate predictions that can be tested with traditional analogue modelling or numerically by first principles equations, before being used in a scenario where no direct analogue exists. Any model must be 'ground truthed' and validated against physical experimentation, numerical problems with known solutions, or observation. The advantages of computer modelling, and of the finite element method (outlined below) are summarised in section 11.2.1.

### 2.6.2 The finite element method

Margetts *et al.* (2005; 2006) presented an early model for investigating dinosaur track formation using the finite element method (FEM), and have compared the results favourably to tracks from the Amherst College Museum of Natural History (ACMNH), highlighting the change in size with depth, and the transmission of force into the soil volume.

The FEM is a numerical analysis technique common in engineering for exploring the mechanics of continuous media, though the method is applicable to a broad variety of mathematical problems that arise in almost all areas of science (Burnet, 1987). The roots of finite element analysis (FEA) lie in finite difference approximations (Richardson, 1910), and engineering elastic continuum problems (Rayfield, 2007; Turner *et al.*, 1956). In simple terms, the method approximates the governing equations of a continuous system by dividing the continuum into 'finite elements,' each of simpler geometry and consequently with simpler governing equations that can be solved and recombined.

As an example of this, consider a circle of radius *r*. In finding the circumference of the circle, one could approximate it to an 8 sided polygon, as in

Figure 2.20, and then calculate the length of a segment using trigonometry. It is then easy to find an approximation of the circumference. Divide the circle into smaller triangles, and the result comes ever closer to the true answer.

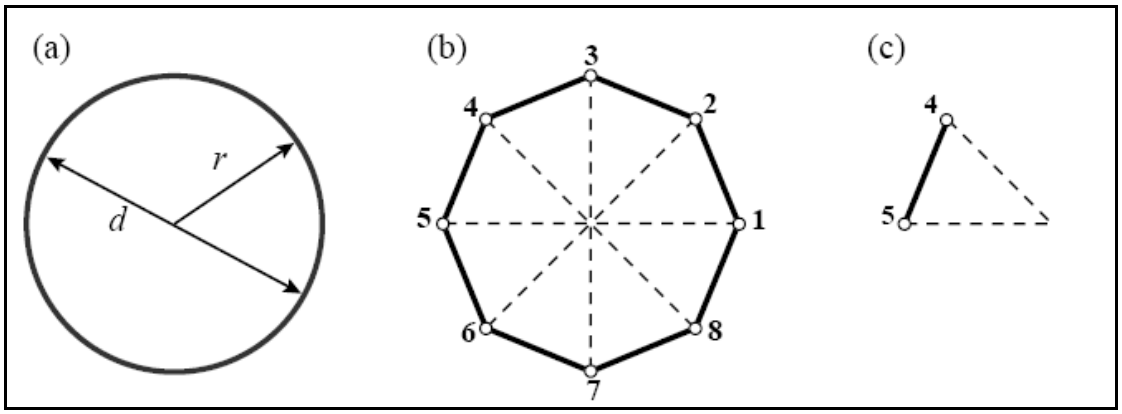


**Figure 2.20 – Analogy for explaining FEA. The circle is replaced with an approximation (an octagon) such that an approximate circumference can be found. Refining the divisions of the circumference leads to a more accurate answer, but takes longer (from Felippa, 2004).**

This is of course a massive over simplification, but provides a useful analogy for how FEA works. A more specific definition of the FEM, though less intuitively easy to understand was stated by Burnet (1987):

*"The FEM is a computer-aided mathematical technique for obtaining approximate numerical solutions to the abstract equations of calculus that predict the response of physical systems subjected to external forces."* (Burnet, 1987, p47).

If it is assumed that a problem requires the description and/or prediction of the response of a system to external influences, then the problem can be considered to have four main concepts (Burnet, 1987):

- The system – the object under study composed of materials. This could be for instance, a mechanical linkage, an aeroplane, or a volume of soil.
- The governing equations – differential, integral, and/or constitutive equations which describe the behaviour of the material composing the system.
- The domain – typically the space occupied by the system, and/or the time over which the system may change.
- Loading conditions – the forces originating externally to the domain that interact with the system.

We can consider these concepts with regard to the problem of vertebrate tracks. The system will be the soil undergoing deformation, the governing equations will determine the behaviour of the soil – its plasticity/elasticity, bearing strength, failure criterion etc. The domain will be the volume of soil considered, and the loading conditions will be the forces applied by the foot. This provides obvious control over such factors as the loading of the foot and the properties of the soil independently to other areas of the model.

Having determined the system and its governing equations, the domain is divided into smaller regions known as elements, with elements generally being made as simple in shape as possible, the most common 3d element shapes being 4-sided tetrahedra, or 8-sided bricks. These elements are defined by nodes, points with x, y, and z coordinates. In low order elements, nodes occur at the corners of the elements, so a tetrahedron will have 4 nodes, whilst a brick will have 8. These nodes are shared with neighbouring elements. In higher order elements, nodes also occur at the midpoint of each edge, giving tetrahedra eight

nodes, and bricks 20. This provides a greater degree of flexibility, but increases the computational expense, making solutions take longer. This collection of elements and nodes is known as the mesh, and this mesh is generated in a pre-processing stage.

The governing equations are then transformed within each element to algebraic equations rather than integral or differential. Because the element equations are identical for all identical elements, they only need to be calculated for a relatively few typical elements, and because each element is much simpler than the domain in shape, the equations may be made less complex. Hence the problem is reduced to a few algebraic equations for a few small elements. The equations within each element are then evaluated and the resulting numbers combined into a much larger set of equations known as the system equations, which are then modified according to the external loads. The resultant equations are then solved, and displayed through the post-processing operation (Burnet, 1987).

Figure 2.21 provides an example to explain the FEA process. A hypothetical problem is given of a bar containing a hole under tension (Figure 2.21a). Because the bar is symmetrical, the domain can be simplified (and only one quarter actually simulated) because the properties and conditions (hence the equations and solutions) will be identical (Figure 2.21b). A mesh is then created. Note that there are many potential meshes, and thus many potential answers of varying accuracy. In this case, a mesh has been produced with more elements in the area expected to be more complicated (Figure 2.21c), this provides a higher resolution and subsequently more accurate answer in the area of most interest. Larger elements can be used away from this area when it is known or expected

that little or no stress will occur in those areas. The equations are then evaluated for each element, and together form the system equations. The system equations are then modified by the boundary conditions (the tension on the bar), and solved. The post processing step then displays the results as in Figure 2.21d and Figure 2.21e, in this case as contours of stress.

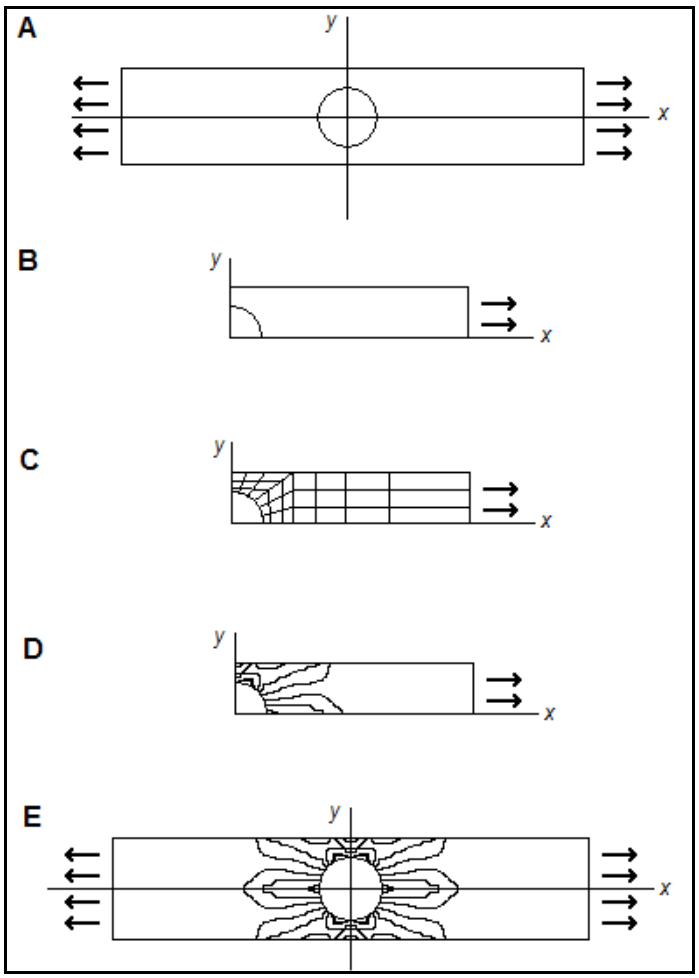


**Figure 2.21 – Example FEA problem and solution showing how symmetry can be used to simplify a problem. Two planes of symmetry allow the full model (A) to be reduced to the form in (B). this form is descritised into elements (C), and solved for values of stress (D) before being recombined into the original form (E). After Burnet (1987)**

### *2.6.2.1 Relevant FEA research.*

The FEM has been used as an analytical technique in engineering and medicine since the 70's and 80's (Rayfield, 2007), but only in the past decade has the

value of FEA in palaeontological research been realised. With few exceptions (see below), almost all of the work carried out in palaeontology using FEA has been on vertebrates, and the biomechanics of bone. Rayfield pioneered much of this work with research into dinosaur skulls and the forces acting upon them (Rayfield, 2004, 2005; Rayfield *et al.*, 2001), and this work has continued with her students (Porro, 2006, 2007). Uses of the method applied to other taxa include foraminifera (Song *et al.*, 1994), insects (Kessel *et al.*, 1998), and echinoids (Philippi and Nachtigall, 1996). In recent years, the application of FEA in dinosaur research has become commonplace (Arbour and Snively, 2009; Manning *et al.*, 2009; Moreno, 2007; Xing *et al.*, 2009c). For a review of FEA in palaeontology, the reader is encouraged to read Rayfield (2007), who discussed the method most comprehensively.

Non-biomechanical palaeontological research involving FEA is much less common. Recent work by Margetts *et al.* (2005, 2006) used finite element analysis to look at dinosaur track formation. A mesh was created to represent a volume of soil. This mesh contained 73,728 8-noded hexahedral elements, and 78,449 nodes. A von Mises soil was used (the source of the governing equations), and nodes were displaced according to the shape of a three-toed dinosaur foot (the loading conditions). The results of the FEA were able to show a definite difference between static and dynamic loading, and also the variation in shape and size of the track with depth (Margetts *et al.*, 2005; Margetts *et al.*, 2006). It is this methodology that will be discussed and expanded upon throughout this thesis.

Whilst dinosaurs interacting with sediment are not particularly common in the FEA literature, a similar scenario with a more industrial use is: that of tyre-

soil interaction (Fervers, 2004; Nakashima and Oida, 2004; Nakashima and Wong, 1993). Fervers (2004) described a 2D FEA simulation of a tyre, over both a rigid ground and a soft soil. The first test described by Fervers was the comparison between FEA model and physical test of the tyre under load; this was then followed by comparison of the model with a physical test of the tyre mounting a curb, and the results of the simulation were shown to be in close correspondence with those from the physical test.

Having shown the FEA model of the tyre to be accurate, it was then simulated moving over a soft soil at two different pressures (7.5 bar and 1.5 bar), under a 30Kn load. The soil used was described by the Drucker-Prager model from the commercial FEA package ABAQUS. This was used to simulate a wet, loose loam (Figure 2.22), and a dry sand (Figure 2.23).

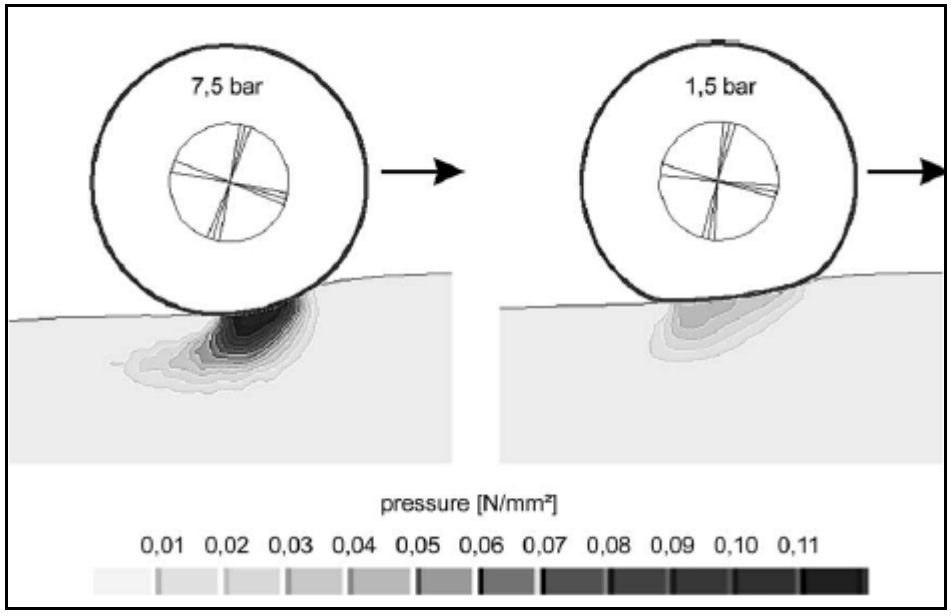


**Figure 2.22 - Soil pressure on loam with high and low tyre pressure (from Fervers, 2004).**

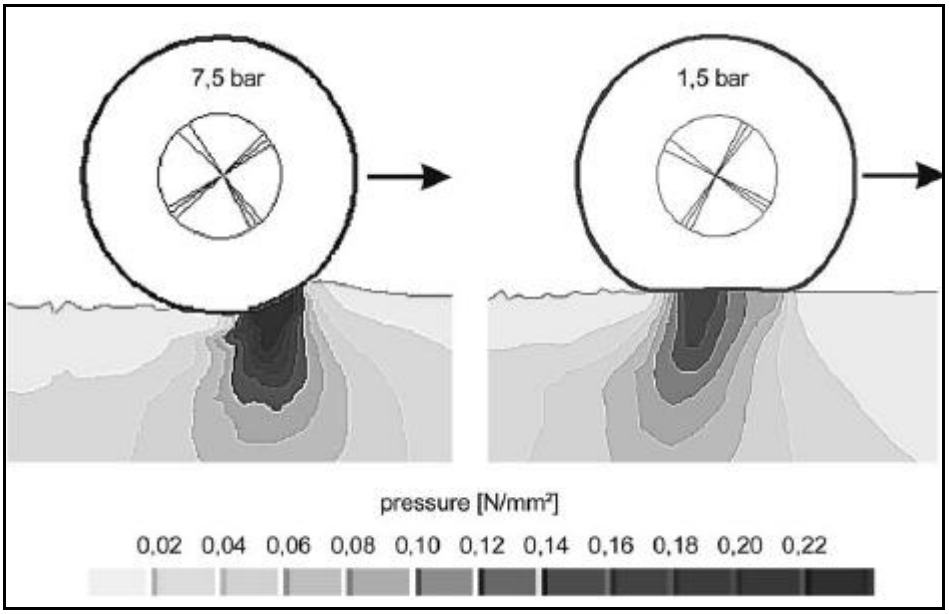


**Figure 2.23 - Soil pressure on dry sand with high and low tyre pressure (from Fervers, 2004).**

Mulungye *et al.* (2007) also investigated tyres and soils, but this time with a flexible pavement on top of the soil. Four tyre pressures were simulated on a finite element mesh modelling asphalt, rock base, sand, and subgrade peat soil. The simulation was run in two dimensions, but both lateral and longitudinal simulations were reported (Mulungye *et al.*, 2007).

Other FEA research involving soils includes Popescu *et al.* (2005; 2006), who used FEA to investigate the effects of random heterogeneity of soil properties on bearing capacity (Popescu *et al.*, 2005), and on the liquefaction of saturated soil (Popescu *et al.*, 2006). Abo-Elnor *et al.* (2004) simulated soil-blade interaction for industrial farming purposes, verifying the model with a compression test using an oedometer both physically and simulated, and showing closely matching results. Scheiner *et al.* (2006) used the FEM to show more effective protection was required for buried pipes, by using FEA to model the loading of oil and gas pipelines due to soil settlements.

#### *2.6.2.2 Parallelisation*

FEA, despite optimisations and shortcuts (e.g. only working with one repeatable part of the whole problem, as in Figure 2.21), is still a very computationally expensive technique – and always will be, because as more power becomes available, more complex problems will be attempted. So an increase in computer power serves not only to speed up current problems, but to allow the tackling of much larger and complex FE models than would otherwise be possible.

Smith (2000) presented a general system for running finite element analysis in parallel, that is dividing the problem over multiple processors and/or computers, and showed the results of this system on a variety of parallel machines (Smith, 2000). This parallelisation was used by Margetts *et al.* (2005, 2006) in the simulation of dinosaur tracks, by dividing the elements and equations equally over the processors. As multi-core processors have become common place in the desktop PC market, most FE software packages and programs have begun to utilize some form of parallelisation. However, the efficient parallelisation of code, so as to be efficient over many hundreds or thousands of processors as found in supercomputers, is still in its infancy.

# Chapter 3 - Fossil tracks.

## *3.1 Documenting fossil tracks.*

Throughout the following sections of this thesis, Tracks and trackways were recorded (where possible or relevant) in the manner outlined by Leonardi (1987) and later Thulborn (1990):

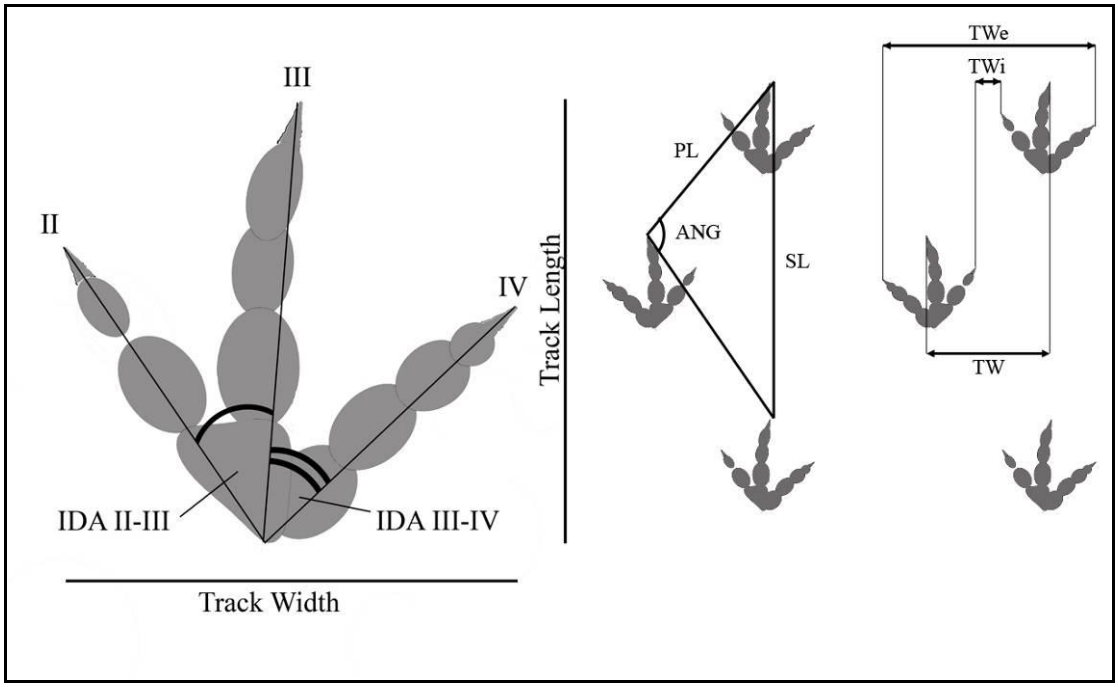


**Figure 3.1 - System for describing tracks and trackways according to Thulborn (1990). IDA = Inter Digital Angle, roman numerals denote digit numbers, ANG = Pace Angulation, PL = Pace Length, SL = Stride Length, TW = Track Width, TWi = Internal Track Width, TWe = External Track Width.**

Where necessary, i.e. when undertracks were clearly present, the terminology from Manning (2004) was applied (see next page):

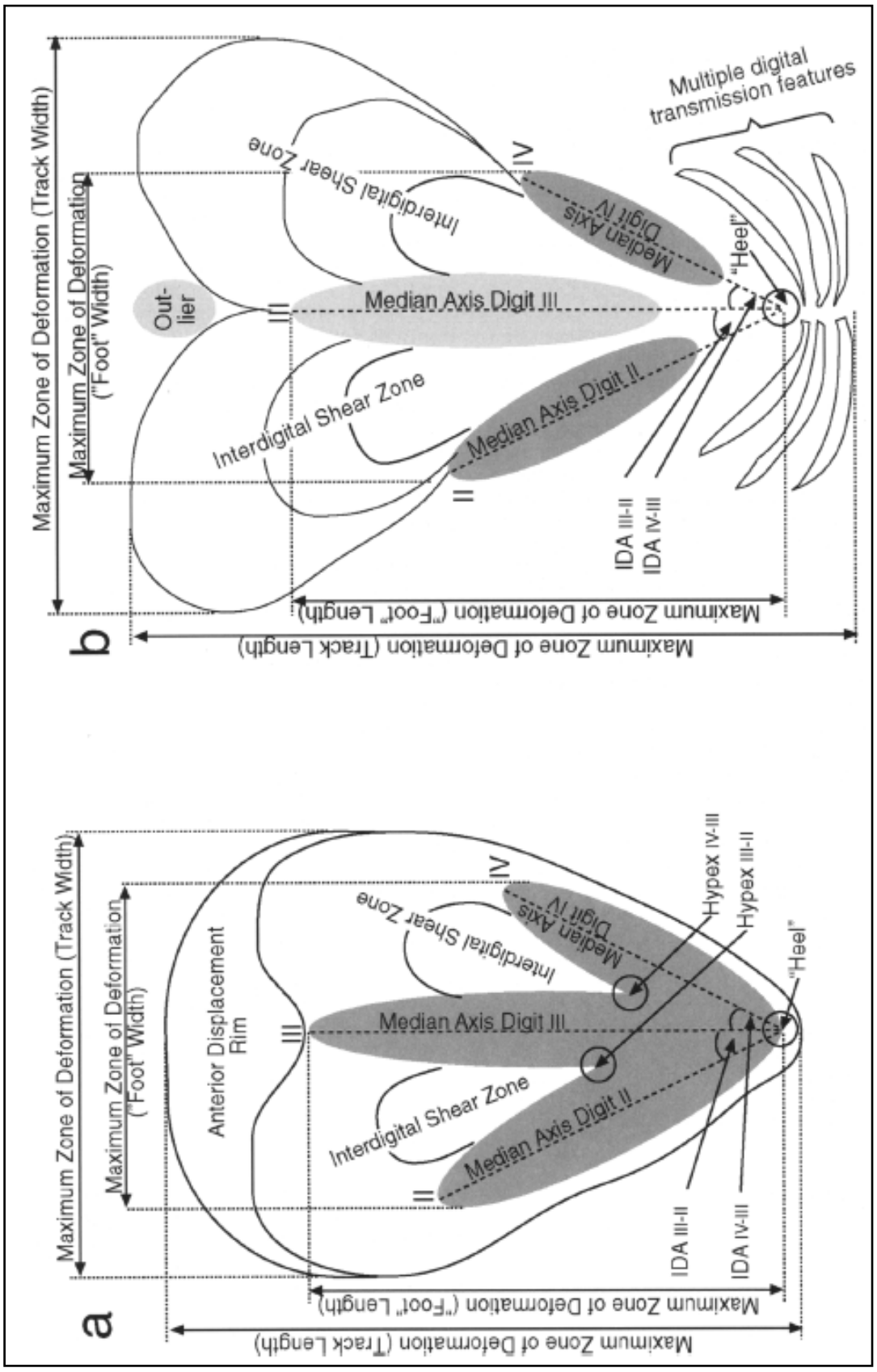


**Figure 3.2 - Track terminology for a) surface track and b) undertrack features, according to Manning (2004) (from Manning 2004).**

Note that the definition of track length varies between systems; Manning uses ‘track length’ and ‘track width’ as synonyms of Maximum Zone of

Deformation (MZD). For this thesis the two terms shall not be used interchangeably, 'track length' shall refer to the impressed deformation and MZD shall refer to the total area deformed, extending to the edges of the displacement rims (see 3.1.1 below).

In instances when photographs were taken, digits were pointed 'up', and low angle light sources were applied from the upper right where possible. This helps to cast shadows so as to capture 3D features.

### 3.1.1 Defining the track extents.

A problem with studying tracks, and particularly when that study extends to the full three dimensional extent of sediment deformation, is how to define the extents of the track itself. At which point can a track be said to end and the surrounding sediment/deformation begin? Is the track length the length of the track's surface outline, or the length at the base of the track? Or is the track length a measure of the disturbance the track maker made (the MZD). Figure 3.3 shows several possible places to measure track length from.

Thulborn (1990:pp 91) highlighted the difficulty and subjective nature in defining the edges of a track. In such a field as vertebrate ichnology where many specimens may vary so widely depending on factors such as foot morphology, limb kinematics, and substrate properties, a move from subjective measuring to more objective recording is always welcome.

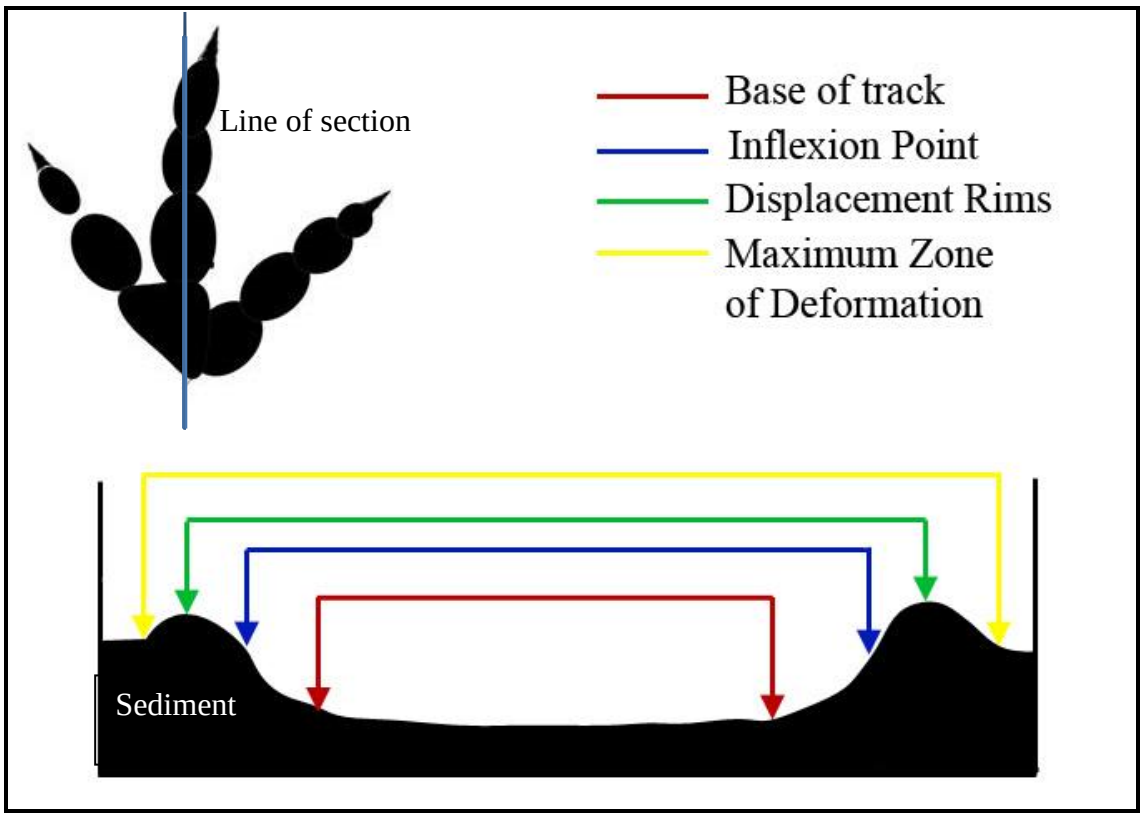


**Figure 3.3 – "Track length" measured at differing points along the axis of a hypothetical track: The base of the track (possible foot-sediment interface); Inflexion Point; Displacement Rim peaks; MZD - the total zone showing deformation caused by loading.**

***What is needed from the measurements of a track?***

Firstly, the need for measurements is one of scale, describing the size of the track to provide a scale for the track-maker's foot. In this case, measurements of length and width of surface tracks should represent the edges of the track-maker's foot. Ideally, the defining edge of the track should be the most extensive points of the contact surface between foot and sediment. Any other point has been deformed by sediment-sediment interaction, rather than directly by the foot (Gatesy, 2003). However, it is not always possible to see where the foot-sediment interaction occurred exactly, and the occurrence of any weathering,

erosion, or separation of layers will usually result in the surface exposed not being that upon which the animal stepped.

Aside from the descriptive need for a defined track, any morphological comparative work requires landmarks that remain consistent throughout all comparisons. Whilst the points defined above (extents of soil-foot contact) may be considered landmarks for surface tracks, such points are non-existent in weathered tracks or undertracks, and so if used would prevent comparisons between surface and subsurface traces.

To define the points at which to measure length and width, and to define the outline of the track, is therefore a complex task. It must be possible to consistently observe anterior, posterior, and lateral points at all levels within a track, and across different tracks. When measured at the track surface, the points should of course represent as closely as possible the corresponding points of the track-maker's foot, such that the measurements for the track are representative of said foot.

***Defining the track outline in fossil specimens.***

Even when the physical track is present, defining the edges of the track is a difficult task. Often a track is measured simply by eye – extents of the track are defined subjectively by the observer. However, attempts to formalise track measurements have been made, and several criteria for defining a track edge have been used in previous literature:

*Landmarks.*

A common method in defining track extents is to use landmarks (Thulborn, 1990). Landmarks can be picked across tracks that are analogous to the geometry of the track, rather than homologous to parts of the animal's foot, e.g. the most anterior point of the track (which may bear no relation to the most anterior part of the foot). The landmark method is usually employed indirectly even when measuring a track in the field, as the posterior and anterior points to measure between are often arbitrary landmarks that designate the point at which the observer has decided track ends.

*Inflexion point.*

The inflexion point is the point at which the slope at the side of the track changes, usually from curving upwards to curving down (Manning, 1999, 2004). If we imagine an indenter with sharp edges indenting a soft substrate, we would see that the inflexion point becomes homologous with the extent of indenter-substrate contact (Allen, 1989, 1997). When the indenter has a curved side (such as a foot), or when the sediment is sufficiently firm as to transmit the force and deform in a large area, the inflexion point moves upwards toward the original surface.

There are numerous occasions however where the inflexion point can be difficult or impossible to measure. Fossil tracks that are weathered and/or found in a rock with a rough surface may contain numerous points of inflexion. Alternatively, a track may be so shallow and the sides sloped so gently that an inflexion point is difficult to ascertain even with digitisation techniques (Bates *et al.*, 2008a; Falkingham *et al.*, 2009) Finally, more complex tracks where

sediment has been convoluted by the foot movement, (such as the Greenland tracks described by Gatesy *et al.* (1999)) may have overhanging sediment, in which case inflexion points will be severely distorted and measurements based on such points will bear no relation to the extent of the track or track-maker's foot.

*Maximum zone of deformation.*

Manning (1999, 2004) highlighted the importance of measuring the maximum zone of deformation (MZD), and noted that a correlation between MZD and the length of the track indentation could potentially relate to other factors such as depth (Manning, 1999). Whilst such a measure is important in understanding the soil mechanics, and therefore conditions, at the time of track formation, such a measure used as "track length" would clearly run into difficulties in tracks such as those reported by Graversen *et al.* (2007) (Figure 3.4) where MZD is so vastly different to the size of the track-maker's pes as to provide no relationship between track and producer, and no information regarding the indented central area.

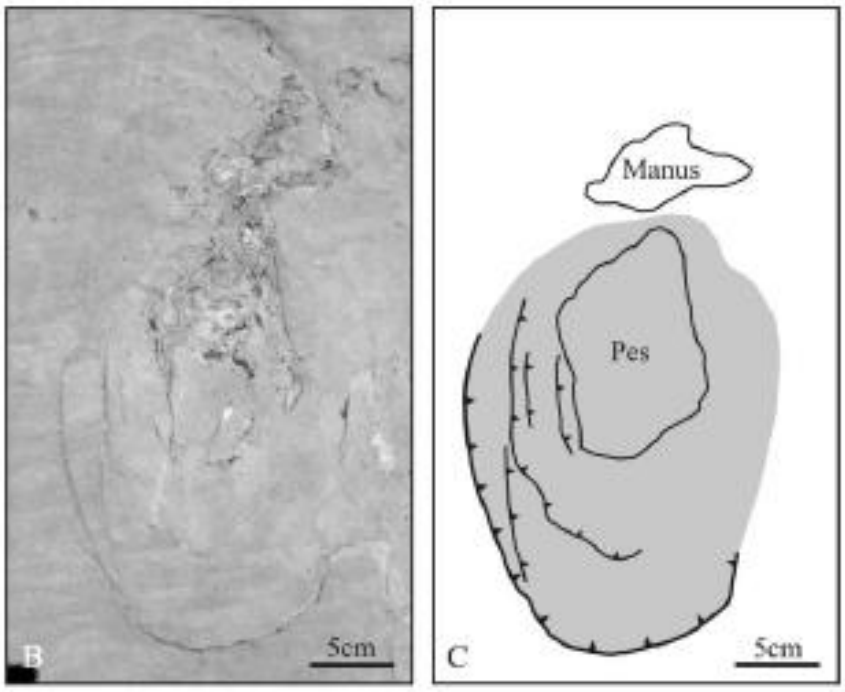


**Figure 3.4 - Manus and pes prints showing large zones of deformation around the track itself. Using MZD as a measure of track length in this case would produce values with little relation to the track maker's foot, and would prove incomparable with tracks made by the same foot in differing conditions (from Graversen *et al.* 2007).**

### *Defining edges of virtual tracks.*

Some of the methods used to measure fossil tracks can be used on virtual tracks. The inflexion point can prove easier to measure in a simulation such as FEA, as track sides are generally smooth, and contain only the single inflexion point. In the case of FEA simulations used in this project where surface nodes are directly displaced, the deformation results in the inflexion point being equal to the extents of the indented foot (that is, the displaced nodes) when measured at the surface.

A digitised track can be contoured according to height, elucidating the position of the track. A contour can then be picked as a landmark. Bates (2006) and Bates *et al.* (2008a; 2008b) used a contour picked from within the

displacement rim, and then used the direction of the trackway to determine the axis of length, and the axis normal to this for width.

Margetts *et al.* (2006) used Mises stress (a scalar function of the principle stresses) to define track outlines in Finite Element simulations of tracks. Only one value of Mises stress forms a solid contour, as this is the point at which the sediment fails. Of course, whilst a simulation of a track may be adapted to output such a value, no such measurement can be made from fossil tracks.

***The Solution?***

What is needed then is a uniform way of defining a track's geometry, not only among surface tracks, but throughout the three dimensional volume of undertracks too. With the advent and increasing popularity of computer simulation of virtual tracks ((Margetts *et al.*, 2005; Margetts *et al.*, 2006), and digitisation of fossil tracks (Bates, 2006; Bates *et al.*, 2009a; Bates *et al.*, 2009b; Bates *et al.*, 2008a; Bates *et al.*, 2008b; Breithaupt *et al.*, 2004; Breithaupt and Matthews, 2001; Breithaupt *et al.*, 2001; Matthews *et al.*, 2005; Matthews *et al.*, 2006), such a method should be applicable to digital and field specimens alike.

For this thesis, (where applicable) a variation on the contour method used by Bates *et al.* (2006) and Bates *et al.* (2006; 2008a; 2008b) has been used. While Bates *et al.*'s method can be made consistent within a single study, such a method involves the arbitrary selection of contours. With computer models, we are presented with the luxury of a smooth surface. As such, for the purposes of this work, the contour will be specified as the contour of 'zero vertical displacement.' That is, the contour defining the sediment that is present at the level of the original undisturbed surface after the track has been formed, or the

point at which the original sediment horizon is cut. While this sediment may have moved laterally, zero y displacement can only occur in two places: 1) between the indentation of the foot and the interior of the displacement rims, and 2) at the extent of any displacement rims. This will prove easy to calculate from virtual models, and presents a good practical solution to identifying track extents in fossil tracks, providing, as it does, an objective definition of track extents.

However, the accuracy and objective nature of computer modelling can lead to complications. The inner contour of zero y displacement will not move far, providing displacement rims are formed. The outer contour, defining the extents of displacement rims however will be affected by very small numbers. Consider the generation of a displacement rim, which curves towards the original surface. Tiny amounts of uplift on the order of $1e^{-6}$ m may extend the contour of zero vertical displacement far beyond what can be seen by eye. Such tiny deformations are a result of numerical problems arising from the digital nature of simulation, and are irrelevant in physical tracks where the deformation attenuates more rapidly and becomes immeasurable against the undulating sediment surface. As such, measurements of the maximum zone of deformation in computer simulations are avoided where possible in this work.

## *3.2 Observations of fossil tracks*

This section details a number of tracks and track sites that have been studied throughout the course of this project. Only by studying fossil tracks can comparisons be drawn with computer simulated tracks, and for this reason details and descriptions of the fossil tracks studied are presented here. The primary locations of fossil tracks studied in this project were: Amherst College Museum of Natural History, Massachusetts, U.S.A, The Zerbst Ranch, Wyoming, U.S.A, and The Mammoth Site of Hot Springs, SD, U.S.A.. Of these tracks, those held in the collections of the Amherst College Museum of Natural history are perhaps the most relevant to this work, offering as they do a look at surface and subsurface layers of tracks made in a fine-grained substrate. Other track sites visited included the Zerbst Ranch in Wyoming, where a high diversity of ichnotaxa could be observed on a single bedding plane, and the Mammoth Site of Hot Springs, South Dakota, where the unique excavation techniques presented the opportunity to view large vertebrate tracks in cross section. These tracksites were selected primarily for the deformation features associated with the tracks. In the case of the Amherst tracks and Mammoth site tracks, subsurface deformation was visible, whilst the Zerbst Ranch site presented tracks associated with cracking and other surface deformation.

### 3.2.1 Amherst College Museum of Natural History

The Amherst College Museum of Natural History (ACMNH) at Amherst College, MA, U.S.A, holds the Hitchcock collection of trackways collected primarily from the Lower Jurassic Connecticut Valley, Massachusetts, USA.

This collection of tracks is amongst the largest in the world, and contains a large amount of track 'books' – blocks of rock containing tracks in which the individual bedding planes have separated. These beds have then been re-attached with metal hinges, literally creating 'books' with pages of stone, each displaying the track volume at a different depth.

Following are the descriptions and measurements taken from selected fossil track specimens held in the collections of the ACMNH, in order to provide examples of track features associated with 3D deformation. Many of the tracks shown here were originally figured and described by Hitchcock (Bates *et al.*, 2008a; Hitchcock, 1858). Throughout the section, multi-part blocks in which the laminae have been split apart will be referred to as 'track-books', each lamina will be referred to as a 'page', and surfaces will be named with the following notation: a number indicating the depth of the leaf (1 being the uppermost sedimentary layer present), and T or B denoting upper surface (**T**op), where tracks are concave, or lower surface (**B**ottom) where tracks are convex. Images and measurements are provided for each track and in each case lower surfaces (with convex tracks) are mirrored to align with surface tracks. Measurements in which the digit is broken or obscured are marked with a '+' after the value. Labels of digits (e.g. II, III, or IV) do not necessarily represent the corresponding digits of the track maker, but are assigned here for ease of description.

#### *3.2.1.1 Track 27/18.*

One of the best examples of track books found in the Hitchcock collection (figured by Manning *et al.*, 2008; Margetts *et al.*, 2006).

Details:

- Museum location: Cabinet 28, Draw 165.
- Track-book consisting of three ‘pages.’
- Single track visible on all surfaces except the underside of the deepest leaf (3B).
- Additional numbers present: 264 (engraved).
- Named: *Ornithopus gracilis*.
- Original Location: not recorded.
- Lithology: Olive grey, silty mudstone with planar bedding.

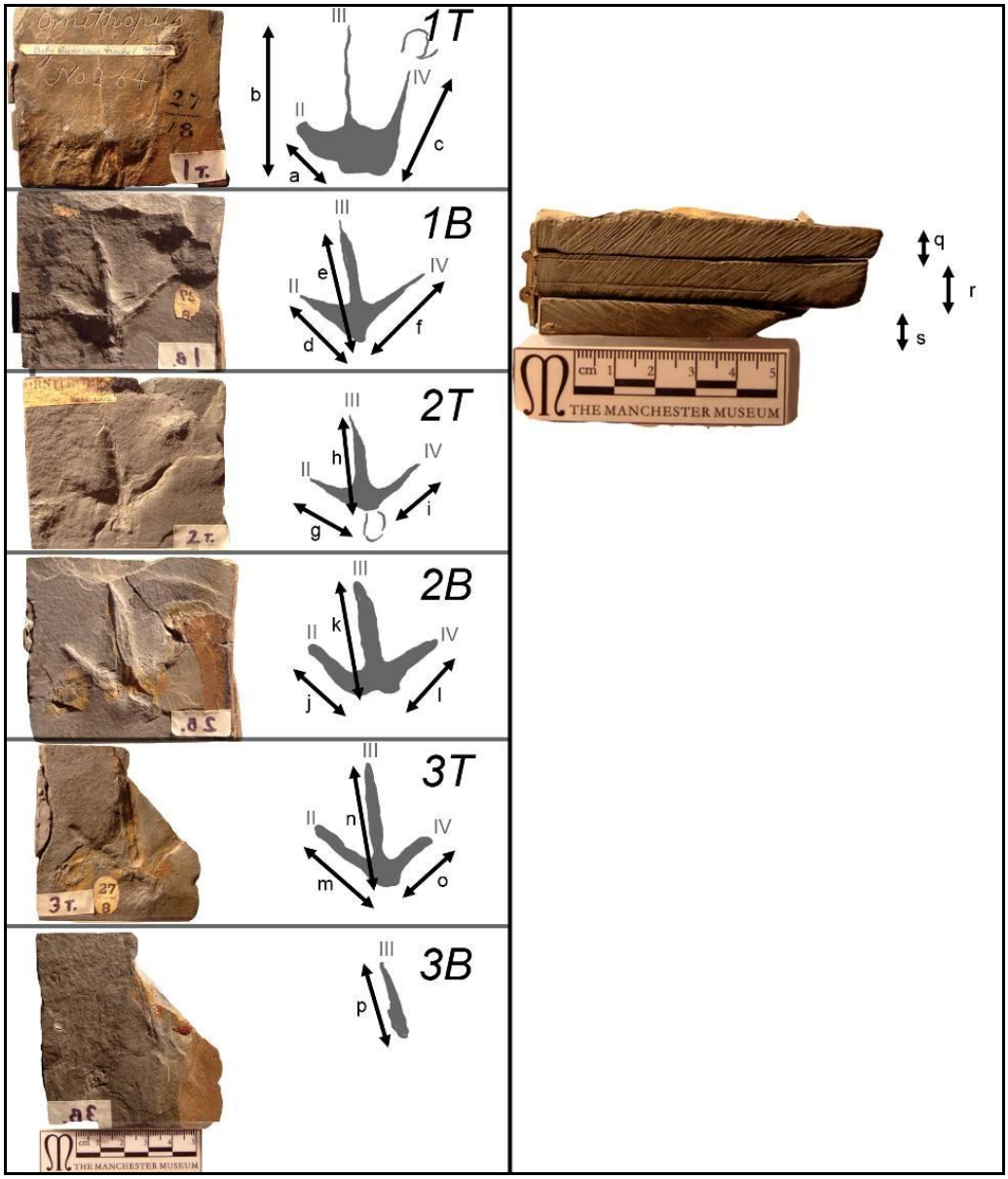


**Figure 3.5 - Track 27/18 on surfaces 1T through 3B:**

**a) Digit II – 34mm, b) Digit III – 68mm, c) Digit IV – 70mm**

**d) Digit II – 34mm, e) Digit III – 48mm, f) Digit IV – 29mm**

**g) Digit II – 32mm, h) Digit III – 48mm, i) Digit IV – 35mm**

**j) Digit II – 40mm, k) Digit III – 59mm, l) Digit IV – 42mm**

**m) Digit II – 46mm, n) Digit III – 44+mm, o) Digit IV – 24+mm**

**p) Digit III – 40+mm, q) Layer 1 thickness – 10mm, r) Layer 2 thickness – 10mm, s) Layer 3 thickness – 8mm. Scale bar= 50mm**

### *3.2.1.2 Track 27/12*

Details:

- Museum Location: Cabinet 28, Draw 166.
- Track-book consisting of three ‘pages.’
- Single track, visible on all surfaces except 1T.
- Additional numbers present: ‘2’ engraved.
- Named: *Ancyropus heteroclitus* / *Sauroidichnites*
- Original Location: Weathersfield.
- Lithology: Coarse grained micaceous siltstone.

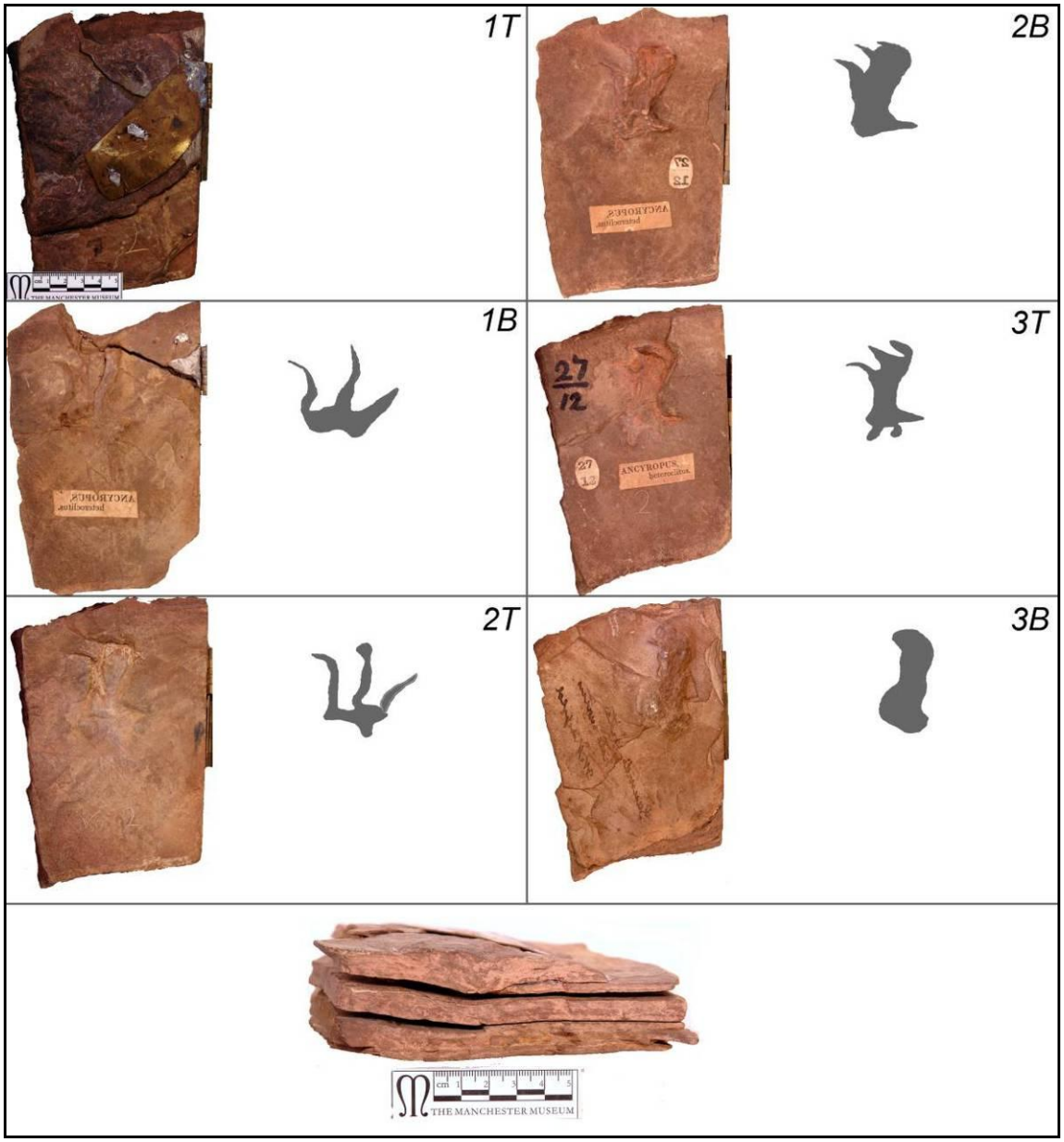


**Figure 3.6 - Track 27/12, Layers 1T through 3B. Specific measurements not taken due to complexity of track morphology. Layer 1 thickness – 12mm, Layer 2 thickness – 9mm, Layer 3 thickness – 10mm. Scale bar = 50mm.**

### *3.2.1.3 Track 27/13*

Details:

- Museum Location: Cabinet 28, Draw 166.
- Track-book consisting of two ‘pages.’
- Three tracks forming trackway, visible on all surfaces except 2B.
- Additional numbers present: none.
- Named: *Xiphopeza triplex*
- Original Location: Turner’s Falls (?).
- Lithology: Olive green micaceous siltstone.

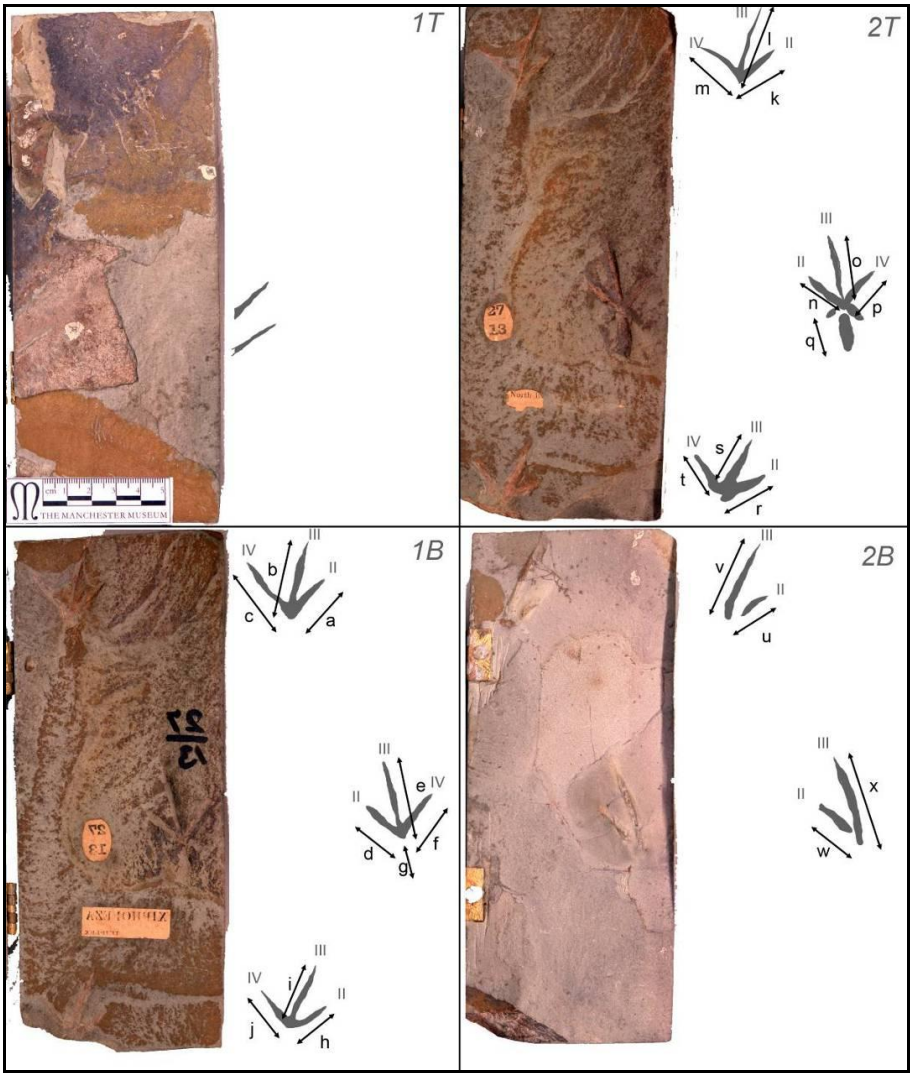


**Figure 3.7 - Track 27/13, layers 1T through 2B:**

**a) Digit II – 19mm, b) Digit III – 31mm, c) Digit IV – 19mm**

**d) Digit II – 16mm, e) Digit III – 30mm, f) Digit IV – 21mm, g) Deformation – 14mm**

**h) Digit II – 19mm, i) Digit III – 31mm, j) Digit IV – 22mm**

**k) Digit II – 21mm, l) Digit III – 32mm, m) Digit IV – 21mm**

**n) Digit II – 20mm, o) Digit III – 31mm, p) Digit IV – 20mm, q) – Deformation – 14mm**

**r) Digit III – 19mm, s) Digit III – 31mm, t) Digit IV – 24mm,**

**u) Digit II – 27mm, v) Digit III – 38mm,**

**w) Digit II – 27mm, x) Digit III – 37mm.**

**Layer 1 thickness – 14mm, r) Layer 2 thickness –8mm, Scale bar = 50mm.**

### *3.2.1.4 Track 27/19*

Details:

- Museum Location:  Cabinet 28, draw 166.
- Track-book consisting of two ‘pages.’.
- Single track visible on all surfaces (plus partial track visible on all surfaces)
- Additional numbers present: ‘14’ (engraved)
- Named: *Triænapus leptodactylus.*
- Original Location: unknown
- Lithology: Ferrigenous micaceous mudstone.

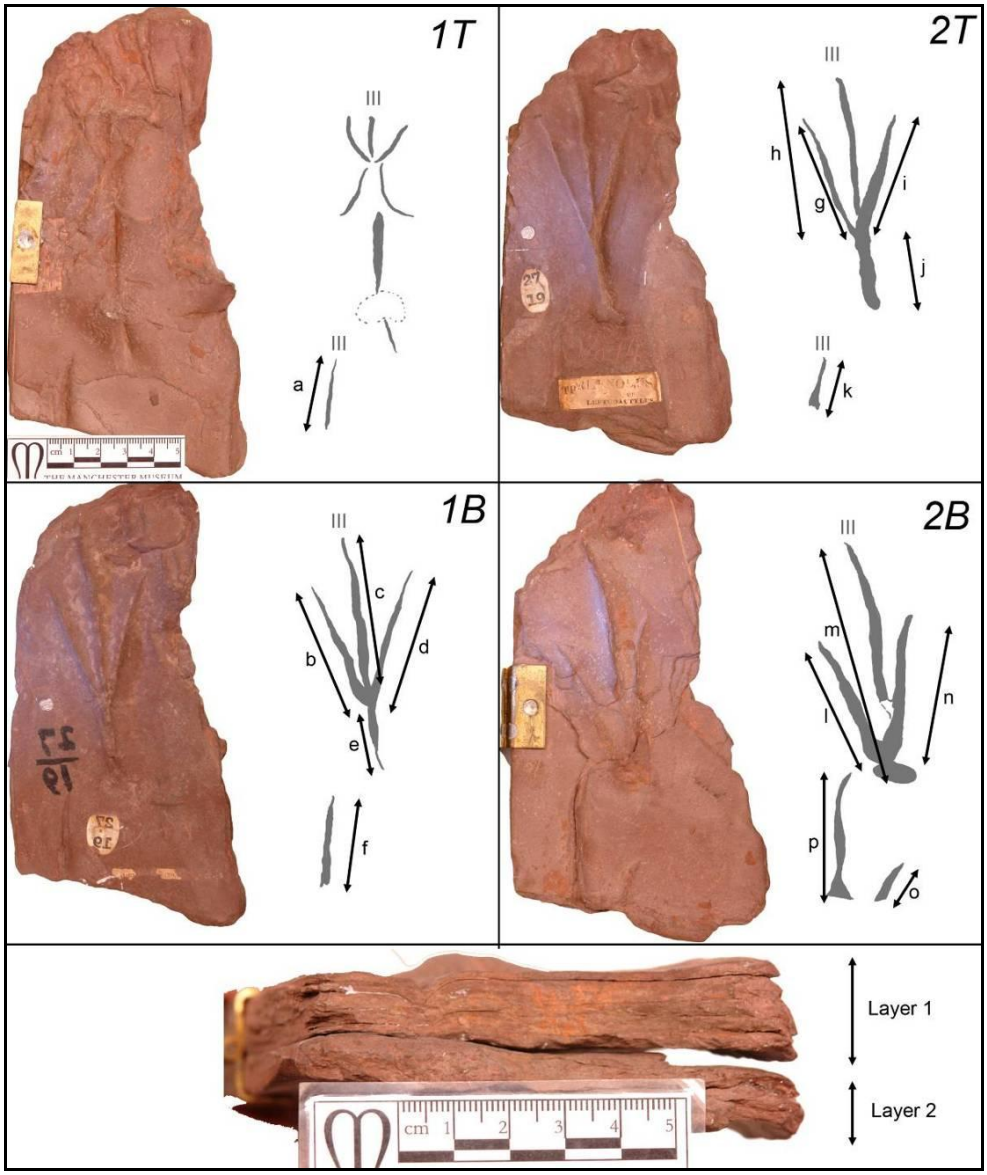


**Figure 3.8 - Track 27/19, layers 1T through 2B:**

**a) Digit III – 27+mm**

**b) Digit II(?) – 55, c) Digit III – 75mm, d) Digit IV – 60mm, e) Reverse structure – 40mm.**

**f) Digit III – 36+mm.**

**g) Digit II(?) – 59, h) Digit III – 71+mm, i) Digit IV – 54mm, j) Reverse structure – 35mm.**

**k) Digit III – 40+mm.**

**l) Digit II(?) – 63mm, m) Digit III – 100mm, n) Digit IV – 65mm,**

**o) Digit II(?) – 20+mm. p) Digit III – 45+mm.**

**Layer 1 thickness – 15mm, Layer 2 thickness – 12mm. Scale bar = 50mm.**

### *3.2.1.5 Track 27/7*

Details:

- Museum Location: Cabinet 28, Draw 180.
- Track-book consisting of four ‘pages.’
- Single sinuous track visible on all layers except 1T. Claw/digit impressions appear on layer 2B (also invertebrate trace; *Conopsoides larvalis*), but become distinct by layer 3B
- Additional numbers present: ‘6’ engraved.
- Named: *Ancyropus heteroclitus*.
- Original Location: unknown.
- Lithology: Coarse grained micaceous siltstone.

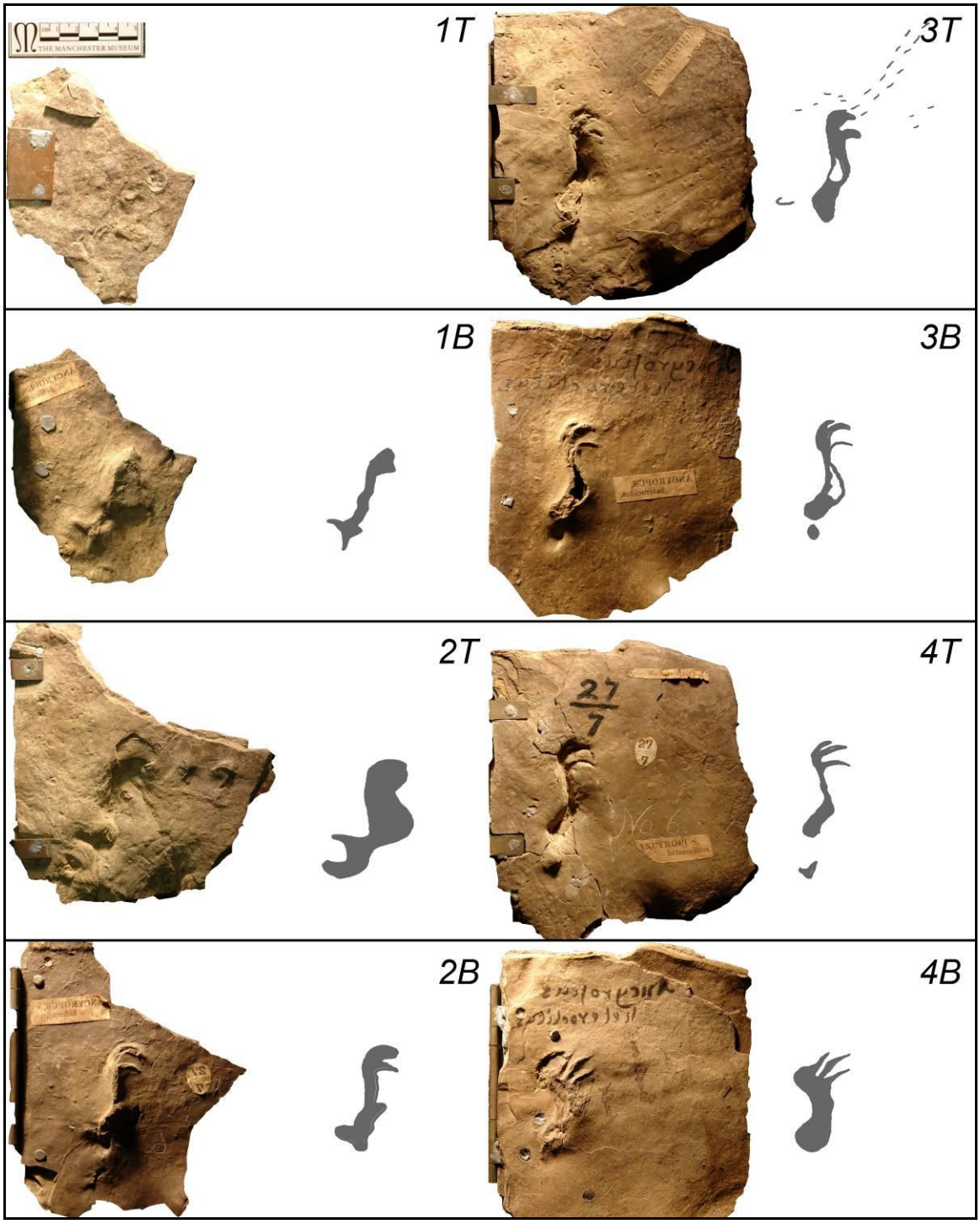


**Figure 3.9 - Track 27/7, Layers 1T through 4B. Specific measurements not taken due to complexity of track morphology. Layer 1 thickness – 6mm, Layer 2 thickness – 8mm, Layer 3 thickness – 5mm, Layer 4 thickness – 8mm. Scale bar = 50mm. Note invertebrate trace on surface 3T.**

### *3.2.1.6 Track 41/21*

Details:

- Museum Location: Cabinet 28, Draw 180.
- Track-book consisting of one ‘page.’
- One tridactyl track visible on both upper and lower surfaces. Very narrow digits on upper surface and much thicker on lower surface. Rock is broken across the tips of two digits displaying sediment deformation throughout.
- Additional numbers present: none
- Named: none
- Original Location: unknown
- Lithology: Ferrigenous micaceous mudstone.

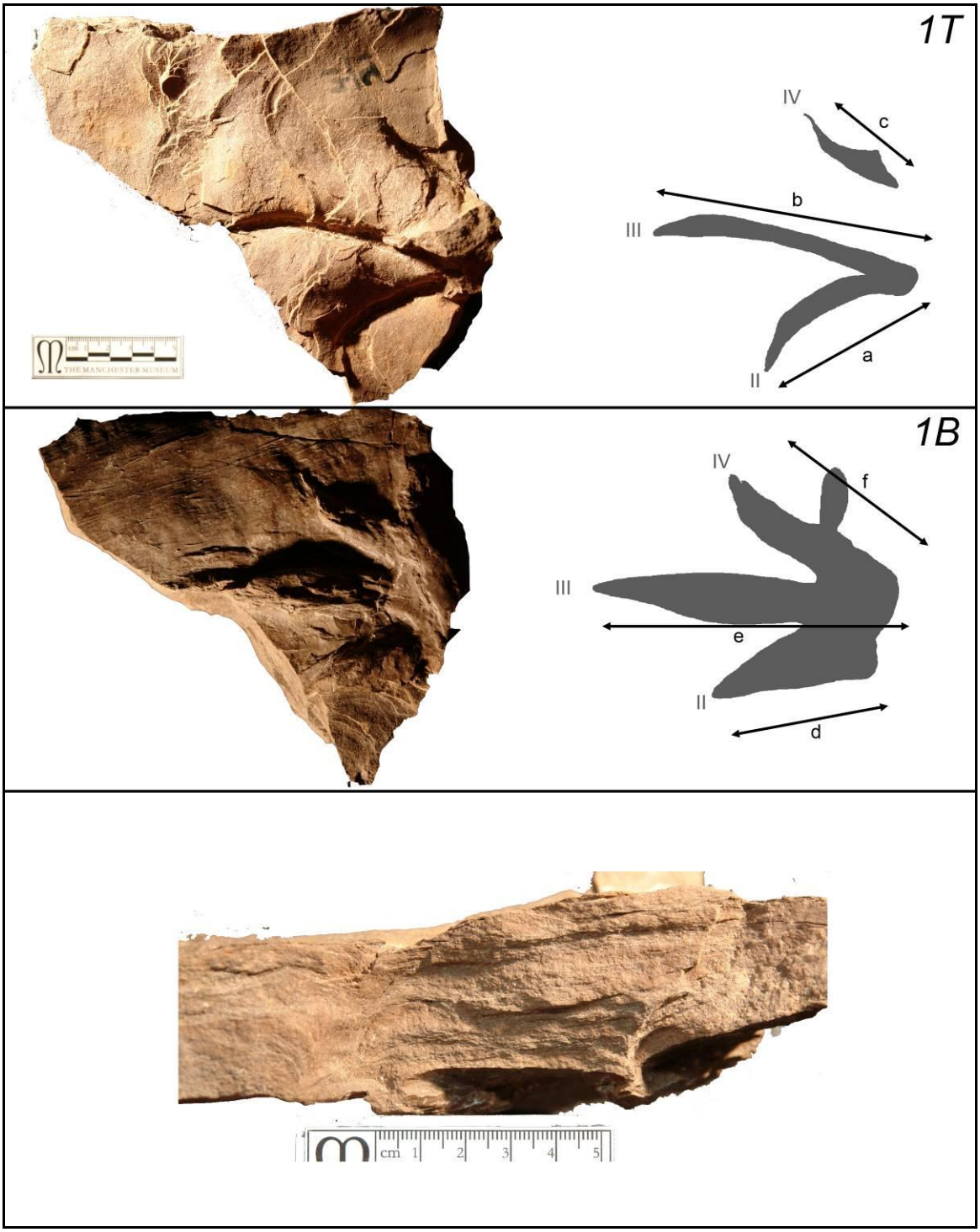


**Figure 3.10 - Track 41/21 on layers 1T and 1B:**

**a) Digit II – 67mm, b) Digit III – 106+mm, c) Digit IV – 47mm, Layer thickness – 37mm.**

**Scale bar = 50mm.**

### *3.2.1.7 Lithology.*

A sample of rock representative of a common lithology in the Amherst tracks (the Ferrigenous micaceous mudstone) was thin-sectioned. This thin-section displayed the very fine grain size (~10-20μm), and also an orientation of grains parallel to the bedding. Plane polarised light (PPL) and cross polarised light (XPL) showed a composition of ~50% quartz, ~30% white mica, and ~20% iron oxide cement. There is a fining upwards texture, with lower, coarser layers containing more iron oxide. Figure 3.11 shows the level of orientation of grains (oriented in the same direction as the large infilling of quartz in the centre of the image). Figure 3.12 displays the individual grains and cement more clearly (taken from centre of Figure 3.11).

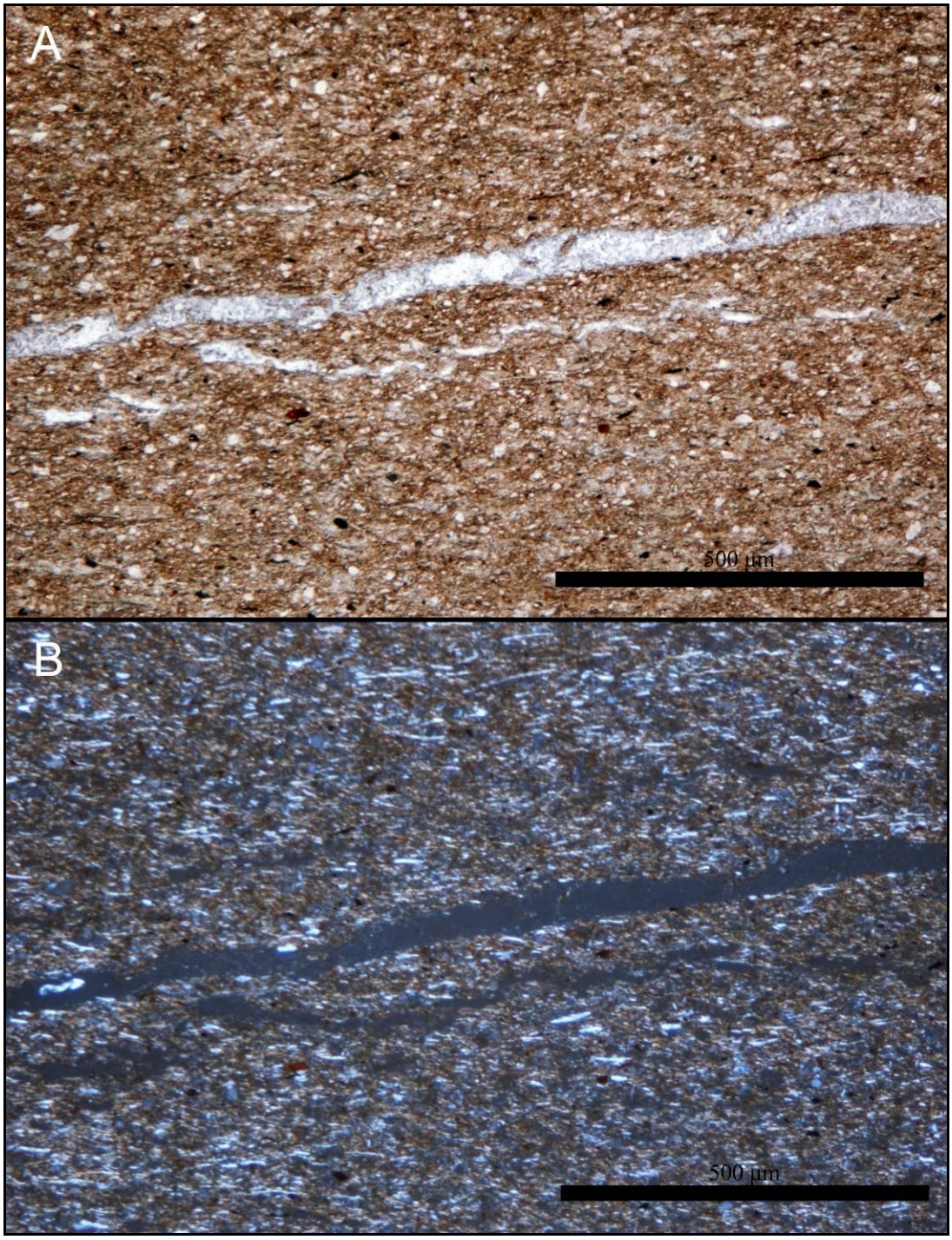


**Figure 3.11 - Thin section of rock representative of ferrigenous micaceous mudstone common among Amherst Tracks under A) PPL and B) XPL. Scale bar = 500 µm. Composition of quartz (white in PPL, 1st order dark grey birefringence in XPL), iron oxide (reddish opaque mineral) and white mica (white in PPL, 3rd order pale blue birefringence in XPL)**

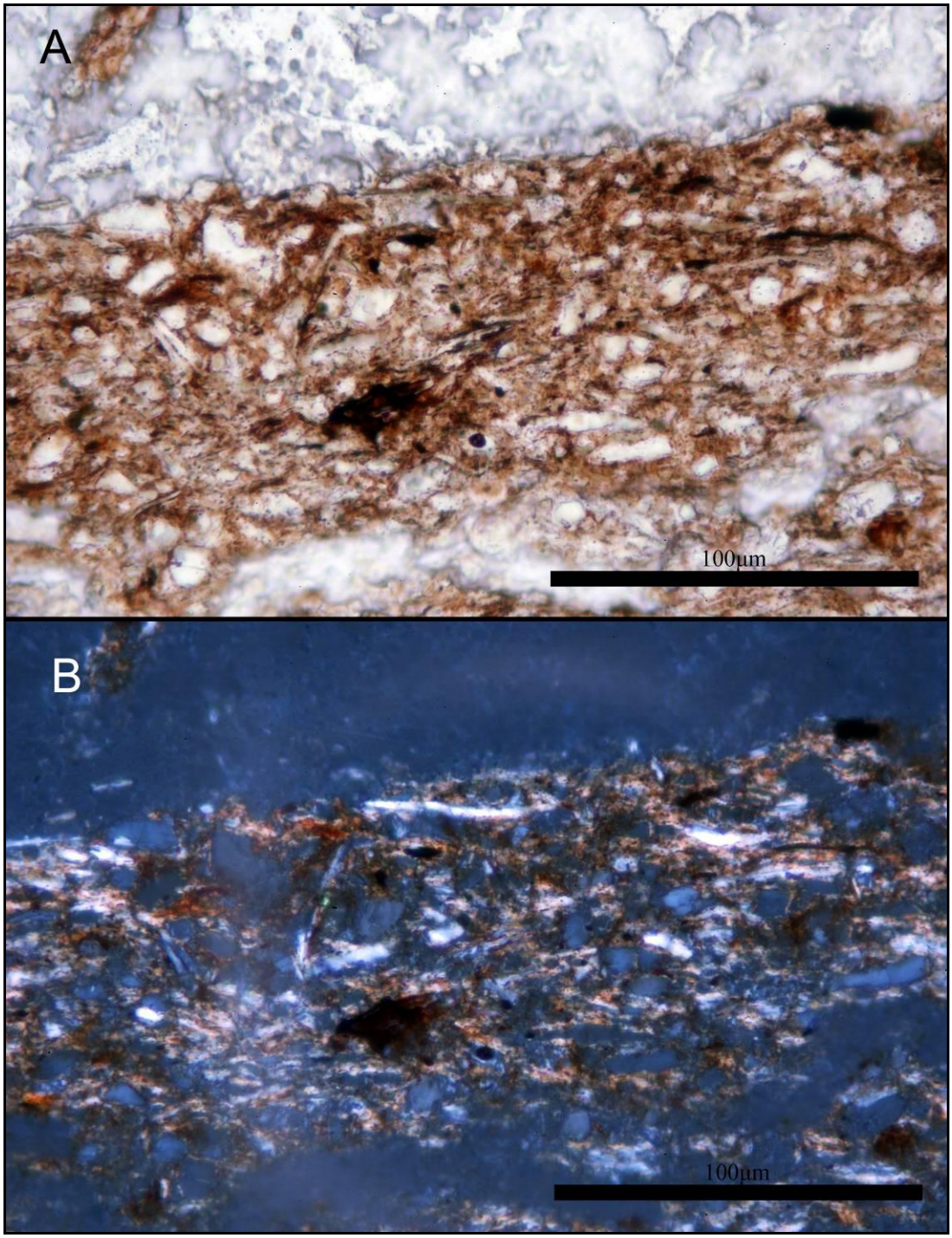


**Figure 3.12 - Close up image of centre of Figure 3.11 in A) PPL and B) XPL. Scale bar = 100µm.**

### *3.2.1.8 Track features of the Amherst collection*

The Amherst tracks present a rare opportunity to examine surface and subsurface deformation within a single track volume. The following features are of note:

*Digit loss/gain*

In most of the tracks and undertracks present in the above track specimens, there are varying degrees of digit loss throughout the track book. This is observed in track 27/18 where on the lowermost surface, only digit III remains visible. In this case, as one may expect, only the greatest weight bearing digit has produced enough force at the surface to transmit to this depth. A similar feature can be seen in track book 27/13 where digit IV has been consistently lost in two tracks of a trackway (with the third track being lost altogether) by the lowermost surface (22 mm depth). This kind of preservational artefact has large implications for ichnotaxonomy and in the assignation of potential producers. Some tracks attributed to dromaeosaurs, for instance, have been done so on the basis of only two digit impressions being present (Xing *et al.*, 2009a).

Both track books 27/13 and 27/19 display reverse digits (halux) on at least one layer, but not on others. Where present (Layer 2T in track book 27/13 and layers 1T-2T in 27/19), these structures appear to be associated with other reverse features. The second track on layer 2T of 27/13 has the appearance of two tidactyl tracks back to back, but this is not supported by surfaces above or below the track. In track book 27/19, the successive track surfaces show what appears to be a reversal in track direction. The tracks present on surfaces 1B and 2T are associated with a reverse pointing structure posterior to the point where the three forward digits converge. However, in layer 2B, the track has increased

in length, and the three digits seem to join at a more posterior position in the track block.

Track book 27/7 can be seen on eight surfaces, but digits only become clear by surface 3B. The shape of these digits changes from recurved to straight as depth of track increases.

*Gross morphological change*

Track books 27/7 and 27/12 both show considerable gross morphological change throughout the total track depth of 20-30 mm. In the case of the former, layers 1T to 3T may be overprints, as little definition is present in the traces. Below 3B, digits become apparent and the trace becomes more defined. Track book 27/12 shows a very different morphology between the first appearance on layer 1B, and the lowermost surface. Towards the upper parts of the track volume, the trace appears tridactyl, but by layer 2B the digits have shifted and the trace appears tetradactyl.

*Track position*

Tracks 27/18 and 27/19 both display a shift in position of the track. In the case of 27/18, the posterior edge of the trace is shifted anteriorly through the track volume (Manning, 2008) (Figure 3.13). In track book 27/19 the general position of the overall track remains the same, but the position of the 'heel' (the point where the three digits converge) shifts posteriorly to a considerable degree. Manning (2008) and Margetts *et al.* (2005; 2006) attribute this shift in track position within the 3D volume to force vectors associated with the foot kinematics and kinetics.

*Interdigital angle*

The gross morphological change seen in track books 27/12 and 27/7 are perhaps unsurprisingly associated with alteration in interdigital angle (IDA). However the IDA of track 27/18 also changes, albeit in a more subtle manner, as reported by Margetts *et al.* (2005; 2006). The IDA also alters in track book 41/21, where the digits can be seen curving away from the middle digit in the upper surface (1T), but appearing straight on the lower surface (1B).

*Track size*

The changes in morphology outlined above for all track books do of course result in differences in measured size. The magnitude of this difference in size between layers varies according to how the track is measured. For instance, in track 27/19 measuring the overall deformation (MZD) sees only a slight change in track length, but measuring from the tip of digit III to the 'heel' results in a considerable change in track length.

Of particular interest in relation to track size with depth is track book 27/18. Manning (2008) and Margetts *et al.* (2005; 2006) noted that the tracks first increase in size, before decreasing in size as depth increases. This is consistent with the bousinesq pressure bulb described in section 2.5.3. The increase in size on the uppermost surface is attributed to being an overprint (Margetts *et al.*, 2006).

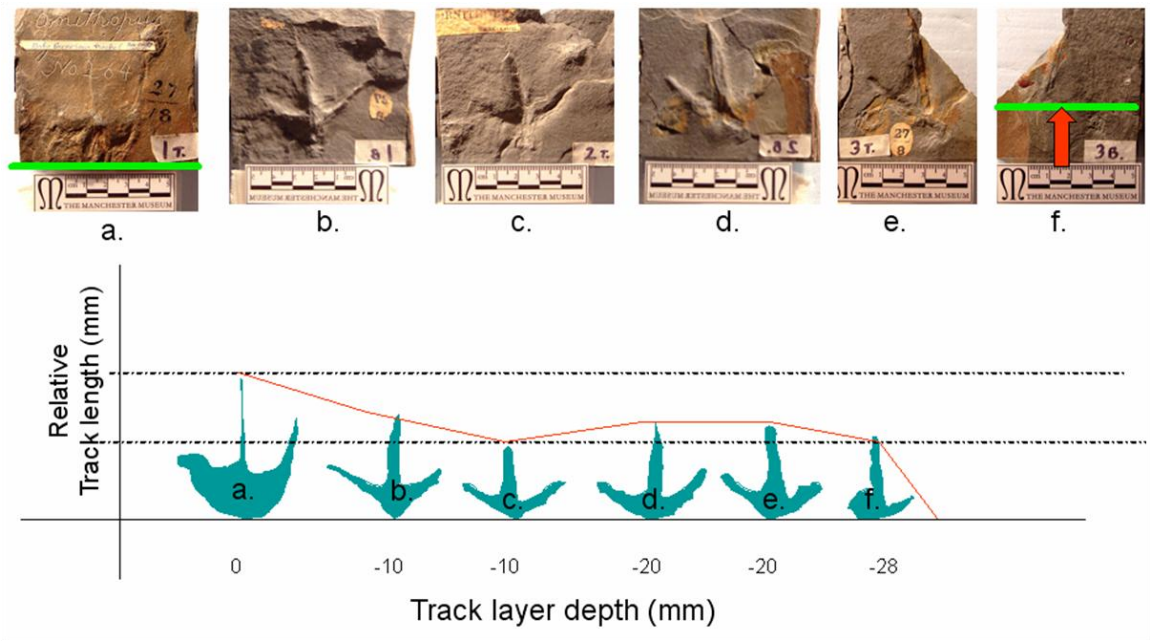


**Figure 3.13 - Track book 27/18 showing change in size and position of the track on each surface. Layers a-f correspond to 1T - 3B respectively. Green line in a and f marks the most posterior point of the track, arrow shows anterior shift of track position. Reproduced from Manning (2008) and Margetts *et al.* (2005; 2006).**

### 3.2.2 The Zerbst Ranch, Wyoming, U.S.A.

The Zerbst Ranch, in Niobrara County, Wyoming, U.S. is privately owned land, on which are numerous tracks in which deformation features are exposed. The track block was found by Leonard Zerbst and contains approximately 20+ tracks from 5+ trackways, dated to the Cretaceous. Only four tracks from a single trackway were originally exposed prior to excavations in 1996. A cast of the block, made in 2002 is on display at the Blacks Hills Institute of Geological Research, Hill City, S.D. The site was described by Lockley *et al.* (2004), who noted the high diversity in ichnotaxa (including tracks attributable to medium and large theropods, large ornithopods, and birds). Many of these tracks were described as having particularly noteworthy features, including skin impressions, well preserved halux impressions, and tail drag marks (Lockley *et al.*, 2004). The tail drag mark was subsequently re-interpreted as a crocodilian trace by Falkingham *et al.* (in press-b; Chapter 5) , further increasing the diversity of the site.

The fossil tracks were made available for viewing by the land owners. Photographs were taken with an 8 mega pixel digital SLR camera under natural light conditions, at mid afternoon in mid-summer. The tracks at the Zerbst Ranch were located on a single slab 12m x 3m in area (Figure 3.14). The selected tracks in Figure 3.14 are those that show features relevant to understanding track formation at and below the surface, or are relevant to understanding sediment conditions at the time the surface was exposed, and are detailed below.

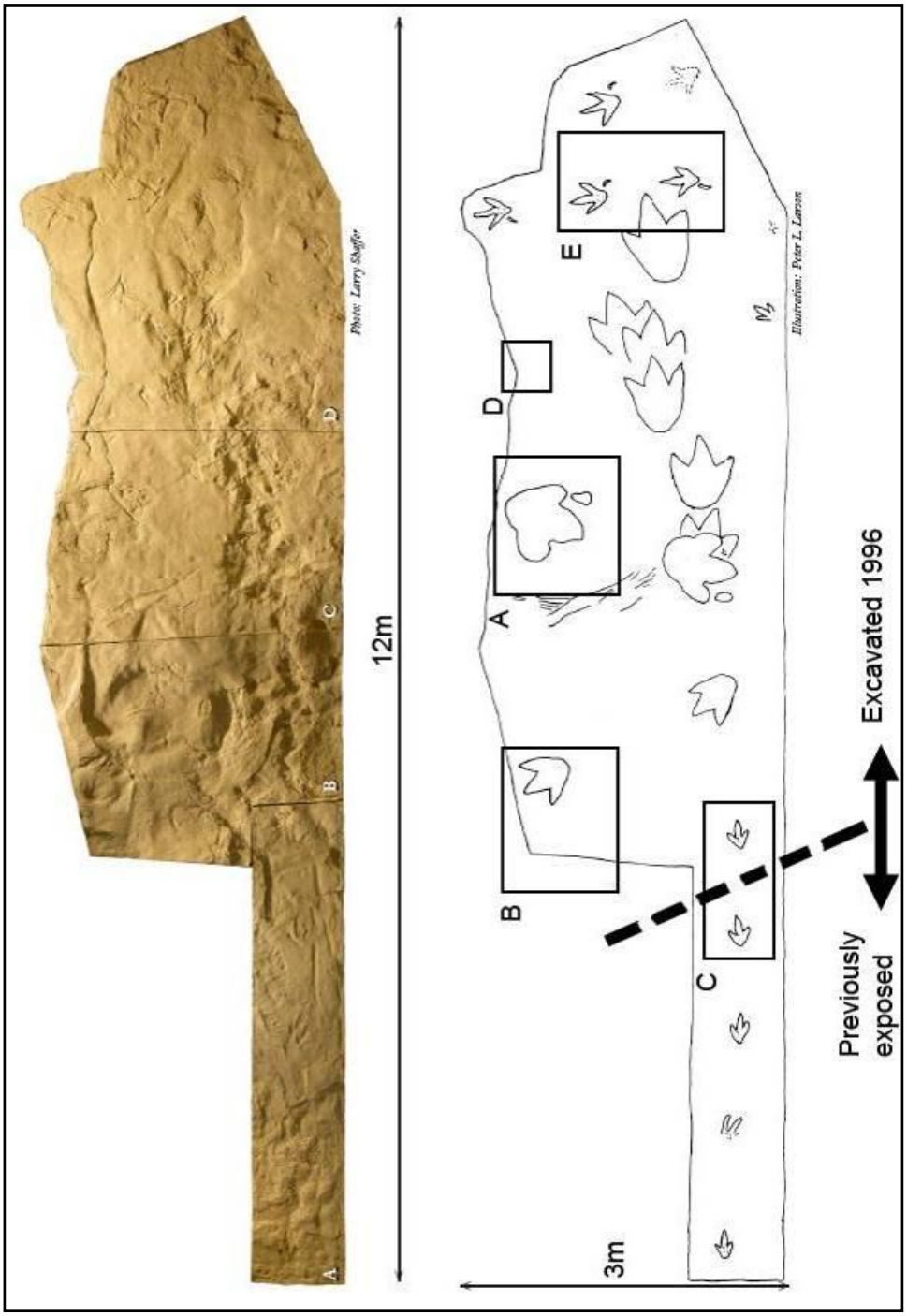


**Figure 3.14 - Outline plan of Zerbst track block, adapted from image courtesy of the Black Hills Institute. Dashed line denotes areas naturally exposed and excavated 1996. Areas A-E are locations of tracks chosen for study. Photo by Larry Schaffer, drawing by Peter L. Larson.**

The bold arrows and dashed line in Figure 3.14 indicate the area which was naturally exposed (to the right) and which area was excavated in 1996 (to the left of the dashed line). A preservational difference can be seen between the upper and lower parts of the track site (top and bottom as in Figure 3.14), this difference can be seen in Figure 3.15.

**Figure 3.15 - Image showing difference in surface and track preservation (view is from left to right relative to Figure 3.14, and view is approx 2m across).**

### *3.2.2.1 General Features of the Zerbst Track Block.*

The rock at the Zerbst Ranch has been dated to the Lance Formation, Upper Cretaceous (Larson, 2003; Lockley *et al.*, 2004). The lithology of the track block at the Zerbst ranch is of a yellow fine grained sand to silt. .

Prevalent over the block surface is an organic film relief (Figure 3.16). This could be misinterpreted as the impression of skin, but the texture appears outside tracks as well as inside tracks. Instead, this texture is possibly the result of an algal mat on the surface of the sediment at or around the time of track formation (Reineck and Singh, 1980). Indeed, the texture is very similar to the 'elephant skin' wrinkle texture described by Porada and Bouougri (2007). Alternatively, this may be the result of some unknown weathering process.


**Figure 3.16 – Texture on track bearing surface indicative of an algal mat. Scale bar = 50mm.**

### *3.2.2.2 Zerbst Track A – Large tridactyl track with sediment deformation structures.*

This track (track A in Figure 3.14) is one of the most interesting tracks at the site. The track appears to have been made by a large tridactyl dinosaur. Lockley *et al.* (2004) proposed a hadrosaurian origin and named the track *Hadrosauropodus sp.*

The track forms part of a trackway, as seen in Figure 3.14. However, it is not entirely clear as to whether the track in question is left or right due to differing orientation between the tracks. In addition to this, the second track is poorly preserved in comparison to the first track. The track has a complex digit impression on the left, as seen below in Figure 3.17. This includes a mark that seems to cut failure structures, potentially a terminal ungal phalanx (TUP) mark. There is also a sinuous swirl-like structure in this digit, and this can be seen in greater magnification in Figure 3.18C.

Of high importance is the surface texture within the track. Unlike the algal mat described above, this structure is regular, and in relief rather than

incuse. This is highlighted in Figure 3.18D. Lockley *et al.* (2004) report this texture as skin impression.

**Figure 3.17 - Track A from the Zerbst track block showing deformation features. Scale bar = 50 mm**

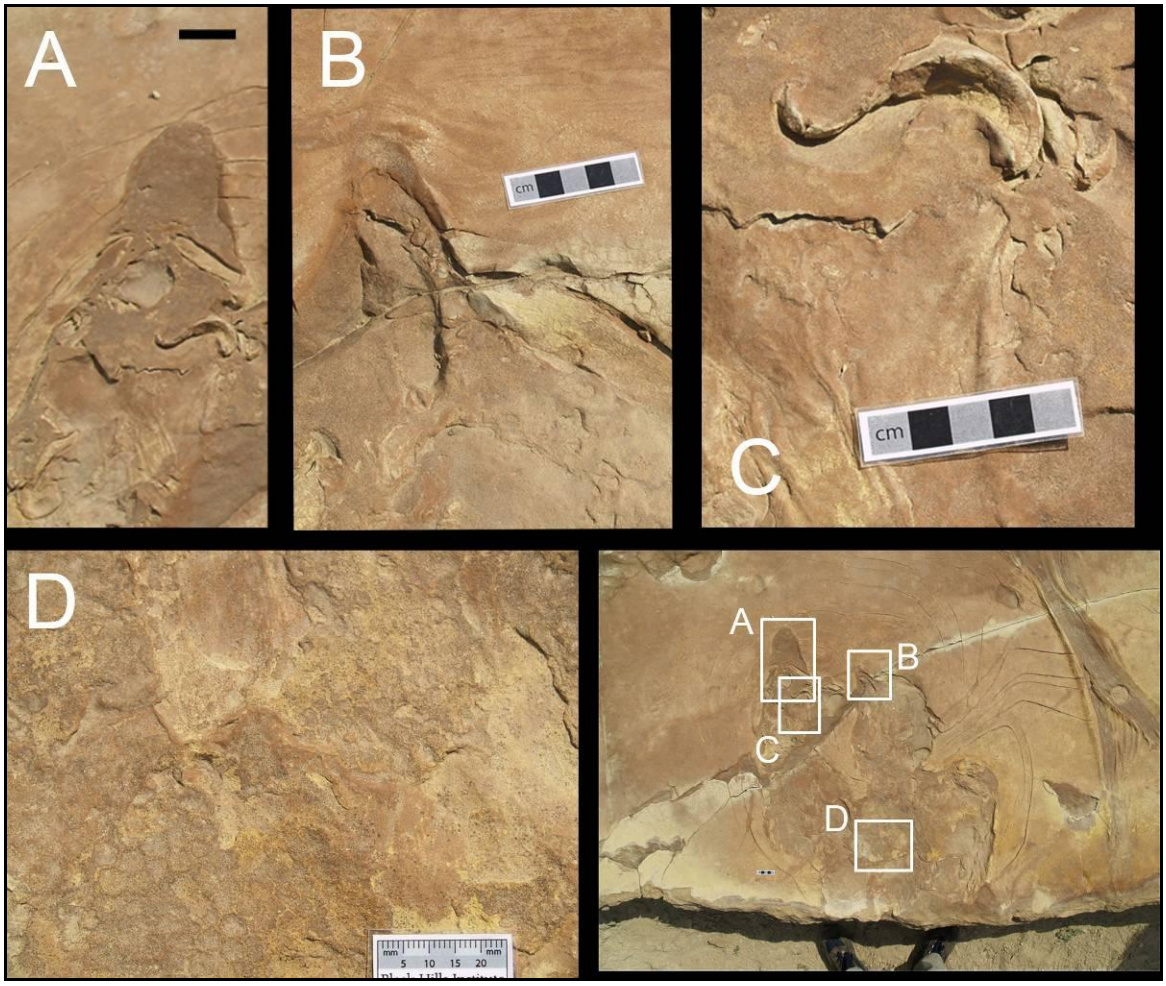


**Figure 3.18 - Image showing close up photos of features within track A (positions outlined in lower right of image). A) Large TUP mark(?) cutting failure features on left digit, B) Smaller TUP-like mark on central digit. C) Sinuous structure found in left digit. D) Regular hexagonal texture (Skin impressions?) within track. Scales in A, B,C = 50 mm, scale in D = 25 mm.**

Significantly, the track displays radial and concentric cracking (Figure 3.17). These cracks loosely follow the outline of the track, but are cut by the digit tips (Figure 3.18 A+B). The fracture lines cut into the crocodilian trace beside the track, indicating that the tridactyl track was made after the crocodilian trace.

#### *3.2.2.3 Zerbst Track B – Tridactyl track with features in relief.*

Track B was unique at the Zerbst site in that parts of the track were in relief, despite all other tracks being incuse, however Track B was poorly defined. The track with relief features was beside another track of similar size which has digits II and IV more clearly defined. The track lengths were approximately 550 mm, and the track widths were approx. 450 mm wide. The tracks were almost parallel. Located centrally between the tracks, but some distance anteriorly was an elongate impression some 200 mm in length.

#### *3.2.2.4 Zerbst Track C – Medium Tridactyl Trackway Displaying Effects of Weathering and Inclusions of Sediment Layers Above.*

Track C was a trackway of four medium sized (~280 mm), well defined tridactyl tracks with no indication of a reverse digit (halux). Pace length was approx. 890 mm, and the trackway width was almost zero (tracks were aligned). There were no visible skin impressions, though outlines of phalangeal pads were visible in both previously exposed and excavated tracks.

Here, the trackway consisted of two areas of varying weathering; one half of the trackway (to the right – see Figure 3.14 and Figure 3.19) was exposed naturally prior to 1996, whilst the rest of the trackway was uncovered in excavations after 1996. This presents the opportunity to observe the effects of weathering on track morphology, whilst trackmaker (and hence foot morphology) remains constant. Length and width of tracks did not alter between pre exposed and excavated tracks, though the depth of the tracks did – those naturally exposed prior to excavation had a more pronounced relief than those

excavated in 1996. Unfortunately, during work at the site, necessary equipment for measuring the relief was unavailable (e.g. a hand held laser scanner). The previously exposed tracks were more obviously weathered, raised areas being more cracked and discoloured than those of the excavated tracks. Additionally, the algal mat texture was found around the excavated track, but not those that had been naturally exposed prior to excavation.

The track exposed during excavation had terminal ungal phalanges (TUP) (claws) preserved in relief (approximately 3-4 mm above surrounding surface), whilst the rest of the track was preserved as an impression. This appeared to be the result of the above layer remaining in the claw marks, rather than a preservational feature resulting from the track's formation. This feature was not observed on the weathered tracks.

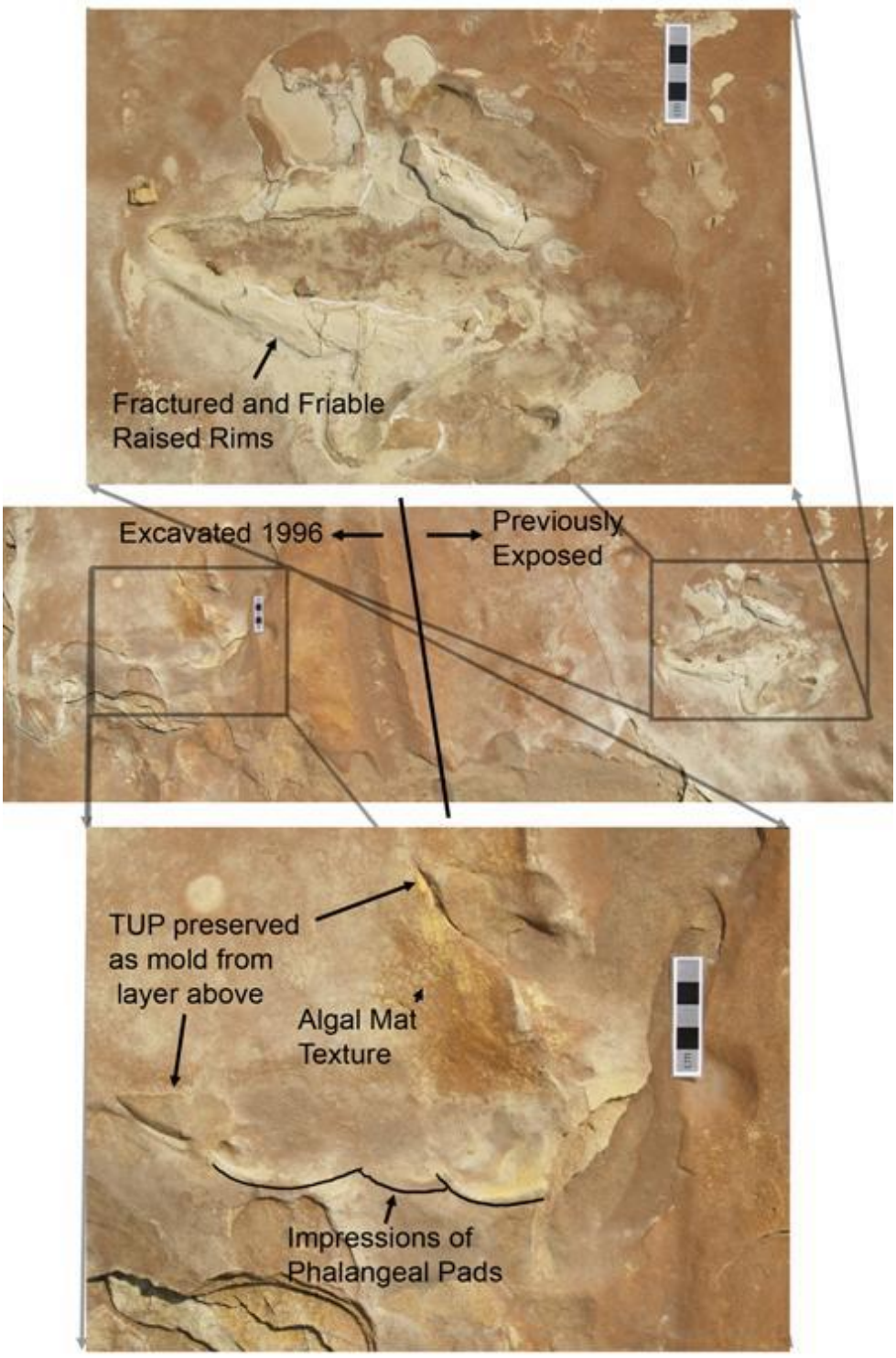


**Figure 3.19 - Two consecutive tracks of type C. (Top) Track from area exposed prior to 1996, (bottom) track excavated 1996. Note inclusions of layer above in the digit tips of the second track. See Figure 3.16 for close up of algal mat texture. Scale bars = 50 mm.**

### *3.2.2.5 Zerbst Track D – Small anisodacytl tracks in very low relief.*

These tracks were very small (~ 70 mm in length) compared to others on the block, and had almost no relief, appearing as faint marks on the surface. Only individual tracks were observed rather than full trackways. The tracks were anisodactyl (see section 2.3.1) in form with a long reverse digit (halux) impression making up 30mm of the track length, and wide toes producing a high interdigital angle. An example of the clearest of these tracks can be seen in Figure 3.20. Despite the shallow relief, rounded structures similar to phalangeal pads can be discerned, as well as small pointed claw marks.

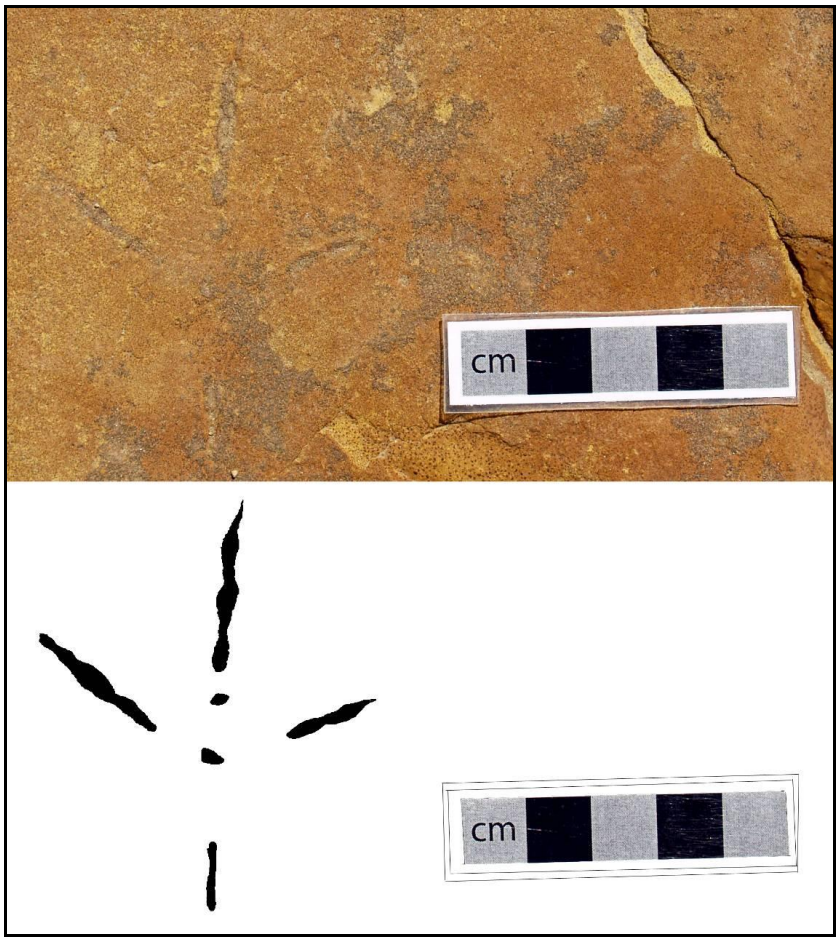


**Figure 3.20 - Small track displaying high interdigital angle and reverse halux structure (pointing backwards). Scale bar = 50mm.**

### *3.2.2.6 Zerbst Track E – Trackway displaying clear reverse digit (halux) structures.*

The tracks outlined as E in Figure 3.14 were approximately 300-350 mm in length, tridactyl but with a clear halux impression. Four tracks constituted 2 trackways with a pace length of 170mm, and displayed a change from poorly defined to well defined, moving down the bedding plane. The tracks were all clearly on the same bedding plane, as can be seen in Figure 3.21. Displacement rim like features were observed around all tracks, but particularly the more defined tracks.

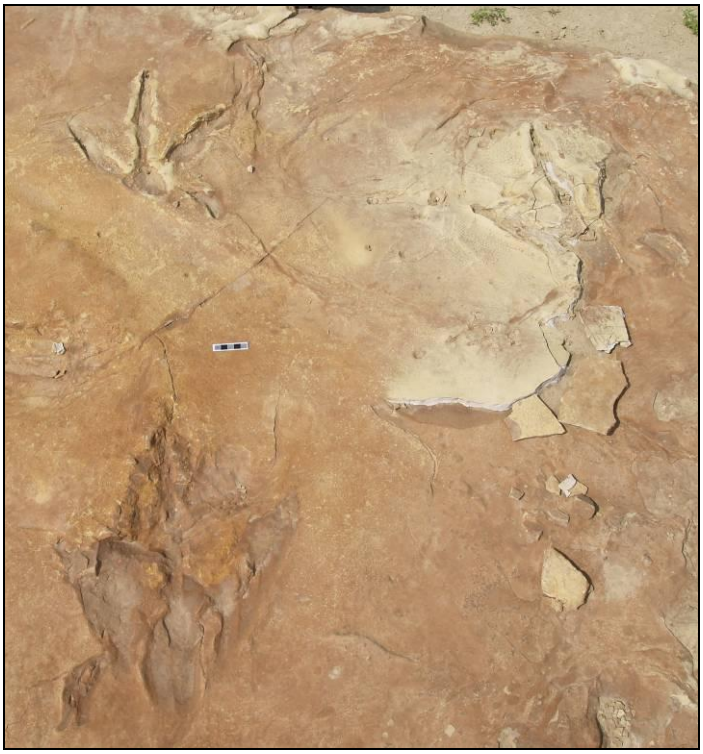

**Figure 3.21 - Tracks 'E' - two trackways, each of two tracks. Lower left of image: Right pes, poorly defined. Upper Left: Well defined left pes print. Scale bar = 5cm.**

### *3.2.2.7 Other tracks in the Zerbst Track Block.*

More large tracks were also present at the site. These were located around the area where preservational quality of tracks decreased, and as such were poorly defined. The impressions of these tracks can be described as a heavily

bioturbated area rather than discrete tracks. It should be noted that the cast at the BHI has these tracks described as being made by a tyrannosaurid because of sharp digits (Larson, 2003), but these were not observed in this instance, perhaps due to subsequent weathering.

#### *3.2.2.8 Important features of the Zerbst track site*

The Zerbst track site offers a number of well preserved, albeit mostly shallow tracks made in fine sand. The presence of a crocodilian trace (Falkingham *et al.*, in press-b; Chapter 5) implies that the area was beside a body of water, and the quality of preservation similarly implies a moist substrate. The concentric cracks around the *Hadropsauropodus* track (track A) are an interesting feature. That the cracks are concentric, and show no signs of buckling or being raised may indicate that they were formed either by the removal of the foot, and collapse towards the track, or that they formed when the substrate dried and shrank, and in doing so formed along the lines of weakness created by the stress distribution from the track.

All of the tracks at the site are very shallow, the deepest being < 1 cm. Such preservation is indicative of a soft, cohesive layer overlying a much firmer substrate. This is consistent with descriptions of the lithology prior to excavation which state that a thin layer of mudstone was located above the now exposd surface (Lockley *et al.*, 2004).

### 3.2.3 The Mammoth Site of Hot Springs, South Dakota, U.S.A.

The Mammoth Site of Hot Springs was first discovered in 1974, and excavations have continued since. The unique way in which the site is excavated, that is, in a methodical section by section approach, means that large areas of the stratigraphy are observable in cross section. This methodology is detailed in Agenbroad and Mead (1994). A number of tracks have been identified in cross section within the site, and interpreted as proboscidian in origin (Agenbroad and Mead, 1994). These tracks provided the opportunity to look at numerous large vertebrate tracks in cross section, often in more than one plane (Figure 3.22). Additionally, bird tracks were discovered at the site, and these too were documented (Falkingham *et al.*, 2010; Chapter 4).

**Figure 3.22 - Deformation structure (track?) visible in two cross sectional planes at the Mammoth Site. Tape is extended to ~ 1 m**

### *3.2.3.1 Geology of the Site.*

Within the Mammoth Site, three distinct (though gradual) episodes of sedimentation have been documented; an initial phase of poorly sorted gravels, a phase of thinly laminated sands and silts, and a final phase of more thinly laminated and finer sediments (Agenbroad and Mead, 1994). The geological setting currently accepted for the site, is that of a sinkhole. In this setting, the initial gravels were deposited by rapid erosion of the sinkhole's walls, the phase

**Figure 3.23 - Photograph showing the excavation technique used at the mammoth site, resulting in platforms with copious exposure in cross section, but few exposed bedding planes. Horizontal FOV ~ 1 m.**

II sediments were deposited within the pond of water caused by local springs, and the final phase of sedimentation occurred sub-aerially when the water table had lowered and spring activity had ceased. Radiocarbon dating from the apatite

of Mammoth bones found in the upper phase II sediments at the site has provided a date of 26,075 (+975/-790) years before present (Agenbroad and Mead, 1994).

No Mammoth remains have been discovered in phase III sediments, but bioturbation from megafauna is recorded from the central area of the depression that would have remained waterlogged the longest (Agenbroad and Mead, 1994). Whilst examining the site, channel structures were found in the same upper layers as the designated megafauna tracks. An example of this can be seen in Figure 3.24.

**Figure 3.24 - An example of a channel-like structure found in the phase III sediments of the Mammoth site. Visible length of tape measure = 350mm**

### *3.2.3.2 Tracks at the Mammoth Site*

Almost all of the large tracks at the Mammoth site were visible in cross section. This was an artefact of the excavation procedure used at the site. This procedure was used to remove blocks of matrix such that the remaining matrix provided a stepped appearance for easy access and for display to the public. The downside to this procedure is that few bedding planes were exposed, meaning surface outlines of tracks were hard to discern, and any trackways were hard to follow unless parallel to the cross sectional surface (Figure 3.23).

Twelve structures, marked by staff at the Mammoth Site as tracks, were examined closely (Figure 3.25 and Figure 3.26). All of the tracks were on the order of 300-600 mm across, and around 300 mm in depth. Many of the labelled tracks consisted of a shaft, at the edges of which were raised rims in the laminations of the rock. The interiors of the tracks all showed highly convoluted laminations that were difficult to follow. The lack of any tracks clearly visible in plan view (i.e. on an exposed bedding plane) limits the use of the subsurface information present. The lack of continuous trackways makes it difficult to distinguish tracks from non-biogenic sedimentary structures such as water upwelling deformation structures (Reineck and Singh, 1980), and it is this author's opinion that many of the structures labelled as tracks are in fact likely to be non-biogenic sediment deformation structures.

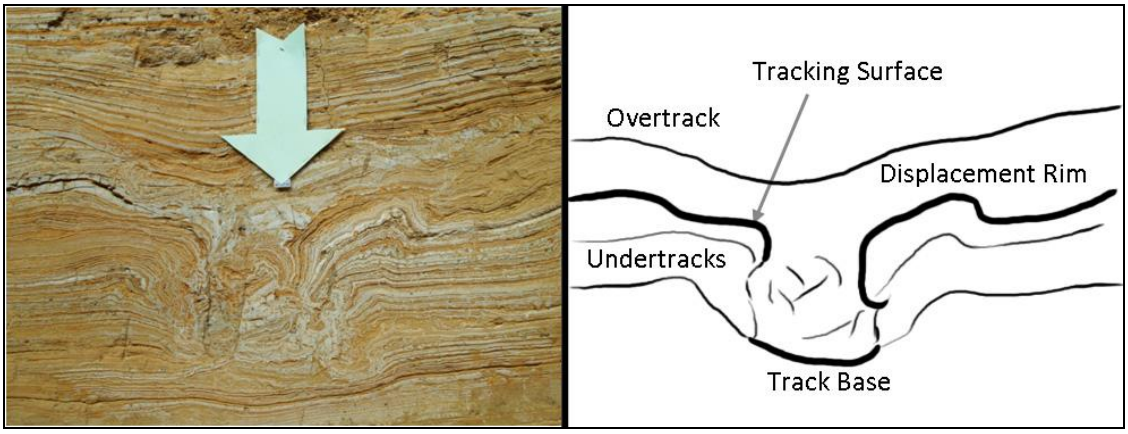


**Figure 3.25 – (Left) Detail image of sedimentary structure labelled as a track. Shaft of green arrow is 0.1 m across. (Right) interpretation of the structure as a track.**

On the small areas of exposed bedding plane, were discovered a number of small vertebrate and invertebrate tracks. The vertebrate tracks were approx. 20mm in length, and consisted of two or three digits. The invertebrate traces were burrows, up to 5mm in diameter, and small trackways of tracks 2-3mm in length. These traces were discovered some 2-3 m below the surface of the site. These tracks were reported by Falkingham *et al.* (2010; Chapter 4).

**Figure 3.26 - Green arrows highlighting structures identified as tracks in the Mammoth site. Each arrow is ~ 0.1 m across.**

# Chapter 4 - First Discovery of Bird tracks at the Mammoth Site of Hot Springs, South Dakota, USA.

A paper published in the peer reviewed journal: Ichnos

Presented in published form.

Reference:

Falkingham, P.L., Thompson, K., Agenbroad, L.D. and Manning, P.L., 2010. *First Discovery of Bird tracks at the Mammoth Site of Hot Springs, South Dakota, USA*. Ichnos, **17**(1): 34-39.

*Ichnos*, 17:34–39, 2010

ISSN: 1042-0940 print / 1563-5236 online
DOI: 10.1080/10420940903358669

Taylor & Francis
Taylor & Francis Group

# Bird Tracks at the Hot Springs Mammoth Site, South Dakota, USA

**Peter L. Falkingham,[1] Larry D. Agenbroad,[2] Kristina Thompson,[2] and Phillip L. Manning[1,3]**

[1]*School of Earth, Atmospheric and Environmental Sciences, University of Manchester, UK*
[2]*Mammoth Site of Hot Springs, South Dakota, USA*
[3]*Department of Earth and Environmental Sciences, University of Pennsylvania, Philadelphia, Pennsylvania, USA*



**The Hot Springs Mammoth Site, South Dakota, USA, has been excavated for over three decades, during which time numerous body fossils have been recorded. The site is particularly well known for the skeletal remains of mammalian megafauna. Bedding plane surfaces were studied that displayed the first record of small vertebrate (avian) and invertebrate traces. While large vertebrate tracks, often observed in cross-section, are well known at the site, the new traces form a hitherto unstudied assemblage.**

**The presence of distinct didactyl and tridactyl avian tracks from the site are described here for the first time. The small (∼20 mm long) tracks and associated invertebrate traces suggest relatively high moisture content in the substrate on surfaces that experienced aerial or subaerial exposure. This is consistent with the interpretation that the upper layers of the site represent the latter stages of a sinkhole setting with a pond undergoing cyclical drying out.**

**Keywords** Avian, bird, track, footprint, Holocene

## INTRODUCTION

The Mammoth Site in Hot Springs is located at the southern extremity of the Black Hills, South Dakota (USA). The site palaeoenvironment has been interpreted as a sinkhole above a breccia pipe, which formed 25,000–26,000 years B.P. (Laury, 1994). The site has been systematically excavated for more than three decades, yielding fossil remains of fish, amphibians, and large mammals, including *Mammuthus* sp. It is the latter which form the majority of the fossil remains at the site. Isolated fragments of bird remains form less than a fraction of 1% of the recovered fauna. These are unidentifiable at order level due to the fragmentary nature of the specimens (Agenbroad and Mead, 1994).

The fine-grained, laminated sediments in many areas of the site (particularly those in the upper parts of the stratigraphy), when exposed in cross-section, display visibly deformed/convoluted bedding, different to the finely laminated planar bedding observed on either side of such structures. These disturbances have been attributed to megafauna bioturbation and include distinct deformation structures that are currently described as *Mammuthus* sp. tracks (Agenbroad and Mead, 1994; Laury, 1994). Invertebrate traces have been previously reported at several levels within the site (Laury, 1994, Mead et al., 1996).

## GEOLOGICAL SETTING

The Mammoth Site sinkhole formed approximately 26,000 years ago when a cavern in the Minnelusa Limestone collapsed (Agenbroad and Mead, 1994). The collapse caused a vertical shaft, consisting of a breccia pipe. The ground surface of the Permo-Triassic Spearfish Formation, a shaley, silty rock formation overlying the limestone, also collapsed into the structure. This opened a 20 m deep 37 m × 46 m sinkhole (Agenbroad and Mead, 1994). The breccia pipe provided a chimney-like opening for a warm spring to well up under artesian pressure to create a steep-sided pond (Agenbroad and Mead, 1994). Where exposed, the sinkhole walls vary in palaeoslope from 60° from the horizontal to overhanging (Agenbroad and Mead, 1990). Eventually the sinkhole in-filled, and the artesian spring was diverted to Fall River by down cutting.

## SEDIMENTOLOGY

The sinkhole fill consists of laminated fine-grained sediments ranging from clay to coarse sand and breccia. These deposits represent reworking and sorting of wall rock, terrace gravels, suspended sediments in an artesian spring, and fine grained

Address correspondence to Phillip L. Manning, School of Earth, Atmospheric and Environmental Sciences, Williamson Building, University of Manchester, Oxford Road, Manchester, M13 9PL, United Kingdom. E-mail: phil.manning@manchester.ac.uk

wind-blown sediment. The depositional energy for moving sediments within the structure was produced by currents from the artesian springs emerging in the north eastern portion of the sinkhole. Three phases of sedimentation have been recognized (Laury, 1980). The initial phase consisted of a coarse grained unit representing, in part, reworking of material from the initial collapse of the sinkhole walls, carrying overlying terraces from the ancestral Fall River. Well-laminated sands and silts represent the second phase of sedimentation. The final phase is characterized as more clay-rich and silt-rich and is heavily bioturbated. This final phase is considered to represent a low energy, shallow water deposit, essentially a mud hole created as spring influence diminished or was diverted to the deepening channel of the Fall River. This layer is believed to have experienced some periods of aerial exposure due to springs diverting to the Lower Fall River (Agenbroad and Mead, 1994). Mammoth remains and megafauna tracks occur in most of the sedimentary phases. The palaeoenvironment of the deposits and the nature of the sediments being deposited have preserved even the most delicate bones, such as hyoids from mammoths. Fish skeletons are also found in low energy portions of the sinkhole (Czaplewski and Mead, 1994), indicating the sinkhole was not a closed system for all of the depositional history.

Over several thousand years, the surrounding strata, the Spearfish Formation, eroded leaving the resistant sinkhole sediments topographically higher (Agenbroad and Mead, 1994).

## DESCRIPTION

The tracks described herein occur on a discrete area of exposed bedding plane (Fig. 1). The sedimentology at this location consists of finely laminated silts and muds. Many of the bedding plane surfaces display a wrinkly texture. This structure forms complex, convoluted rounded ridges on the surface of the muds (Fig. 2). Two vertebrate tracks with distinct digital impressions are exposed and measure approximately 20 mm in length (from tip of middle digit to the posterior convergence of the toes). Both tracks are isolated features and are not part of exposed trackways, though this may be a function of limited bedding surface exposed.

Track 1 (Fig. 3) displays two distinct digits, 20 mm and 12 mm in length, preserved as very shallow impressions. Total track length and width is 20 mm and 14 mm, respectively. Interdigital angle between visible digits is 47°. There is also an impression at the posterior of the track where a halux would be expected to touch the substrate and a faint mark representing a third digit, though this impression is much less distinct than the others.

Track 2 (Fig. 4) also displays 2 digits measuring 25 mm and 8 mm in length. The area of rock where a third digit would be expected has been removed. Track length is 25 mm and track width is 16 mm; interdigital angle between visible digits is 60°. Distinct phalangeal pads can be observed on digit III, which terminates with a sharp claw mark. Close to track 2 is an invertebrate trace approximately 60 mm in length and a sharply incised sinusoidal feature measuring ∼20 mm (Fig. 4).

In addition to these clear tracks, several less distinct impressions can be seen on the same bedding plane as track 1. These marks are regularly spaced, shallow circular depressions <10 mm in diameter that appear to represent either faint surface features or transmitted tracks.

## INTERPRETATION

There are several interpretations for the wrinkled texture observed on the bedding planes of silts and muds, upon

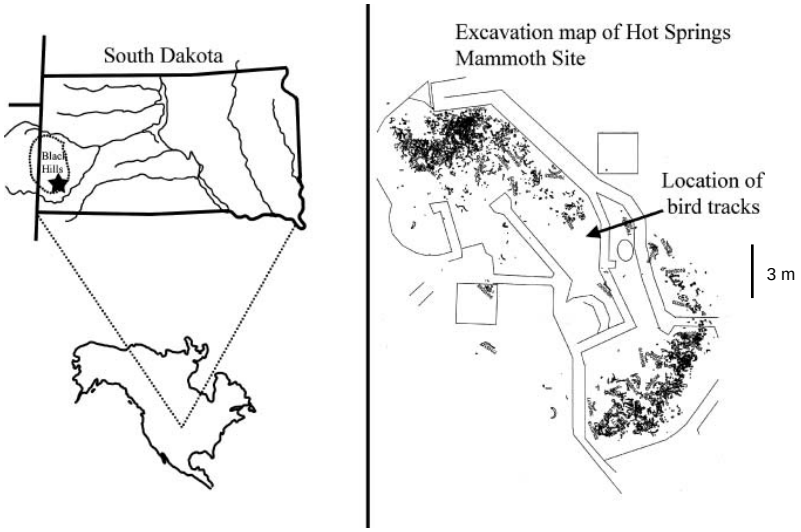


FIG. 1. **Left:** Star indicates the location of the Mammoth Site of Hot Springs, located to the south of the Black Hills, South Dakota, USA. **Right:** Excavation map from the Mammoth Site, arrow shows location of exposed bedding planes containing bird tracks.

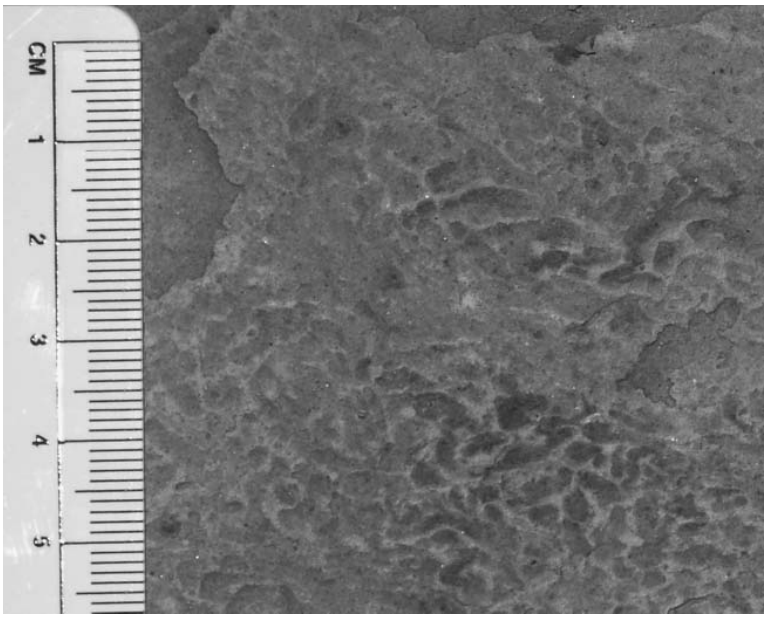


FIG. 2. Photograph of "Wrinkle" structure, possibly produced by a microbial mat. Scale bar is in mm.



which the tracks and traces are preserved. The first is that the texture represents a microbial mat. The complex convoluted nature of the texture is morphologically similar to that of Kinneyia structures (Porada and Bouougri, 2007). Kinneyia-like structures are described as "likely formed below the sediment-water interface by gas build-up beneath buried microbial mats" (Hagadorn and Bottjer, 1999, p. 74).

Modern mats typically require an absence of predators, for example, gastropods, and such conditions may be met in areas where mats are at least occasionally subaerially exposed (Porada and Bouougri, 2007).

Alternatively, Allen (1985) described similar wrinkle marks from the intertidal zone of the Severn Estuary, England. The structures described by Allen were created by finely interbedded

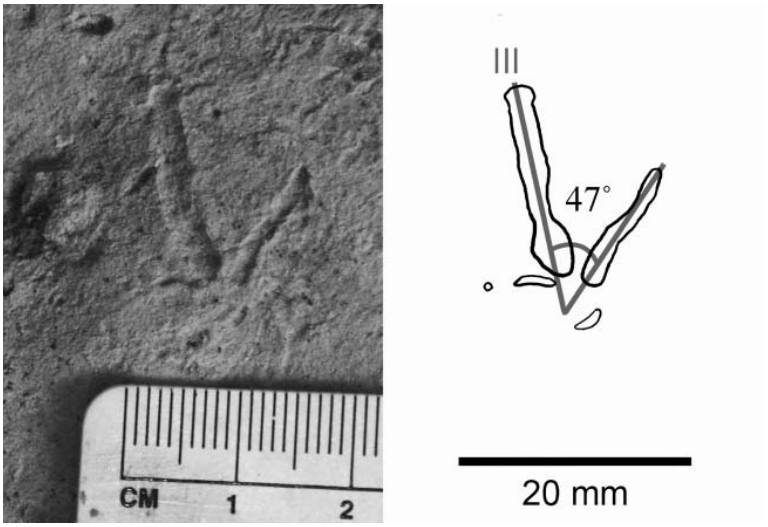


FIG. 3. Photograph and outline of tridactyl track 1. Digit III (middle digit) is labeled. Only two digits are clearly recorded by the sediment, though a mark at the posterior of the foot may be a halux impression. The faint trace to the left of the track is where a third digit would be expected. Scale bar = 20 mm.

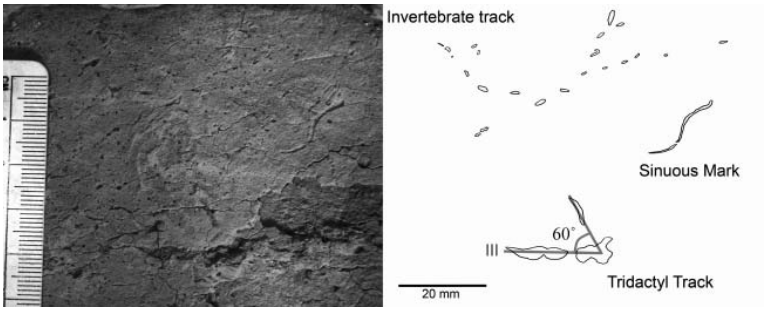


FIG. 4. Photograph and outline of tridactyl track 2, sinuous feature, and invertebrate trace. Digit III (middle digit) of track 2 labeled. Note the level of detail present (phalangeal pads and claw mark). Scale bar = 20 mm.

sand and mud. These structures were noted to form when an ebbing tide had exposed the sediment but while the sediment was still saturated by water—either by high pore fluid pressures as water drains away or through liquefaction of the mud by wave action with tide withdrawal. Reineck and Singh (1980) also describe wrinkle marks or "Runzelmarken" as forming on sediment surfaces that are partly cohesive and covered by a thin film of water (<10 mm). A strong wind blowing over the surface causes wrinkles to develop either as ripple-like features or as a honeycomb form, with thinner water films producing smaller, more closely spaced wrinkles (Reineck and Singh, 1980).

The interpretations provided by both models are consistent with the palaeoenvironments of the Mammoth Site, supporting that these areas were located in the upper layers of the site and were exposed to periods of aerial or subaerial exposure.

The tracks display two clear digits, with faint impressions from the halux and third digit also present on one track. While track 1 appears to have been formed/preserved primarily as an

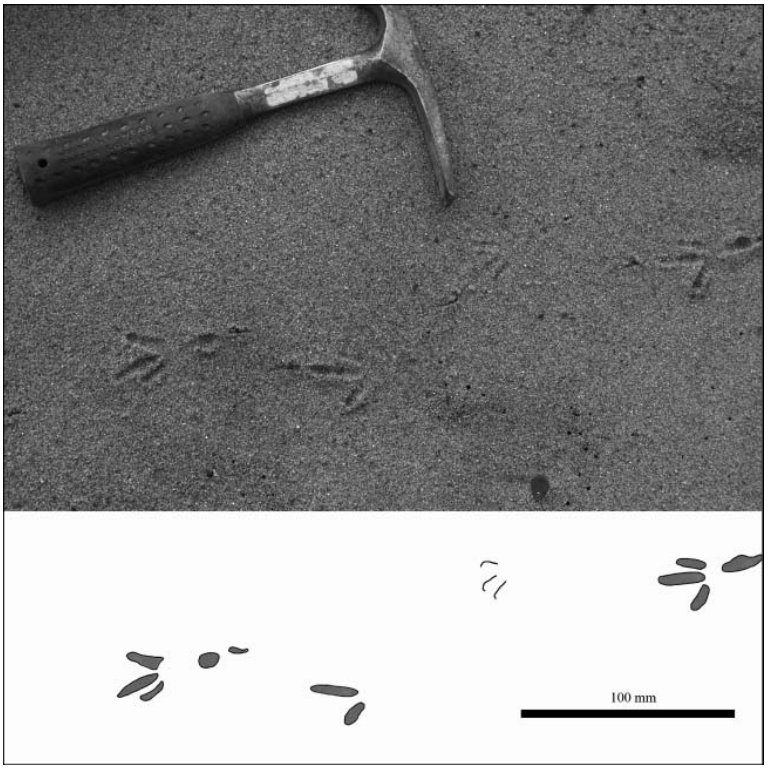


FIG. 5. Photograph and outline of a trackway made by a small bird in fine, moist beach sand, Sandown Bay on the Isle of Wight (UK). Note that the first (right) and last (left) tracks display all three digits and a reverse halux impression. The third track is only impressed as two digits (III and IV), whilst the second track is barely preserved at all. Scale bar = 100 mm.

impression of two digits (the third leaving a far less obvious impression), the sediment next to track 2 where the third digit should be is missing. The lack of a distinct third digit on track 1 may be a function of the weight distribution on the foot and/or that the track is an undertrack (Manning, 2004). Such an undertrack might be formed at a depth of only 1–2 mm, as observed in many of the Lower Jurassic Massachusetts tracks (PLM and PLF, pers. obs.). The detail present in track 2 indicates it was most likely exposed at the surface upon which the animal walked. Modern bird tracks made in fine sand by a tridactyl foot can be seen to "lose" a digit, even within a trackway, due to very local substrate properties (particularly moisture content) and weight distribution over the foot (Fig. 5).

The more numerous circular marks found on the same layers may represent feeding traces of birds (Lockley et al., 1992). Alternatively the traces may be more deeply transmitted undertracks that have lost detail and definition. If this is the case, these marks would appear to represent trackways rather than individual tracks. Unfortunately the marks are nondescript and posses no identifiable features. Future excavation of the site and thin sectioning of the structures may help to confirm their origin.

The sinusoidal mark found next to track 2 has sharply incised edges and curves sharply. While this may have been formed by a burrowing animal predominantly in the layer above (the layer now removed), the morphology of the mark is consistent with a fish swimming trace where the tip of the caudal fin scours the surface of the substrate (De Gibert et al., 1999). Such a trace is indicative of at least very shallow water over the sediment.

We suggest that the makers of these small tridactyl tracks were likely to have been small birds feeding or drinking at the water's edge.

## CONCLUSION

The didactyl and tridactyl traces reported in this paper represent the first small vertebrate tracks discovered at the Hot Springs Mammoth Site. The significance of this find is twofold. First, these tracks add to the represented ichnofauna of the site. The only bird remains from the site previously discovered were small and fragmentary and thus unidentifiable. While specific taxon cannot be inferred from these tracks, in situ evidence is provided for birds with a foot size of around 20 mm being present at the Mammoth site when an active depositional basin.

Located centrally in the site, approximately 1.5–2 m from the surface of excavations, the presence of small, detailed bird tracks in which the foot has been placed flat against the substrate indicates the sediment was moist. If covered by water at the time of track formation, the depth of water cannot have been more than a few cm. This is supported by the presence of wrinkle structures. Periods of aerial exposure would dry out the sediment, preserving the "wrinkled structure." This provides us with three phases: 1) submerged substrate, as evidenced by the fish trace; 2) subaerial exposure, as evidenced by the wrinkle structures; and 3) aerial exposure (the drying of the sediment). Bird tracks may have been formed at any stage (providing the water was shallow enough during phase 1, though the tracks presented here were most likely formed during phases 2 and/or 3.

The palaeoenvironment for this location and depth at the site is therefore suggested to be that of a shallow pond or pool of water (or the shore of a somewhat larger pond) subject to periodic drying. This is consistent with the current interpretation that toward the latter stages of deposition within the sinkhole, local springs dried up or were diverted, leaving the remaining depression to alternately fill with rain or ephemeral streams, which then dried up. However, the presence of small bird traces in lower stratigraphic levels of the site is not ruled out and would entail a revision of the depositional history of parts of the site.

Small tracks such as those described here may have been previously overlooked due to the excavation techniques employed at the site, where removal of overburden often occurs at an angle to bedding. It is therefore cautioned that at sites where archaeological style excavation removes overburden systematically, the surfaces of bedding planes are not disregarded.

## ACKNOWLEDGMENTS

We would like to thank NERC for providing a grant with which Falkingham was able to conduct fieldwork (ref: NER/S/A/2006/14033) and Dr. Nicholas Minter (University of Bristol) and Dr. John Pollard (University of Manchester) for useful discussion and comments. We would also like to thank Dr. Alice Giannetti and one anonymous reviewer for helpful comments and reviews.

## REFERENCES

Agenbroad, L. D. and Mead, J. I. 1994. The Hot Springs mammoth site: A decade of field and laboratory research in paleontology, geology and paleoecology. Fenske Printing Inc., Rapid City, SD, 457 p.

Allen, J. R. L. 1985. Physical sedimentology. George Allen & Unwin, London, 272 p.

Czaplewski, N. J. and Mead, J. I. 1994. Late Pleistocene small mammals from Hot Springs mammoth site, South Dakota. *In* Agenbroad, L. D. and Mead, J. I. (eds.), The Hot Springs mammoth site: A decade of field and laboratory research in paleontology, geology, and paleoecology. Hot Springs, South Dakota, The Mammoth Site, 136–149.

De Gibert, J. M., Buatois, L. A., Fregenal-Martinez, M. A., Gabriela Mangano, M., Ortega, F., Poyato-Ariza, F. J., and Wenz, S. 1999. The fish trace fossil Undichna from the Cretaceous of Spain. *Palaeontology*, 42:409–427.

Hagadorn, J. W. and Bottjer, D. J. 1999. Restriction of a late Neoproterozoic biotype: Suspect-microbial structures and trace fossils at the Vendian-Cambrian transition. *Palaios*, 14: 73–85.

Laury, R. L. 1980. Paleoenvironment of a late Quaternary mammoth-bearing sinkhole deposit, Hot Springs, South Dakota. *Geological Society of America Bulletin*, pt. 1, v. 91: 465–475.

Laury, R. L. 1994. Palaeoenvironment of the Hot Springs mammoth site. In Agenbroad, L. D. and Mead, J. I. (eds.), The Hot Springs mammoth site: A decade of field and laboratory research in paleontology, geology, and palaeoecology. Fenske Printing, Rapid City, SD: 28–68.

Lockley, M. G., Yang, S. Y., Matsukawa, M., Fleming, F., and Lim, S. K. 1992. The track record of Mesozoic birds: Evidence and implications. *Philosophical Transactions: Biological Sciences*, 336(1277): 113–134.

Manning, P. L. 2004. A new approach to the analysis and interpretation of tracks: Examples from the dinosauria. *In* McIlroy, D. (ed.), The application of ichnology to palaeoenvironmental and stratigraphic analysis, volume 228:93–123.

Mead, J. I., Hevly, R. H., and Agenbroad, L. D. 1994. Late Pleistocene invertebrate and plant remains, mammoth site, Black Hills, South Dakota. *In* Agenbroad, L. D. and Mead, J. I. (eds.), The Hot Springs mammoth site: A decade of field and laboratory research in paleontology, geology, and palaeoecology. Fenske Printing, Rapid City, SD: 117–135.

Porada, H. and Bouougri, E. H. 2007. Wrinkle structures—a critical review. *Earth-Science Reviews*, 81:199–215.

Reineck, H. E. and Singh, I. B. 1980. Depositional sedimentary environments. Springer Verlag, Berlin, 542 p.

# Chapter 5 - A Crocodylian trace from the Lance Formation (Upper Cretaceous) of Wyoming.

A paper accepted for publication in the peer reviewed journal: New Mexico Museum of Natural History and Science Bulletin.

Presented in published form.

Reference:

Falkingham, P.L., Milàn, J. and Manning, P.L., 2010. *A Crocodilian trace from the Lance Formation (Upper Cretaceous) of Wyoming*. In: Milàn, J., Lucas Spencer, G., Lockley, M. and Spielmann, J. (Editors), Crocodylian tracks and traces. New Mexico Museum of Natural History and Science Bulletin. **51**, pp. 171-174.

Milàn, J., Lucas, S.G., Lockley, M.G. and Spielmann, J.A., eds., 2010, Crocodyle tracks and traces. New Mexico Museum of Natural History and Science, Bulletin 51.



# A CROCODYLIAN TRACE FROM THE LANCE FORMATION (UPPER CRETACEOUS) OF WYOMING

PETER L. FALKINGHAM[1], JESPER MILÀN[2,3] AND PHILLIP L. MANNING[1,4]

[1] School of Earth, Atmospheric and Environmental Science, University of Manchester, Williamson Building, Oxford Road, Manchester, M13 9PL, UK; peter.falkingham@manchester.ac.uk;
[2] Department of Geography and Geology, University of Copenhagen, Øster Voldgade 10, DK-1350, Copenhagen K, Denmark;
[3] Geomusem Faxe, Østsjællands Museum, Østervej 2, DK-4640 Faxe, Denmark, jesperm@oesm.dk;
[4] Department of Earth and Environmental Science, University of Pennsylvania, 254-b Hayden Hall, 240 South 33rd Street, Philadelphia, PA 19104-6316, USA; phil.manning@manchester.ac.uk

**Abstract—**A 1.5-m-long double sinusoidal trace from the Lance Formation of Wyoming, U.S.A, is attributed a crocodylian origin. The trace forms part of a diverse tracksite containing dinosaur and bird tracks. The double sinusoidal nature of the trace is suggested to have originated from the dual undulatory motion of body and tail. Other features such as scute and claw marks are comparable with modern crocodyle traces, even though clear footprints have not been identified. The trace therefore expands upon the already diverse dinosaurian ichnofauna of the Lance Formation to include crocodylians.

## INTRODUCTION

The preserved traces of animals provide an important source of information for the study of fossil faunal assemblages. Even when the trackmaker is not identifiable to any significantly low taxonomic level, traces can provide information regarding palaeoenvironment and substrate consistency ( Thulborn and Wade, 1989; Thulborn, 1990; Lockley, 1991; Milàn and Bromley, 2006, 2008; Falkingham, 2009; Falkingham et al., 2009). Nevertheless, if the trackmaker can be identified to a reasonable taxonomic level, some interpretation of paleoecology and biomechanics can be inferred (e.g., Thulborn and Wade, 1989; Gatesy et al., 1999; Day et al., 2004; Myers and Fiorillo, 2009;), complementing osteological information.

Presented here is a detailed description of a trace from the Lance Formation of Wyoming, previously described as a potential tail drag mark (Lockley et al., 2004). The trace is located on a track-bearing outcrop in association with a number of dinosaur and bird tracks and trackways. The track assemblage includes large dinosaur tracks (> 60 cm), of both theropod and ornithopod origin, mid-sized (~ 30 cm) tracks of likely theropod origin, and small (~ 5 cm) bird tracks ( Lockley and Rainforth, 2002; Larson, 2003; Lockley et al., 2004). The trace discussed here is closely associated with a trackway consisting of two tracks of probable hadrosaurian origin (ichnogenus *Hadrosauropodus).*

## GEOLOGICAL SETTING

Lockley et al. (2004) described both the geological setting of the Lance Formation and of the locality. The description of the locality is summarized here for convenience. The site covers a small (3 m x 15 m) outcrop located on private land belonging to the Zerbst Ranch, so specific geographical location is not disclosed. The major track-bearing surface (including the trace redescribed here) is located on the upper surface of an upward-fining sandstone. Lockley et al. (2004) reported a palaeoflow direction of 319°.

Above the main track-bearing surface was a layer of fine-grained sandstone 0.1 m thick. This layer was removed during an earlier excavation (Lockley and Rainforth, 2002), but contained a number of bird tracks preserved as casts, together with ripples and raindrop impressions ( Lockley and Rainforth, 2002; Lockley et al., 2004; Falkingham et al., 2009). The track-bearing horizon was interpreted as being the top of a channel sandstone, with mud-draped ripples containing bird tracks and raindrop impressions being indicative of a short-lived small body of water such as a pond, suggesting drying up and abandonment of a channel (Lockley et al., 2004).

## MATERIAL/TRACK DESCRIPTION

The trace (Fig. 1) consists of a double sinusoidal mark approximately 1.5 m in length, running north-south. It is truncated at one end by the impression of a dinosaur track. The other end appears to have been cut somehow, and there is no relief, positive or negative, compared to the surrounding bedding plane. The trace is present over a short area to the anterior of the second (right) hadrosaur track (as illustrated by Lockley et al., 2004, fig. 8), extending the length of the trace to approximately 2.5 m, though the surface of the rock beyond the second hadrosaur track (in the same trackway) was heavily weathered when the site was visited in the field season of 2007, and subsequently this part of the trace is now barely visible. The trace possesses a flat base, differentiated from the bedding surface by coloration (shaded area, Fig. 1). This contrast in coloration is also present in many of the dinosaur tracks occurring on the same track-bearing surface.

This interior surface of the trace displays striations running longitudinally, parallel to the long axis. A single linear feature is present in the narrower of the two sinusoidal marks, running along the center of the trace (Fig. 1a). At the southern end of the trace, a series of parallel striations are seen between the two sinusoidal marks (Fig. 2c).

The trace also shows raised rims approximately 1 cm in height. These rims are present for the entire length of the trace. Importantly, the rims are cut by concentric fractures associated with the first (left) dinosaur track (Fig. 1b). These fractures are 2-4 mm in width, in-filled, and have both a concentric and a radial relationship to the outline of the dinosaur track. Located to the right (east) of the trace, near the second (right) hadrosaur track are a series of three curved marks that sharply incise the substrate (Fig. 1e). On the left side of the trace, two additional impressions are present. One of these is interpreted as a possible footprint (Fig. 1b).

A second long trace was illustrated by Lockley et al. (2004, fig. 3) to the east of the trace discussed here. However, this was no longer present at the site, as the area had been eroded and broken up by the field season of 2007.

## NEW INTERPRETATION

In the original interpretation of the track, Lockley et al. (2004) suggested the trace might be the drag mark from the tail associated with the nearby hadrosaur tracks with which it is aligned. However, a number of morphological features suggest another explanation for the “tail-drag” trace. The double sinusoidal trace observed is very similar to the trace of extant crocodylians dragging both their body and tail along the ground.

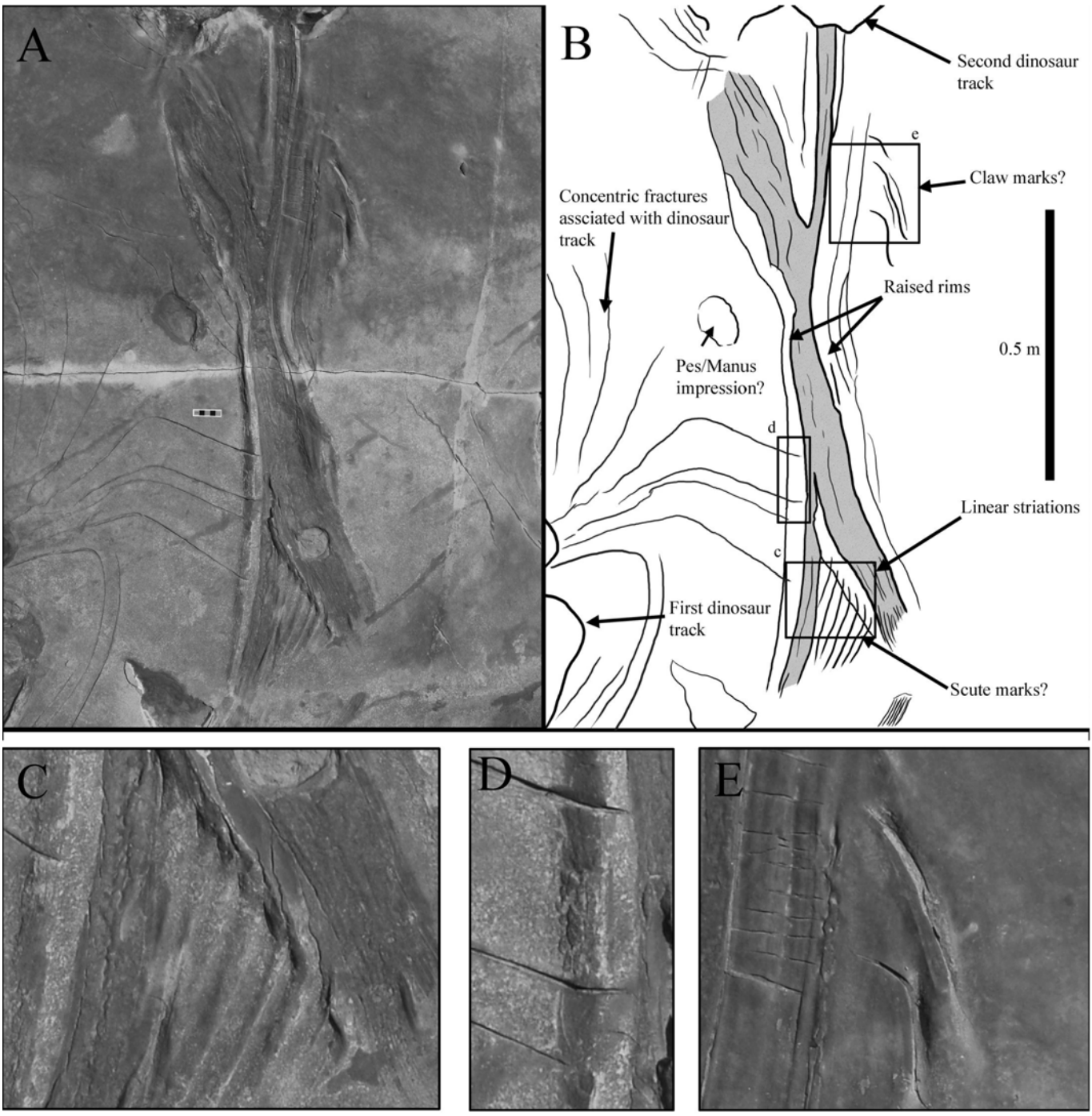


FIGURE 1. **a**, Field photograph of the double sinusoidal trace. **b**, Interpreted outline diagram, indicating the main morphological features of the trace. **c**, Close-up photo of the interpreted scute marks. **d**, Fractures associated with the nearby dinosaur track cutting the raised ridge of the trace. **e**, Subparallel drag marks from claws.

The gait, posture and body plan of crocodylians results in a typical "undulatory" motion of the body, with the belly and the tail leaving distinct, intersecting sinusoidal traces (Milàn and Hedegaard, 2010). As noted below, the tail trace may be wider than the body trace. However, no clear manus or pes traces are seen, even though a possible left footprint is indicated in Figure 1b, and we infer that the set of parallel traces on the right side (Fig. 1c) represent claw traces caused by foot motion.

The trackway from a subadult, female, Slender-snouted crocodile, *Crocodylus cataphractus*, with a total body length of 149 cm, shows intersecting sinusoidal traces from the body and tail (Fig. 2a-b) as seen in the fossil trace described here. In addition, the feet of the crocodile were dragged along the sediment towards the next step, producing parallel, curved drag marks from the claws (Fig. 2a-b), akin to the impressions observed in the specimen from the Lance Formation (Fig. 1c). The parallel features interpreted as scute marks in the specimen from the Lance Formation (Fig. 1a) are similar to what is observed in the belly imprint of an adult, female *Tomistoma schlegeli*, measuring 270 cm (Fig. 2c). Here, the broad, transverse scutes that protect the belly of the crocodile have left clear impressions in the sediment, and interestingly, the belly imprint is intersected by the drag mark from the

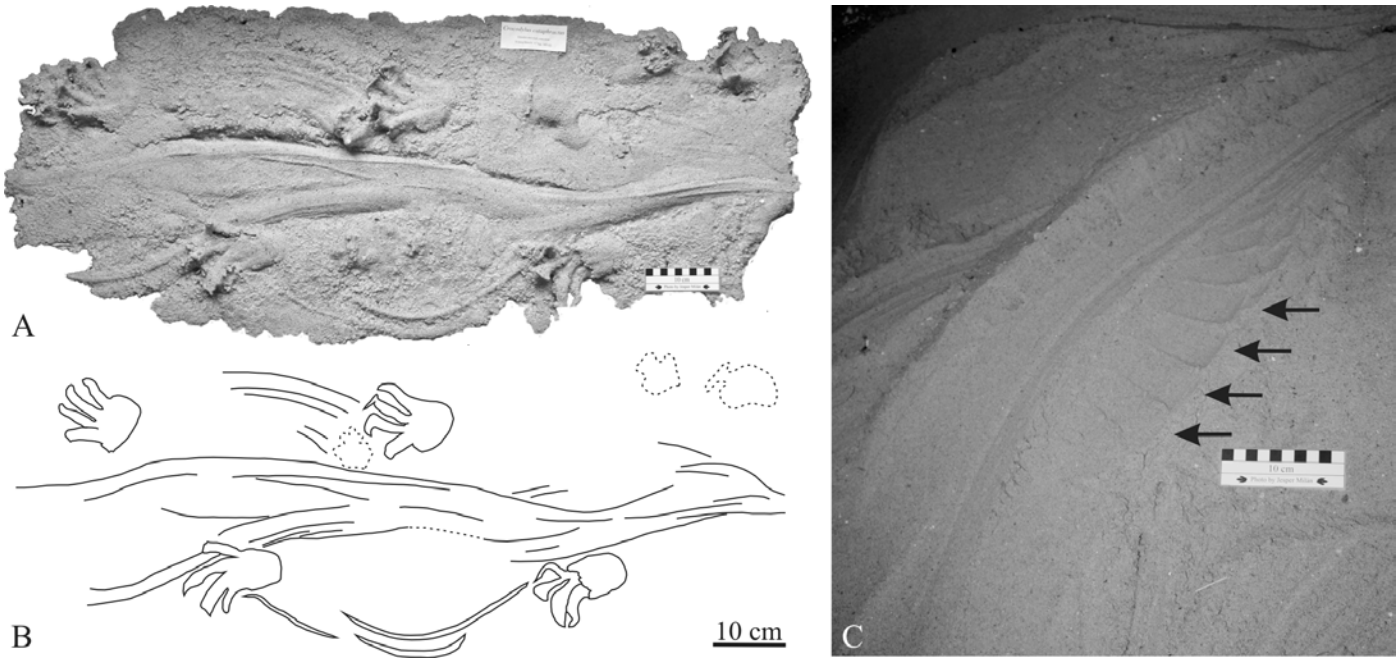


FIGURE 2. Trackways from extant crocodylians, showing similar features to the specimen from the Lance Formation. **A**, Plaster cast of the trackway from a subadult *Crocodylus cataphractus*, dragging its belly and tail in an intersecting sinusoidal pattern. Notice the curved drag marks from the claws. **B**, Interpretive drawing of the trackway. **C**, Belly imprint of an adult *Tomistoma schlegeli*, intersected by its tail trace. Notice the imprints of the transverse scutes covering the belly of the animal.

tail, as the animal progressed forward.

In the trace fossil from the Lance Formation, the thinner of the double sinusoidal traces appears to have been made first, as the wide mark overprints the narrower at the southern end of the trace. Assuming the two marks are associated with body and tail drag, this would imply that the wider of the two traces is attributable to the tail, and the narrower to the body. In extant species of crocodiles, the tail is normally the part of the body producing the most pronounced drag marks and the most sinusoidal movement (Milàn and Hedegaard, this volume). As the more deeply impressed tail is swiping sideways during progression, the resulting tail trace appears wider than the trace from the belly.

## DISCUSSION

The previous study by Lockley et al. (2004) was rightly tentative in suggesting the trace was a "possible" tail drag mark, and noted in their paper that the trace appeared to be cut by the second footfall in the *Hadrosauropodus* trackway, leaving the interpretation "subject to criticism" (Lockley et al., 2004, p. 243). The authors further provided four alternative scenarios to account for this:

1. The impression of the second track means that the tail "skimmed over" the impression, and did not leave a mark. However, as noted by Lockley et al. (2004), the tracks at the Zerbst Ranch are all very shallow, so this scenario is unlikely.
2. The action of the animal passing over the substrate compacted the sediment, so that when the tail passed over the track, no deformation was achieved.
3. The trace was made by another animal that passed by previously.
4. The trace was made by something other than a tail in motion, a plant stem for instance.

The above scenarios offer plausible explanations for the cutting of the trace by the second footfall and of the levees by the fractures associated with the first footfall. However, the presence of fracture lines extending from around the first footfall, but cutting the displacement rim/levee of the trace in question, imply that the trace described here was made prior to the dinosaur tracks. This effectively rules out scenarios 1 and 2, and suggests the trace has an origin not associated with the dinosaur trackway. This is further supported by the angle of the trace being somewhat different than the angle of the dinosaur trackway.

By comparing the trace with trackways generated by extant crocodiles we propose that the third scenario (that the trace was made by another animal prior to the ornithopod) offers the most plausible explanation that explains the morphological features found in the trace. The "hour-glass" shape trace in association with two ornithopod tracks as noted by Lockley et al. (2004) is here interpreted as the double sinusoidal trace from the tail and body of a crocodylian, which was later crossed by the path of an ornithopod dinosaur. This double sinusoidal trace is preserved with scute marks and associated claw impressions as seen in modern crocodylian traces. This interpretation is further supported by the presence of crocodylian fossils from within this facies in the Lance Formation (Breithaupt, 1997).

## CONCLUSION

The "hour-glass"-shaped trace from the Maastrichtian Lance Formation is here interpreted to be the trace of a crocodylian. The gait, posture and body plan of crocodylians produces an "undulatory" motion resulting in the distinct intersecting sinusoidal traces of the body and tail of the animal. This expands the already diverse ichnofauna from the Lance Formation to include crocodylian tracks as well as tracks from multiple taxa of dinosaurs and birds.

## ACKNOWLEDGMENTS

PLF fieldwork and subsequent research was funded by NERC award NER/S/A/2006/14033. The research of JM was supported by the Danish Natural Science Research Council. René Hedegaard from Krokodille Zoo is thanked for his hospitality and access to study extant crocodylians. The authors wish to thank Martin Lockley and Octavio Mateus, whose helpful reviews greatly improved the manuscript.

## REFERENCES


Breithaupt, B., H., 1997, Lance Formation; *in* Currie, P.J., and Padian, K., eds., Encyclopedia of Dinosaurs: San Diego, California/London, UK, Academic Press, p. 394–395.

Day, J.J., Norman, D.B., Gale, A.S., Upchurch, P., and Powell, H.P., 2004, A Middle Jurassic dinosaur trackway site from Oxfordshire, UK: Palaeontology, v. 47, p. 319–348.

Falkingham, P.L., 2009, Diversity in fossil vertebrate track assemblages: Preservational bias due to sediment consistency and animal mass: Journal of Vertebrate Paleontology, v. 29, p. 93A.

Falkingham, P.L., Margetts, L., Smith, I.M., and Manning, P.L., 2009, Reinterpretation of palmate and semi-palmate (webbed) fossil tracks; insights from finite element modelling: Palaeogeography, Palaeoclimatology, Palaeoecology, v. 271, p. 69-76.

Gatesy, S.M., Middleton, K.M., Jenkins, F.A., and Shubin, N.H., 1999, Three-dimensional preservation of foot movements in Triassic theropod dinosaurs: Nature, v. 399, p. 141–144.

Larson, P.L., 2003, An important trackway site from the Lance Formation (Late Cretaceous) of Niobrara County, Wyoming, with new information on behavior in *Tyrannosaurus rex*: Journal of Vertebrate Paleontology, v. 23, p. 70A.

Lockley, M., and Rainforth, E., 2002, The tracks record of Mesozoic birds and pterosaurs: An ichnological and paleoecological perspective; *in* Chiappe, L., and Witmer, L.M., eds., Mesozoic birds above the heads of dinosaurs: Berkeley, University of California Press, p. 405–418.

Lockley, M.G., 1991, Tracking dinosaurs: Cambridge, Cambridge University Press, 252 p.

Lockley, M.G., Nadon, G., and Currie, P.J., 2004, A diverse dinosaur-bird footprint assemblage from the Lance Formation, Upper Cretaceous, eastern Wyoming: Implications for ichnotaxonomy: Ichnos, v. 11, p. 229–249.

Milàn, J., 2008, The impact of sediment consistency on track and undertrack morphology: Experiments with emu tracks in layered cement: Ichnos, v. 15, p. 19–27.

Milàn, J., and Bromley, R.G., 2006, True tracks, undertracks and eroded tracks, experimental work with tetrapod tracks in laboratory and field: Palaeogeography Palaeoclimatology Palaeoecology, v. 231, p. 253–264.

Milàn, J., and Hedegaard, R., 2010, Interspecific variation in tracks and trackways from extant crocodylians: New Mexico Museum of Natural History and Science Bulletin, this volume.

Myers, T.S., and Fiorillo, A.R., 2009, Evidence for gregarious behavior and age segregation in sauropod dinosaurs: Palaeogeography, Palaeoclimatology, Palaeoecology, v. 274, p. 96–104.

Thulborn, R.A., 1990, Dinosaur tracks: London, Chapman & Hall, 410 p.

Thulborn, R.A., and Wade, M., 1989, A footprint as a history of movement; *in* Gillette, D.D. and Lockley, M.G., eds., Dinosaur tracks and traces: Cambridge, Cambridge University Press, p. 51–56.

# Chapter 6 - Finite element analysis methods

## *6.1 Software development*

The primary software used for conducting FEA simulations of tracks was codenamed PalaeoFEM and is originally based on program p122.f90, from Smith and Griffiths (2004), written in FORTRAN 90. FORTRAN 90 is predominantly an engineering programming language and contains many functions that would otherwise have to be user-created in a language such as C, specifically functions dealing with matrices – an integral part of finite element analysis. The program was co-developed with Dr Lee Margetts (University of Manchester) and used the ParaFEM Libraries (www.ParaFEM.org.uk), providing parallel code, as used by Margetts *et al.* (2005; 2006). Throughout the course of this research, the FEA program used was added to and updated numerous times.

### 6.1.1 Preprocessing

#### *Mesh Generation*

In order to create inputs for the analyses; meshes, loading conditions, and boundary conditions had to first be generated in a separate pre-processing stage. This code was written by the author. A finite element mesh consists of a series of elements, defined by nodes located at the corners (and with higher order elements, at mid-point of each edge). Figure 6.1 shows a simple 4 element mesh. PalaeoFEM requires an input mesh (*.d) of the form:

```
*THREE_DIMENSIONAL
*NODES
 [NODE_ID]        [X_COORD]        [Y_COORD]                  [Z_COORD]
                  …
                  …
*ELEMENTS
[ELEMENT_ID]     [DIMENSIONS]     [NODES]     [ELEMENT]     [NODE_ID]     [MATERIAL]
                  …
                  …
```

The first line defines the mesh as three dimensional. The next line, *NODES indicates that the following section contains values for each node; the Node ID number, and the XYZ coordinates in 3D space. These values are separated by a tab, and continue until all nodes are listed. These are then followed by details for each element: the element ID number, the number of dimensions (in this case always three), the number of nodes that make up the element, the element type (hexahedral, tetrahedral etc) then values listing each node by ID number that makes up the element. The final column denotes a material type, to allow each element to have differing properties. The order in which the nodes are listed is important, and follows the spiralling sequence seen in Smith and Griffiths (2004), and shown in Figure 6.1.

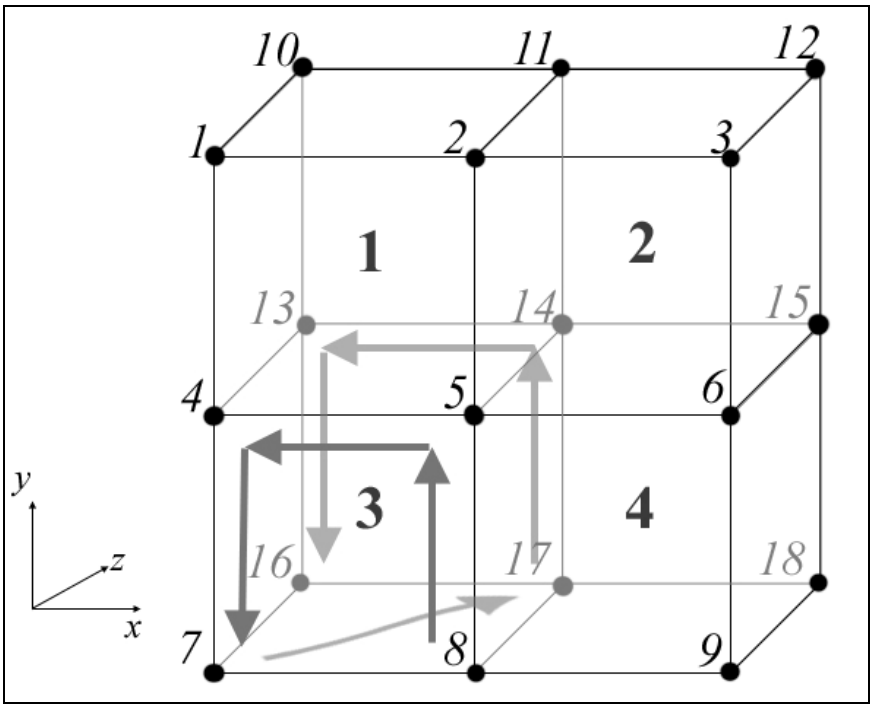


**Figure 6.1 - Node and Element generation in the mesh generation program MeshGen. Here, the order of nodes for element 3 is highlighted – the order found in the *.d file would be 8, 5, 4, 7, 17, 14, 13, 16.**

## *Boundary conditions*

In order for an FE mesh to be stable, parts of the mesh need to be restrained, specifically at the boundaries. If the FE mesh represents a volume of soil, the boundary conditions represent the container in which the soil is held. For PalaeoFEM, this requires an input file (*.bnd) listing the restrained nodes, and the direction (x, y, or z) in which the node is restrained from moving. For the simulations discussed herein, each side of the soil volume was restrained such that nodes could move freely in the plane of the side, but were unable to move outwards or inwards to the soil, these nodes were considered to be on 'rollers.'

The base of the mesh was restrained in all directions, and all other nodes were free to move in all directions.

### *Loading*

With a mesh generated and suitable boundary conditions set, the remaining input is the applied loads. For the work carried out in Chapter 7 (Falkingham *et al.*, 2009), displacement values were generated for each node to be displaced by. For Chapters 8-10 (Falkingham *et al.*, in prep, in review; Falkingham *et al.*, in press-a), the ability for the software to apply forces, rather than displacements, to nodes was implemented, allowing for a more realistic loading scenario. Individual nodes of an element were loaded according to Smith and Griffiths (2004), in which forces are distributed proportionally over the constitutive nodes of a loaded element. In order to apply the loads to a representation of a foot (a complex geometrical feature), the mesh generation program utilised image files. A white on black image of a foot (in *.ppm format) was read by the software and divided into a grid of the same resolution as the surface of the FE mesh. Grid squares occupied by the image (i.e. where pixel values were > 0) were counted as 'loaded,' while other squares were counted as 'empty.' An additional layer of elements was then generated on the surface of the previous mesh in (Figure 6.2). These elements were given material properties sufficiently higher than those of the soil (100x) so as to make the indenter essentially rigid. An overall load was then distributed over all elements on the surface of the 'foot.'

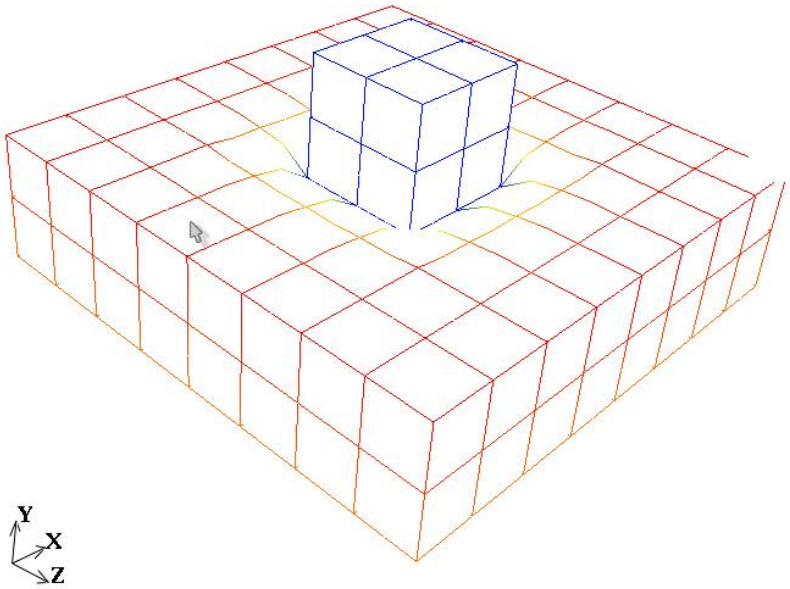


**Figure 6.2 - Simple mesh with 'foot' added to the surface of the soil.**

### *Reducing element number*

Because FEA is fundamentally an approximation method (section 2.6.2), smaller elements, and subsequently higher resolution meshes are necessary for increased accuracy. Also, in order to avoid boundary effects, an FE mesh needs to be ~3.5-4.5 times the foot length in all dimensions (Allen, 1997; Potts and Zdravković, 1999, 2001), requiring a much larger mesh than the area of soil of interest. However, increasing element number also increases solution time. Efficient meshes therefore use dense meshes in areas where the greatest stresses are expected, and larger elements away from this area. The mesh generation program implements a scaling algorithm for creating a dense mesh beneath the foot, but with larger elements further away from the area of indentation (Figure 6.3). This is accomplished in the mesh generation program by multiplying previous element size by a user-specified factor. The same technique has also been applied in the geomechanics literature to optimise finite element meshes

(e.g. Hambleton and Drescher, 2008; Potts and Zdravković, 2001; Smith and Griffiths, 2004).

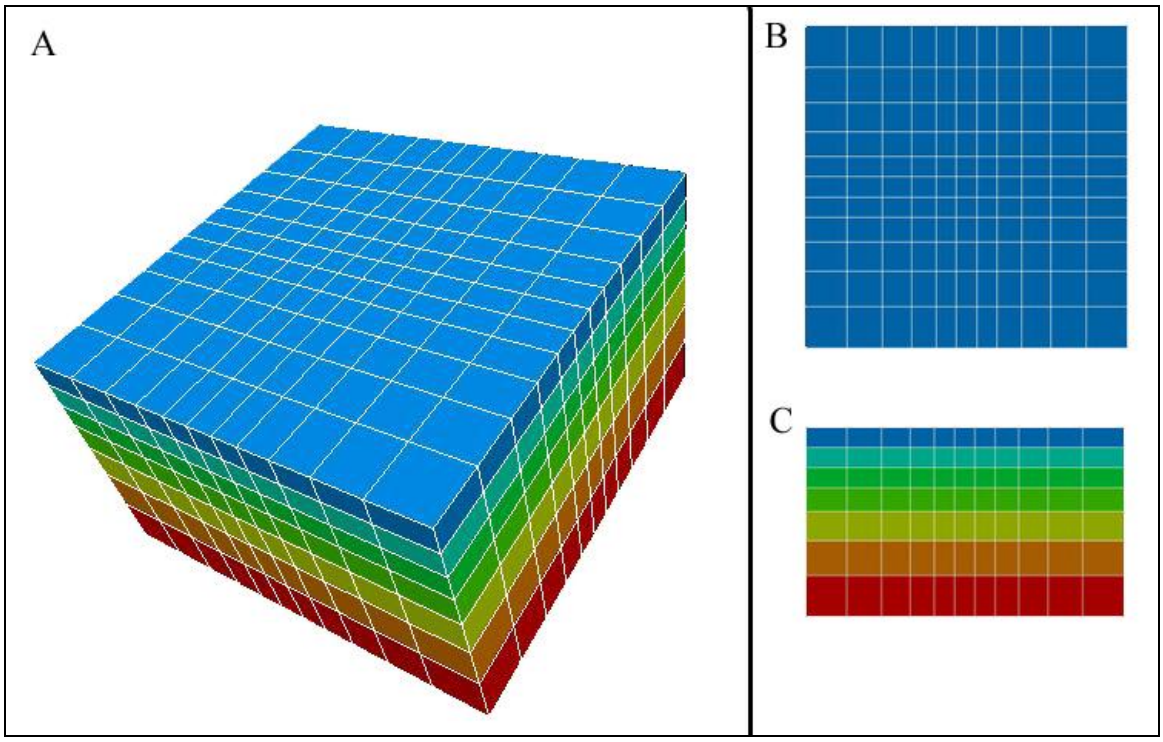


**Figure 6.3 - A simple mesh produced by MeshGen - a dense core of 3x3 small elements can be seen on the surface (B), and at the side (C), surrounded by larger elements scaling by a factor of 1.2 away from the core. This resulted in a mesh containing 847 elements.**

### 6.1.2 Analysis - PalaeoFEM

Having generated the required input files with MeshGen (see above), all inputs were passed to PalaeoFEM for the analysis. Multiple load files were possible, allowing for quasi-dynamic loading conditions (e.g. heel-toe). PalaeoFEM used the von Mises elastic-perfectly-plastic constitutive soil model (see section 2.5.5). This required three inputs to define the soil properties: Undrained shear strength (*Cu*), Young's Modulus (*E*), and Poisson ratio (*v*).

The output of the analysis consisted of displacement files (*.dis) listing all nodes and displacements in the x, y, and z coordinates, and a results file

(*.res) recording such variables as analysis time, iterations needed to find a solution etc. The *.dis files were combined with the original mesh in the visualisation stage.

### 6.1.3 Step 3: Post processing/Visualisation

The primary visualization package for output from PalaeoFEM was based on AVS/Express 7.2 by Advanced Visual Systems Inc. AVS/Express is a module based network system, whereby 'networks' are produced of modules, each of which adds visualisation in a different way. For instance, a slice module may be combined with a magnitude module to display a slice through the soil volume, coloured according to the magnitude of displacement a node has undergone. AVS/Express presented an extremely versatile method for visualising the output of PalaeoFEM. Figure 6.4 shows a relatively simple example of an AVS network used to visualise FEA data.

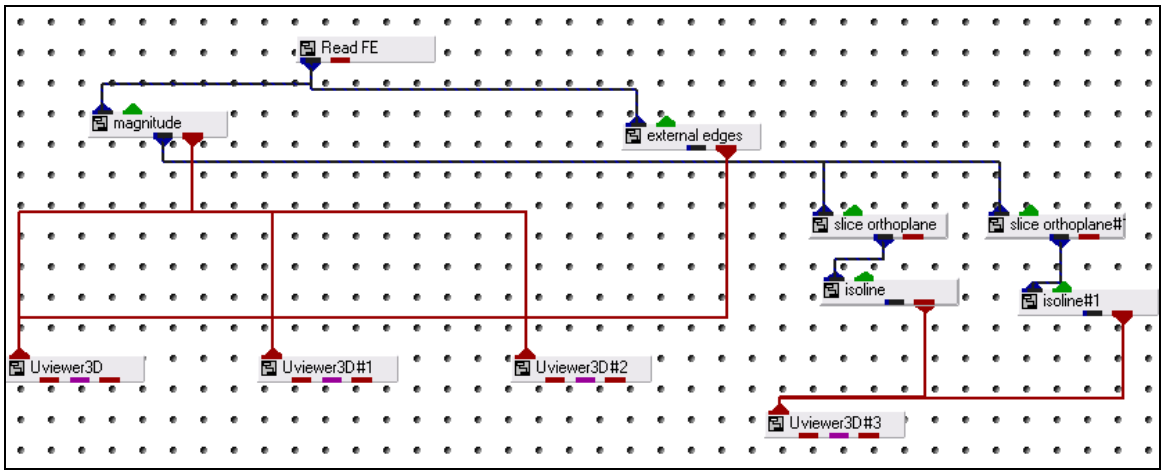


**Figure 6.4 - An AVS network. This network outputs an overall view of the mesh from 3 different angles, and produces an image of 2 isoline planes perpendicular to each other on a forth viewer.**

In 2009 a package was developed by Research Computing Services, University of Mancheser based on AVS/Express that provided a user interface

directly, rather than requiring the construction of a network. This software (ParaFEM-Viewer) was subsequently used. Details of ParaFEM-Viewer can be found at http://wiki.rcs.manchester.ac.uk/community/Projects/ParaFEM-Viewer at time of writing.

### 6.1.4 Hardware

PalaeoFEM was specifically designed so as to be able to run on a range of hardware platforms, ranging from laptops to UK supercomputing facilities such as HECToR and HPCx (www.hector.ac.uk and www.hpcx.ac.uk respectively). Table 6.1 summarises the capabilities of all systems PalaeoFEM was run on. Both HPCx and Horace (University of Manchester) were decommissioned in 2010.

| *Name* | *No. CPUs* | *Speed of each CPU (Ghz)* | *RAM per CPU (GB)* |
|---|---|---|---|
| **Laptop** | 2 | 2.2 | 1 |
| **Workstation** | 8 | 2.8 | 4 |
| **Terra** | 20 | 1.96 | 4 |
| **Horace** | 192 | 1.6 | 2 |
| **HPCx** | 2560 | 1.5 | 2 |
| **HECToR** | 22656 | 2.3 | 2 |

**Table 6.1- Computing resources, and computational power associated with each.**

PalaeoFEM used MPI (Message Passing Interface) in order to take advantage of multiple processors, ranging from a dual core laptop, to a 22,000 processor supercomputer. It is of course advantageous to be able to utilise the

processing power of multiple processing units for a single computational task, as this can reduce the time taken for the task to complete, allowing for larger analyses, or greater numbers of smaller analyses in a given time.

A common serial program works by sequentially executing lines of code. The processor has an attached block of memory in which it can store variables and results to perform further calculations on. In order to utilise more than one processor, each process within the code must be spread over different processors, such that calculations can take place simultaneously. Two multi-processor systems allow for this, the first being shared memory, perhaps where 2 or 4 cores are found on a single processor (as is now common in consumer PCs), and the second being a distributed memory system, in which each processor has its own block of memory, this may be a cluster of workstations or a supercomputer (Pacheco, 1997).

MPI, the Message Passing Interface, constitutes a library of functions that can be called from a C or Fortran program (Pacheco, 1997). A program using MPI must be built from the ground up to include MPI instructions. Such a program cannot be run in serial. MPI spawns all threads at the start of the code (determined by the number of processors the code is running on). The programmer can then distribute calculations over threads. Using commands to broadcast variables to all (or specific) threads, MPI can be used on shared or distributed memory systems, from workstation clusters to supercomputers (Pacheco, 1997).

Because MPI programs use the instructions throughout the program, and message passing is made explicitly, it is possible to achieve near perfect speed ups (double processor number results in halved run time). However, overheads

are still incurred as messages are passed and as file input/ouput is undertaken. These overheads become less significant as problem size (and run time) increase, so larger problems are scalable to a larger number of processors. The standard documentation is available at www.mpi-forum.org at the time of writing.

## *6.2 Software testing*

When using computational techniques, it is important to test the validity and capabilities of the technique before carrying out experiments. Any errors in the model would obviously produce false results, so it is important to run simulations in which the results are already known, either through theory or physical experimentation. Described in this section are a number of tests and experiments run to both validate the model and to find its capabilities. After each iteration of software development, visual validation was first undertaken to confirm the simulation was reaching completion in a somewhat expected manner, and then numerical validation was carried out to ensure the results matched those predicted by geotechnical theory.

### 6.2.1 Visual validation

The first validation test to undertake is a visual comparison between the software and a known problem. Whilst such a check does not provide details on the accuracy of the simulation, it does provide a qualitative comparison such that more detailed analyses need not be run if the visual validation fails. PalaeoFEM was visually validated with a known problem from Smith and Griffiths (2004). This is a footing problem, in which a foundation load is applied to the surface of a soil constrained on all sides.

The problem in the text was a two dimensional one, so to adapt it for PalaeoFEM, the 3$^{rd}$ dimension was treated as the two dimensional wall continuing back, and the loaded nodes continuing in the same fashion (Figure 6.5C). The known solution and the solution calculated by PalaeoFEM did not

show any abhorrent behaviour, and were sufficiently similar as to visually validate the program.

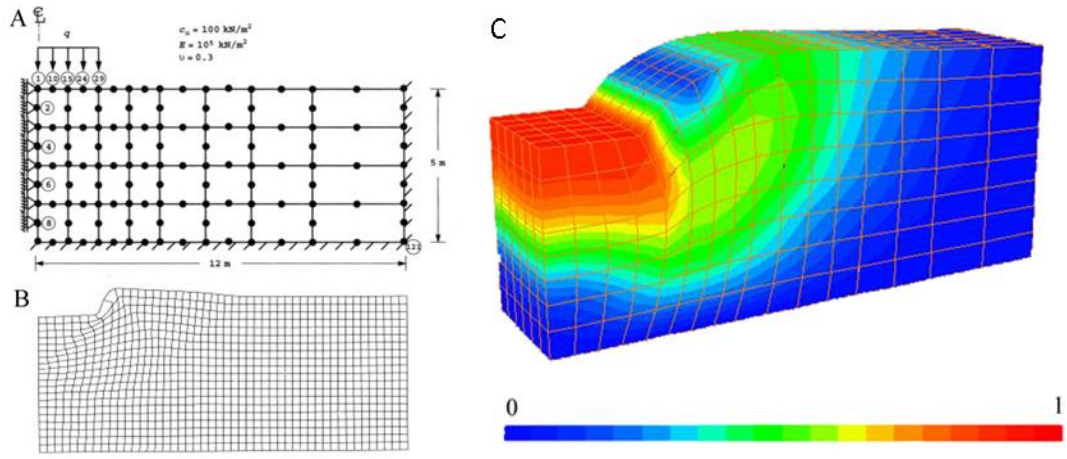


**Figure 6.5 - The problem (A) and known solution (B) from Smith and Griffiths (2004). In this problem, a trench is impressed at one end of a wall of soil. This wall is constrained such that the nodes at the left and right hand sides may only move up and down (free in the y-axis), and the nodes on the base are fixed. (C) The same problem, albeit in 3D reproduced in PalaeoFEM.**

### 6.2.2 Numerical validation

In order to numerically validate PalaeoFEM, the problem outlined above was re-created. However, stricter controls over the size of the Z axis were required. The problem used by Smith and Griffiths (2004) was a plane-strain problem. However, the mesh generation software was developed only with 3D meshes in mind, and so to create a plane strain problem, a 3D mesh was generated 1 element deep (0.5 m). Recalling the von Mises failure criterion described in section 2.5.5, we can see that the von Mises failure surface is defined differently for plane-strain or triaxial conditions. As such, the value of *Cu* used in

PalaeoFEM was equal to $\sqrt{3} * Cu$. Figure 6.6 shows the results of PalaeoFEM compared with the data from Smith and Griffiths (2004).

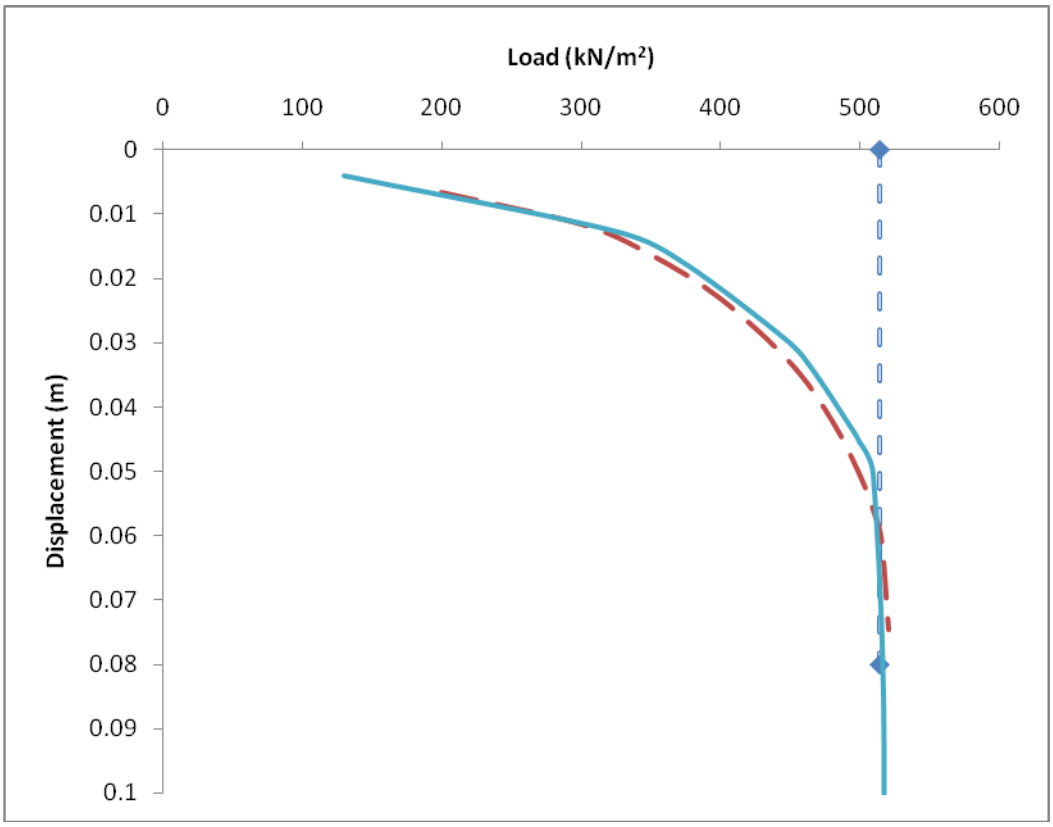


**Figure 6.6 - Reproduction of problem in Smith and Griffiths (dashed line), and PalaeoFEM (mesh = 0.5 m depth plane strain) (solid line). Theoretical bearing capacity (Prandtl load) is shown at 514 kN/m$^2$.**

The code used in PalaeoFEM is based on code from Smith and Griffiths (2004). Therefore, it is necessary to corroborate results between PalaeoFEM and other FEA software; in this case Abaqus 6.8.2. In order to do this, a mesh was generated to simulate a 5 x 5 x 5 m block of soil ($Cu$ = 57 kN/m$^2$, $E$ = 100,000 MPa, $v$ = 0.4) being indented by a 1 x 1 x 1 m indenter. A load of 700 kN/m$^2$ was used to ensure failure and produce the entire elastic-plastic range of behaviour. Mesh resolution was sufficiently high as to avoid artefacts (see section 6.2.3 below). Results were compared between Abaqus and PalaeoFEM,

and then compared with predicted displacements from soil mechanics theory, whereby elastic deformation is calculated by:

$$S_i = \frac{qB}{E}(1 - v^2)\, I_s.$$

Where q = load, B = breadth of indenter, $E$ = Young's Modulus, and $I_s$ = an influence factor (Craig, 2004). For a rigid square indenter, the influence factor is 1.02. This equation is only accurate at calculating displacement until first yield. Once plastic deformation occurs, it becomes very difficult to predict displacement (D'Appolonia *et al.*, 1971). Instead, the ultimate bearing capacity was compared between Abaqus, PalaeoFEM, and theory (see section 2.5.4).

PalaeoFEM and Abaqus showed idential results, indicating that PalaeoFEM was working correctly regardless of input parameters. As can be seen from Figure 6.7, there is very close agreement between the FEA simulations and the predicted response of the soil, both in the elastic region, and in prediction of ultimate bearing capacity. The FEA software can be considered numerically validated.

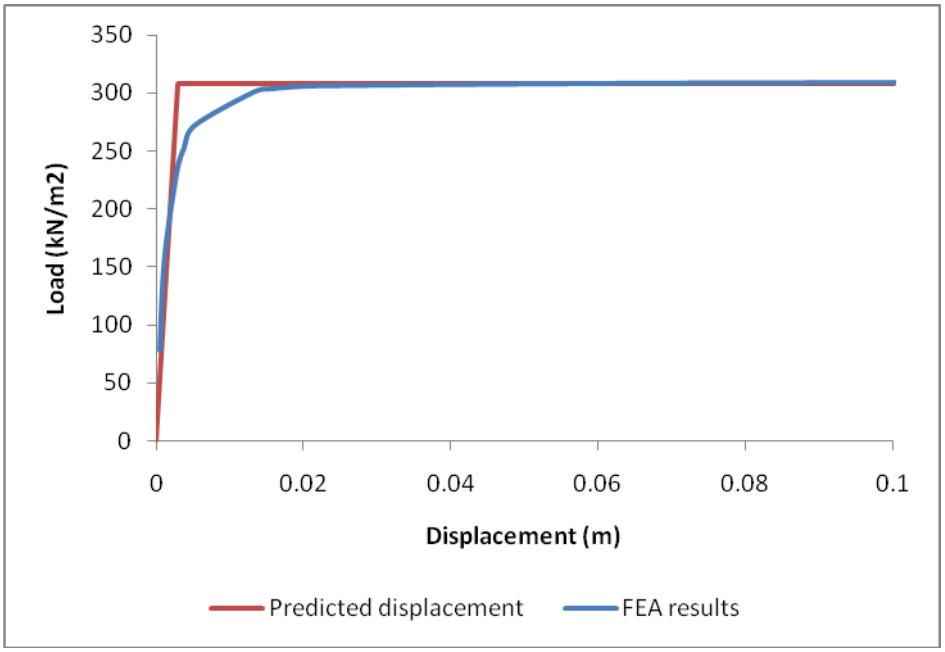


**Figure 6.7 - Graph showing predicted elastic-perfectly-plastic response of soil and results from FEA simulation.**

### 6.2.3 Effects of mesh density.

The accuracy of a finite element analysis is directly related to the size and number of elements making up the mesh. However, an increase in element number raises the complexity of the model, and consequently increases solution time. There is therefore a trade off between accuracy and solution time. The number of elements required for a given accuracy will vary problem to problem, and overall element number can be reduced whilst maintaining accuracy (see section 6.1.1 above).

A simple model is presented here to illustrate the overall effects of element number on solution time and accuracy. The model was composed of a soil block 5 x 5 x 5 m, with a 1 x 1 x 1 m cube on the surface to act as an indenter. Elements were set at 1 $m^3$, 0.5 $m^3$, 0.25 $m^3$, 0.125 $m^3$, and 0.0834 $m^3$ resulting in mesh sizes of 126, 1008, 8064, 64512, and 217728 elements. Decreasing an element in size by halving the length of each side results (in the

case of a uniform mesh) in multiplying the total element number by 8. One can see that after only a few refinements using this approach, element numbers can soon become unmanageable.

A load was applied greater than the predicted bearing capacity so as to cause the soil to fail such that the entire elastic-plastic deformation could be observed. Figure 6.8 shows the results of these simulations. It can be seen that at low mesh resolutions, results differ wildly from expected theoretical results. Mesh refinement is necessary several times before failure occurs close to the predicted value. It should be noted that due to the nature of FEA being an approximation method, the results will never converge on the 'true' answer, but will remain slightly above. The nature of any given problem (e.g. problem size, expected magnitude of deformation) will define the accuracy required by a simulation, and mesh refinement must be undertaken accordingly. Unless otherwise stated, all further experiments in this thesis used an iterative approach to determining the correct mesh density.

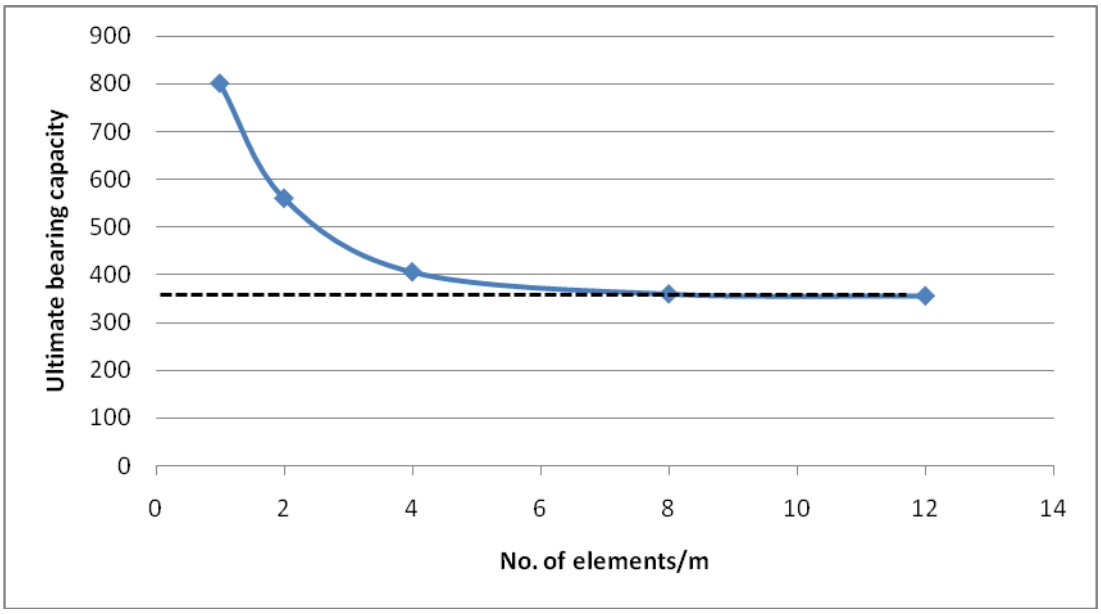


**Figure 6.8 - Graph showing load required for failure in meshes of various sizes. Dashed line indicates theoretical bearing capacity for a soil where *Cu* = 57 kN/m$^2$, loaded by a square footing.**

### 6.2.4 Scalability

A series of experiments were run on HECToR using PalaeoFEM to investigate the scalability of the program over large numbers of processors. Two meshes were generated, the first made up from approximately 1 million elements (1,102,059 nodes), and the second from approximately 4 million elements (4,203,216 nodes). Both were given similar static loading conditions, creating 3,197,350 and 12,362,600 equations for the 1 million and 4 million element meshes respectively. Each mesh was then solved on a number of processor cores from 6 to 250. For each run, the speedup and efficiency of the program were calculated, where:

**Speedup($x$) = time taken on 1 core / time taken on $x$ cores**

and

**Efficiency($x$) = Speedup($x$) / $x$**

If $x$ is the number of cores.

Due to the large nature of these problems, it was unfeasible to run the 1 million element mesh on any less than 6 cores, and the 4 million element mesh on any less than 12. For this reason, the lowest number of cores on which the program was run were used to approximate time taken on 1 core (e.g. time taken on 6 cores / 6). Time taken, speedup and efficiency with number of cores are given in Table 6.2 and Table 6.3 and plotted in Figure 6.9 and Figure 6.10 for the 1 million and 4 million element meshes respectively.

Generally, the speed at which solutions were reached for the two problems were as expected: the larger mesh took longer, but proved to be more scalable, achieving an efficiency of 0.55 when run on 250 cores compared with 0.35 for the smaller mesh on the same number of cores. This higher efficiency on more processing cores results from fewer overheads (passing information between threads etc) in proportion to time spent in calculations. This higher efficiency represents a better exploitation of parallelism.

It is of note that we see super linear speedup when the larger mesh is run on 24 cores. Super linear speedup is when efficiency greater than 1 is achieved. This may occur when a problem is too large to fit in the memory of a lesser number of cores.

*One million element mesh:*

| No. of Cores | Elapsed Time (sec): | Speedup | Efficiency |
|---|---|---|---|
| 6 | 15207.563 | 6 | 1.0000 |
| 12 | 8185.893 | 11.1462 | 0.9289 |
| 24 | 4376.3 | 20.8491 | 0.8687 |
| 36 | 3096.918 | 29.4622 | 0.8184 |
| 48 | 2509.882 | 36.3531 | 0.7574 |
| 60 | 2083.904 | 43.7842 | 0.7297 |
| 72 | 1838.225 | 49.6359 | 0.6894 |
| 96 | 1509.226 | 60.4562 | 0.6298 |
| 120 | 1312.888 | 69.4972 | 0.5791 |
| 150 | 1230.06 | 74.1769 | 0.4945 |
| 200 | 1153.687 | 79.0873 | 0.3954 |
| 250 | 1045.749 | 87.2504 | 0.3490 |

**Table 6.2 - Time taken, speedup and efficiency for 1 million element mesh. Six cores were used to approximate time taken on 1 core (problem too large to run on less than 6 cores).**

*Four million element mesh:*

| No. of Cores | Elapsed Time (sec): | Speedup | Efficiency |
|---|---|---|---|
| 6 | | Could not run | |
| 12 | 21923.362 | 12.0000 | 1.0000 |
| 24 | 10666.657 | 24.6638 | ***1.0277*** |
| 36 | 7509.397 | 35.0335 | 0.9732 |
| 48 | 6078.73 | 43.2788 | 0.9016 |
| 60 | 5028.127 | 52.3217 | 0.8720 |
| 72 | 4457.753 | 59.0164 | 0.8197 |
| 96 | 3351.796 | 78.4894 | 0.8176 |
| 120 | 2847.9 | 92.3770 | 0.7698 |
| 150 | 2482.271 | 105.9837 | 0.7066 |
| 200 | 1999.003 | 131.6058 | 0.6580 |
| 250 | 1895.083 | 138.8226 | 0.5553 |

**Table 6.3 - Time taken, speedup and efficiency for 4 million element mesh. Twelve cores were used to approximate time taken on 1 core (problem too large to run on less than 12 cores). Note that 24 cores produced a 'super linear speed up,' see text for explanation.**

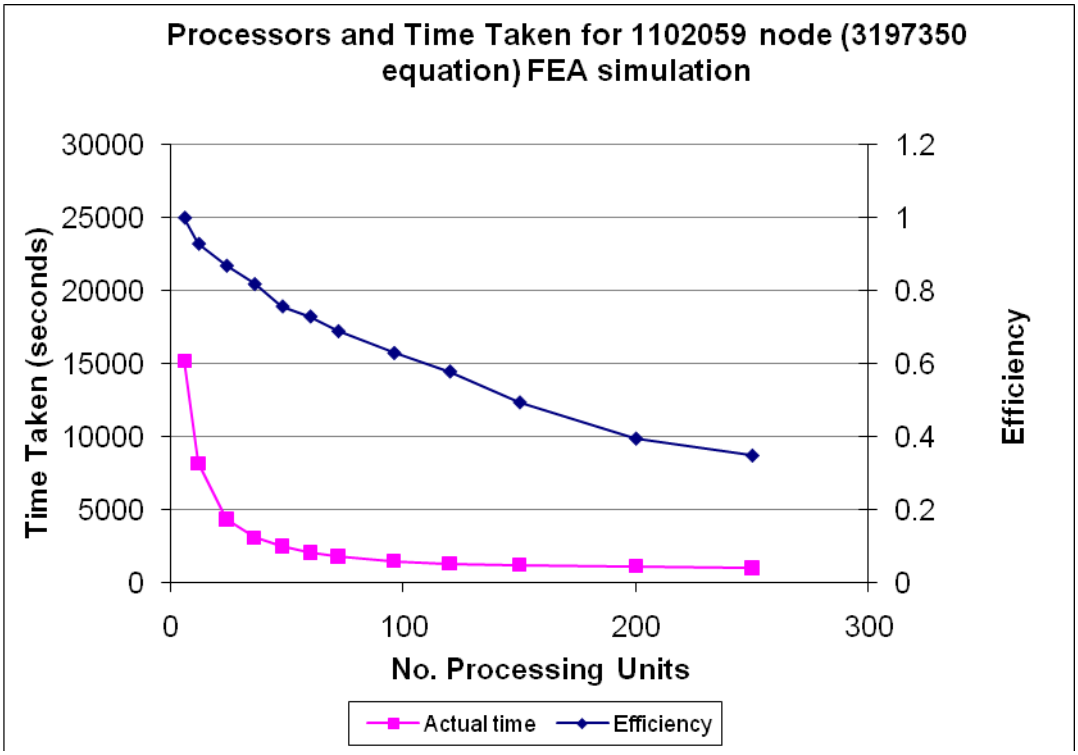


**Figure 6.9 - Efficiency and time taken against processor core number for 1 million element mesh.**

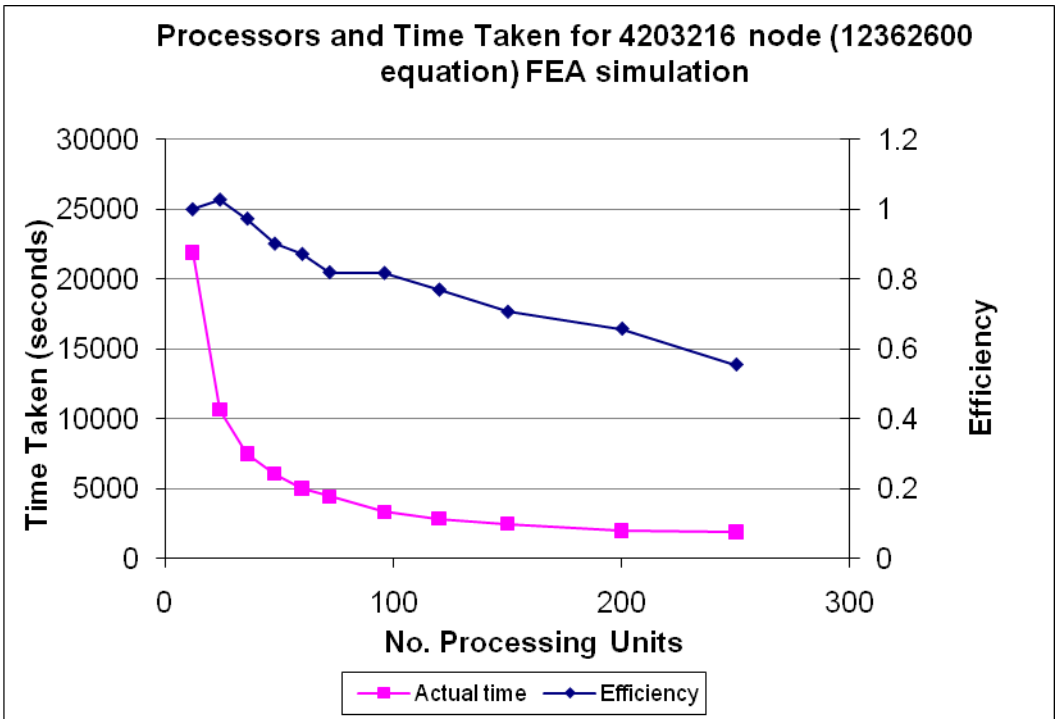


**Figure 6.10 - Efficiency and time taken against processor core number for 4 million element mesh**

# Chapter 7 - Reinterpretation of palmate and semi-palmate (webbed) fossil tracks; insights from finite element modelling

A paper published in the peer reviewed journal Palaeogeography, Palaeoclimatology, Palaeoecology.

Presented in published form.

Reference:

Falkingham, P.L., Margetts, L., Smith, I.M. and Manning, P.L., 2009. *Reinterpretation of palmate and semi-palmate (webbed) fossil tracks; insights from finite element modelling*. Palaeogeography, Palaeoclimatology, Palaeoecology, **271**(1-2): 69-76.

Palaeogeography, Palaeoclimatology, Palaeoecology 271 (2009) 69–76

Contents lists available at ScienceDirect

Palaeogeography, Palaeoclimatology, Palaeoecology

journal homepage: www.elsevier.com/locate/palaeo

# Reinterpretation of palmate and semi-palmate (webbed) fossil tracks; insights from finite element modelling

Peter L. Falkingham [a,*], Lee Margetts [a,b], Ian M. Smith [c], Phillip L. Manning [a,d]

[a] University of Manchester, School of Earth, Atmospheric and Environmental Sciences, Williamson Building, Oxford Road, Manchester, M13 9PL, England, United Kingdom
[b] University of Manchester, Research Computing, England, United Kingdom
[c] University of Manchester, School of Mechanical, Aerospace and Civil Engineering, England, United Kingdom
[d] The Manchester Museum, University of Manchester, England, United Kingdom

ARTICLE INFO

*Article history:*
Received 26 March 2008
Received in revised form 1 August 2008
Accepted 15 September 2008

*Keywords:*
Cretaceous
Footprint
Track
FEA
Bird
Dinosaur

ABSTRACT

A track from the Late Cretaceous previously described as being generated by a semi-palmate bird was studied with the aid of high resolution laser scanning. Substrate conditions at the time of track formation were diagnosed (fine-grained, soft, waterlogged sediment) and used to constrain a finite element track simulator. The indentation of a non-webbed virtual tridactyl foot in such conditions created a resultant track with features analogous to 'webbing' between digits. This 'webbing' was a function of sediment deformation and subsequent failure in 3D, specific to rheology. Variation of substrate conditions and interdigital angle was incrementally stepped. Apparent webbing impressions were clearly developed only within a limited range of sediment conditions and pedal geometry.

The implications of this work are that descriptions of 'webbed' tracks should account for the possibility that webbing was indirectly formed through sediment failure and not necessarily the direct impression of a webbed foot. Additionally, dating the earliest occurrence of webbed feet in the fossil record, and potentially extending phylogenetic ranges, should be treated with caution when based upon evidence from tracks.



## 1. Introduction

Fossil vertebrate tracks are a source of information on the size, speed, limb kinematics and even behaviours of the animals that made them (Day et al., 2004; Manning, 2004 and references therein). In many cases, the fossil tracks provide information that is not preserved in skeletal remains. The record of palmate and semi-palmate (webbed) Cretaceous birds, for instance, is almost exclusively ichnological (Yang et al., 1995; Lockley and Rainforth, 2002; Lockley et al., 2004), with only a single web-footed specimen described to date (You et al., 2006).

Records of webbed bird tracks extend into the Early Cretaceous (Lim et al., 2000; Kim et al., 2006), and thereafter are not uncommon (e.g. Yang et al., 1995; Lockley and Rainforth, 2002; Lockley et al., 2004). The appearance of webbed bird tracks at this time has been interpreted as evidence of a considerable diversification of shore birds.

Sarjeant (1967) described a number of tracks from the Middle Triassic of Mapperly Park, Nottingham (UK) and described *Swinnertonichnus* as a small theropod track that displayed webbing, a feature not currently reported in body fossils of dinosaurs. These tracks were reinterpreted by King and Benton (1996) who observed no such evidence of webbing, noting that if substrate conditions were good enough to preserve interdigital webbing, claw impressions should also be present.

Track morphology is dependant upon a number of interacting factors, including limb kinematics, limb morphology and substrate properties. Once exposed, a track is subjected to the effects of weathering and erosion, which may further modify the geometry (Bates, 2006; Henderson, 2006; Bates et al., 2008). In order to recover information regarding the trackmaker, the interaction of these factors must be taken into account. These controlling factors will vary with sediment particle size and distribution, density, along with the air and/or water occupying the pore spaces between the particles. A clear example of this is demonstrated when water content is increased, reducing the amount of air filling the voids, resulting in the sediment volume becoming less compressible. The bulk density of the sediment increases, as does the shear strength, until the critical saturation point is reached, water then begins to push the particles apart, and the sediment fails (Karafiath and Nowatzki, 1978). In terms of track formation, a waterlogged sediment would prove soft, and easily deformed, but the incompressibility would lead to sediment being forced upwards around the foot to form displacement rims (Manning, 2004).

The effects of the limb–sediment interaction impact heavily upon the *volume* of sediment, and not just the surface in contact with the foot (Allen, 1989, 1997; Manning, 1999, 2004; Milàn et al., 2004; Milàn, 2006; Milàn and Bromley, 2006, 2008; Manning et al., in review). The

* Corresponding author. Fax: +44 1612753947.
*E-mail address:* Peter.Falkingham@manchester.ac.uk (P.L. Falkingham).

0031-0182/$ – see front matter © 2008 Elsevier B.V. All rights reserved.
doi:10.1016/j.palaeo.2008.09.011

consequence of this is that a track must be treated as a full three-dimensional volume, and not simply a surface feature representing the two-dimensional outline of the trackmaker's foot. Force will not only be transmitted downwards below the foot, but also out and up as sediment moves along the path of least resistance, according to Rankine's theory of shear (Craig, 1997; Manning, 2004).

The primary implications of complex deformation generated by a dynamic load are that tracks may appear substantially different to the morphology of the trackmaker's foot, depending on such conditions as those listed above, as well as which track surface within the volume is exposed. The fossil track collection at the Amherst College Museum of Natural History contains numerous examples where this is the case, with single trackways containing traces with varying numbers of digits, or individual tracks preserved as 'books' where several layers of rock have been peeled apart to reveal subsurface features. Each 'page' of the book may have a considerably different morphology to the last (Margetts et al., 2006; Manning et al., in review).

The 3D nature of tracks has been the focus of analogue modelling by track workers over the past decade (Allen, 1989, 1997; Manning, 1999, 2004; Milàn et al., 2004; Milàn, 2006; Milàn and Bromley, 2006; Manning, 2008; Milàn and Bromley, 2008). Such work has provided a quantitative approach to investigating the effects of substrate properties on track morphology, at the surface and within the sediment volume. Such physical modelling, however, is time consuming and in many cases requires physical sectioning and extraction of subsurface layers within the volume. This extraction process is destructive, disrupting the relative position of track surfaces within the volume.

The advance of computer power, combined with software design that takes advantage of multiple processors simultaneously, means that complex simulations such as the deformation of a substrate volume under dynamic loading conditions can be run to completion in feasible time frames. Such a simulation has many advantages over physical modelling, including precise and independent control of variables, and complete freedom to view a structure in three (or even four) dimensions non-destructively.

With this in mind we aim to test the hypothesis that web-like features may be formed as a function of sediment, and not automatically assumed to be of semi-palmate/palmate origin. A comparison of fossil tracks and finite element modelling (FEA) of substrate under dynamic loading is used herein to test this hypothesis.

### 1.1. The finite element method

Finite element analysis (FEA) is a numerical analysis technique common in engineering for exploring the mechanics of continuous media, though the method is applicable to a broad variety of mathematical problems that arise in almost all areas of science (Burnet, 1987; Smith and Griffiths, 2004). In simple terms, the method approximates the governing equations of a continuous system by dividing the continuum into 'finite elements.'

Many palaeontologists will primarily associate FEA with its use in testing load and subsequent stress within bones (Rayfield et al., 2001; Rayfield, 2004, 2005). Rayfield (2007) provides a review of the uses of FEA in palaeontology and also of the method itself.

A volume of sediment is composed of individual grains (of varying size and form), as well as water and air in pore spaces. However, a given volume of sediment, sufficiently large in relation to its constituent grains, can be considered as a single entity. This entity will have properties that define its behaviour under load (assuming homogeneity, heterogeneous volumes can be treated as 'blocks' of differing homogeneous volumes). As such, a volume of sediment can be treated as a continuum, and studied using FEA. This has been the case in the engineering fields for several decades, and the use of FEA for solving problems involving soils and sediments is now common place; for example, soil settlement (Scheiner et al., 2006), tire–soil interaction (Nakashima and Wong, 1993; Shoop, 2001; Fervers, 2004; Nakashima and Oida, 2004; Shoop et al., 2006) and building foundation problems (Johnson et al., 2006). A framework is therefore in place for defining and solving problems of soil deformation under load. This framework can be used to study vertebrate track formation.

## 2. Materials and methods

### 2.1. Fossil track

The specimen used as an example of a semi-palmate track was a cast of *Sarjeantopodus semipalmatus* (Lockley et al., 2004). The original fossil is held in the collections of the University of Colorado Dinosaur Tracks Museum (specimen no: CU-MWC224.4). The original locality was in eastern Wyoming, (U.S.A.), though was located on private land so exact locality data is withheld (Lockley et al., 2004). Found in the Late Cretaceous Lance Formation, the track horizon was located as casts on the underside of a 0.1 m thick, fine-grained sand/mud layer, situated a few centimetres above a major dinosaur track layer (Lockley and Rainforth, 2002; Lockley et al., 2004). The track horizon where CU-MWC224.4 was located also preserved raindrop impressions and small ripples.

In addition to the specimen (cast), a hand held laser scanner was used to generate a 3D digital surface of the track. The scanner used was a Polhemus FastScan Cobra capable of achieving >0.1 mm resolution. This allowed virtual manipulation of the track, including viewing the surface as an impression rather than a cast, and also allowing profile sections to be taken non-destructively. A digital representation of the track was directly compared with a surface generated by the FEA.

### 2.2. Finite element simulations

The software used herein was developed in-house, being a modified version of a three-dimensional finite element program in Smith and Griffiths (2004). The program uses a von Mises elasto-plasticity model to represent the plastic behaviour of the sediment.

A relatively simple cuboid mesh was created from hexahedral elements, each defined by eight nodes. To increase efficiency and decrease run time whilst maintaining a high resolution output, a scaling factor produced larger elements away from the source of loading (the 'foot'), and smaller elements beneath the load where deformation would be most intense and complex. The simulation was run at the meter scale for ease of use, though the results are directly scalable. The mesh measured 2 m×2 m at the surface, and was 1 m deep. This large size prevented any boundary effects caused by fixed nodes at the edges of the soil volume. Whilst the elements were arranged in 1 cm layers, these layers were given uniform properties creating a homogeneous sediment.

Loading was achieved through the direct displacement of surface nodes defining a track outline. The outline represents a generic tridactyl foot measuring 0.6 m in length (Fig. 1).

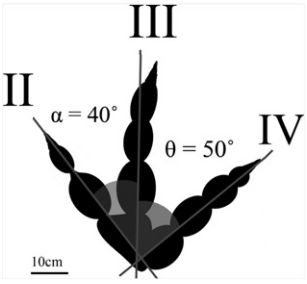


**Fig. 1.** Outline used to represent tridactyl foot. Interdigital angle (IDA) between Digits II and III — 40°, IDA between Digits III and IV — 50°. Foot length=60 cm.

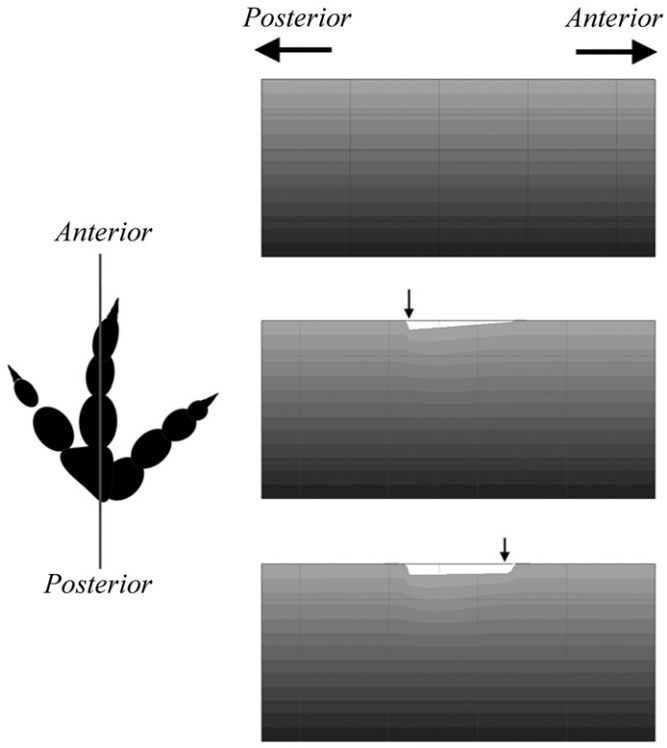


**Fig. 2.** Three cross-sections through a soil volume undergoing dynamic loading (top — prior to loading; centre — after 'heel' nodes are displaced; bottom — after full loading cycle). Sections are taken as indicated by the line through the track on the left.

The nodes were displaced in such a manner that the most posterior nodes (those forming the rear of the virtual foot) were vertically displaced first, followed by the anterior nodes (Fig. 2). This approximated a heel–toe step cycle where the centre of mass passes anteriorly over the foot, as opposed to a static loading scenario in which all nodes are displaced uniformly, a difference comparable to that between an animal standing still on a sediment, and an animal walking over that sediment. Manning et al. (in review) showed the difference in results obtained from static and dynamic loading regimes, where the dynamic loading produced more extensive zones of shear and deformation than static loading.

The sediment was defined by three parameters: undrained shear strength ($u$), Young's modulus ($E$) and Poisson's ratio ($v$). The undrained shear strength controls the stiffness and resistance of the sediment to shearing, the Young's modulus is the modulus of elasticity, and the Poisson's ratio is the measure of compressibility (the ratio of compression in one axis to extension along the normal axis), with 0.5 being incompressible and 0 being entirely compressible. Typical values for shear strength and Poisson's ratio are given in Tables 1 and 2 respectively. The Young's modulus varies and is defined according to these parameters.

**Table 1**
Undrained strength classification of clays according to BS 8004:1986 (from Craig, 1997)

| Consistency | Undrained strength (kN/m$^2$) |
|---|---|
| Very stiff or hard | >150 |
| Stiff | 100–150 |
| Firm to stiff | 75–100 |
| Firm | 50–75 |
| Soft to firm | 40–50 |
| Soft | 20–40 |
| Very soft | <20 |

**Table 2**
Typical values for Poisson's ratio in various substrates (from Bowles, 1968)

| Material | Typical values for Poisson's ratio |
|---|---|
| Saturated clay | 0.4–0.5 |
| Rock | 0.1–0.4 |
| Sand, gravely sand | 0.3–0.4 |
| Silt | 0.3–0.35 |
| Sandy clay | 0.2–0.3 |
| Loess | 0.1–0.3 |

The properties used for the experiment were chosen to represent a waterlogged fine sand/mud such as that found at the side of a body of water, following the palaeoenvironment and sedimentological interpretation offered by Lockley et al. (2004). As such, a high Poisson's ratio was used: $v$=0.499, and a low shear strength: $u$=45 kN/m$^2$ consument to the sediment conditions prevailing at the time of track formation (Lockley et al., 2004).

Saturated sediment, by definition, has a large amount of pore water occupying intergranular spaces. The relative incompressibility of water compared with the air it has replaced increases the Poisson's ratio to approach incompressibility. However, a saturated sediment also begins to loose cohesion between grains, as water both lubricates movement and forces grains apart, thus the shear strength decreases with increased moisture content (Smith, 1981), resulting in a soft sediment.

## 3. Fossil description

The fossil is a natural cast and is hence seen in positive relief (Fig. 3). The track has three prominent digits, and was described to be a left track, with a 'web-like' structure occurring prominently between the central and right digits (II and III), and less pronounced between the central and left digits (III and IV) (Lockley et al., 2004). This interdigital structure appears as a 'platform' when viewed in profile (Fig. 4). A reversed digit is also present at the posterior of the track at an angle to the central axis. The central part of the foot, where the digits converge, is not impressed clearly. Track length is ~95 mm from tip of Digit III to the tip of the reversed digit; and track width is also ~95 mm from tip of Digit II to tip of Digit IV.

Shallow sinuous asymmetric ripples are present on the surface, more visible in the profile image taken from the laser scan than the original natural cast (Fig. 5). Small circular impressions are also present, and are concentrated on the crests of the ripples. These impressions are distributed unevenly over the ripples, occurring more on the stoss side of the ripple (Figs. 3 and 5).

## 4. Simulated track description

The finite element track displayed features consistent with wet, soft sediment deformation, including displacement rims and an uneven surface (Manning, 1999). Of particular interest with regard to this paper, is the form of the displacement rim between Digits III and IV. Here, the sediment is stepped (Figs. 6 and 7), creating a visible line between the digits from the tip of Digit IV to approximately half way along Digit III. Additionally, there is a smaller ridge of similar form between Digits III and II, though this structure is less pronounced, extending from digit tip to digit tip.

An advantage to the FEA model is to easily look within the sediment and view surfaces at any level within the 3D volume. At 50 cm depth below the track surface, and though the track has become faint by this depth, being less than 1 cm in relief, there is still a distinct failure structure between the digits comparable to the surface track (Fig. 8).

A second FEA track was produced with a higher shear strength ($u$=65 kN/m$^2$, approximating a 'firm' clay). However, this track did not show any signs of failure between digits.

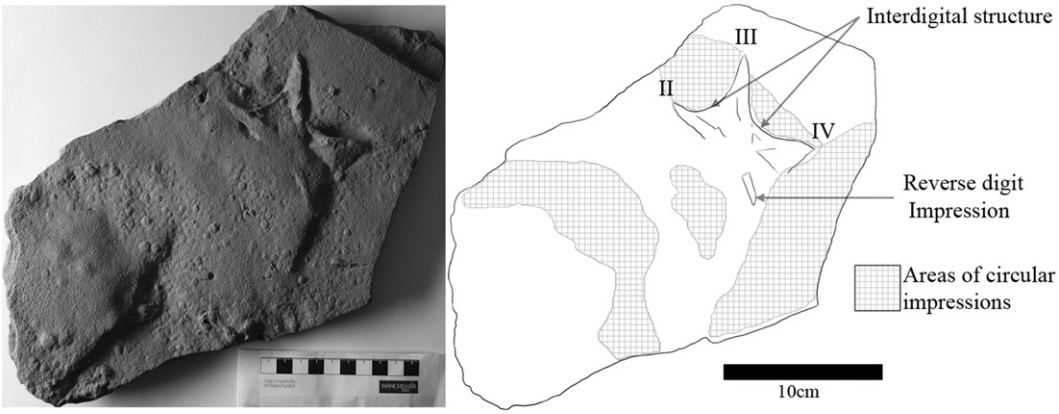


**Fig. 3.** Photograph and outline drawing of cast of CU-MWC224.4 highlighting interdigital features, locations of circular impressions and digits of track. Scale bar = 10 cm, light source from the left.

Also, two further experiments were undertaken to investigate the effects of interdigital angle. In the first experiment, Digit IV was rotated to create a smaller interdigital angle (25°), and a narrower foot, whilst in the second experiment the procedure was reversed and the digit was rotated back to produce a larger interdigital angle (95°) (Fig. 9). Substrate conditions were identical to the original experimental

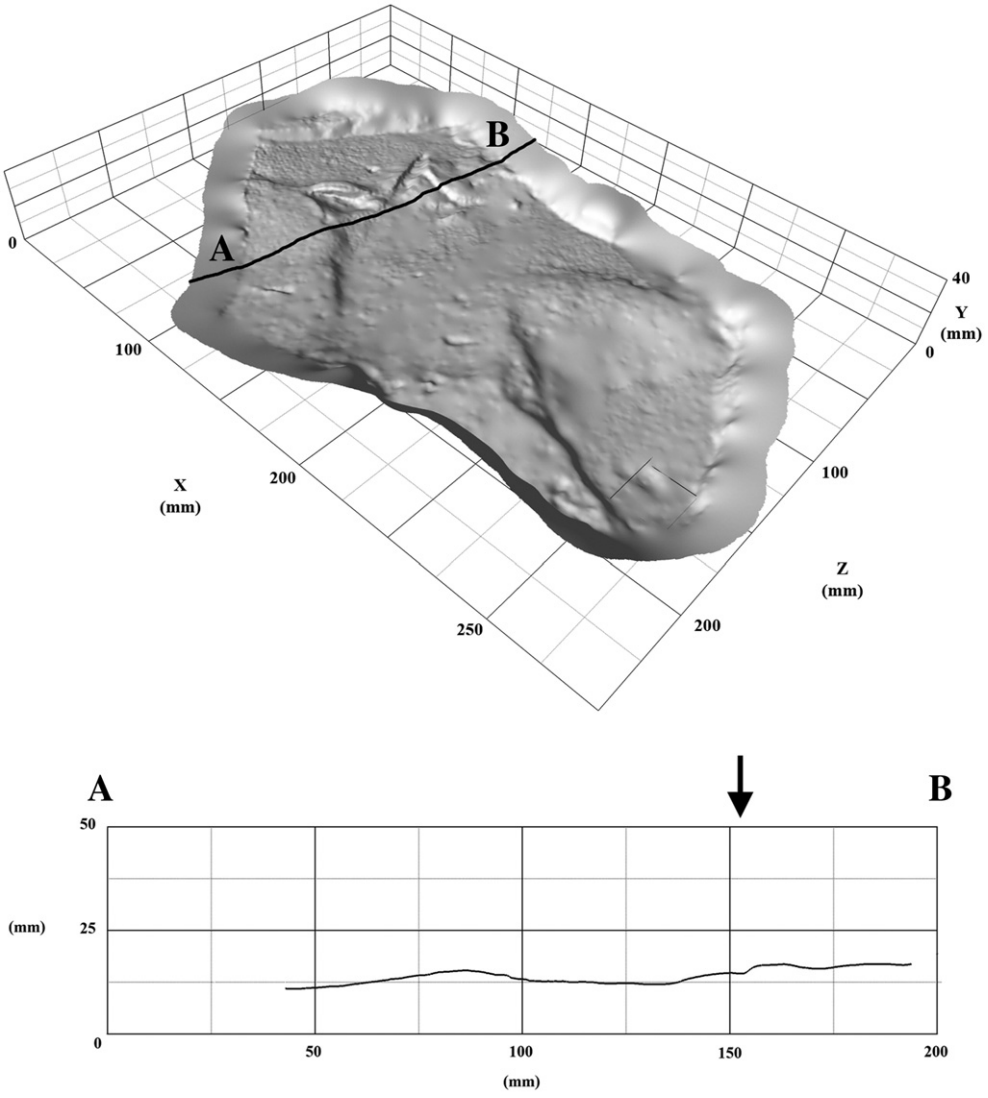


**Fig. 4.** Laser scanned surface (overturned) and profile of CU-MWC224.4. Arrow above profile indicates structure referred to as 'webbing impression.' Light in upper image is from the left.

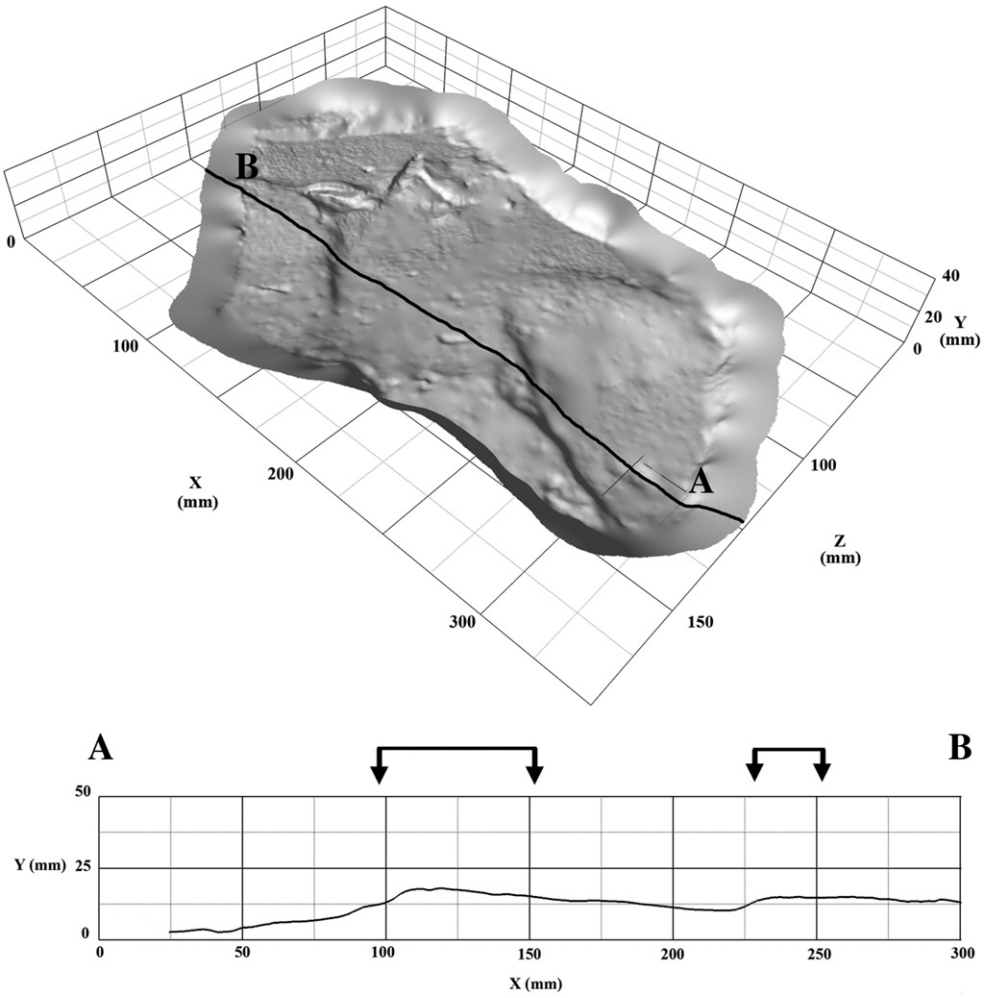


**Fig. 5.** Laser scanned surface (overturned) and profile of CU-MWC224.4. Arrows above profile indicate areas of concentrated raindrop impressions. Light in upper image is from the left.

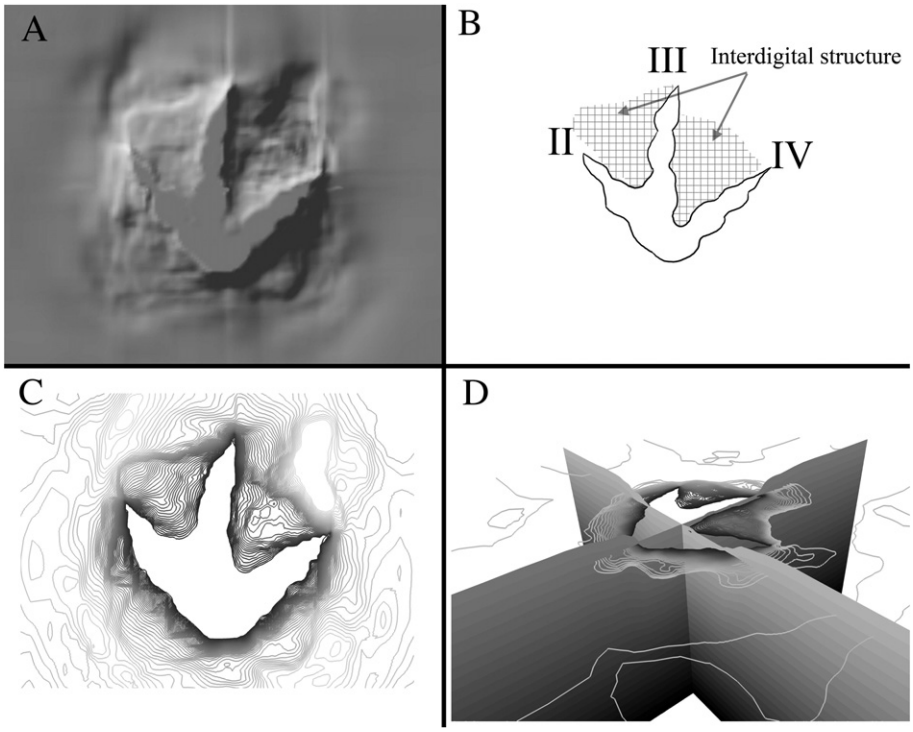


**Fig. 6.** A) Simulated track formed in virtual substrate comparable to wet, soft sediment, light source is from the lower right. B) Interdigital structures are labelled. C) Two-dimensional map of isolines of displacement, closer contours indicate steeper gradient. Note steepest gradients at extents of interdigital structures. D) Location of 2D displacement map relative to 3D volume.

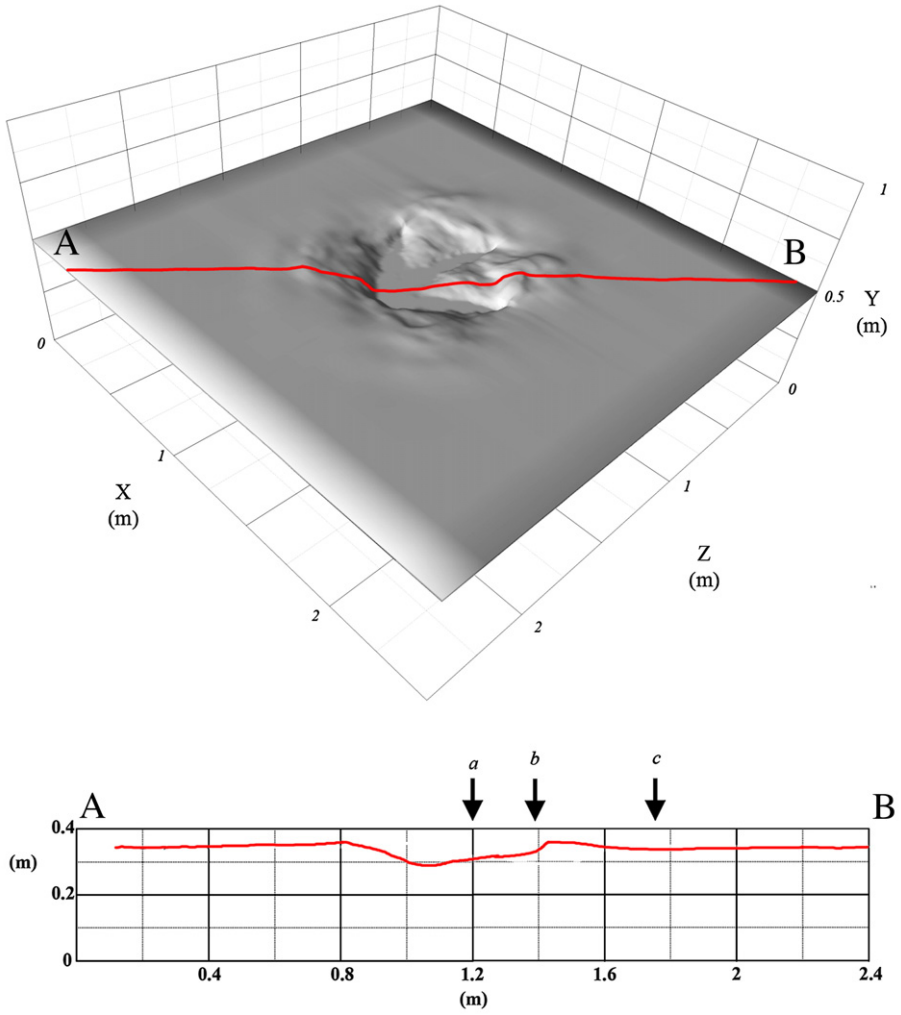


**Fig. 7.** Surface track and cross-sectional profile of finite element track. Arrows labelled 'a' 'b' and 'c' mark; the start of sediment displacement beyond the foot–sediment interface, the 'stepped' structure in the displacement and the extremity of the displacement rim respectively.

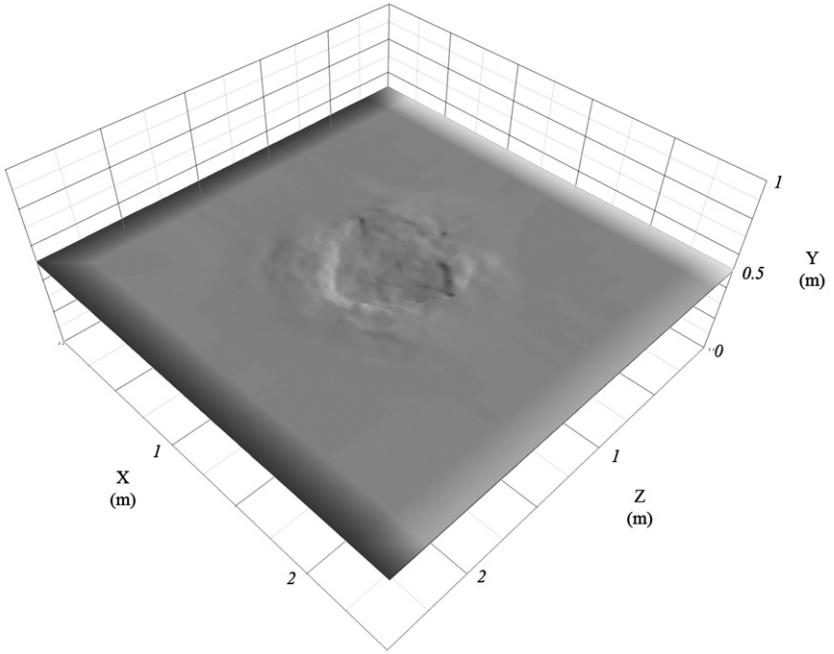


**Fig. 8.** Surface at 50 cm depth below surface seen in Fig. 7.

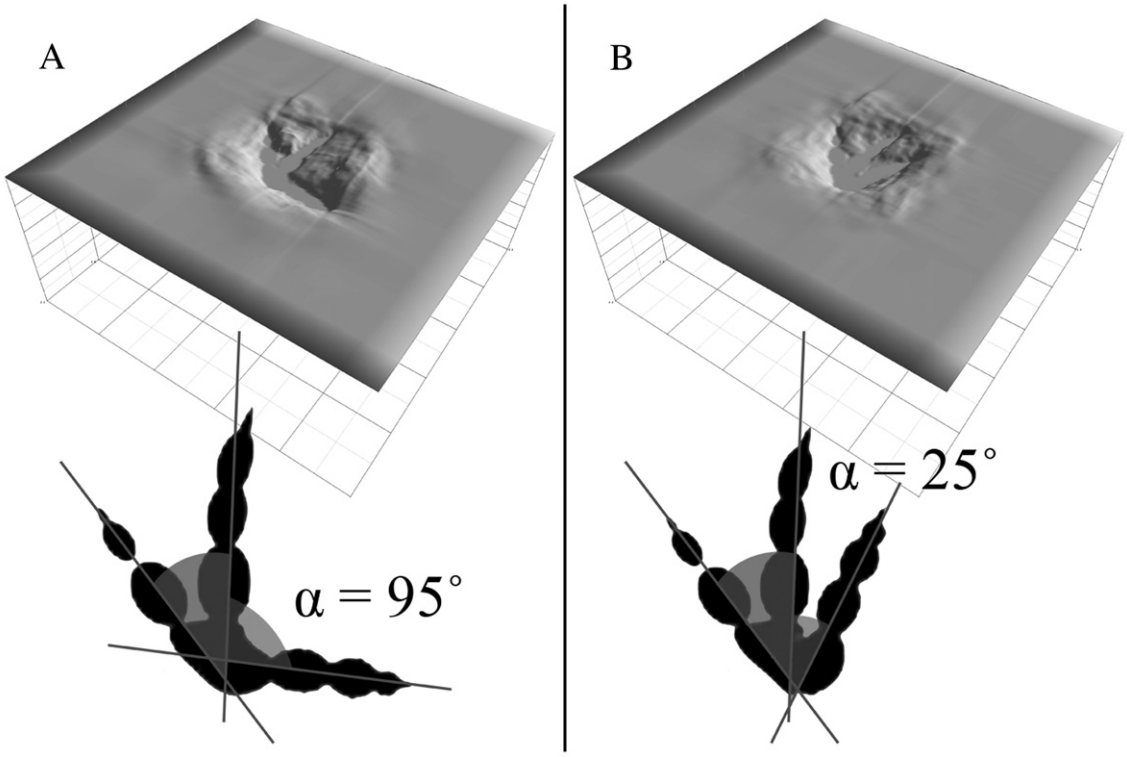


**Fig. 9.** Experiments in which wider (A) and narrower (B) interdigital angles between Digits III and IV were used.

conditions. In neither experiment was a feature analogous to 'webbing' visible.

## 5. Discussion

The fossil track CU-MWC224.4 has previously been interpreted as being generated by a semi-palmate (webbed) bird foot (Lockley et al., 2004). The surface upon which the track is located is rippled and covered with circular impressions interpreted as rain pitting. The ripples are shallow and asymmetric, which are consistent with the palaeoenvironmental interpretation of shallow water at the edge of a channel. The raindrops occur almost exclusively on the crests of ripples, implying some difference between the crests and the troughs affecting the formation and/or preservation of raindrop impressions. We propose standing water of a few mm, which occupied the topographic lows, leaving the drier ripple crests exposed. Reineck and Singh (1980, p. 61) suggest that raindrops falling on a freshly exposed rippled surface will form better impact impressions on the relatively drier crests than the wet troughs. This is supported by the presence of raindrops extending further over the stoss side of the ripples, creating a palaeo-waterline. The interpreted environmental setting is of wet, waterlogged fine-grained sediment located at the edge of flowing water, supporting the original interpretation (Lockley et al., 2004).

Taking this into account, the finite element model was created with similar properties to a fine-grained, saturated substrate. The indentation of a tridactyl foot resulted in a track with a feature very similar to the 'webbing' described in CU-MWC224.4. This structure formed through sediment failure as the sediment was pushed up between the toes, and then collapsed. This 'interdigital shear' was described by Manning (1999, 2004), and represents a peak of stress within the sediment that causes shearing. The interdigital shear was present in subsurface deformation to a considerable depth.

When interdigital angle was increased or decreased for Digits III and IV, the simulation did not produce web-like structures. This implies a specific IDA in tridactyl feet conducive to forming web-like structures through sediment failure, in this case the resultant 'webbed' track had an IDA of 50° where 'webbing' formed (between Digits III and IV). It should be noted here that the fossil track CU-MWC224.4 has interdigital angles of 50° and 90° between Digits II and III and III and IV respectively, and the prominent webbing is only located between Digits II and III. Where the IDA is large, a much smaller structure is observed.

Given the palaeoenvironment in which the track was formed, we propose that rather than webbing, these structures are a function of sedimentary environment, foot morphology, digit position, and rheology. Such a scenario accounts for the trackway described by Lockley et al. (2004, Fig. 15a), where only two of the three tracks in a single trackway appear to have 'webbing', and this 'webbing' varies between individual tracks. Alternatively, in a firm substrate it is conceivable that a webbed foot may leave no evidence of webbing as the weight bearing digits support the web above the substrate surface. If this were the case however, the tracks would be considerably shallower.

The presence of an algal or microbial mat on the surface of the sediment would alter the properties of the upper few mm. Providing the foot did not puncture the substrate surface, the microbial mat may provide adhesion between grains to prevent the failure seen in the FEA models. If however the foot did puncture the mat, the adhesive properties offered would hold the platformed sediment in place, potentially exaggerating the 'webbed' effect.

The ideal conditions for sediment failure to produce a 'webbed' track (wet, soft, fine-grained sediment), coincide with the conditions in which one would expect waterbirds with palmate feet to be found, leading to inherent complications in interpreting palmate tracks. Sediment deformation, however, may be considered the most likely/parsimonious explanation in specific cases, especially when 'webbed' tracks would extend the phylogenetic range of palmate birds, or would imply the presence of interdigital webbing in groups such as dinosaurs that currently have no supporting evidence for such an interpretation.

## 6. Conclusions

Using new methods including FEA and high resolution laser scanning, we have shown the mechanism by which a track can be produced with a palmate or semi-palmate morphology, even when the foot itself is not webbed. In this case, the example track used indicated a waterlogged substrate. This is supported with the FEA simulations in which low shear strength and high Poisson's ratio (soft and incompressible) produced 'semi-palmate' tracks.

Saturated, soft, fine-grained substrate is ideal for this type of sediment failure, but is also the predicted sediment in which to find palmate tracks. This means that we present only an alternative hypothesis, rather than a replacement. However, the implications of this apply to all palmate/semi-palmate tracks in the fossil record, suggesting care should be taken when describing such tacks in the future. Descriptions of track features should look for direct evidence of webbing (e.g. skin impression) or sediment failure, especially when the tracks occur outside the phylogenetic range of palmate birds as defined by other fossils.

## Acknowledgements

We would like to thank NERC for providing a grant to Falkingham (ref: NER/S/A/2006/14033), P. Larson for access to cast material, and Karl Bates for constructive comments and discussion during the writing of the paper. Also Finn Surlyk, Jesper Milàn, and Brent Breithaupt for constructive reviews of the manuscript. The finite element simulations were carried out using HECToR, through EPSRC project EP-F055595-1.

## References

Allen, J.R.L., 1989. Fossil vertebrate tracks and indenter mechanics. Journal of the Geological Society 146, 600–602.

Allen, J.R.L., 1997. Subfossil mammalian tracks (Flandrian) in the Severn Estuary, SW Britain: mechanics of formation, preservation and distribution. Philosophical Transactions of the Royal Society of London. Series B, Biological Sciences 352, 481–518.

Bates, K.T., 2006. The application of Light Detection and Range (LIDAR) imaging to vertebrate ichnology and geoconservation (M. Phil Theses), University of Manchester, Manchester, 347 pp.

Bates, K.T., Rarity, F., Manning, P.L., Hodgetts, D., Vila, B., Oms, O., Galobart, À., Gawthorpe, R., 2008. High-resolution LiDAR and photogrammetric survey of the Fumanya dinosaur tracksites (Catalonia): implications for the conservation and interpretation of geological heritage sites. Journal of the Geological Society, London 165, 115–127.

Bowles, J.E., 1968. Foundation Analysis and Design. McGraw-Hill, New York. 659 p.

Burnet, D.S., 1987. Finite Element Analysis from Concepts to Applications. Addison-Wesley Publishing Company, Reading, M.A. 844 pp.

Craig, R.F., 1997. Soil Mechanics. Chapman & Hall, London. 485 pp.

Day, J.J., Norman, D.B., Gale, A.S., Upchurch, P., Powell, H.P., 2004. A Middle Jurassic dinosaur trackway site from Oxfordshire, UK. Palaeontology 47, 319–348.

Fervers, C.W., 2004. Improved FEM simulation model for tire–soil interaction. Journal of Terramechanics 41, 87–100.

Henderson, D.M., 2006. Simulated weathering of dinosaur tracks and the implications for their characterization. Canadian Journal of Earth Sciences 43, 691–704.

Johnson, K., Lemcke, P., Karunasena, W., Sivakugan, N., 2006. Modelling the load-deformation response of deep foundations under oblique loading. Environmental Modelling & Software 21, 1375–1380.

Karafiath, L.L., Nowatzki, E.A., 1978. Soil mechanics for off-road vehicle engineering. Series on Rock and Soil Mechanics. Trans Tech publications, Aedermannsdorf. 515 pp.

Kim, J.Y., Kim, S.H., Kim, K.S., Lockley, M., 2006. The oldest record of webbed bird and pterosaur tracks from South Korea (Cretaceous Haman Formation, Changseon and Sinsu Islands): more evidence of high avian diversity in East Asia. Cretaceous Research 27, 56–69.

King, M.J., Benton, M.J., 1996. Dinosaurs in the Early and Mid Triassic? — The footprint evidence from Britain. Palaeogeography, Palaeoclimatology, Palaeoecology 122, 213–225.

Lim, J.-D., Zhou, Z., Martin, L.D., Baek, K.S., Yang, S.Y., 2000. The oldest known tracks of web-footed birds from the Lower Cretaceous of South Korea. Naturwissenschaften 87, 256–259.

Lockley, M., Rainforth, E., 2002. The tracks record of Mesozoic birds and pterosaurs: an ichnological and paleoecological perspective. In: Chiappe, L., Witmer, L.M. (Eds.), Mesozoic Birds above the Heads of Dinosaurs. University of California Press, Berkeley, pp. 405–418.

Lockley, M.G., Nadon, G., Currie, P.J., 2004. A diverse dinosaur-bird footprint assemblage from the Lance Formation, Upper Cretaceous, Eastern Wyoming: implications for ichnotaxonomy. Ichnos 11, 229–249.

Manning, P.L., 1999. Dinosaur track formation, preservation and interpretation: fossil and laboratory simulated dinosaur track studies. Ph.D Thesis, University of Sheffield (England).

Manning, P.L., 2004. A new approach to the analysis and interpretation of tracks: examples from the dinosauria. In: McIlroy, D. (Ed.), The Application of Ichnology to Palaeoenvironmental and Stratigraphic Analysis. Special Publications, Geological Society, London, pp. 93–123.

Manning, P.L., 2008. *T. rex* speed trap. In: Carpenter, K., Larson, P.L. (Eds.), *T. rex* Symposium Volume. Indiana University Press, Bloomington, pp. 205–231.

Manning, P.L., Margetts, L., Leng, J., Smith, I.M., Falkingham, P.L., in review. Using computer simulation to gain a new perspective on dinosaur trackways.

Margetts, L., Smith, I.M., Leng, J., Manning, P.L., 2006. Parallel three-dimensional finite element analysis of dinosaur trackway formation. In: Schweiger, H.F. (Ed.), Numerical Methods in Geotechnical Engineering. Taylor & Francis, London, pp. 743–749.

Milàn, J., 2006. Variations in the morphology of emu (*Dromaius novaehollandiae*) tracks reflecting differences in walking pattern and substrate consistency: ichnotaxonomic implications. Palaeontology 49, 405–420.

Milàn, J., Bromley, R.G., 2006. True tracks, undertracks and eroded tracks, experimental work with tetrapod tracks in laboratory and field. Palaeogeography, Palaeoclimatology, Palaeoecology 231, 253–264.

Milàn, J., Bromley, R.G., 2008. The impact of sediment consistency on track and undertrack morphology: experiments with emu tracks in layered cement. Ichnos 15, 19–27.

Milàn, J., Clemmensen, L.B., Bonde, N., 2004. Vertical sections through dinosaur tracks (Late Triassic lake deposits, East Greenland) — undertracks and other subsurface deformation structures revealed. Lethaia 37, 285–296.

Nakashima, H., Wong, J.Y., 1993. A three-dimensional tire model by the finite element method. Journal of Terramechanics 30, 21–34.

Nakashima, H., Oida, A., 2004. Algorithm and implementation of soil–tire contact analysis code based on dynamic FE-DE method. Journal of Terramechanics 41, 127–137.

Rayfield, E.J., 2004. Cranial mechanics and feeding in *Tyrannosaurus rex*. Proceedings of the Royal Society of London. Series B, Biological Sciences 271, 1451–1459.

Rayfield, E.J., 2005. Using finite-element analysis to investigate suture morphology: a case study using large carnivorous dinosaurs. Anatomical Record. Part A, Discoveries in Molecular Cellular and Evolutionary Biology 283A, 349–365.

Rayfield, E.J., 2007. Finite element analysis and understanding the biomechanics and evolution of living and fossil organisms. Annual Review of Earth Planetary Sciences 35, 541–576.

Rayfield, E.J., Norman, D.B., Horner, C.C., Horner, J.R., Smith, P.M., Thomason, J.J., Upchurch, P., 2001. Cranial design and function in a large theropod dinosaur. Nature 409, 1033–1037.

Reineck, H.E., Singh, I.B., 1980. Depositional Sedimentary Environments. Springer Verlag, Berlin. 542 pp.

Sarjeant, W.A.S., 1967. Fossil footprints from the Middle Triassic of Nottingham and the Middle Jurassic of Yorkshire. Mercian Geologist 3, 269–282.

Scheiner, S., Pichler, B., Hellmich, C., Eberhardsteiner, J., 2006. Loading of soil-covered oil and gas pipelines due to adverse soil settlements — protection against thermal dilatation-induced wear, involving geosynthetics. Computers and Geotechnics 33, 371–380.

Shoop, S.A., 2001. Finite element modelling of tire–terrain interaction. ERDC/CRREL TR-01-16, U.S. Army Corps of Engineers, Engineer Research and Development Center.

Shoop, S., Kestler, K., Haehnel, R., 2006. Finite element modeling of tires on snow. Tire Science and Technology 34, 2–37.

Smith, M.J., 1981. Soil Mechanics. George Godwin, London. 168 pp.

Smith, I.M., Griffiths, D.V., 2004. Programming the Finite Element Method. Wiley, Chichester. 628 pp.

Yang, S.Y., Lockley, M., Greben, R., Erikson, B.R., Lim, S.Y., 1995. Flamingo and duck-like bird tracks from the Late Cretaceous and Early Tertiary: evidence and implications. Ichnos 4, 21–34.

You, H.-L., Lamanna, M.C., Harris, J.D., Chiappe, L.M., O'connor, J., Jl, S.-A., Lu, J.-C., Yuan, C.-X., Li, D.-Q., Zhang, X., Lacovara, K.J., Dodson, P., Ji, Q., 1995. A nearly modern amphibious bird from the early cretaceous of northwestern China. Science 312 (5780), 1640–1643.

# Chapter 8 - Fossil vertebrate tracks as palaeopenetrometers: Confounding effects of foot morphology

A paper accepted for publication in the journal PALAIOS.

Presented as a manuscript formatted for the journal.

Reference:

Falkingham, P.L., Margetts, L. and Manning, P.L., 2010. *Fossil vertebrate tracks as palaeopenetrometers: Confounding effects of foot morphology*. PALAIOS. **25**(6):356-360

# FOSSIL VERTEBRATE TRACKS AS PALAEOPENETROMETERS: CONFOUNDING EFFECTS OF FOOT MORPHOLOGY

FALKINGHAM, P. L.[1]*, MARGETTS, L.[1, 2] and MANNING, P. L.[1, 3]

[1]*School of Earth, Atmospheric and Environmental Science, University of Manchester, Williamson Building, Oxford Road, Manchester, M13 9PL, UK.*

[2]*Research Computing, University of Manchester, Devonshire House, Oxford Road, Manchester, M13 9PL, UK.*

[3]*Department of Earth and Environmental Science, University of Pennsylvania, 254-b Hayden Hall, 240 South 33rd Street, Philadelphia, PA 19104-6316.*

*Email: peter.falkingham@manchester.ac.uk*

*Corresponding author



Keywords: Dinosaur, bird, footprint, finite element analysis, soil mechanics.

## ABSTRACT

**The depth to which a vertebrate track is indented can provide a wealth of information, being a direct result of the weight, duty factor, and limb kinematics of the animal as well as media (=substrate or sediment) consistency. In order to recreate the formation of the track and elucidate media consistency at the time of track formation, such factors as animal mass, duty factor, and foot morphology must be taken into consideration. This study uses Finite Element Analysis and physical modeling to demonstrate for the first time that the shape of the foot is an important factor that influences the depth to which the sediment is penetrated. In cohesive sediment, less compact morphology allows more sediment to move vertically upwards at the edges of the foot, dissipating force at the surface, and retarding transmission of load vertically down into the sediment. The reverse of this effect is seen in noncohesive sediment. Foot morphology, therefore, has a direct impact on preservation potential, both of surface tracks and undertracks that is irrespective of the pressure exerted on the sediment surface by the foot and independent of mass and duty factor.**

## INTRODUCTION

In this paper, the effect of foot morphology on track depth is investigated by using Finite Element Analysis (FEA) to indent a series of abstract foot geometries. As a measure of foot morphology, a metric derived from circumference, or edge length, has been used, where edge length can be defined as the boundary between foot and sediment when seen in plan view. FEA has previously been applied to the study of track formation to show that interdigital

webbing may arise as an effect of media deformation, rather than as the impression of true webbing (Falkingham et al., 2009), and to illustrate subsurface deformation and undertrack formation beneath vertical and heel-toe cycle loads (Margetts et al., 2005; Margetts et al., 2006; Falkingham et al., 2007; Falkingham et al., 2008).

While vertebrate ichnotaxa may be difficult to constrain to specific environmental or media conditions, we are provided with tracks produced in multiple media with relatively consistent loading conditions (e.g., pressure, force vectors, pedal morphology, etc), resulting in track morphologies that may vary to a considerable degree due entirely to media consistency (Manning, 2004; Milàn and Bromley, 2006, 2008; Díaz-Martínez et al., 2009). Even if two different animals that share foot morphology and limb kinematics are separated temporally and spatially, there may be enough consistency in loading conditions that differences in the tracks—magnitude of displacement rims, radial cracks, track depth—can be used to infer media conditions at the time of track formation in different strata. Much of this sedimentary variation may be linked to water content (e.g., Platt and Hasiotis, 2006), which is in turn controlled by environmental factors (e.g., Hasiotis, 2007). In a cohesive media, water content directly determines both the shear strength of the material (through creating cohesion between particles) and the Poisson ratio (compressibility). Extremes of moisture content prevent track formation either because the media is too loose, or too liquid (Laporte and Behrensmeyer, 1980; Platt and Hasiotis, 2006).

Given that track depth is a function of the force applied through the sole of the foot over a given media, there is therefore the potential to use tracks as paleopenetrometers (Lockley, 1987; Allen, 1989; Nadon and Issler, 1997;

Nadon, 2001), whereby the depth of a track may be used to gauge the media consistency at the time of track formation, and subsequently used to refine paleoenvironmental interpretations (Lockley, 1986; Nadon and Issler, 1997; Nadon, 2001; Platt and Hasiotis, 2006). In order to do so with confidence, other confounding factors influencing the depth of a track must be understood and taken into account.

## METHODS

Two experiments were carried out to investigate the effects of varying pedal complexity on penetration of the media, one in which FEA was used to explore the effects of indenter morphology, and a second in which physical modeling was used to investigate the differing response of sand and mud. Physical modeling was necessary due to the inability of the computer model to model granular (i.e. sandy) substrates. FEA provides a means for investigating stress and strain within a continuous medium under load, and is now a tried and tested technique in paleontology. See Rayfield (2007) for a comprehensive review of the method, and Falkingham et al. (2007; 2008; 2009) and Margetts et al (2005; 2006) for details of the method as applied to track simulations.

The first experiment involved generating geometrically abstract shapes to act as indenters, which maintained a consistent surface area, but differed in complexity. The same pressure was then applied to the surface of each indenter. By using geometrically abstract shapes, complete control over shape complexity could be achieved, and FEA meshes consisting of relatively few elements used, facilitating rapid analysis (Rayfield, 2007).

These analyses were undertaken using a program written by us using ParaFEM (www.parafem.org.uk), a freely available parallel finite element library. The program was validated using a series of geotechnical engineering test problems, such as the bearing capacity of a smooth flexible footing (Smith and Griffiths, 2004). Results of these validation examples were compared with empirical solutions and with analyses carried out using Abaqus/CAE version 6.8-2 (http:// www.simulia.com/).

A second experiment was carried out using physical modeling. Indenters of equivalent shape as those used in experiment 1 were cut from wood and used to indent natural media.

*Measuring shape.*—In order to draw comparisons between indenters of differing morphology, a metric was required. As a measure of shape, edge length—the circumference of the indenter—was used as this varies with shape for a given sized indenter. Using absolute circumference or a ratio of edge length to surface area, however, provides a function that varies with size; a small square has a higher circumference to surface area ratio than a larger square. To take account of this, edge length was normalized using equation 1.

$$e' = (e/4)^2/A \qquad \text{(Eq. 1)}$$

Where $e'$ is the normalized edge length, $e$ is edge length, or circumference, of the indenter, and $A$ is the surface area of the indenter. A square will always have an $e'$ value of 1, regardless of size, whilst less compact morphologies will have a higher value, but one that will remain constant as size varies.

## Experiment 1

An FEA mesh representing a volume of elastic-perfectly-plastic soil was created using 20-node hexahedral elements and given the properties of a stiff mud [Young's Modulus = 100,000 kPa, Poisson Ratio = 0.4, Shear Strength = 100 kN/m$^2$ (Leach, 1994)]. On the surface of this mesh, an indenter was created, and given a Young's Modulus and Shear Strength sufficiently high as to make the indenter nondeformable relative to the media. This is a technique used by FEA users in geotechnical engineering to model rigid indenters (Potts and Zdravković, 1999, 2001). The elements used to define the indenter were arranged in seven different configurations, forming seven indenters, each with a surface area of nine units$^2$, but with edge lengths ranging from 12 units (the minimum possible for nine elements) to 20 units (the maximum possible) (Fig. 1). Corresponding values of *e'* ranged from 1 to 2.78. Two variations were created each for edge lengths of 14 and 20 units, one (Fig. 1C, F) more complex than the other (Fig. 1B, G). A uniform pressure of 10 units per unit area was applied to the surface of each indenter to provide a vertical load.

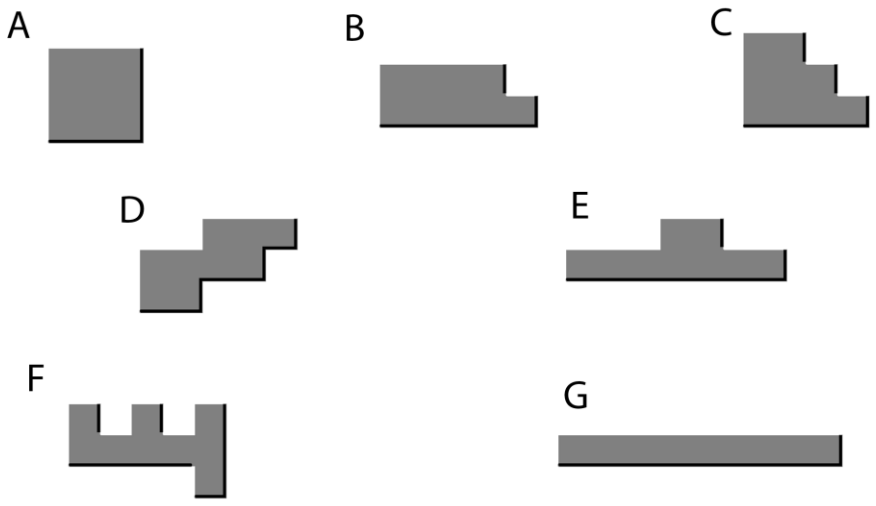


**Figure 1 - Indenter shapes used in experiment 1 (surface area = 9 units2) in plan view. Indenters are subsequently referred to as 1A, 1B etc.**

A second series of indenters were generated to explore the effects of indenter size on track depth, and each had a surface area of 16 square units (using 16 elements), providing a greater range of *e'* (1 to 4.52) (Fig. 2). The same pressure was applied as for the above scenario, and the soil properties remained constant. The parameters of each indenter are summarized in Table 1.

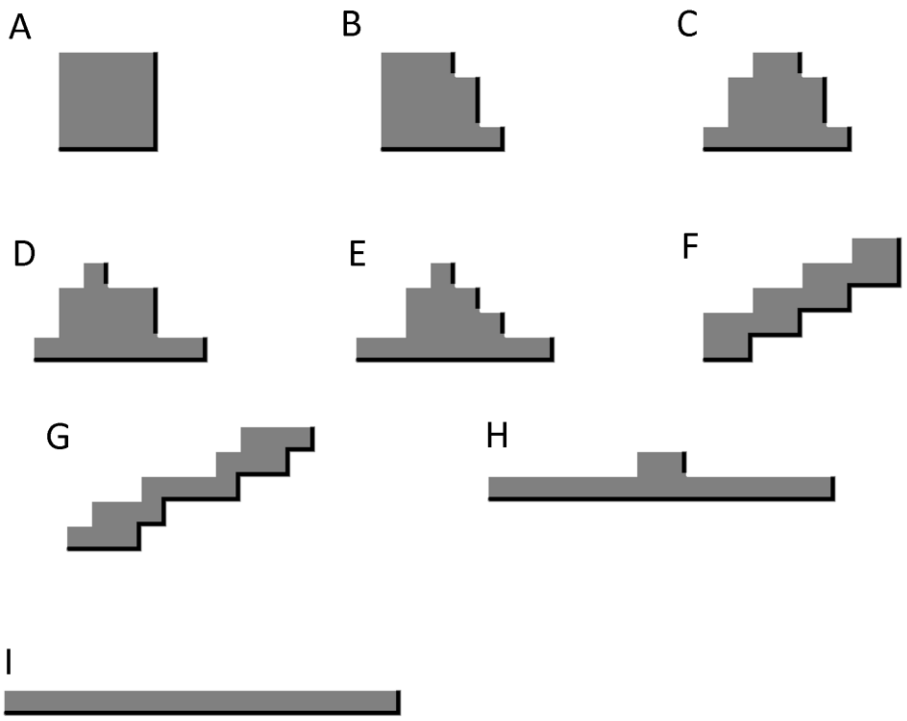


**Figure 2 - Indenter shapes with surface area = 16 units2, viewed in plan view. Subsequently referred to as indenters 2A to 2I. See table for details of edge lengths.**

There are many more possible indenter shapes that would retain constant surface area over a range of edge lengths, but it is not feasible to attempt to model them all here. The indenters used herein represent most of the extreme forms of complexity and simplicity.

In order to avoid effects of low-resolution meshes, a series of analyses were run on consecutively higher resolution meshes until the difference in final

result became negligible. Final mesh sizes were on the order of 400,000

| Indenter | Surface Area (units$^2$) | Edge length (units) | Edge to surface area ratio | Normalised Edge Length (*e'*) |
|---|---|---|---|---|
| 1A | 9 | 12 | 1.33 | 1 |
| 1B | 9 | 14 | 1.56 | 1.36 |
| 1C | 9 | 14 | 1.56 | 1.36 |
| 1D | 9 | 16 | 1.78 | 1.78 |
| 1E | 9 | 18 | 2 | 2.25 |
| 1F | 9 | 20 | 2.22 | 2.78 |
| 1G | 9 | 20 | 2.22 | 2.78 |
| 2A | 16 | 16 | 1 | 1 |
| 2B | 16 | 18 | 1.125 | 1.26 |
| 2C | 16 | 20 | 1.25 | 1.56 |
| 2D | 16 | 22 | 1.375 | 1.89 |
| 2E | 16 | 24 | 1.5 | 2.25 |
| 2F | 16 | 26 | 1.625 | 2.64 |
| 2G | 16 | 30 | 1.875 | 3.52 |
| 2H | 16 | 32 | 2 | 4 |
| 2I | 16 | 34 | 2.125 | 4.52 |

**Table 1 - Details of indenter surface area, edge length, edge length to surface area ratio, and e'.**

elements. Figure 3 shows how meshes were refined.

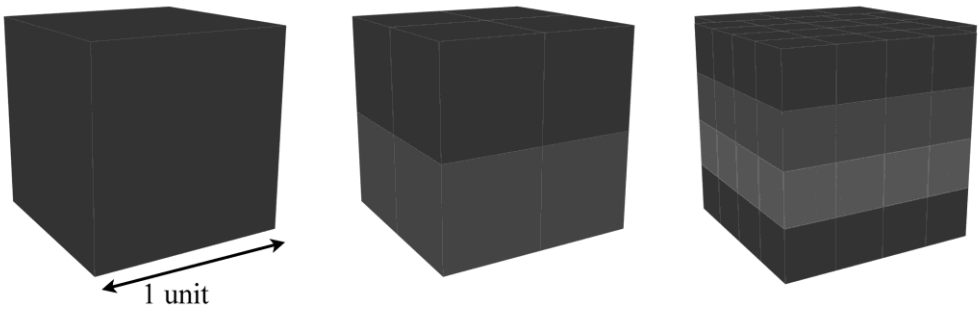


**Figure 3 - Increasing mesh resolution. Left; element size = 1 unit$^3$, Middle; elements with dimensions 50 % smaller (volume 25 % of original), and Right; smallest elements used (0.25 units$^3$). Each image is shown to the same scale.**

Experiment 2

For this experiment, indenters matching those used in experiment 1 (Fig. 1) were made from wood. These indenters were used to indent a soft mud with shear strength of ~5-10 kN/m$^2$ as measured *in situ* with a penetrometer. A consistent pressure of 3 kN/m$^2$ was slowly applied through each indenter using the penetrometer. Subsequent displacement was then measured. The above procedure was repeated for dry, fine-grained sand. These experiments were carried out numerous times and recorded depths were averaged for each indenter.

## RESULTS

### Experiment 1

Maximum displacement was plotted against edge length (Fig. 4). The maximum depth to which the indenters displaced the sediment decreased as complexity (given by *e'*) increased. The most complex shape (Fig. 1F), however, does not follow the pattern, instead indenting to a greater depth than the 'simple' indenter of edge length 20 (Fig. 1G). The data show an overall decrease in maximum vertical displacement corresponding to an increase in *e'*.

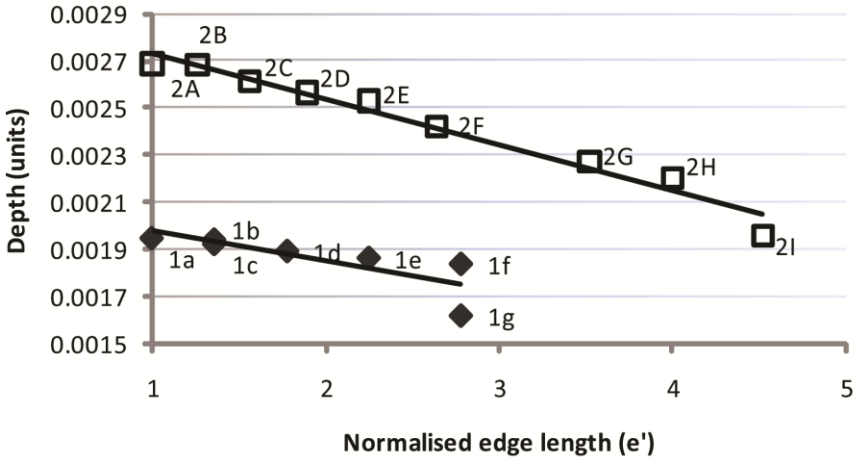


**Figure 4 - Graph plotting maximum vertical displacement beneath indenters of varying edge length, for indenters consisting of 9 or 16 elements, with subsequent surface area of 9 or 16 units$^2$ (diamonds and squares, respectively).**

Experiment 2

The values for depth of indentation in the mud and dry sand are shown in Figure 5. The indenters in mud showed slight reduction in depth with increasing *e'*, it can be seen that indenters 1G and 1F (*e'* = 2.78) both indented to a lesser degree than did indenter 1A (*e'* = 1), showing an extreme of only 50% of the depth of indenter 1A. The sand showed the reverse trend seen in the experiments with mud and in the FEA simulations; an increase in *e'* produced a greater depth of indentation. There is still the dichotomy between indenters 1B and 1C, and between 1Fand 1G.

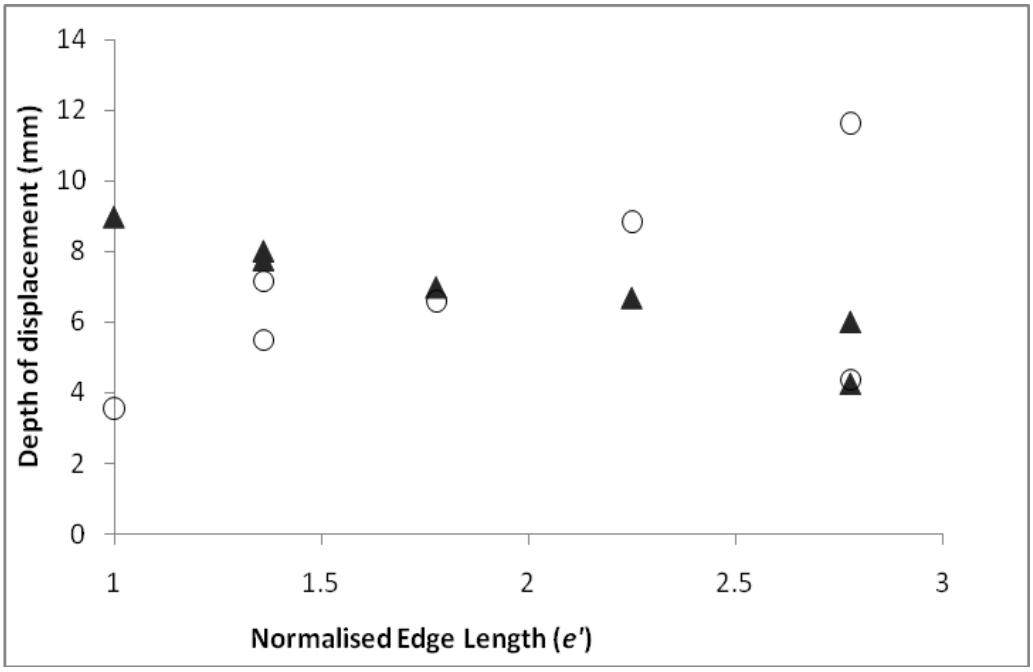


**Figure 5 - Mean depths of indentation for indenters 1A– 1F in mud (triangles) and dry sand (circles). Increasing normalized edge length results in a decrease in depth indented in cohesive mud, but an increase in noncohesive sand.**

## DISCUSSION

The results from experiment 1 show a general trend for decreasing displacement as edge length (*e'*) increases (Figs. 4, 6). Experiment 2 shows this trend in cohesive media, but that the reverse is true in noncohesive sand. This is consistent with soil mechanics theory; a noncohesive sand will displace to the greatest extent at the edges of an indenter because values of Young's Modulus vary with confining pressure (Craig, 2004). Sediment grains are able to move past each other, and as a result grains located between protrusions of indenters are not pulled downwards by cohesion, unlike in muds and clays.

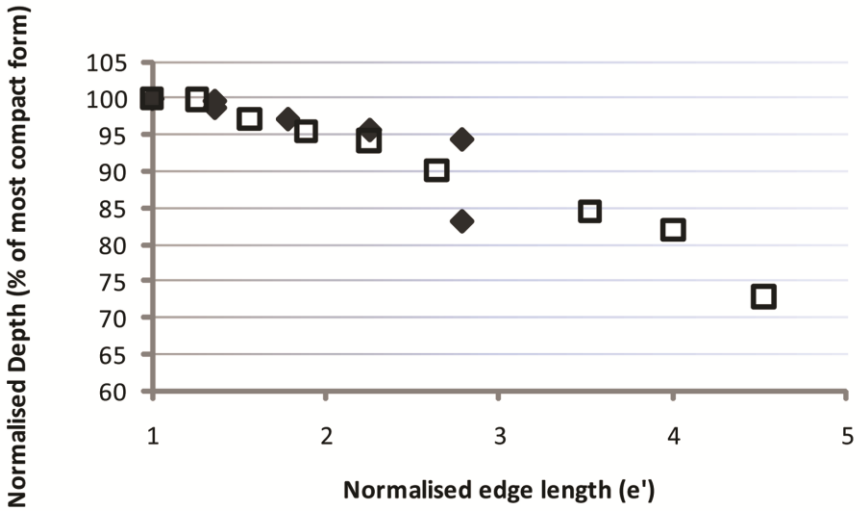


**Figure 6 - Data for normalized edge length against maximum displacement (normalized as a percentage of the most compact indenter) as recorded from FEA simulations of geometric shapes. Both sets of data show a close similarity in trend (Diamonds: surface area = 9 units$^2$, Squares: surface area = 16 units$^2$).**

Penetration in cohesive media decreased by nearly 20% when normalized edge length was increased from shortest to longest (most compact shape, to least compact). When displacement is normalized to a percentage of the depth indented by the most compact form, it can be seen that size of indenter does not significantly affect the pattern (Fig. 6).

The larger indenters (surface area = 16 units$^2$) penetrated to greater depths than the smaller set of indenters (Fig. 4). Even though pressure remains constant, indenter size affects penetration depth independently of shape. This is consistent with geotechnical theory, which shows a relationship between footing size and bearing capacity of a soil (Zhu et al., 2001; Kumar and Khatri, 2008).

The implication for vertebrate paleoichnology is that two dissimilar foot morphologies may indent to very different track depths even when the same pressure is applied. A sauropod track may be deeper than a theropod track, for instance, not due to the weight of the animal, which when distributed over the

surface area of the foot creates an equal pressure to the smaller animal, but due to the morphology and geometry of the foot being larger, and more compact in shape.

The mechanism by which normalized edge length affects track depth can be explained through soil mechanics. As the load is applied, the media is displaced. At the surface, beside the indenter, the path of least resistance allows the sediment to move upwards (Fig. 7). Directly beneath the indenter, sediment can only move vertically down, creating a 'dead zone' (Allen, 1989, 1997; Manning, 2004). As such, an indenter with a high edge to surface area ratio provides relatively more opportunity for sediment to move upwards around the indenter. The result is that energy is lost at the surface, rather than transmitted vertically, and shallower tracks are produced. This is in agreement with Jackson et al. (2009) who noted that it was the widest parts of indenters that transmitted displacement most deeply.

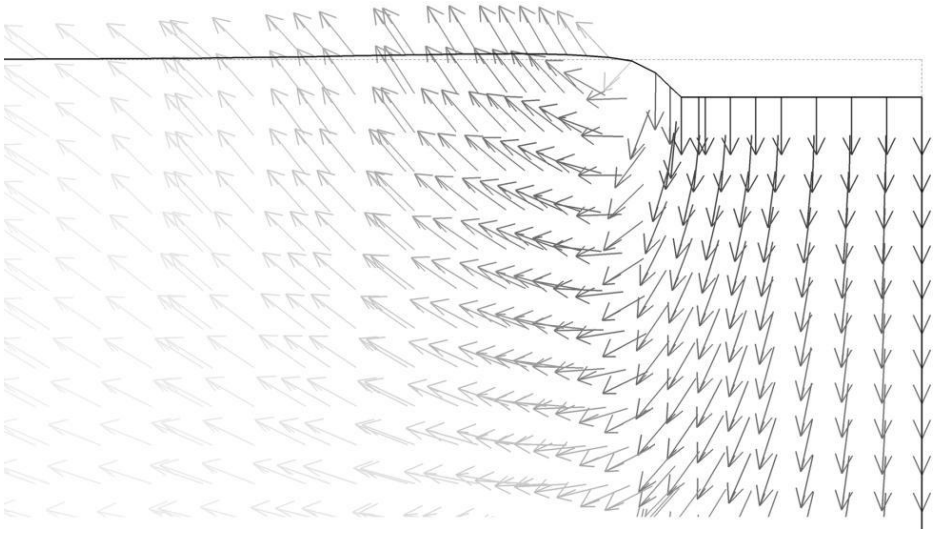

**Figure 7 - Vectors of displacement beneath the corner of a loading template. Sediment is forced vertically down beneath the center of the indenter, but moves outwards and upwards at the edge of the indenter, according to Prandtl theory. A higher edge length to surface area ratio provides more opportunity for sediment to move upwards and laterally, reducing energy transmitted down.**

There are exceptions to this, however, where an increase in edge length can lead to indentation to a greater degree. For example, indenter 1F, despite having a normalized edge length of 2.78, indented further than indenter 1G with equal edge length (Fig. 4), this is because the media was unable to move upwards in the small gaps present in indenter 1F due to cohesion. The stiffness of the media prevented easy movement, and instead the areas between protrusions were forced down, essentially decreasing the effective *e'* for indenter 1F. By creating a more complex shape (with more corners), the effects of a stiff, cohesive media mean that effective *e'* is reduced. This is exaggerated in a low-resolution finite element mesh where only a single element is present between indenting elements (e.g. in indenter 1F) and is unable to deform to an extent allowing it to pass between the protrusions of the indenter. Such a scenario highlights the importance of choosing the correct FEA mesh resolution.

In order to use vertebrate tracks as paleopenetrometers, estimates of mass and speed must be used in conjunction with observed or implied pedal morphology and geometry. It is not enough to say that two tracks, made by animals of similar size with similar sized feet represent comparable indenters, pedal morphology must also be constant.

Investigating the effects of pedal morphology also brings insight to advantageous pedal forms. These experiments indicate that an animal with a given mass may be provided with an advantage towards reducing the depth to which its feet sink in soft media, either through an increase of the surface area of the foot, which subsequently reduces pressure, or by an increase in the edge length of the foot. Such an advantage may be linked to the morphology of the feet of wading birds. Many wading birds possess long, slender toes with no

interdigital webbing (Brown et al., 1987; Paulson, 1992). Such animals traverse soft media regularly. Increasing surface area of the foot directly would be disadvantageous towards moving the foot through water. By increasing edge to surface area ratio and employing the effect described here, however, a low surface area can be maintained whilst the effect of sinking into soft media may be reduced.

## CONCLUSIONS

Tracks made by two animals of comparable size (mass and pedal surface area) in similar media conditions may nevertheless be of differing depth. The complexity of the foot morphology, as measured using the normalized edge length *e'*, is one cause of this variation in depth. Cohesion of the media means that areas not directly in contact with the indenter are still displaced down by neighboring media, essentially decreasing effective pressure. The effects of morphology are reversed in noncohesive media, where increasing relative edge length results in greater depth of tracks. Neoichnological and laboratory experiments and observations must, therefore, be used comparatively only with similar media if meaningful comparisons are to be drawn. Size also has an independent effect on total displacement; larger indenters penetrate the media to a greater extent, when morphology and pressure are kept constant.

## ACKNOWLEDGEMENTS

PLF was funded by NERC award NER/S/A/2006/14033. HPCx project e46 funded through EPSRC grant EPF055595-1. We also acknowledge support from Louise Lever for assisting with the FEA visualization, James Jepson and

Karl Bates for comments on an early draft, and Research Computing Services at the University of Manchester for providing free access to the local HPC system Horace. We also thank Stephen T. Hasiotis and two anonymous reviewers whose comments helped to improve the manuscript.

## REFERENCES


ALLEN, J.R.L., 1989, Fossil vertebrate tracks and indenter mechanics: Journal of the Geological Society, v. 146, p. 600-602.

ALLEN, J.R.L., 1997, Subfossil mammalian tracks (Flandrian) in the Severn Estuary, SW Britain: Mechanics of formation, preservation and distribution: Philosophical Transactions of the Royal Society of London Series B-Biological Sciences, v. 352, p. 481-518.

BROWN, R., FERGUSON, J., LAWRENCE, M., and LEES, D., 1987, Tracks and Signs of the Birds of Britain and Europe: Christopher Helm, London, 232 p.

CRAIG, R.F., 2004, Craig's Soil Mechanics: Spon Press, Abingdon, 447 p.

DÍAZ-MARTÍNEZ, I., PÉREZ-LORENTE, F., CANUDO, J.I., and PEREDA-SUBERBIOLA, X., 2009, Causas de la variabilidad en icnitas de dinosaurios y su aplicación en icnotaxonomía., Actas de las IV Jornadas Internacionales sobre Paleontología de Dinosaurios y su Entorno, p. 207-220.

FALKINGHAM, P.L., MANNING, P.L., and MARGETTS, L., 2007, Finite Element Analysis of Dinosaur Tracks: Journal of Vertebrate Paleontology, v. 27, p. 73A.

FALKINGHAM, P.L., MARGETTS, L., and MANNING, P.L., 2008, Using finite element analysis to aid interpretation of dinosaur tracks: Journal of Vertebrate Paleontology, v. 28, p. 76A.

FALKINGHAM, P.L., MARGETTS, L., SMITH, I.M., and MANNING, P.L., 2009, Reinterpretation of palmate and semi-palmate (webbed) fossil tracks;

insights from finite element modeling: Palaeogeography, Palaeoclimatology, Palaeoecology, v. 271, p. 69-76.

JACKSON, S.J., WHYTE, M.A., and ROMANO, M., 2009, Laboratory-controlled simulations of dinosaur footprints in sand: a key to understanding vertebrate track formation and preservation: PALAIOS, v. 24, p. 222-238, doi: 10.2110/palo.2007.p07-070r.

KUMAR, J., and KHATRI, V.N., 2008, Effect of footing width on $N_\gamma$: Canadian Geotechnical Journal, v. 45, p. 1673-1684.

LAPORTE, L.F., and BEHRENSMEYER, A.K., 1980, Tracks and substrate reworking by terrestrial vertebrates in Quaternary sediments of Kenya: JOURNAL OF SEDIMENTARY RESEARCH, v. 50, p. 1337-1346.

LEACH, R., 1994, Engineering Properties of Wetland Soils, WRP Technical Note SG-RS-1.2, p. 1-7.

LOCKLEY, M.G., 1986, The paleobiological and paleoenvironmental importance of dinosaur footprints: PALAIOS, v. 1, p. 37-47.

LOCKLEY, M.G., 1987, Dinosaur trackways and their importance in paleoenvironmental reconstruction., *in* Czerkas, S., and Olson, E.C., eds., Dinosaurs Past and Present: Los Angeles County Museum, Los Angeles, p. 81-95.

MANNING, P.L., 2004, A new approach to the analysis and interpretation of tracks: examples from the dinosauria, *in* McIlroy, D., ed., The Application of Ichnology to Palaeoenvironmental and Stratigraphic Analysis., p. 93-123.

MARGETTS, L., SMITH, I.M., and LENG, J., 2005, Simulating Dinosaur Track Formation, COMPLAS, Barcelona

MARGETTS, L., SMITH, I.M., LENG, J., and MANNING, P.L., 2006, Parallel three-dimensional finite element analysis of dinosaur trackway formation., *in* Schweiger, H.F., ed., Numerical Methods in Geotechnical Engineering: Taylor & Francis, London, p. 743-749.

MILÀN, J., and BROMLEY, R.G., 2006, True tracks, undertracks and eroded tracks, experimental work with tetrapod tracks in laboratory and field: Palaeogeography Palaeoclimatology Palaeoecology, v. 231, p. 253-264.

MILÀN, J., and BROMLEY, R.G., 2008, The Impact of Sediment Consistency on Track and Undertrack Morphology: Experiments with Emu Tracks in Layered Cement: Ichnos, v. 15, p. 19 - 27.

NADON, G.C., 2001, The Impact of Sedimentology on Vertebrate Track Studies, *in* Tanke, D.H., and Carpenter, K., eds., Mesozoic Vertebrate Life: Indiana University Press, Bloomington, p. 395-407.

NADON, G.C., and ISSLER, D.R., 1997, The compaction of floodplain sediments: Timing, magnitude, and implications: Geoscience Canada, v. 24, p. 37-44.

PAULSON, D.R., 1992, The Phylum Chordata: Classification, external anatomy, and adaptive radiation., *in* Wake, M.H., ed., Hyman's comparative vertebrate anatomy: University of Chicago Press, Chicago, p. 795.

PLATT, B.F., and HASIOTIS, S.T., 2006, Newly discovered sauropod dinosaur tracks with skin and foot-pad impressions from the Upper Jurassic Morrison Formation, Bighorn Basin, Wyoming, USA: PALAIOS, v. 21, p. 249-261.

POTTS, D.M., and ZDRAVKOVIĆ, L., 1999, Finite element analysis in geotechincal engineering: Theory.: Thomas Telford, London, 440 p.

POTTS, D.M., and ZDRAVKOVIĆ, L., 2001, Finite element analysis in geotechnical engineering: Application.: Thomas Telford, London, 427 p.

RAYFIELD, E.J., 2007, Finite Element Analysis and Understanding the Biomechanics and Evolution of Living and Fossil Organisms: Annual Review of Earth and Planetary Sciences, v. 35, p. 541-576.

SMITH, I.M., and GRIFFITHS, D.V., 2004, Programming the Finite Element Method: Wiley, Chichester, 628 p.

ZHU, F., CLARK, J.I., and PHILLIPS, R., 2001, Scale Effect of Strip and Circular Footings Resting on Dense Sand: Journal of Geotechnical and Geoenvironmental Engineering, v. 127, p. 613-621.

# Chapter 9 - Simulating sauropod manus only trackways

A paper accepted for publication in the journal Biology Letters.

Presented as a manuscript formatted for the journal.

Reference:

Falkingham, P.L., Bates, K.T., Margetts, L. and Manning, P.L., 2010. *Simulating sauropod manus only trackways.* Submitted to Biology Letters.

DOI: 10.1098/rsbl.2010.0403

# Simulating Sauropod Manus Only Trackway Formation Using Finite Element Analysis

FALKINGHAM, P. L.[1]*, BATES, K. T.[2], MARGETTS, L.[1, 3], & MANNING, P. L.[1, 4]

[1]School of Earth, Atmospheric and Environmental Science, University of Manchester, Williamson Building, Oxford Road, Manchester, M13 9PL, UK.

[2]Adaptive Organismal Research Group, Faculty of Life Sciences, University of Manchester, Stopford Building, Manchester, M13 9PL, UK.

[3]Research Computing Services, University of Manchester, Kilburn Building, Oxford Road, Manchester, M13 9PL, UK.

[4]Department of Earth and Environmental Science, University of Pennsylvania, 254-b Hayden Hall, 240 South 33rd Street, Philadelphia, PA 19104-6316, USA.

*Email: peter.falkingham@manchester.ac.uk*

*Fax: +44 (0) 1612753947*

**Summary**

The occurrence of sauropod manus-only trackways in the fossil record is poorly understood, limiting their potential for understanding locomotor mechanics and behaviour. To elucidate possible causative mechanisms for these traces, finite element analyses were conducted to model the indentation of substrate by the feet of *Diplodocus* and *Brachiosaurus*. Loading was accomplished by applying mass, centre of mass, and foot surface area predictions to a range of substrates to model track formation. Experimental results show that when pressure differs between manus and pes, as determined by the distribution of weight and size of respective autopodia, there is a range of substrate shear strengths for which only the manus (or pes) produce enough pressure to deform the substrate, generating a track. If existing reconstructions of sauropod feet and mass distributions are correct, then different taxa will produce either manus or pes only trackways in specific substrates. As a function of this work, it is predicted that the occurrence of manus- or pes-only trackways may show geo-temporal correlation with the occurrence of body fossils of specific taxa. This reinterpretation also significantly revises and rejects the behavioural and ecological models formally used to explain such traces.

**Key Words**: Dinosaur, Track, FEA, Centre of mass,

## Introduction

Palaeobiologists strive to understand the behaviour of extinct animals, but are frustrated by the redundancy of vestigial body fossil evidence. Trace fossils present us with direct evidence of how past animals interacted with their surrounding biota and environment, significantly furthering understanding of organism behaviour and functional evolution in the fossil record (Liu et al., 2010; Milner et al., 2009). Interpretation of manus-only sauropod trackways as swimming traces infers a degree of otherwise unknown aquatic ability in these giant animals. Some authors have suggested the sauropod trackmaker was buoyed up by water and 'punted' off the bottom with their forefeet (Bird, 1944; Henderson, 2004; Ishigaki, 1989; Thulborn, 1990). However, others have challenged this idea in favour of a preservational bias towards manus prints, attributing the occurrence of trackways somewhat vaguely to substrate conditions and undertrack phenomena (Lockley et al., 1994; Vila et al., 2005). These studies have presented evidence against a swimming origin for manus-only trackways, but as yet no causative mechanism relating to track formation or preservation has been proposed. To what extent are manus-only trackways linked to the specific aspects of trackmaker biology and locomotor mechanics? Alternatively, can prevailing sedimentological conditions at the time of track formation fully account for their occurrence, or do they represent an unknown taphonomic artefact of the rock record? Understanding of this phenomenon is important, not only for understanding sauropod behaviour and ecology, but fundamentally for interpretations of the trackway record of all quadrupedal tetrapods. Interpretations of the habitual locomotor mode in groups with uncertain and potentially diverse gaits will be misinformed if systematic bias leads to consistent loss of manus or pes prints in the fossil record. For example, prosauropod and hadrosaurian dinosaurs have been

reconstructed as bipedal, quadrupedal or as capable of both forms of locomotion by different workers based on interpretation of skeletons (see Galton and Upchurch, 2004; Sellers et al., 2009 for reviews). Pes-only trackways assigned to these groups may not represent evidence for a bipedal gait if instead there is simply a bias against manus preservation.

This paper presents the first attempt to investigate the mechanisms underpinning the formation of manus-only sauropod trackways by combining computer simulation with geotechnical theory.

**Material and Methods**

Finite Element Analysis (FEA) was used to model the response of a homogenous, cohesive substrate to the calculated load from a sauropod manus and pes. For each analysis, an indenter was generated atop a meshed volume of soil, composed of 20-node hexahedral elements. The indenters were generated and scaled to represent sauropod autopodia. Two sauropods were used; *Diplodocus* and *Brachiosaurus* because they represent distinct sauropod groups, and have been suggested to have considerably different centre of mass (CM) positions (Henderson, 2006). Indenter morphology was based on predicted track outlines for the two taxa by Wright (2005; Fig. 9.3) and scaled according to the specimens used in calculating mass by Henderson (2006) (Figure 1). The indenters were given material properties to make them rigid in comparison with the substrate, consistent with interpretations of the sauropod manus as a functionally rigid, block-like structure (Bonnan, 2003).

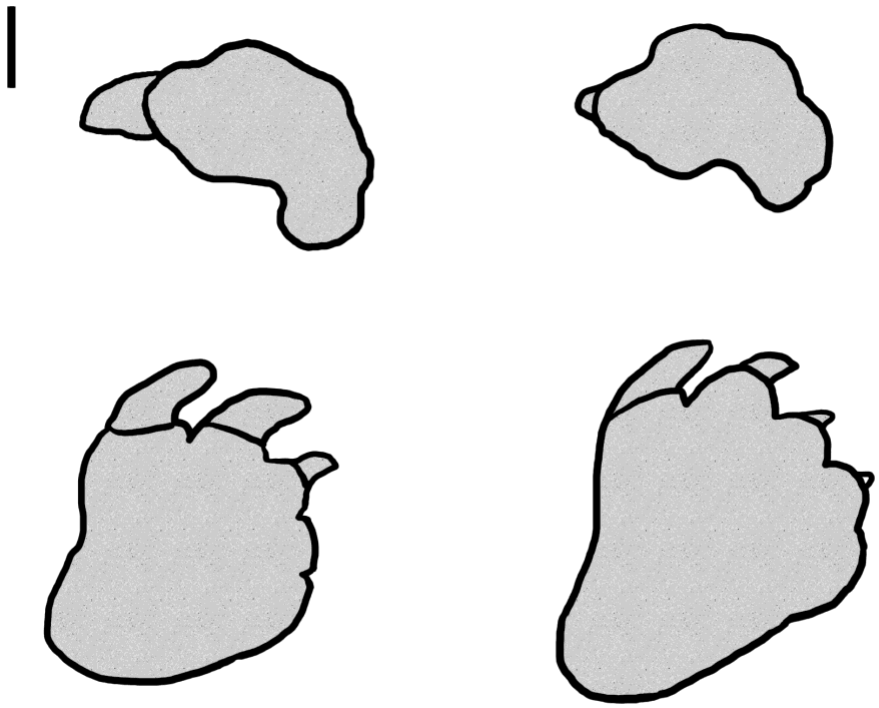

**Figure 1 -** Pes and manus outlines used to create indenters. Left; *Diplodocus* (based on *Apatosaurus*), and right; *Brachiosaurus*. Scale bar = 0.2 m. Redrawn from Wright (2005; Fig. 9.3).

Fossil trackways suggest that the manus and pes were planted in a predominantly vertical manner in sauropods, as opposed to having any considerable horizontal component (Milàn et al., 2005). The walking velocities and limb kinematics of sauropods are unknown, so to avoid unfounded assumptions, loads equal to the animal's weight (mass multiplied by gravity) were used throughout this study. Load was distributed over the 'foot' surface in a vertical manner and apportioned to fore and hind limbs according to the gleno-acetabular position of the CM (Henderson, 2006). This force was distributed between a single fore- and hind-foot to represent a quadrupedal limb cycle during walking, essentially treating the animal as two linked bipeds (Alexander, 1989). This is a simplification of the true force vectors and underfoot pressures of sauropods, but is sufficient for the purposes

of this initial analysis, and can be elaborated upon in future studies. The mass and CM position for the two dinosaurs used are shown in Table 1. After initial loading, providing the substrate had not failed, the load was removed and the substrate allowed to recover the elastic portion of deformation.

| | Mass (kg) | CM (% Gleno-Acetabular distance) | Weight applied to foot (kN) | Foot Surface Area ($m^2$) | Pressure ($kN/m^2$) |
|---|---|---|---|---|---|
| ***Brachiosaurus manus*** | 25,922 | 37.4 | 95.1 | 0.144 | 662.3 |
| ***Brachiosaurus pes*** | | 62.6 | 159.2 | 0.401 | 396.58 |
| ***Diplodocus manus*** | 11,449 | 11.5 | 12.9 | 0.158 | 81.93 |
| ***Diplodocus pes*** | | 88.5 | 99.4 | 0.345 | 288.36 |

**Table 1 - Values used to simulate track generation by manus and pes of *Diplodocus* and *Brachiosaurus*. Mass and CM values from Henderson (2006).**

For each experiment, the shear strength of the soil (*Cu)* was lowered until the substrate could no longer support the applied load in order to find the minimum shear strength required to support the animal. The elastic modulus (*E)* was altered accordingly to be 1000 x *Cu* (Leach, 1994), and Poisson's ratio (*v*) was set at 0.3. Whilst plastic deformation does occur prior to failure, the extent of this deformation is relatively minor on the scale of an animal's foot, and only occurs close to the bearing capacity. In order to produce a track deeper than a centimetre or so (very shallow when the pes of the animal may be up to a meter in length), a cohesive substrate must fail. Having found the value of *Cu* corresponding to failure, it may be generally considered that substrates with greater *Cu* will not deform sufficiently to produce a track, whilst weaker substrates will not support the foot and a track will be formed. FEA simulations were undertaken using ParaFEM (www.parafem.org.uk), as in Falkingham et al (In Press; 2009)

## Results

FEA results suggest that if there is a difference in pressure between manus and pes, resulting from weight distribution and/or foot surface area, then there is a range of substrates in which only the manus or pes can create tracks. Using hypothesized pes and manus morphology (Wright, 2005) combined with CM and mass estimates (Henderson 2006), *Diplodocus* cannot produce manus only trackways, but would be expected to produce pes-only trackways when $Cu = 13 – 45$ kN/m$^2$, and *Brachiosaurus* would be expected to produce manus-only trackways between $Cu = 65 – 110$ kN/m$^2$ . If the simulated tracks are visualised, and failure is halted at 5 cm depth to represent a firmer subsurface layer, virtual trackways are generated as in Figure 2. It can be seen for *Brachiosaurus* that at low values of *Cu*, both manus and pes indent and create obvious tracks, complete with raised displacement rims. As *Cu* increases, the pes impressions fail to indent to any significant depth, leaving only manus impressions until *Cu* becomes so high that neither manus nor pes can significantly indent the substrate (Figure 2).

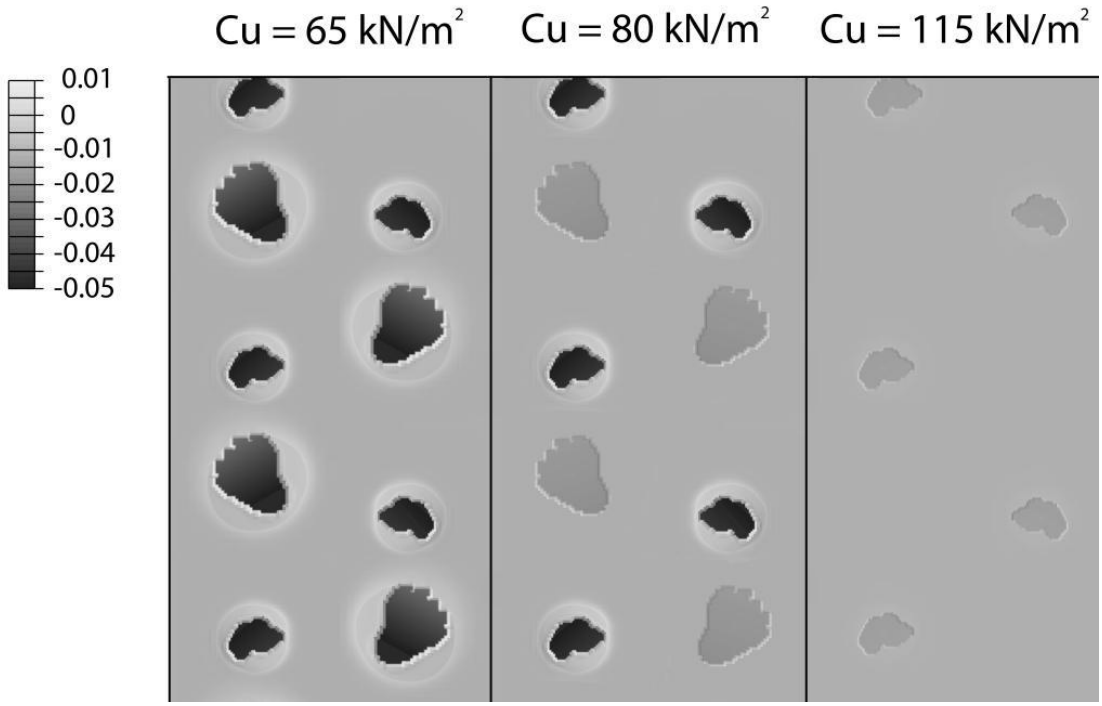


**Figure 2 - (a) Required *Cu* to support manus and pes of *Diplodocus* and *Brachiosaurus*. Foot morphology and mass/CM estimates used predict that *Diplodocus* would leave pes-only trackways in substrates with 13 < *Cu* < 45 kN/m$^2$, and *Brachiosaurus* would leave manus-only trackways when 65 < *Cu* < 110 kN/m$^2$. (b) Composite trackways generated from FEA results of separate *Brachiosaurus* manus and pes simulations. Deformation was artificially stopped at 5 cm to prevent complete failure and to represent a firmer subsurface layer.**

## Discussion

Computer analysis allows specific control over experimental inputs, and by modifying input parameters related to soil properties and loading conditions (reflecting trackmaker biology) it is possible to demonstrate the factors responsible for producing manus-only trackways. These results demonstrate that formation of a track in a cohesive substrate relies upon having a *Cu* sufficiently low at the surface that the applied load cannot be supported. In homogenous substrates, the deformation prior to failure is relatively small until the bearing capacity is reached, at which point failure occurs. Based on current predictions of CM position (Henderson, 2006) and sauropod foot shape and size (Wright, 2005), there were potentially large disparities between the pressures exerted by the manus and pes in different sauropod dinosaurs. These different pressures mean that the range of substrates (based on *Cu* value) capable of recording both manus and pes impressions varies considerably for sauropod taxa. In *Brachiosaurus,* where CM is positioned relatively anteriorly, the range of substrates in which only the manus will produce tracks may be large, resulting in a higher likelihood of manus-only trackway formation.

Such a scenario clearly precludes the need to invoke elaborate mechanisms for manus-only trackway formation such as swimming (or punting) sauropods. Therefore, a manus-only trackway may not necessarily be evidence of a very soft, submerged substrate, but instead of a substrate sufficiently firm as to prevent track formation by the pes of these large animals, having considerable consequences for palaeoenvironmental interpretations. Undertrack preservational bias is secondary to the mechanism described here, as notable undertracks will only form in substrates in which the surface track has made a significant impression. In complex heterogenous substrates, undertrack formation will likely become important, though we hypothesise

that the mechanism described here of differing pressures between manus and pes will still be primary. The novel methods presented provide a means to explore this.

The difference observed in predicted pressures of manus and pes in sauropods is not consistent with such distribution in extant elephants, where CM position and manus/pes area ratio are approximately equal (Henderson, 2006). Future research may show a relationship between CM and foot surface area in extant taxa, and it may be possible that such a relationship could be used to validate or constrain CM estimates of extinct taxa, though we acknowledge the reconstruction of pedal soft tissue morphology from only osteological material, particularly of larger animals, is not straightforward.

That manus- or pes-only trackways can be formed by obligate quadrupeds highlights the need for caution when interpreting locomotor mode from trackways. The presence of a bipedal trackway may not be evidence of bipedalism. Such confounding information supports the need for further gait reconstructions based on osteology, and then supported by trackway evidence, particularly where locomotor mode is disputed or potentially variable (e.g. hadrosaurs, prosauropods).

This work highlights the need for confident mass estimates, CM predictions, and soft tissue morphology reconstructions of extinct animals in order to understand their palaeobiology and evolution, not only through body fossils, but also tracks and trackways. Future research in this area shall focus on determining if there is a geo-temporal relationship between manus-only trackways and sauropod phylogeny, given that a phylogenetic shift in CM position has been posited by some authors (Henderson, 2006).

**Acknowledgements**

PLF and KTB were funded by NERC grants (NER/S/A/2006/14033 and NER/S/A/2006/14101). FEA run on HPCx, through EPSRC grant EPF055595-1

**References**


Alexander, R.M., 1989, Dynamics of Dinosaurs & other extinct giants: Chichester, Columbia University Press, 167 p.

Bird, R.T., 1944, Did *Brontosaurus* ever walk on land?: Natural History, v. 53, p. 60-67.

Bonnan, M.F., 2003, The evolution of manus shape in sauropod dinosaurs: Implications for functional morphology, forelimb orientation, and phylogeny: Journal of Vertebrate Paleontology, v. 23, p. 595-613.

Falkingham, P.L., Margetts, L., and Manning, P.L., In Press, Fossil vertebrate tracks as palaeopenetrometers: Confounding effects of foot morphology: Palaios.

Falkingham, P.L., Margetts, L., Smith, I.M., and Manning, P.L., 2009, Reinterpretation of palmate and semi-palmate (webbed) fossil tracks; insights from finite element modelling: Palaeogeography, Palaeoclimatology, Palaeoecology, v. 271, p. 69-76.

Galton, P.M., and Upchurch, P., 2004, Prosauropoda, *in* Weishampel, D.B., Dodson, P., and Osmólska, H., eds., The Dinosauria. 2nd Ed.: Berkeley, CA, University of California Press, p. 232-258.

Henderson, D.M., 2004, Tipsy punters: sauropod dinosaur pneumaticity, buoyancy and aquatic habits: Proceedings of the Royal Society of London Series B-Biological Sciences, v. 271, p. S180-S183.

—, 2006, Burly Gaits: Centers of mass, stability, and the trackways of sauropod dinosaurs: Journal of Vertebrate Paleontology, v. 26, p. 907-921.

Ishigaki, S., 1989, Footprints of swimming suropods from morocco, *in* Gillette, D.D., and Lockley, M.G., eds., Dinosaur tracks and traces: Cambridge, Cambridge University Press, p. 83-86.

Leach, R., 1994, Engineering Properties of Wetland Soils, WRP Technical Note SG-RS-1.2, p. 1-7.

Liu, A.G., McIlroy, D., and Brasier, M.D., 2010, First evidence for locomotion in the Ediacara biota from the 565 Ma Mistaken Point Formation, Newfoundland: Geology, v. 38, p. 123-126.

Lockley, M.G., Pittman, J.G., Meyer, C.A., and Santos, V.F., 1994, On the common occurence of manus-dominated sauropod trackways in Mesozoic carbonates.: Gaia, Revista de Geociencias, Museu Nacional de Historia Natural, Lisboa, Portugal, v. 10, p. 119-124.

Milàn, J., Christiansen, P., and Mateus, O., 2005, A three-dimensionally preserved sauropod manus impression from the Upper Jurassic of Portugal: Implications for sauropod manus shape and locomotor mechanics: Kaupia v. 14, p. 47-52.

Milner, A.R.C., Harris, J.D., Lockley, M.G., Kirkland, J.I., and Matthews, N.A., 2009, Bird-Like Anatomy, Posture, and Behavior Revealed by an Early Jurassic Theropod Dinosaur Resting Trace: PLoS ONE, v. 4, p. e4591.

Sellers, W.I., Manning, P.L., Lyson, T., Stevens, K., and Margetts, L., 2009, Virtual palaeontology: gait reconstruction of extinct vertebrates using high performance computing: Palaeontologia Electronica.

Thulborn, R.A., 1990, Dinosaur Tracks: London, Chapman & Hall, 410 p.

Vila, B., Oms, O., and Galobart, À., 2005, Manus-only titansaurid trackway from Fumanya (Maastrichtian, Pyrenees): further evidence for underprint origin: Lethaia, v. 38, p. 211-218.

Wright, J., 2005, Sauropod tracks and their importance in the study of the functional morphology and paleoecology of sauropods, *in* Curry Rogers, K.A., and

Wilson, J.A., eds., The Sauropods: Evolution and Paleobiology: London, University of California Press, Ltd., p. 252-284.

# Chapter 10 - The 'Goldilocks' effect: Preservational bias in vertebrate track assemblages

A paper submitted for peer review to the journal Proceedings of the Royal Society: Interface.

Presented as a manuscript formatted for the journal.

Reference:

Falkingham, P.L., Bates, K.T., Margetts, L. and Manning, P.L., in review. *The Goldilocks effect: Preservational bias in vertebrate track assemblages*. Submitted to Proceedings of the Royal Society: Interface.

# Preservational bias in vertebrate track assemblages related to size and substrate

FALKINGHAM, P. L.[1]*, BATES, K. T.[2], MARGETTS, L.[1, 3] & MANNING, P. L.[1, 4]

[1]School of Earth, Atmospheric and Environmental Science, University of Manchester, Williamson Building, Oxford Road, Manchester, M13 9PL, UK. [2]Computational and Evolutionary Biology Research Group, Faculty of Life Sciences, University of Manchester, Jackson's Mill, PO BOX 88, Sackville Street, Manchester, M60 1QD, UK. [3]Research Computing, University of Manchester, Devonshire House, Oxford Road, Manchester, M13 9PL, UK. [4]The Manchester Museum, University of Manchester, Oxford Road, Manchester, M13 9PL, UK.

*Email: peter.falkingham@manchester.ac.uk*

*Fax: +44 (0) 1612753947*

**Abstract:**

Using finite element analysis, virtual tracks were simulated for four dinosaur taxa; *Struthiomimus*, *Tyrannosaurus*, *Brachiosaurus,* and *Edmontosaurus*, in a range of substrate conditions in order to investigate the extent of bias in the ichnological record attributable to body mass/size. Outlines of autopodia were created based on osteology and published soft-tissue reconstructions. Loads were applied vertically to the feet equivalent to the weight of the animal (mass x gravity), distributed accordingly to fore- and hind-limbs where relevant. Ideal, semi-infinite elastic-plastic substrates showed a strong bias towards the largest animals the substrate could support without collapsing, given that small animals failed to indent the substrate, and larger animals would be unable to traverse the area without becoming mired. If a firm subsurface layer is assumed, a more complete assemblage is possible, though there remains a strong bias towards larger, heavier animals. The depths of fossil tracks within an assemblage may indicate thicknesses of mechanically distinct substrate layers at the time of track formation, even when the lithified strata appear compositionally homogenous. This increases the effectiveness of using vertebrate tracks as palaeoenvironmental indicators. Additionally, simulated undertracks are examined, and it is shown that complex deformation beneath the foot may not be indicative of limb kinematics as has been previously interpreted, but instead ridges and undulations at the base of a track may be the result of displacement vectors and pedal morphology.

**Key words:** Footprint, FEA, Trackway, computer modelling, Dinosaur

## Introduction

The fossil record offers a unique window on the history of ancient life and environments and the interactions between biosphere, lithosphere and atmosphere through geological time. However, the body fossil record is notoriously incomplete (Benton and Storrs, 1994; Maxwell and Benton, 1990) and may in fact be fundamentally biased by environmental and taxon-specific factors that potentially hamper our interpretations of ecological and evolutionary dynamics through deep time (Benson et al., 2010; Mannion et al., in press).

Interdependent environmental and taxon-specific biases are equally likely to affect the ichnological or trace fossil record. A vertebrate track is a function of foot anatomy, forces applied, and substrate properties (Padian and Olsen, 1984). Variation of any of these parameters will inevitably lead to differences in formational or preservational potential between tracks (Minter et al., 2007). Allen (1997) noted over a decade ago that a widespread understanding of track formation lagged behind knowledge of anatomical aspects and distributions of fossil tracks, and despite a number of rigorous studies in the intervening years (Gatesy et al., 1999; Manning, 1999, 2004; Milàn, 2006; Milàn and Bromley, 2006, 2008; Milàn et al., 2004), this still remains the case. However, fossil vertebrate tracks provide a wealth of information about the behaviour, ecology, and palaeoenvironment of extinct animals that is unavailable from body fossils, and would otherwise be lost (Allen, 1997; Lockley, 1991; Thulborn, 1990). Biases of the ichnological record due to animal size have profound implications for studies which attempt secondary or 'higher-level' (Witmer, 1995) inferences from assemblages of vertebrate tracks. Any attempt to interpret faunal diversity from track assemblages may be omitting large quantities of data. It is therefore imperative that the process of track formation and the variables associated with environment and animal biology are investigated.

In this paper, computer simulation is used to explore the potential for size bias in the vertebrate track record by simulating a variety of tracks from a number of dinosaur taxa in cohesive substrates. The bias is examined in surface and subsurface planes (true tracks and undertracks), across a variety of sediment conditions. Understanding such a bias has profound implications for identification and interpretation of faunal associations in track bearing strata. Previous work on track formation using computer simulation has explored

independently the effects of substrate consistency (Falkingham et al., 2009), foot anatomy (Falkingham et al., in press), and force (Falkingham et al., in review). This paper aims to present a combined study in which all of the quantifiable variables of track formation are considered as a whole system, in the hope of elucidating the extent of preservational bias inherent in the vertebrate track record.

*Track Formation*

As an animal moves over a given substrate, it exerts a compressive force on that substrate. This force is determined by the producer's body mass and locomotor kinematics. A standing animal will exert a force equal to its weight, in a vertical manner, distributed between autopodia (Alexander, 1989). As the animal begins to move faster, the force applied increases as a function of duty factor (proportion of the step cycle a foot is in contact with the ground), and gains a horizontal component (Alexander, 1977; Mossman et al., 2003). This force will, if of sufficient magnitude, deform the sediment and produce a track. An animal's gait or behaviour may create considerable variation between tracks, even within a single trackway (Bates et al., 2008b; Day et al., 2002; Díaz-Martínez et al., 2009; Minter et al., 2007), due to differing magnitudes and vectors of the forces involved. The locomotor kinematics may in turn be dictated or influenced by the sediment conditions (Marty et al., 2006), a deep soft mud for instance may cause an animal to move more carefully, or in an unusual manner (Milàn et al., 2005).

The relationship between the size of an animal and the load applied to the substrate is not straightforward however, because larger, heavier animals will tend to have larger feet than smaller, lighter animals, and consequently a larger surface area in contact with the substrate. Given that pressure is a measure of force over area, the resultant pressure exerted on the sediment surface is a function not only of the animal's mass (as weight), but also the geometry of the autopodia. Quadrupedal animals benefit from more feet in contact with the ground, further reducing the load on the substrate beneath any single foot, as compared with a similar sized biped. In addition to size, foot morphology also plays a role in determining the magnitude of deformation, expressed as the depth of a track. Differing shapes present different paths for sediment movement,

resulting in variable distributions of force which affect the extent to which any given foot may indent a substrate (Falkingham et al., in press).

The mechanical properties of a cohesive substrate such as mud or clay may be numerically parameterised according to cohesiveness, compressibility, and stiffness (Craig, 2004). Non-cohesive substrates such as sand further incorporate parameters such as friction angle. These parameters define the maximum load required to deform the substrate, and therefore the range of track-makers for which the formation of tracks and trackways becomes possible (Allen, 1997).

The deformation associated with track formation occurs not only at the surface, but extends beneath that surface as subsurface deformation, creating a track volume, rather than a single surface. If one were to expose a sedimentary layer within such a track volume, the exposed surface would display undertracks that vary in geometry and morphology compared to the original surface track (Allen, 1989, 1997; Hitchcock, 1858; Lockley, 1991; Manning, 1999, 2004; Milàn and Bromley, 2006, 2008; Milàn et al., 2004; Thulborn, 1990).

*Computer Modelling of Tracks.*

Interpretations of fossil tracks can be aided and supported by data from experimentation, either through analogue track experiments using extant taxa and indenter mechanics (Allen, 1989, 1997; Gatesy et al., 1999; Manning, 2004; Milàn, 2006; Milàn and Bromley, 2006, 2008) or digitally, using for instance finite element analysis (FEA) (Falkingham et al., in review; Falkingham et al., 2007; Falkingham et al., 2008, in press; Falkingham et al., 2009; Margetts et al., 2005; Margetts et al., 2006) or 3D reconstruction (Bimber et al., 2002; Gatesy et al., 1999; Manning, 2008). By providing a closed system in which experimental variables (e.g. sediment moisture content, loading kinematics etc) are known, laboratory simulated traces can provide quantitative data to constrain interpretations of fossil specimens. Note that the modelling and simulation of track formation is not to be confused with the digitisation of fossil specimens, for instance through the use of laser scanning (Bates et al., 2009a; Bates et al., 2008a; Bates et al., 2008b) or photogrammetry (Breithaupt et al., 2004; Breithaupt et al., 2001; Matthews et al., 2006).

Finite element analysis has become commonplace in palaeontology during recent years, especially with its applications in biomechanics, investigating stresses within bones (Moazen et al., 2008; Porro, 2007; Rayfield, 2004, 2005; Rayfield et al., 2001; Ross, 2005; Witzel and Preuschoft, 2005; Xing et al., 2009). The reader is directed to Rayfield (2007) for a review of FEA in palaeontology, and also of the method itself.

A volume of sediment, sufficiently large in relation to its constituent grains, can be considered as a single continuous entity. This entity will have properties that define its behaviour under load, much like any other object such as a bone. As such, a volume of sediment can be treated as a continuum, and studied using FEA. This has been the case in the engineering fields for several decades, and the use of FEA for solving problems involving soils and sediments is now common place. It is only a small conceptual step from using FEA to model building foundations and farming machinery, to modelling the deformation of sediment beneath an animal's foot.

Computational approaches such as FEA are advantageous over physical modelling, enabling quantifiable and repeatable experiments in considerably less time. The greatest advantage comes from being able to specify absolute values of input parameters, which is difficult to achieve with physical modelling. This means that sediment properties and the nature of loading can be precisely controlled and repeatedly and systematically altered to measure their effects on resultant track geometry. The virtual environment allows for removal of substrate layers, visualisation of stress fields, time-dependant analysis during track formation, and the ability to manipulate and view the resultant track in any manner (e.g. in cross section), whilst retaining the original. Digital models can also be easily transferred to other packages to study further lines of enquiry, e.g. for applying different weathering models, or comparison with laser scans of real tracks.

## Methods

*The virtual foot.*

The following experiments used parallel FEA software developed by LM and PLF, using the freely available ParaFEM libraries (www.parafem.org.uk) to model track formation (see Falkingham et al., in review; Falkingham et al., in press; Falkingham et al., 2009; Margetts et al., 2005; Margetts et al., 2006). A number of dinosaur tracks were simulated over a range of substrates in order to explore bias in track formation resulting from substrate or taxa specific factors.

In observing the effects of animal size coupled with environmental conditions, the Dinosauria present the largest range in body masses, and variation in morphology, of all terrestrial vertebrate taxa. Coupled with a vast quantity of research describing dinosaur tracks spanning more than a century and a half (Delair and Sarjeant, 1985; Hitchcock, 1858; Lockley, 1986, 1987, 1991; Sarjeant, 1974, 1990), and the presence of modern analogues (at least for the Theropoda) in the form of birds, dinosaurs provide the ideal basis on which to further our understanding of fossil track formation, and the size related biases associated therewith. Four dinosaurs (*Struthiomimus*, *Edmontosaurus*, *Tyrannosaurus*, and *Brachiosaurus*) were chosen to create a varied virtual track assemblage on a cohesive substrate, representing a range of body masses, and including obligate bipeds, an obligate quadruped, and a facultative biped (Table 1). These particular taxa were chosen because they all have published data on body mass and centre of mass (CM) position, and represent a wide range in size, mass, and pedal morphology. The taxa were not selected in order to create some geo-temporally correct assemblage.

| Trackmaker | Mass (kg) | Force (kN) | Foot length (m) | Foot Surface Area (m2) | Pressure (kN/m2) |
|---|---|---|---|---|---|
| *Struthiomimus* | 423 | 4.15 | 0.336 | 0.026 | 161.21 |
| *Edmontosaurus* (biped) | 813 | 7.98 | 0.29 | 0.052 | 151.92 |
| *Edmontosaurus* Quadruped manus | 813 | 2.55 | 0.12 | 0.011 | 241.39 |
| *Edmontosaurus* Quadruped pes | 813 | 5.42 | 0.29 | 0.052 | 103.31 |
| *Tyrannosaurus* | 7654 | 75.09 | 0.72 | 0.234 | 320.26 |
| *Brachiosaurus* manus | 25922 | 95.11 | 0.6 | 0.144 | 662.29 |
| *Brachiosaurus* pes | 25922 | 159.19 | 0.87 | 0.401 | 396.58 |
| *Edmontosaurus** | 813 | 7.98 | n/a | 0.063 | 126.46 |
| *Brachiosaurus** | 25922 | 254.29 | n/a | 0.545 | 466.59 |

**Table 1 - Mass, weight, foot metrics and pressures used to represent various dinosaur taxa used in this study. Data for *Struthiomimus, Edmontosaurus,* and *Tyrannosaurus* from Bates et al (2009b), and data for *Brachiosaurus* from Henderson (2006). **Edmontosaurus* and *Brachiosaurus* are also shown with pressure values from manus and pes combined.**

In accordance with the three factors determining track formation (force, foot anatomy, and substrate), each taxa provided values for two inputs: applied force and shape of the foot. To apply a reasonable force, the body mass for each dinosaur was taken from the literature (Bates et al., 2009b; Henderson, 2006 see Table 1). Animals spend a very small proportion of their time moving at anything more than a walking speed, therefore it would be expected that most tracks are made by walking animals, and indeed this is corroborated by the numbers of trackways showing walking, rather than running gaits (Alexander, 1989; Thulborn, 1990). A slow movement was therefore assumed for each animal. When moving slowly, an animal will take shorter strides than if it were moving faster (Alexander, 1976, 1977). This means that the hip joint and centre of mass (CM) will move a shorter distance horizontally from the contact between the foot and the ground, resulting in a smaller angle of ground reaction force (Alexander, 1977). As such, for the purposes of this paper, a purely vertical component to the applied force was assumed. Force distributed through feet in

contact with the ground was taken as the weight of the animal, calculated as mass x gravity (9.81 $m/s^2$). An animal of 100 Kg would therefore exert a vertical force upon the ground of 981 N.

For a biped, maximum force is transmitted through a single foot when the opposite foot is raised, so the pressure applied in this case was equal to the weight of the animal divided by the surface area of a single foot. In the case of quardrupedalism, centre of mass plays a role in determining how much of the animal's weight is distributed to the fore and hind limbs, after which the two sets of limbs can be treated separately as bipeds (Alexander, 1977). Centre of mass estimates for *Edmontosaurus* and *Brachiosaurus* were taken from the literature (see Bates et. al 2009 for *Edmontosaurus* CM and Henderson 2004 for *Brachiosaurus*) and used to apportion force between fore- and hind-limbs. The amount of the animal's weight given to each pair of limbs was equal to the relative position of the CM between the pelvic and pectoral girdles, i.e. a CM 60% of the way from the pectoral girdle to the pelvic girdle would imply a weight distribution of 60% to the hind limbs, and 40% to the fore limbs (Henderson, 2006) (Figure 1). Treating the animal as two linked bipeds with appropriate weights is sufficient for the purposes of these experiments (see Alexander, 1977, for walking models of quadrupeds represented as two bipeds in tandem). Whilst this may be a very simplified solution that ignores the effects of complex gaits, walking velocities and limb kinematics of dinosaurs are unknown. Employing the loading regime outlined above avoids incorporating additional unfounded assumptions into the simulations. It is hoped that future studies may build on this approach to include complex kinematics and kinetics associated with full locomotor reconstructions. Consideration is given to the effects of duty factor and locomotion in the discussion section.

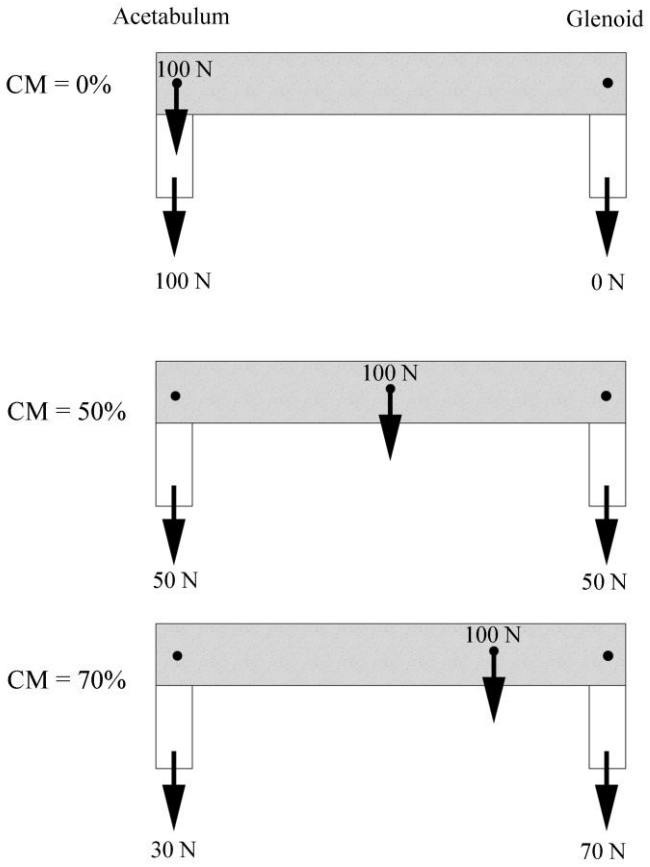


**Figure 1 - Loads beneath fore- and hind- limbs as determined by CM position. A CM position of 50% gleno-acetabular position applies equal load to both fore- and hind- limbs. As the CM is positioned more anterior or more posterior, more load is applied to the fore-limbs or hind-limbs respectively.**

Hadrosauridae have been interpreted as primarily bipedal with facultative quadrupedalism at either low (Galton, 1970; Weishampel and Horner, 1992), or high (Sellers et al., 2009) speeds, based on anatomical features in the forelimbs suggestive of either mode of locomotion, and trackway evidence also supporting both gait reconstructions (Lockley and Wright, 2001; Moratalla et al., 1992; Thulborn, 1990). *Edmontosaurus* tracks were therefore simulated as being made by both a bipedal animal, and a quadrupedal animal.

The indenters, or 'virtual feet' were created by producing outlines around ventral views of reconstructed skeletal autopodia. Skeletal geometry was scaled to the same size as the specimens used by Bates (2009b) and Henderson (2006) so as to remain consistent with mass estimates. The outlines were then increased in size to account for soft tissue. The outline of the *Edmontosaurus* manus does

not follow the osteology as closely as the other indenters, instead being based on the hadrosaur specimen MRF 03 (though scaled to the specimen used by Bates et al. 2009), as figured in Sellers et al. (2009, Fig. 5), where the manus takes a 'mitten' like form. This is supported by hadrosaur manus tracks illustrated by Lockley and Wright (2001), and described as "crescent shaped" by Currie (1983). The indenters representing the manus and pes of *Brachiosaurus* were generated as in Falkingham et al. (in review), from reconstructions by Wright (2005). These outlines defined the nodes and elements that would be loaded on the FE substrate volume (Figure 2). The indentation of the meshed 'foot' resulted in a flat track. Whilst fossil tracks are rarely flat indentations, for the purposes of examining the effects of body mass, a flat foot was sufficient, and allowed for far quicker solution times than would be possible if employing complex curved FE meshes.

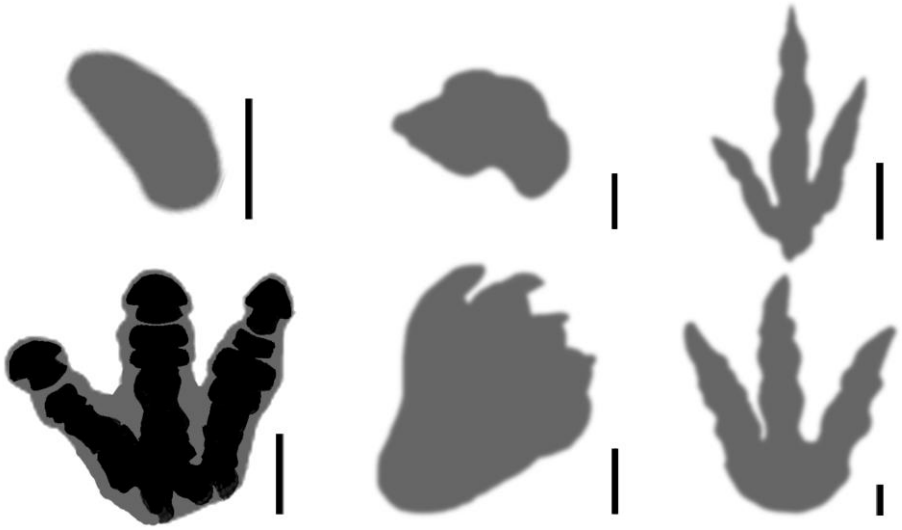

**Figure 2 – Foot outlines used to create indenters. Left, *Edmontosaurus* manus (above) and pes (below), middle, *Brachiosaurus* manus (above) and pes (below) (adapted from Wright (2005), and right, *Struthiomimus* (above), and *Tyrannosaurus* (below). Scale bars = 0.1 m. *Edmontosaurus* pes shows how foot outline was derived based on osteology.**

For each animal, a volume of substrate was created for each foot to be indented into. Only one pes needed to be indented for each bipedal condition, and only one manus and one pes for the *Brachiosaurus* and quadrupedal *Edmontosaurus*.

*The virtual substrate.*

An elastic-perfectly-plastic von Mises model was applied in order to model a cohesive substrate. The mechanical properties of the substrate were defined by the Undrained Shear Strength (*Cu*), the Young's Modulus (*E*), and the Poisson's Ratio (*v*). These parameters relate respectively to:

- The strength of the substrate, that is, how much stress is needed before failure of the sediment (permanent deformation). Essentially a measure of cohesion between grains, shear strength is most strongly affected by water content (Marty et al., 2006). Values of *Cu* according to the British Standards for Geotechnical Engineering are summarised along with field testing methods in Table 2.
- The stiffness of the substrate – how much deformation is recoverable through elastic behaviour before (and after) plastic deformation takes place. The value of Young's modulus is typically 1000x the value of *Cu* in cohesive substrates (Leach, 1994).
- The compressibility of the substrate. In an entirely incompressible substrate, $v = 0.5$. Such a substrate will not change in volume when deformed, resulting in expansion equal to compression along an axis perpendicular to that of the primary stress. An incompressible substrate could be considered to be a fully saturated sediment, in which void space air has been completely replaced by water (note: though water is technically compressible to some extent, at the magnitude of forces dealt with here, it can safely be considered incompressible). Typical values for saturated clay and mud would be 0.4 - 0.5 (Newcomb and Birgisson, 1999).

| Stiffness state | Undrained strength ($kN/m^2$) | Test |
|---|---|---|
| **Hard** | >300 | Can be scratched by thumb nail |
| **Very Stiff** | 150-300 | Can be indented by thumb nail |
| **Stiff** | 75-150 | Can be indented slightly by thumb |
| **Firm** | 40-75 | Thumb makes impression easily |
| **Soft** | 20-40 | Finger pushed in up to 10 mm |
| **Very soft** | <20 | Finger easily pushed in up to 25 mm |

**Table 2 - Undrained strength ($C_u$) classification of clays according to BS 8004:1986, along with simple field tests (from Craig, 2004)**

Many palaeontological FEA studies concerning stress within bone use elastic models, in which there is a linear relationship between stress and strain (Figure 3A), determined by *E*. The introduction of a failure criterion (*Cu*) however, produces an elastic-perfectly plastic model, whereby initial loading deforms the material in a recoverable elastic manner (Line O-Y' in Figure 3B) until the substrate reaches a plastic state. Further loading equals or exceeds the bearing capacity and results in failure, where the substrate can no longer support the load (Line Y'-P in Figure 3B). When the load is removed, recovery occurs along a line parallel to the original elastic deformation (Line Y''-U in Figure 3B). On the scale of individual elements, this relationship is clear and well defined, but over an entire mesh, where some elements may be in a plastic state and others in an elastic one, the relationship becomes less defined, with a curved portion where plastic deformation occurs (Figure 3C).

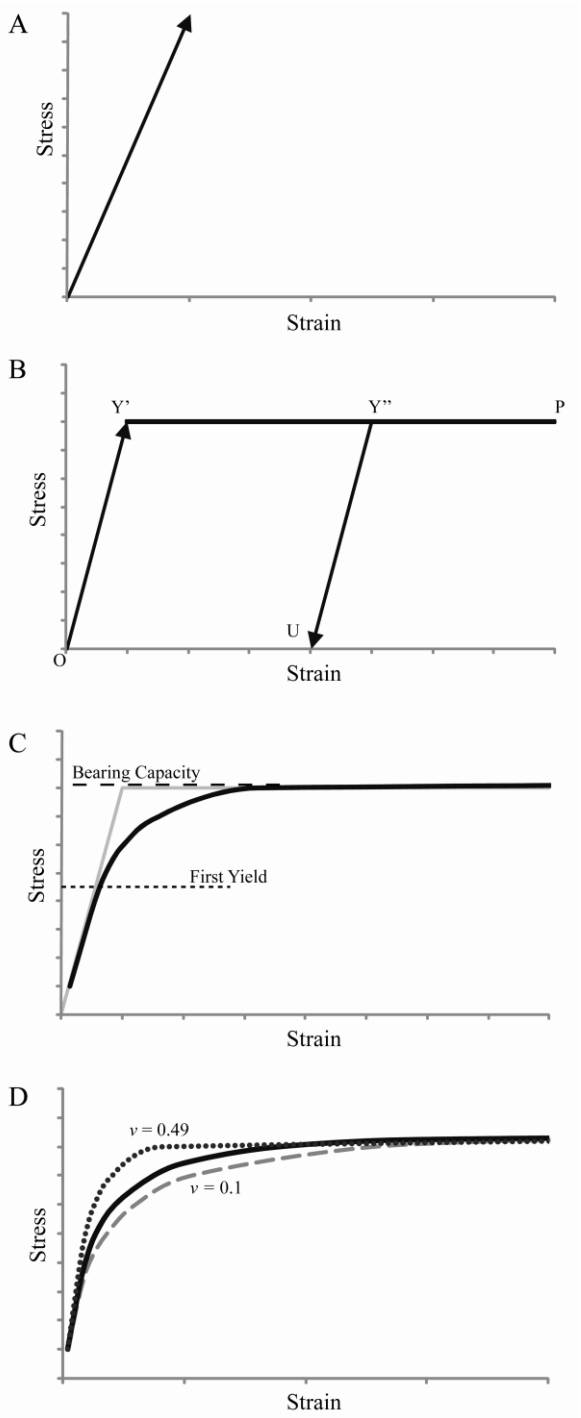


**Figure 3 - A) elastic stress-strain relationship, B) elastic-perfectly-plastic stress-strain relationship. Initial elastic deformation occurs along line O-Y' until stress exceeds the strength of the substrate, at which point failure occurs and deformation takes place along line Y'-P. If loading is halted at Y'', and then removed, elastic recovery occurs along line Y''-U, parallel to initial deformation O-Y'. C) The effects of an elastic-perfectly-plastic model distributed over a substrate volume, in which parts are in plastic failure, and others are in the elastic region. D) The effects of Poisson ration on the overall form of the stress-strain relationship within a substrate; dotted line shows $v$ = 0.49, solid line shows $v$ = 0.3, and dashed line shows $v$ = 0.1.**

The use of an elastic-plastic model can be computationally very expensive. This is due to numerical complexities when loading the substrate at levels where stress approaches the failure point. At this point, even the smallest of loads can result in very large deformations. For this reason, simulations involving large numbers of elements were run on the HPCx and HECToR supercomputing services, taking advantage of the parallel nature of the FEA software.

A soft clay-like substrate was reproduced in the FEA simulations using 20-node hexahedral elements. The 20-node element is required in this case because of the nature of the deformation; indenting into soft substrate causes a large gradient of deformation from negative vertical displacement beneath the edge of the indenter, to positive vertical displacement adjacent to the indenter. Eight-node elements lack the numerical flexibility to deal with such a gradient, and so by increasing the number of nodes defining the element, a more accurate solution can be found. The volume of substrate modelled was equal to 4 x the foot length in all dimensions in order to avoid boundary effects (Allen, 1997).

*The process of indenting.*

In order to create tracks to a depth corresponding to each animal's mass, it was important to load nodes with force, rather than directly displace them. Whilst the foot of an animal can move at joints and the soft tissue is deformable to an extent, as a whole the foot can be considered rigid compared to the non-rigid substrate. In order to create a rigid loaded area, rigid-body interface elements were generated above the area on the mesh that would be loaded (Potts and Zdravković, 1999), essentially creating a solid meshed foot on the surface of the virtual substrate. The weight of the animal was then applied to the interface elements to generate a uniform load over the foot. After an initial loading step was complete, a time step with zero loading was applied in order to allow the substrate to recover the elastic part of the deformation, as would be the case in the formation of a real track.

For each indenter, substrates were generated with a high *Cu*, and this was incrementally lowered until the substrate could no longer support the load (i.e. bearing capacity was exceeded). In all cases, *E* was equal to 1000 x *Cu*, and $\nu$ =

0.4. Maximum depth of indentation beneath the virtual foot was recorded in each experiment, as this value is a fair indication of the degree to which a track is observable. Additionally, surface tracks and undertracks were visualised and qualitatively observed.

**Results**

There is a very narrow range of *Cu* values for any given pressure that allow the formation of significantly deep surface tracks (Figure 4). If *Cu* is higher than this value, indenters fail to deform the substrate to an appreciable degree, attaining maximum track depths of less than a millimetre. Given that many of the autopodia used were tens of cm in length, such deformation cannot realistically be considered to be an observable track. Lower values of *Cu* than this narrow range cannot support the applied load, and the substrate fails. The maximum load a substrate can support beneath an indenter can be approximated by calculating the bearing capacity of a circular indenter under the specified load using the following equation (Skempton, 1951):

Bearing capacity = $Cu\ (2+\pi) * S$
Where S is a shape factor equal to 1 + 0.2 x (breadth/length).

Using this equation, it can be seen that a substrate for which Cu = 100 kN/m$^2$ will fail when the load on a circular indenter reaches 616.8 kN/m$^2$. The approximated failure point for circular indenters at any given load is plotted as a line in Figure 4. This prediction is not the true value of bearing capacity for any specific track however, due to variations in foot morphology deviating from a circular shape. However, as can be seen from Figure 4, this approximation is sufficiently close as to highlight the relationship.

Below the minimum value of *Cu*, a track will be formed providing there is a firmer substrate layer beneath, in which case the tracks will be of a maximum depth approximately equal to the thickness of the surface substrate. If there is no firmer subsurface layer, the substrate cannot support the load, and the animal in question will be unable to traverse the area without becoming mired.

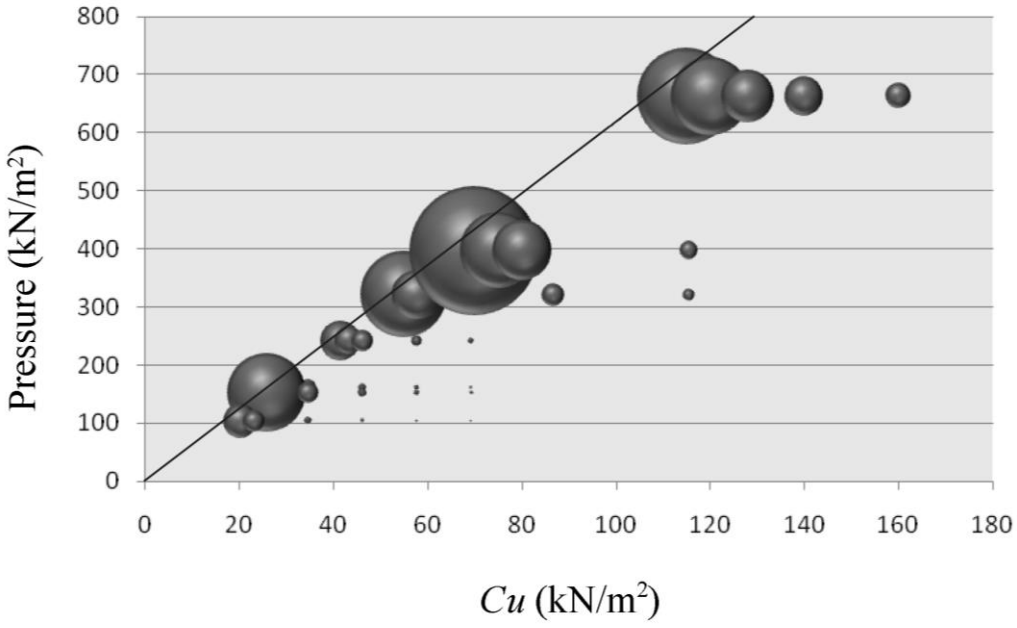


**Figure 4 – Bubble plot of maximum track depth for a given load on varying substrates. Size of bubbles represents maximum depth of track. Line shown denotes the predicted minimum *Cu* required to support any given load applied to a perfectly circular indenter. Tracks are only formed to any significant depth at values approximately equal to those defined by the line. Above and to the left of the line, the substrate is too soft to support the load and fails entirely, whilst below and to the right of the line, loads are insufficient to produce tracks of significant depth.**

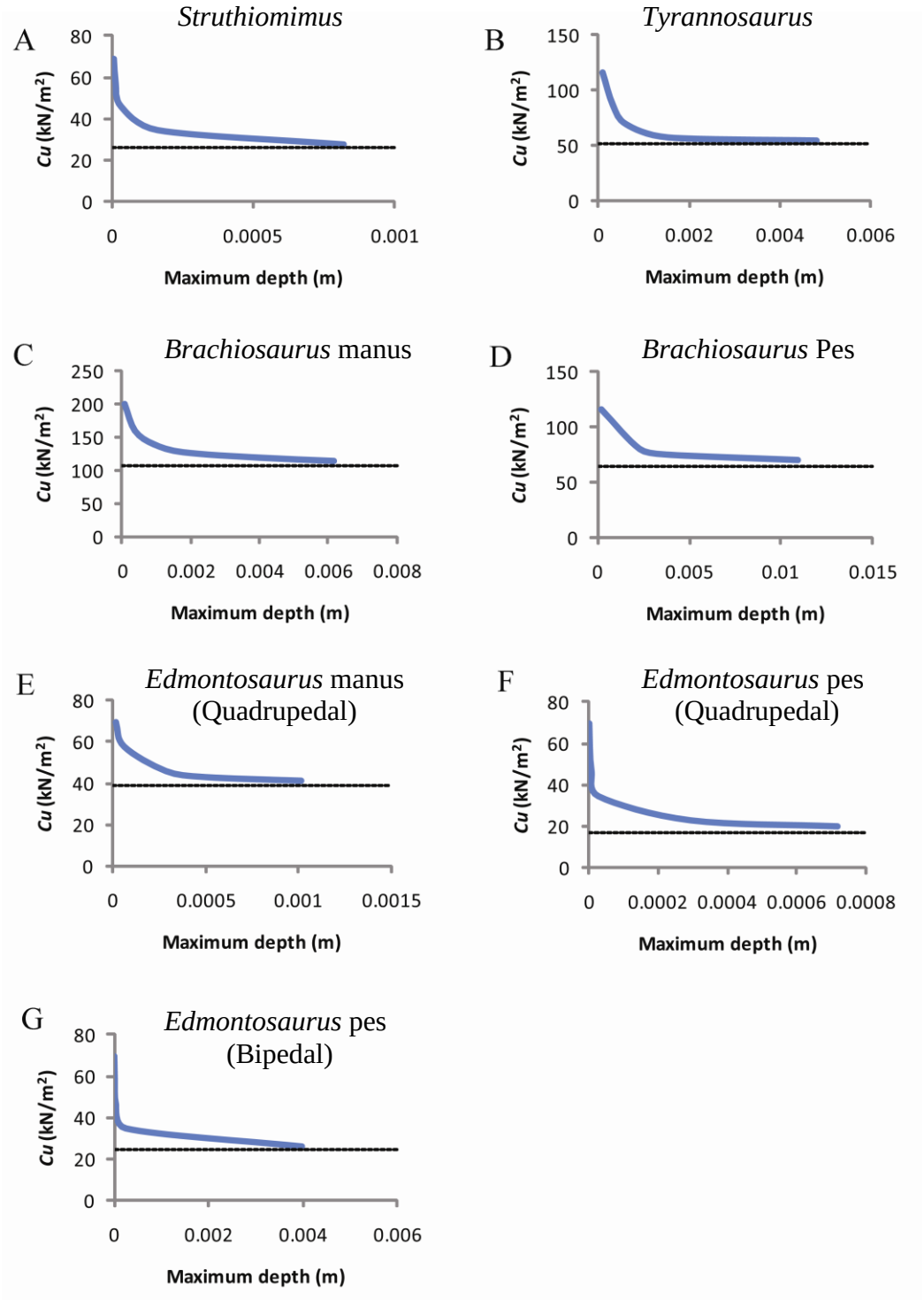


**Figure 5 – Graphs showing maximum track depth and substrate *Cu* for each indenter. A) *Struthiomimus*, B) *Tyrannosaurus*, C) *Brachiosaurus* manus, D) *Brachiosaurus* pes, E) *Edmontosaurus* manus (quadrupedal loading), F) *Edmontosaurus* pes (quadrupedal loading), and G) *Edmontosaurus* pes (bipedal loading). Each graph shows there is a very narrow range in which tracks are generated, but the substrate is still able to support the load.**

The range of *Cu* in which tracks of significant depth can be generated is very small regardless of foot morphology or load (Figure 5). This limits tracks made in truly homogenous substrates to an extremely narrow range of forces, and subsequently producer sizes. Combining the FEA simulations to produce a track surface shows that a theoretically ideal, semi-infinite homogenous substrate is likely to record tracks only from a very limited range of pressures. However, if a firmer substrate layer is assumed 0.05 m beneath the surface (track formation is halted when maximum depth reaches 0.05 m), then all tracks made by animals with a sufficiently high load to deform the surface substrate are formed. In such a scenario there is a clear bias towards larger, heavier animals (Figure 6).

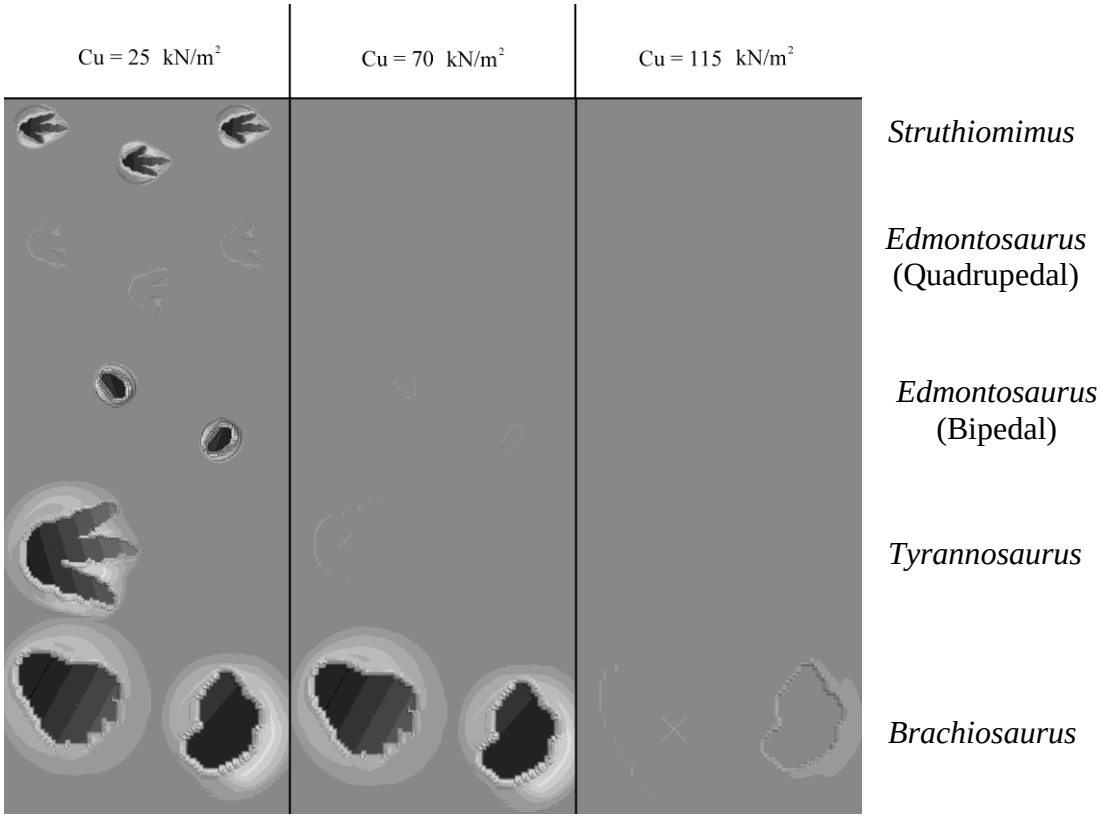


**Figure 6 – Predicted track assemblages generated from composite FEA simulations, assuming a firm subsurface layer at 0.05 m depth (track simulations halted after failure when maximum depth reaches 0.05 m). When the surface substrate layer has low *Cu*, all animals produce observable tracks, the larger animals supported by the firmer subsurface layer. At high *Cu* only large animals produce enough force to indent the substrate and generate tracks. Darker shading represents deeper parts of the track.**

## Discussion

From the results presented here, a key observation is that in simulating track formation in a semi-infinite elastic-perfectly-plastic substrate, generation of tracks to any significant depth is difficult to achieve. This is because the load required to plastically deform the substrate, and the maximum load which the substrate can support are very close, implying that a very specific pressure is required to generate a noticeable track in an homogenous substrate. There is therefore a 'goldilocks' quality to homogenous substrates regarding possible track formation, where a substrate must be 'just right' in terms of shear strength in order to record the tracks of an animal. A faunal assemblage recorded as tracks will be strongly biased towards the largest animals the substrate can support, resulting in a very low diversity of recorded body sizes. Taxa exerting more pressure beneath their feet than the substrate can support will avoid the area or become mired, whilst animals producing less pressure than is required to create a track will not leave observable impressions.

Ideal, semi-infinite, homogenous substrates may be rare in nature, occurring perhaps only at mud flats and salt marshes etc. More commonly, substrates are polyphasic, with heterogeneous mechanical properties varying vertically and laterally. If we consider the scenario of a series of substrate layers becoming progressively firmer with depth (Figure 7), it is observed that any animal creating sufficient load as to deform the uppermost substrate will generate a track. Refining this stratification such that *Cu* increases gradually with depth results in the intuitive case that heavier animals generate deeper tracks. There is therefore a greater range of possible substrates in which larger animals can generate tracks than smaller animals.

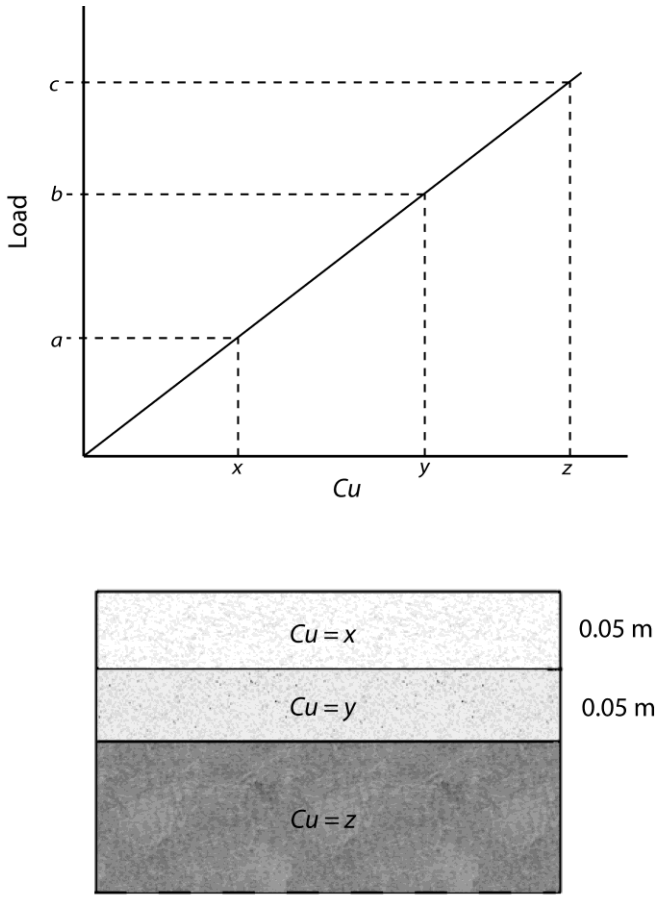


**Figure 7 – Hypothetical scenario in which three substrate layers are considered, in which *Cu* increases with depth. Animals producing loads that cause the surface layer to fail, but not the subsequent layer (a < load < b) will create tracks of 0.05 m maximum depth. Animals producing loads sufficient to deform layer two, but insufficient to deform layer 3 (a < b < load < c) will generate tracks to 0.1 m depth. Animals producing loads above the bearing capacity of layer three (load > c) will be unable to traverse the substrate, whilst animals producing less pressure than is required to deform the surface layer (load < a) will not generate tracks.**

If a substrate is stratified with mechanically distinct layers, depths and surface areas of present tracks can be used to determine the depth and mechanical properties of these layers at the time of track formation. A track bearing surface on which small and medium tracks are impressed to a similar depth, yet on which tracks made by larger animals appear deeper, will indicate a mechanically homogenous surface layer as deep as the small and medium tracks (after accounting for subsequent weathering/erosion). Such consideration of tracks as palaeo-penetrometers may prove useful in interpretations of palaeoenvironment.

The experiments carried out in this study have used body mass to apply a force through the autopodia in a number of taxa. Loading in this way assumes a direct linear relationship between body mass and force. This was done to avoid incorporating unfounded assumptions into the simulations, and to allow rapid simulation. Nevertheless, consideration must be given to the effects of locomotion; duty factor and limb kinetics and kinematics. As an animal begins to move, the ground reaction force (GRF) gains a horizontal (forward-backward) component in order to move the animal forwards (Mossman et al., 2003). This force vector may also incorporate a lateral component depending on the animal's gait. As speed increases, the magnitude of the ground reaction force also increases. In terms of pressure applied then, the pressure beneath an animal's foot will increase as speed increases. As an animal increases in speed, the minimum *Cu* increases, such that a substrate that previously would be incapable of recording an animal standing or moving slowly, may fail beneath the foot of a running animal.

Peak ground reaction force (GRF) measured from various extant taxa positively correlates with speed, and for living bipeds is often in the range of 1.5 times body weight when walking and 2 – 4 times body weight when running (Hutchinson, 2004 and references therein). Gatesy et al. (2009) showed that in larger taxa, possible peak GRFs appeared to be considerably less than in smaller animals. Smaller animals are perhaps more able to engage in relatively faster locomotion than larger animals. Indeed Alexander (1989) noted that tracks made by a theropod of ~600kg (0.38 m foot length) appeared to be the largest set of dinosaur tracks to show running. As a result, it may be that smaller animals are more likely or able to apply a greater pressure to the surface of the substrate, counteracting some of the bias towards larger animals.

Examining the biases inherent in track formation as a consequence of animal size permits discussion of genuine and artificial signals regarding diversity as interpreted from track sites. A track site limited to large producers, e.g. a purely sauropod track assemblage, is likely to be a preservational artefact, or indistinguishable from such. Smaller animals may have been abundant at such a site, but unable to produce tracks in the substrate. Allen (1989) noted in his discussion of the Flandrian deposits of the inner Bristol Channel and Severn Estuary, that the fauna represented by tracks lacked records of smaller mammals

such as foxes and dogs, arguing this was a preservational rather than ecological issue.

Given that there is strong bias towards greater underfoot pressures, the preservation potential of track assemblages representing mixed age groups (herd behaviour) is greatly reduced. There will be a strong bias towards preserving only the largest members of the group. If the adults within a group are particularly large, as in the case of sauropods for instance, the range of substrates traversable by the group will be constrained by the minimum substrate strength that can support the largest animals. As such, tracks from smaller individuals become far less likely to form and subsequently preserve, because the substrates over which the animals move are not soft enough to record the passage of smaller, juvenile forms.

The presence on a single track bearing surface of both small and large tracks, indented to approximately the same depth (evidently halted by a firmer subsurface layer) is likely to be indicative of true diversity in the area at the time of track formation (providing effects of time averaging can be removed). Presence of small, shallow tracks and large, deep tracks may not be indicative of true diversity however, if the large deep tracks are particularly deep. In such a scenario, it is possible that medium sized animals produce too great a pressure underfoot to be supported by the soft surface layer, but sink too far to traverse the area. This highlights the importance of considering not just the tracks present at a track site, but their total 3D morphology including foot anatomy and track depth, in order to make interpretations about faunal diversity.

**Discussion of individual track features**

The simulations undertaken for this study present an opportunity to investigate track features at the original track surface, and in subsurface undertracks. Specific features related to autopodia morphology and undertrack depth are discussed here.

The values of mass, foot morphology, and CM position used for the *Edmontosaurus* produce differing pressures between manus and pes (151.93 $kN/m^2$ and 103.31 $kN/m^2$ respectively). These differing pressures imply substrates of different *Cu* are required to support the loads, which in turn creates a range of substrates (*Cu* = 20 – 40 $kN/m^2$) where the manus causes the substrate

to fail, but the pes does not. In such substrates, if underlain by a firmer layer, only the manus will generate tracks. This is the same mechanism as described in detail by Falkingham et al. (in review) for sauropods. It is interesting to note that the pressure beneath the pes when bipedal locomotion is assumed is less than for the manus in a quadrupedal mode of locomotion. Depending on the validity of the mass, CM, and foot outline input parameters used here, this may support the hypothesis that differing modes of locomotion may be have used for traversing different substrates. The values employed in this study would suggest quadrupedalism to be potentially more advantageous on firmer substrates, where the manus will not sink, whilst a bipedal mode of locomotion would allow traversal of softer substrates.

As described above for the *Edmontosaurus* track simulations, and as described by Falkingham et al (in review), there are a range of substrates in which only the manus, and not the pes, of *Brachiosaurus* produce enough pressure to deform the substrate. When the subsurface undertracks generated by manus and pes are visualised, important features can be observed. The bowl like form of the *Brachiosaurus* pes (Figure 8) is reminiscent of a number of reported sauropod tracks (e.g. Ensom, 2002). The simulations here indicate that such a bowl-like form is characteristic of undertracks, potentially to a considerable depth.

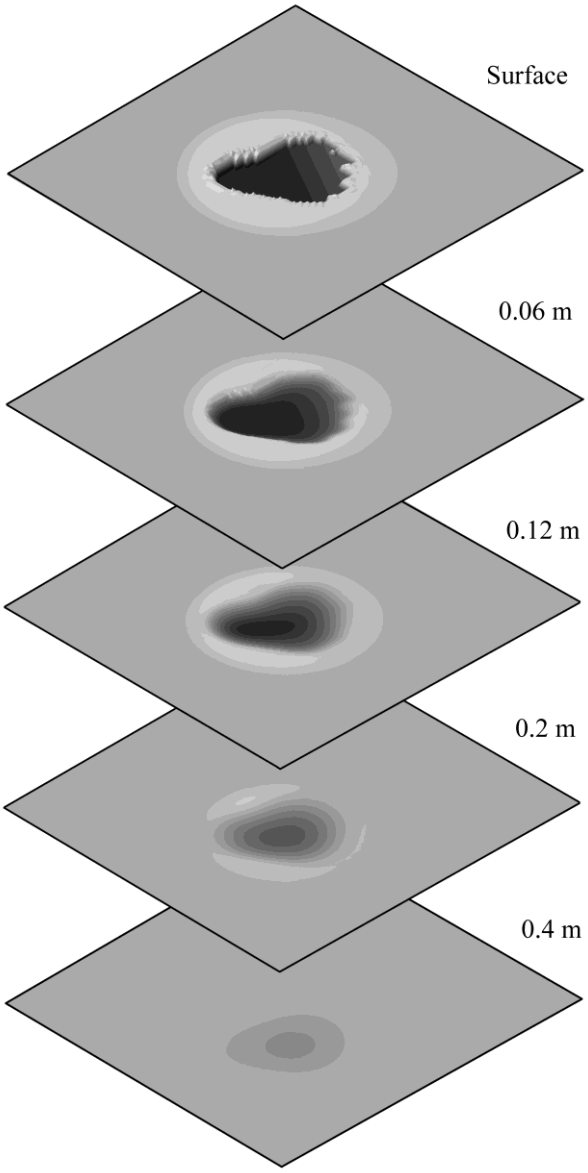


**Figure 8 – Series of undertracks as generated by the *Brachiosaurus* pes, seen in isometric view. Note the bowl-like form of successive undertracks, as compared with the flat interior and distinct outlines of the uppermost tracks. Darker shading represents deeper parts of the track.**

When the *Brachiosaurus* manus is observed as a series of undertracks, the development of a ridge running transversely across the track can be seen (Figure 9A,B). This ridge appears superficially similar to the undulating track surface that results from three phase movement of the foot (Manning, 2004; Thulborn and Wade, 1989). However, with full control of all input variables, it is known that in this case the loading was carried out in an entirely vertical

manner, through a flat foot, and so the ridge cannot be a function of limb kinematics or foot anatomy. Instead, this ridge is produced through the displacement of sediment according to Prandtl theory (Craig, 2004). As substrate is deformed by a load, it is pushed down and out from beneath the indenter (Figure 9C). The base of the actively deforming zone of substrate undulates against the rigid, non-moving zone. A cross section through this area results in a subsurface track containing a ridge of non-deformed substrate. This effect is seen in the *Brachiosaurus* manus track because of the round shape of the indenter. Note that other described ridges in sauropod tracks (e.g. Hwang et al., 2008) may appear different to those outlined here, and we do not necessarily suggest this mode of ridge formation for those cases.

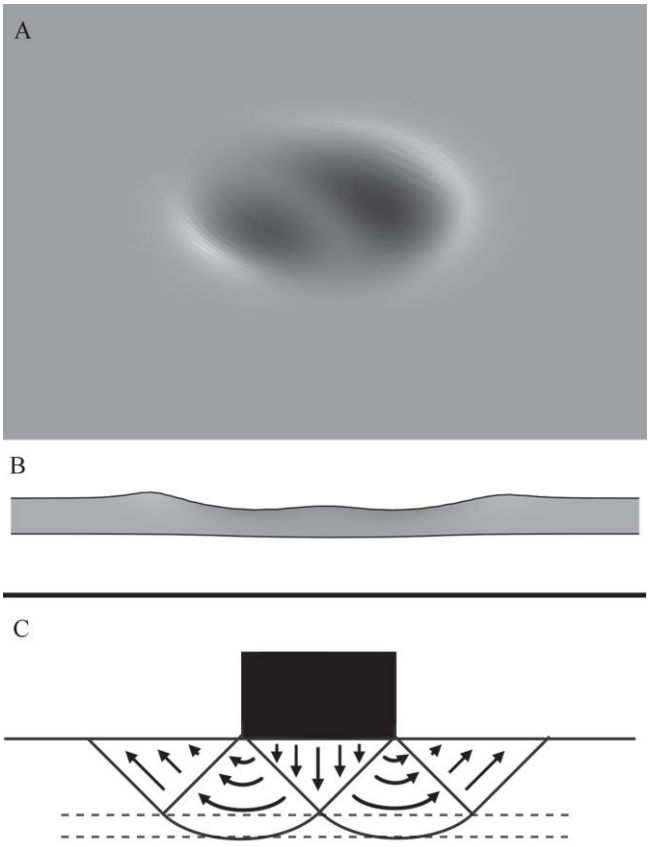


**Figure 9 – A) Isometric and B) cross section views of sauropod manus undertrack at a depth of 0.2 m (track generated in substrate of *Cu* = 110 kN/m$^2$ and halted when track depth reached 0.05 m). Note the transverse ridge running medio-laterally through the track, appearing similar to the three-phase track described by Manning (fig 6a; 2004; fig. 12.7; 2008). Darker shading represents deeper parts of the track. C) Theoretical displacement beneath a strip load in a cohesive substrate. If a track is exposed in a layer corresponding to that marked, tracks may appear to contain an internal ridge running across the widest part of the track (C modified from Allen, 1997).**

Both theropod tracks (*Struthiomimus* and *Tyrannosaurus*) indented to a considerably greater degree at the posterior of the virtual foot (Figure 10). The pes of the *Edmontosaurus* also exhibited this feature, albeit to a lesser extent. This effect is a function of the shapes of the indenters as seen in Falkingham et al. (in press). The appearance of a deeper posterior track portion under uniform loading of a flat indenter has important consequences for interpretations of limb kinematics from fossil tracks. The development of a deeper track beneath a larger, more consolidated part of the foot would mean that the 'two phase' interaction of the foot (weight bearing, and toe off) described by Thulborn and Wade (1989) could potentially produce a track with the appearance of a 'three-phase' foot-substrate interaction (which precedes the above phases with touch-down), where the heel and toes are deeper than the centre portion of the track (Manning, 2004, 2008). Trackways for which interpretations of locomotion have been made based on the 'pitch' of the track (Day et al., 2002; Mossman et al., 2003) must consider as an alternative, or at least confounding factor, varying shear strength (as a function of water content) throughout the total substrate layer at the time of track formation. Alternatively, variations in track 'pitch' may be influenced by grain size or compositional differences, given that sand responds in the opposite manner to muds (Falkingham et al., in press), allowing greater deformation beneath digits. Further research is required in order to clarify the relationship between substrate composition, limb kinematics, and pitch of track.

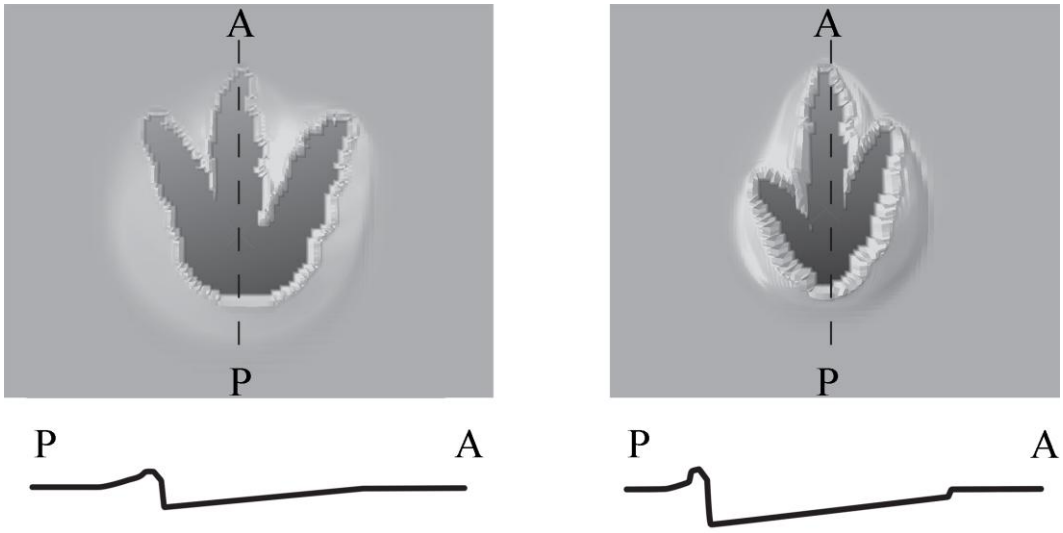


**Figure 10 - *Tyrannosaurus* (left) and *Struthiomimus* tracks (right) viewed in plan and cross section though digit III. Vertical dispalcement is greater at the posterior of the track due to the compact nature of the indenter in this area. Darker shading represents deeper parts of the track.**

Comparison between the *Struthiomimus* and *Tyrannosaurus* tracks simulated in this study indicates the extent to which interdigital angle (IDA) affects substrate penetration. The low interdigital angle of the digits of the *Struthiomimus* pes create an indenter that is more elongated and than the more splayed digits of the *Tyrannosaurus* pes. As the shape of an indenter becomes more elongated, it can be seen that the shape factor used in Equation 1 approaches 1. This reduces the bearing capacity relative to a circular or square indenter. It is beyond the scope of this study to support or reject the hypothesis that there may be a correlation between IDA and substrate, though it is hoped that future research may investigate this potential indicator of palaeosubstrate. Given that it has already been shown that IDA can change with depth within a single track volume (Margetts et al., 2006), and that as presented here it may vary with substrate consistency (as a deliberate behaviour of the animal, spreading the digits to spread the load when traversing soft mud for instance), IDA represents a poor character for describing ichnotaxa, but nevertheless represents important information regarding the producer and the substrate at the time of track formation.

## Conclusions

The simulation of tracks from a series of dinosaur taxa ranging in size from 400 kg to 25,000 kg shows a linear relationship between body mass and substrate shear strength required to produce observable tracks. The point of failure for a given track, and subsequently the shear strength of the substrate at the time of track formation can be approximated by calculating the bearing capacity required for a circular indenter of equal size and load. Variations around this approximation are due to the effects of foot shape

Tracks of significant depth are not possible in homogenous substrates without the presence of a firmer subsurface layer, because failure of the substrate will result in the animal being unable to traverse the area. A homogenous substrate will only record tracks from the largest animals that substrate can support without failing. There is, however, a strong bias towards tracks made by larger animals if there is a firmer substrate beneath a softer layer. This has wide ranging implications for interpretations of palaeodiversity and palaeoecology based on vertebrate track assemblages.

Presence of small and large tracks indented to the same depth on a single track-bearing surface (assuming time averaging can be accounted for) offer the highest possibility of presenting a true representation of faunal diversity in the area at the time of track formation. Caution is strongly advised in making any interpretations of faunal diversity or population dynamics from track assemblages where all tracks have been produced by similar sized producers. Such assemblages are most likely to represent a strongly biased preservation.

Specific features regarding track and undertrack formation have been noted for this range of indenters based on dinosaur taxa. Bowl-like sauropod pedal impressions are likely to be undertracks, probably of significant depth. Internal ridges may form in tracks either due to the vectors of displacement beneath a uniform load (as in the *Brachiosaurus* manus), or as a result of autopodia morphology causing non-uniform displacement under uniform loading (as in the tridactyl tracks).

The approach used here, of computer simulation using FEA, has allowed the generation of tracks and associated undertracks for a range of animal sizes that would be difficult to replicate using physical modelling. Employing computational methods has also catered for constancy in input variables between

experiments, and has provided the ability to easily and systematically manipulate those variables. We recognise that this study makes a number of assumptions and simplifications in terms of loading, and expect subsequent research to build on the methods used here to produce more complex models. Many of the conclusions and observations recorded here are related to the mechanics of substrates under load, and we hope that this will encourage further research into the effects of complex limb kinematics and kinetics on track formation, in light of the confounding geotechnical effects described here.

**Acknowledgements**

PLF and KTB were funded by the Natural Environment Research Council (NER/S/A/2006/14033, and NER/S/A/2006/14101 respectively). FEA simulations were run on the HPCx supercomputing service, using EPSRC grant EPF055595-1, awarded to LM. We would also like to thank James Jepson for commenting on an early draft of the manuscript.

**References**


Alexander, R.M., 1976. Estimates of Speeds of Dinosaurs. Nature, 261(5556): 129-130.

Alexander, R.M., 1977. Mechanics and scaling of terrestrial locomotion. In: T.J. Pedley (Editor), Scale effects in animal locomotion. Academic Press, London, pp. 93-110.

Alexander, R.M., 1989. Dynamics of Dinosaurs & other extinct giants. Columbia University Press, Chichester, 167 pp.

Allen, J.R.L., 1989. Fossil vertebrate tracks and indenter mechanics. Journal of the Geological Society, 146: 600-602.

Allen, J.R.L., 1997. Subfossil mammalian tracks (Flandrian) in the Severn Estuary, SW Britain: Mechanics of formation, preservation and distribution. Philosophical Transactions of the Royal Society of London Series B-Biological Sciences, 352(1352): 481-518.

Bates, K.T. et al., 2009a. Digital imaging and public engangement in palaeontology. Geology Today, 25(3): 95-100.

Bates, K.T., Manning, P.L., Hodgetts, D. and Sellers, W.I., 2009b. Estimating body mass properties of dinosaurs using laser imaging and 3D computer modelling. PLoSONE, 4(2).

Bates, K.T., Manning, P.L., Vila, B. and Hodgetts, D., 2008a. Three Dimensional Modelling and Analysis of Dinosaur Trackways. Palaeontology, 51(4): 999.

Bates, K.T. et al., 2008b. High-resolution LiDAR and photogrammetric survey of the Fumanya dinosaur tracksites (Catalonia): Implications for the conservation and interpretation of geological heritage sites. Journal of the Geological Society, London, 165(1): 115-127.

Benson, R.B.J., Butler, R.J., Lindgren, J. and Smith, A.S., 2010. Mesozoic marine tetrapod diversity: mass extinctions and temporal heterogeneity in geological megabiases affecting vertebrates. Proceedings of the Royal Society B: Biological Sciences, 277(1683): 829-834.

Benton, M.J. and Storrs, G.W., 1994. Testing the quality of the fossil record: Paleontological knowledge is improving. Geology, 22(2): 111-114.

Bimber, O., Gatesy, S.M., Witmer, L.M., Raskar, R. and Encarnacao, L.M., 2002. Merging fossil specimens with computer-generated information. Computer, 35(9): 25-30.

Breithaupt, B.H., Matthews, N. and Noble, T., 2004. An Integrated Approach to Three-Dimensional Data Collection at Dinosaur Tracksites in the Rocky Mountain West. Ichnos, 11: 11-26.

Breithaupt, B.H., Southwell, E.H., Adams, T. and Matthews, N.A., 2001. Innovative Documentation Methodologies in the Study of the Most Extensive Dinosaur Tracksite in Wyoming. 6th Fossil Research Conference Proceedings Volume: 113-122.

Burnet, D.S., 1987. Finite Element Analysis From Concepts to Applications. Addison-Wesley Publishing Company, Reading, M.A., 844 pp.

Craig, R.F., 2004. Craig's Soil Mechanics. Spon Press, Abingdon, 447 pp.

Currie, P.J., 1983. Hadrosaur Trackways from the Lower Cretaceous of Canada. Acta Palaeontologica Polonica, 28: 63-73.

Day, J.J., Norman, D.B., Upchurch, P. and Powell, H.P., 2002. Biomechanics - Dinosaur locomotion from a new trackway. Nature, 415(6871): 494-495.

Delair, J.B. and Sarjeant, W.A.S., 1985. History and bibliography of the study of fossil vertebrate footprints in the British isles: supplement 1973-1983. Palaeogeography, Palaeoclimatology, Palaeoecology, 49(1-2): 123-160.

Díaz-Martínez, I., Pérez-Lorente, F., Canudo, J.I. and Pereda-Suberbiola, X., 2009. Causas de la variabilidad en icnitas de dinosaurios y su aplicación en icnotaxonomía., Actas de las IV Jornadas Internacionales sobre Paleontología de Dinosaurios y su Entorno, pp. 207-220.

Ensom, P.C., 2002. Vertebrate trace fossils in the Purbeck limestone group of southern England. Special Papers in Palaeontology, 68: 203-220.

Falkingham, P.L., Bates, K.T., Margetts, L. and Manning, P.L., in review. Simulating sauropod manus only trackways.

Falkingham, P.L., Manning, P.L. and Margetts, L., 2007. Finite Element Analysis of Dinosaur Tracks. Journal of Vertebrate Paleontology, 27(3): 73A.

Falkingham, P.L., Margetts, L. and Manning, P.L., 2008. Using finite element analysis to aid interpretation of dinosaur tracks. Journal of Vertebrate Paleontology, 28(3): 76A.

Falkingham, P.L., Margetts, L. and Manning, P.L., in press. Fossil vertebrate tracks as palaeopenetrometers: Confounding effects of foot morphology. PALAIOS.

Falkingham, P.L., Margetts, L., Smith, I.M. and Manning, P.L., 2009. Reinterpretation of palmate and semi-palmate (webbed) fossil tracks; insights from finite element modelling. Palaeogeography, Palaeoclimatology, Palaeoecology, 271(1-2): 69-76.

Galton, P.M., 1970. The posture of hadrosaurian dinosaurs. Journal of Paleontology, 44(3): 464-473.

Gatesy, S.M., Bäker, M. and Hutchinson, J.R., 2009. Constraint-Based Exclusion of Limb Poses for Reconstructing Theropod Dinosaur Locomotion. Journal of Vertebrate Paleontology, 29(2): 535-544.

Gatesy, S.M., Middleton, K.M., Jenkins, F.A. and Shubin, N.H., 1999. Three-dimensional preservation of foot movements in Triassic theropod dinosaurs. Nature, 399(6732): 141-144.

Henderson, D.M., 2006. Burly Gaits: Centers of mass, stability, and the trackways of sauropod dinosaurs. Journal of Vertebrate Paleontology, 26(4): 907-921.

Hitchcock, E., 1858. Ichnology of New England. A Report on the Sandstone of the Connecticut Valley, Especially its Fossil Footmarks. W. White, Boston, MA [reprinted 1974 by Arno Press, New York], 220 pp.

Hutchinson, J.R., 2004. Biomechanical modeling and sensitivity analysis of bipedal running ability. 1. Extant taxa. Journal of Morphology, 262: 421-440.

Hwang, K.-G., Lockley, M.G., Huh, M. and Paik, I.S., 2008. A reinterpretation of dinosaur footprints with internal ridges from the Upper Cretaceous Uhangri Formation, Korea. Palaeogeography, Palaeoclimatology, Palaeoecology, 258(1-2): 59-70.

Leach, R., 1994. Engineering Properties of Wetland Soils.

Lockley, M.G., 1986. The paleobiological and paleoenvironmental importance of dinosaur footprints. PALAIOS, 1(1): 37-47.

Lockley, M.G., 1987. Dinosaur Tracks Symposium Signals a Renaissance in Vertebrate Ichnology. Paleobiology, 13(2): 246-252.

Lockley, M.G., 1991. Tracking Dinosaurs. Cambridge University Press, Cambridge, England., 252 pp.

Lockley, M.G. and Wright, J.L., 2001. Trackways of large quadrupedal ornithopods from the cretaceous: A review. In: D.H. Tanke and K. Carpenter (Editors), Mesozoic Vertebrate Life. Indiana University press, Bloomington, Indiana, pp. 428-442.

Manning, P.L., 1999. Dinosaur track formation, preservation and interpretation: fossil and laboratory simulated dinosaur track studies. Ph.D Thesis, University of Sheffield (England).

Manning, P.L., 2004. A new approach to the analysis and interpretation of tracks: examples from the dinosauria. In: D. McIlroy (Editor), The Application of Ichnology to Palaeoenvironmental and Stratigraphic Analysis. Special Publications, Geological Society, London, pp. 93-123.

Manning, P.L., 2008. *T.rex* speed trap. In: K. Carpenter and P.L. Larson (Editors), T. rex Symposium Volume. Indiana University Press., Bloomington & Indianapolis, pp. 205-231.

Mannion, P.D., Upchurch, P., Carrano, M.T. and Barrett, P.M., in press. Testing the effect of the rock record on diversity: a multidisciplinary approach to elucidating the generic richness of sauropodomorph dinosaurs through time. Biological Reviews.

Margetts, L., 2002. Parallel Finite Element Analysis. PhD Thesis, University of Manchester, Manchester, U.K.

Margetts, L., Smith, I.M. and Leng, J., 2005. Simulating Dinosaur Track Formation, COMPLAS, Barcelona.

Margetts, L., Smith, I.M., Leng, J. and Manning, P.L., 2006. Parallel three-dimensional finite element analysis of dinosaur trackway formation. In: H.F. Schweiger (Editor), Numerical Methods in Geotechnical Engineering. Taylor & Francis, London, pp. 743-749.

Marty, D., Meyer, C. and Billion-Bruyst, J.-P., 2006. Sauropod trackway patterns expression of special behaviour related to substrate consistency? An example from the Late Jurassic of northwestern Switzerland. Hantkeniana, 5: 38-41.

Matthews, N.A., Noble, T.A. and Breithaupt, B.H., 2006. The application of photogrammetry, remote sensing and geographic information systems

(GIS) to fossil resource management. Bulletin New Mexico Museum of Natural History and Science, 34: 119-131.

Maxwell, W.D. and Benton, M.J., 1990. Historical Tests of the Absolute Completeness of the Fossil Record of Tetrapods. Paleobiology, 16(3): 322-335.

Milàn, J., 2006. Variations in the morphology of emu (*Dromaius novaehollandiae*) tracks reflecting differences in walking pattern and substrate consistency: ichnotaxonomic implications. Palaeontology, 49: 405-420.

Milàn, J. and Bromley, R.G., 2006. True tracks, undertracks and eroded tracks, experimental work with tetrapod tracks in laboratory and field. Palaeogeography Palaeoclimatology Palaeoecology, 231(3-4): 253-264.

Milàn, J. and Bromley, R.G., 2008. The Impact of Sediment Consistency on Track and Undertrack Morphology: Experiments with Emu Tracks in Layered Cement. Ichnos, 15(1): 19 - 27.

Milàn, J., Christiansen, P. and Mateus, O., 2005. A three-dimensionally preserved sauropod manus impression from the Upper Jurassic of Portugal: Implications for sauropod manus shape and locomotor mechanics. Kaupia 14: 47-52.

Milàn, J., Clemmensen, L.B. and Bonde, N., 2004. Vertical sections through dinosaur tracks (Late Triassic lake deposits, East Greenland) - undertracks and other subsurface deformation structures revealed. Lethaia, 37(3): 285-296.

Minter, N.J., Braddy, S.J. and Davies, R.B., 2007. Between a rock and a hard place: arthropod trackways and ichnotaxonomy. Lethaia, 40(4): 365-375.

Moazen, M., Curtis, N., Evans, S. and Fagan, M., 2008. The role of cranial sutures in a lizard skull: a finite element analysis investigation. Journal of Vertebrate Paleontology, 28(3): 117A.

Moratalla, J.J., Sanz, J.L., Jiménez, R. and Lockley, M.G., 1992. A quadrupedal ornitjopod trackway from the lower Cretaceous of La Rioja (spain): Inferences on gait and hand structure. Journal of Vertebrate Paleontology, 12(2): 150-157.

Mossman, D.J., Brüning, R. and Powell, H.P., 2003. Anatomy of a Jurassic Theropod Trackway from Ardley, Oxfordshire, U.K. Ichnos, 10: 195-207.

Newcomb, D.E. and Birgisson, B., 1999. Measuring in situ mechanical properties of pavement subgrade soils. Transportation Research Board, 73 pp.

Padian, K. and Olsen, P.E., 1984. Footprints of the Komodo Monitor and the Trackways of Fossil Reptiles. Copeia(3): 662-671.

Porro, L., 2007. Feeding and Jaw Mechanism in *Heterrodontosaurus tucki* Using Finite Element Analysis. Journal of Vertebrate Paleontology, 27(3): 131A.

Potts, D.M. and Zdravković, L., 1999. Finite element analysis in geotechincal engineering: Theory. Thomas Telford, London, 440 pp.

Rayfield, E.J., 2004. Cranial mechanics and feeding in Tyrannosaurus rex. Proceedings of the Royal Society of London Series B-Biological Sciences, 271(1547): 1451-1459.

Rayfield, E.J., 2005. Using finite-element analysis to investigate suture morphology: A case study using large carnivorous dinosaurs. Anatomical Record Part a-Discoveries in Molecular Cellular and Evolutionary Biology, 283A(2): 349-365.

Rayfield, E.J., 2007. Finite Element Analysis and Understanding the Biomechanics and Evolution of Living and Fossil Organisms. Annual Review of Earth and Planetary Sciences, 35: 541-576.

Rayfield, E.J. et al., 2001. Cranial design and function in a large theropod dinosaur. Nature, 409(6823): 1033-1037.

Ross, C., F., 2005. Finite element analysis in vertebrate biomechanics. The Anatomical Record Part A: Discoveries in Molecular, Cellular, and Evolutionary Biology, 283A(2): 253-258.

Sarjeant, W.A.S., 1974. A history and bibliography of the study of fossil vertebrate footprints in the British isles. Palaeogeography, Palaeoclimatology, Palaeoecology, 16(4): 265-378.

Sarjeant, W.A.S., 1990. A name for the trace of an act: approaches to the nomenclature and classification of fossil vertebrate footprints. In: K.

Carpenter and P.J. Currie (Editors), Dinosaur systematics: perspective and approaches. Cambridge University Press, pp. 265-278.

Sellers, W.I., Manning, P.L., Lyson, T., Stevens, K. and Margetts, L., 2009. Virtual palaeontology: gait reconstruction of extinct vertebrates using high performance computing. Palaeontologia Electronica(12.3.11A).

Skempton, A.W., 1951. The Bearing Capacity of Clays. Proc. Building Research Congress, 1: 180-189.

Smith, I.M. and Griffiths, D.V., 2004. Programming the Finite Element Method. Wiley, Chichester, 628 pp.

Thulborn, R.A., 1990. Dinosaur Tracks. Chapman & Hall, London, 410 pp.

Thulborn, R.A. and Wade, M., 1989. A Footprint as a History of Movement. In: D.D. Gillette and M.G. Lockley (Editors), Dinosaur Tracks and Traces. Cambridge University Press, Cambridge, pp. 51-56.

Weishampel, D.B. and Horner, J.R., 1992. Hadrosauridae. In: D.B. Weishampel, P. Dodson and Osmólska (Editors), The Dinosauria. University of California Press, London, pp. 534-561.

Witmer, L.M., 1995. The extant phylogenetic bracket and the importance of reconstructing soft tissues in fossils. In: J.J. Thomason (Editor), Functional Morphology in Vertebrate Paleontology. Cambridge University Press, Cambridge, pp. 19-33.

Witzel, U. and Preuschoft, H., 2005. Finite-element model construction for the virtual synthesis of the skulls in vertebrates: Case study of *Diplodocus.* The Anatomical Record Part A: Discoveries in Molecular, Cellular, and Evolutionary Biology, 283A(2): 391-401.

Wright, J., 2005. Sauropod tracks and their importance in the study of the functional morphology and paleoecology of sauropods. In: K.A. Curry Rogers and J.A. Wilson (Editors), The Sauropods: Evolution and Paleobiology. University of California Press, Ltd., London, pp. 252-284.

Xing, L., Yong, Y.E., Chunkang, S.H.U., Guangzhao, P. and Hailu, Y.O.U., 2009. Structure, Orientation and Finite Element Analysis of the Tail Club of *Mamenchisaurus hochuanensis*. Acta Geologica Sinica - English Edition, 83(6): 1031-1040.

# Chapter 11 - Discussion

## *11.1 Summary of preceding chapters, and wider implications of this work.*

The preceding chapters (7-10) each present peer-reviewed contributions to the science of vertebrate ichnology, employing FEA as a method. That such work has been carried out successfully is testament to the use of FEA in investigating track formation. The validity of the method, including the advantages and limitations will be discussed later. First however, the discussions and conclusions of each piece of work will here be summarised.

### 11.1.1 The effects of substrate on track formation.

Chapter 7 (Falkingham *et al.*, 2009), in which webbed tracks were formed by non-webbed autopodia when the substrate was very soft, illustrates clearly the effects which substrate consistency can have upon the final morphology of a vertebrate track. Despite being a somewhat subtle feature, the artificial webbing produced in this particular study could, if found in a fossil track, considerably affect interpretations of foot morphology, and subsequently producer. This in turn may affect higher level interpretations, e.g. timing of evolutionary events or palaeodiversity.

Anfinson *et al.* (2009), whilst referring to *Sarjeantopodus* as a webbed track commented that the trace was "*incorrectly re-interpreted as an artefact by Falkingham et al. (2009)*," though offered no further explanation as to why this re-interpretation was incorrect. In the same volume, Lockley *et al.* (2009) stated that they remained "*sceptical of recent claims that such web traces are*

*preservational artefacts (Falkingham et al., 2009)*" though once again did not elaborate further. Regardless of whether the specific track (*Sarjeantopodus semipalmatus*) used for comparison in Chapter 7 (Falkingham *et al.*, 2009) shows true or artificial webbing, the conclusions of that work did not state that all webbing in tracks is artificial, but rather presented an alternative mechanism for their formation, a distinction evidently misunderstood by Anfinson *et al.* (2009) and Lockley *et al.* (2009), but acknowledged in other works (Raguel *et al.*, 2009; Sellers *et al.*, 2009; Xing *et al.*, 2009b). The experimental work nevertheless shows that webbed tracks can be formed by non-webbed feet.

The deformation of substrate beneath any uniform load or indenter may lead to the inclusion of other features within a track that appear to be related either to foot anatomy or complex limb kinematics. Some of these features were illustrated and discussed in Chapter 10 (Falkingham *et al.*, in prep). The appearance of ridges in the base of the sauropod manus undertracks appears superficially similar to the predicted ridges associated with three-phase limb movement described by Thulborn and Wade (1989), and figured by Manning (2004). However, in the experimental scenario, loading was a known condition, and no such dynamic motion was applied to the foot. Whilst it is indeed likely that a medio-lateral ridge will form beneath a three-phase foot due to pressure distributions during the foot cycle, consideration must also be given to the possibility that such features may represent artefacts of substrate movement according to Prandtl theory (see Figure 2.15).

It was shown in Chapter 10 (Falkingham *et al.*, in prep) that any given cohesive substrate has a 'Goldilocks' quality, where a very small range of loads for any indenter will result in significant plastic deformation without failure. The

consequence of this is that the composition of track assemblages, i.e. which animals have produced tracks, can be useful in determining substrate, and hence environmental, conditions when the tracks were formed.

This 'Goldilocks' quality can also be seen in the validation data used in Figure 6.6, where first yield occurs at a load of approximately 300 kN/m$^2$, and failure occurs when loading reaches the bearing capacity of 514 kN/m$^2$ (Smith and Griffiths, 2004). Though failure occurs at a considerably higher load than first plastic yield, it can be seen that maximum deformation only reaches 0.06 m before the substrate fails to support the load. Considering that the indenter in this case is a strip footing 5 m in width, 0.06 m deformation is very small. A depth of 0.05 m – just 1 % of the width of the indenter – is attained at a load of ~500 kN/m$^2$ – very close to the ultimate bearing capacity of the substrate. Subsequent unloading will further reduce this maximum depth when the indenter is removed due to elastic recovery, leaving a very shallow impression.

In order for tracks of clearly observable depth to form in cohesive substrates then, a firmer subsurface layer is required to support the load applied by the animal. This may take the form of a gradient in shear strength created by compaction of deeper sediments, or it may be the result of stratified, mechanically distinct layers within a substrate volume (including for instance a rigid base). In non-cohesive, grain supported, substrates such as sand, the inclusion of a friction angle (Figure 2.11and Figure 2.12) provides an increasing resistance to shear as confining stress increases, essentially providing a shear strength gradient with depth. This is why, though the sand on a beach may appear quite homogenous, a person does not sink when walking across it. The

muds of a tidal flat however, will often fail beneath a person's foot, resulting in sinking to a considerable depth.

The failure modes involved in track formation (general, local, and puncture shear) were shown in to be directly related to the Poisson's ratio of the substrate (see Figure 2.17). This provides numerical reasoning for associating strong displacement rims of tracks with saturated sediments at the time that track was formed, and can be combined with observations of apparent faunal diversity to aid in palaeoenvironmental interpretations.

### 11.1.2 The effects of foot morphology on track formation

Foot anatomy can have a varying degree of influence upon final track morphology. Obviously, the outline of the foot directly determines the overall shape of the track, as has been seen throughout this work. Foot morphology and geometry also determine the pressure applied to the substrate (given that pressure = force/area), and hence are direct factors in determining the depth to which a track indents, and whether the substrate can support the load or not. But foot anatomy can also have more subtle effects. As seen in Chapter 7 (Falkingham *et al.*, 2009), the generation of 'webbed' tracks occurred only when the interdigital angle was around 50°. If the outline of the foot was altered, either by spreading or closing the digits, the artificial webbing was not formed.

Chapter 8 (Falkingham *et al.*, in press-a) explored solely the effects of indenter morphology and geometry, and showed that an increasingly complex, distributed shape indented to a lesser degree than a more compact form such as a square, even when loaded equally. The extremes of shapes used in that study may be considered as abstract representations of the compact form of a sauropod foot, or the splayed digits of a tridactyl theropod. The differences in substrate

penetration can be attributed to a difference between applied pressure, and effective pressure. The cohesive nature of the substrates used meant that complex indenters would pull sediment down from around the edge of the indenter. A greater relative edge length emphasised this effect, essentially increasing the area of sediment deformed, and subsequently reducing the effective pressure.

The effect of indenter morphology on track depth noted in Chapter 8 (Falkingham *et al.*, in press-a) was generally subtle, though was shown to lead to differences in track depth of up to 20% between most and least compact forms. In Chapter 10 (Falkingham *et al.*, in prep) it was shown that each indenter used in the study varied in closeness to the predicted minimum *Cu* for a circular indenter.

Indenter morphology also affected the distribution of displacement within a track. The deeper posterior parts of tracks generated by tridactyl feet could potentially be misinterpreted as the result of limb kinematics. In their description of trackways from Ardley Quarry, Oxfordshire, Mossman *et al.* (2003) noted differences in the pitch of the base of the tracks, and attributed this to differences in ground reaction forces associated with acceleration and deceleration, as determined by stride lengths. However, the correlation between stride length and track pitch was not supported beyond the first nine tracks. Alternatively, given that sand and mud act differently under load (Chapter 2, Chapter 8 (Falkingham *et al.*, in press-a), and Chapter 10 (Falkingham *et al.*, in prep)), variations in pitch of tracks within a trackway are theoretically possible if the substrate undergoes a subtle compositional change from cohesive substrate to grain supported non-cohesive substrate, i.e. if the proportions of very fine and fine grains alter over

the length of the trackway. Such an explanation for change in pitch does not require any complex explanations based on limb kinematics or locomotion, though is impossible to support without examining the lithology of the site in great detail.

### 11.1.3 The effects of force on track formation

In Chapter 7 (Falkingham *et al.*, 2009), direct displacement was used to generate a track, as in previous simulation based work by Margetts *et al.* (2005; 2006), and as in physical experimental work (Allen, 1989, 1997; Milàn, 2006; Milàn and Bromley, 2006). This created a flat track of a specified depth in a homogenous substrate. Subsequent studies (chapters 8-10) generated tracks through an applied force. The 'Goldilocks' effect of homogenous, cohesive substrates meant that track generation still had to be halted at a predetermined depth as with the direct displacement method, but the use of force rather than vertical displacement allowed the indenters to move more freely, in a manner determined by soil mechanics rather than predetermined, resulting in tilted track bases as in the tridactyl tracks simulated in Chapter 10 (Falkingham *et al.*, in prep).

Throughout the work in this PhD, in studies where force has been used rather than direct displacement of surface nodes (i.e. Chapters 8-10), only a vertical component of the applied force has been considered, as in previous physical experimental work (Allen, 1989, 1997; Jackson *et al.*, 2009; Milàn, 2006; Milàn and Bromley, 2006). The force applied through an animal's foot is a complex vector which can change in magnitude and direction throughout the step cycle (Biewener, 2003). However, in extinct animals such as dinosaurs, these vectors and magnitudes are unknown, and indeed would vary to such a

large extent even for one individual animal, that attempting to reconstruct them at this point would only incorporate unfounded assumptions into the simulations. Even with a simplified loading regime, important effects related to the applied force can be observed in the preceding chapters, particularly Chapters 9 and 10.

The distribution of force in quadrupedal animals, according to published mass and centre of mass estimates of dinosaurs, when combined with the surface area of the fore- and hind- feet can create very different pressures, which in turn produce tracks of differing depths. This forms trackways consisting of only the pes *or* the manus. This is an important finding, as it means that there is no need for explanations involving buoyancy or locomotor mechanics in order to explain such trackways.

### 11.1.4 A framework for track formation.

The three factors discussed previously; force, substrate, and foot anatomy, wholly determine track formation. Given that $E$ is proportional to $Cu$ (Leach, 1994), and that the range of $v$ for naturally occurring cohesive substrates is relatively small, usually between 0.4 and 0.5 (Newcomb and Birgisson, 1999), substrates can be quantified according to the shear strength. Force is a complex vector, though if considered as creating an underfoot pressure, the contribution of loading to track formation may be treated as a scalar. Foot morphology is somewhat more difficult to accurately parameterise without using techniques such as geometric morphometrics (Belvedere, 2008), though the equation derived in Chapter 8 (Falkingham *et al.*, in press-a) provides a simple numeric means to quantify shape.

The relationship between load and $Cu$ has been shown in Chapter 10 (Falkingham *et al.*, in prep). **Error! Reference source not found.**There is a

specific failure plane, below which tracks are not formed due to the firmness of the substrate, and above which substrate failure occurs, and a firmer subsurface layer is required in order for an animal to traverse the area, and leave tracks. Interpreting vertebrate track assemblages in light of this complete framework can be used to constrain substrate conditions at the time of track formation, based on minimum *Cu* required to support any given animal represented in the assemblage.

For example, if the tracksite at the Zerbst Ranch (section 3.2.2) is considered, it can be seen that there are tracks made by medium and large animals, and these tracks are all on the order of ~5 – 10 mm in depth. The only tracks by smaller animals are the very shallow (< 1 mm) bird tracks. It is clear from the bird tracks that smaller animals were in the area at the time of track formation, yet their presence is barely recorded. Using the framework presented here, it could be predicted that the surface substrate (~10 mm in depth) had a low enough shear strength to fail beneath the feet of medium and large dinosaurs, but sufficiently high as to support the birds with minimal deformation. This surface layer was underlain by a substrate firm enough to support even the largest dinosaurs recorded at the site with minimal deformation.

## *11.2 FEA as a method for investigating vertebrate tracks.*

### 11.2.1 Advantages

The use of FEA has allowed for the simulation of tracks made by very large animals, specifically the 25,000 kg *Brachiosaurus* (see Chapters 9 & 10). Undertaking such an experiment physically would require specialist loading equipment and a very large soil volume of uniform properties. Such a soil volume would require considerable time and expertise in order to be given specific properties including *Cu*, *E*, and *v* (though see section 11.2.2 below). Additionally, very different equipment would be required for physically simulating tracks made by smaller animals (for instance the *Struthiomimus*), and if a separate soil volume was used, ensuring sediment properties remained constant would be difficult.

The versatility of digital visualisation has meant that undertracks can be viewed at any level within a simulated track (whilst retaining the original). This proved useful in Chapter 7 where it was shown artificial webbing extended throughout the track volume, and vital in Chapter 10 where subsurface features were examined, particularly in sauropod tracks. The ridge located in the undertrack of the *Brachiosaurus* manus is extremely sensitive to depth within the track volume owing to the mechanism of its formation (see Chapter 10 for details). A physical experiment in which undertracks are exposed at pre-determined levels (e.g. by the plaster of paris method as used by Manning (2004)) would be likely to miss such features.

When optimization techniques were utilised, such as reducing element number at the edges of the soil volume, solution times became acceptably fast, taking ~12 hours on an eight core workstation, and significantly less when using HPC facilities. Altering of input files to change substrate parameters or loading was accomplished with shell scripts, and meant that a series of simulations systematically altering variables could be run in short order, with minimal user interaction. Despite a considerable set-up and preparation time (including development of the FEA software, the mesh generation software, and creation of initial meshes), FEA offers a fast, repeatable, and quantifiable method with which to study track formation.

### 11.2.2 Limitations of FEA in the study of fossil tracks

A simulation or computer model, no matter how accurate and precise, can only produce an output as accurate as the inputs were to begin with. Though the model has been validated and shown to be in agreement with geotechnical theory (Chapter 6), the input parameters regarding substrate and load need to be determined outside of the program. It is very difficult to measure substrate parameters *in situ* to any real accuracy (Craig, 2004; Smith, 1981). The use of penetrometers and shear vanes provide reasonable measurements of shear strength, but calculation of Young's modulus and Poisson's ratio is extremely difficult without moving a sample of the soil to the lab (Smith, 1981). As such, an FEA simulation in which a modern track is reconstructed is only as accurate as the methods used to determine the mechanical properties of the substrate.

Further difficulties arise in attempting to reconstruct precise substrate properties from a fossilised track. Trying to simulate specific tracks may therefore be of limited use. Instead, the strengths of FEA simulation of track

formation lie in observing trends and features associated with ranges of substrate properties.

These limitations are not restricted solely to FEA simulation however, and are perhaps not as great as may first seem apparent. Allen (1989, 1997) used plasticine to model the muds of the Severn Estuary, and Milàn and Bromley (2006, 2008) used cement to examine undertracks beneath the foot of an emu. Despite these substrates not representing the exact properties of the medium in which the respective (sub)fossil tracks were made, important insights were nevertheless made.

The FEA software used throughout this thesis and the publications herein has been developed with cohesive substrates as the focus. This was a deliberate design decision from the beginning of software development, as many of the best tracks, in terms of details preserved, are formed in fine muds, rather than coarser sands (pers. obs., also see section 3.2.1). The inclusion of a friction parameter and the use of a Mohr Coulomb failure criterion (see section 2.5.5) have subsequently been incorporated into the ParaFEM libraries, and will allow future work on sand-like substrates.

Because the finite element method is designed to model the response of a continuum to stress, standard FEA code does not handle discontinuities without complex and computationally expensive re-meshing during analysis. This means that features such as concentric cracks around tracks (e.g. Figure 3.17) are visible in simulations only as peaks of stress. It is also impractical with standard FEA code to simulate ejecta and removal of substrate by the foot (Allen, 1997). Recent advances in FEA, such as the eXtended Finite Element Method (XFEM) have lead to FEA code designed to simulate crack propagation and

discontinuities (Belytschko and Gracie, 2007), though the extent to which this is useful for track simulations remains to be seen.

# Chapter 12 - Conclusions and further work

## *12.1 Conclusions and significance of work undertaken.*

1. Hitherto undiscovered bird tracks have been reported from the Mammoth Site of Hot Springs, South Dakota, U.S.A. These tracks add to the faunal assemblage recorded from the site, and provide direct evidence of shallow water located towards the central, upper part of the site.

2. A trace located in Wyoming, U.S.A. that had previously been described as produced by the dragging motion of a dinosaur tail has been reinterpreted as the trace of a crocodilian, extending the recorded fauna of the site.

3. Pre-processing mesh generation software was developed that included optimization routines in order to reduce solution times whilst maintaining high levels of accuracy. This was accomplished by using larger elements further away from the area of interest.

4. Webbed tracks can be formed in specific substrates (soft, waterlogged muds) even when the indenting foot is not webbed. Caution should be employed when describing such tracks, especially with single tracks that do not form part of a trackway.

5. Foot shape affects the extent to which displacement of substrate occurs. More compact morphologies result in deeper indentations than more splayed morphologies. This is related to the cohesion in muds. In non-cohesive substrates, this effect is reversed.

6. Assuming current published reconstructions of sauropods are correct, the distribution of force to manus and pes, determined by centre of mass position, can result in wildly different pressures beneath each. This in turn may lead to a wide range of substrates in which only the fore- or hind- feet can produce tracks. This provides a mechanism for manus-only trackway formation that does not rely on complex locomotor or soil mechanics.

7. Homogenous, semi-infinite cohesive substrates are poor track bearing media, exhibiting a 'Goldilocks' quality whereby only the largest animals the substrate can support leave observable tracks. Those tracks that are generated will typically be very shallow.

8. If underlain by a firmer substrate, there is a clear bias towards larger animals. Track assemblages containing only the tracks of large animals should not be considered appropriate for making interpretations regarding faunal diversity and palaeoecology.

9. Finite element analysis presents a rapid, tested method with which to explore vertebrate track formation.

## *12.2 Future work.*

In the immediate future, code pertaining to PalaeoFEM and Meshgen will be hosted on the internet and made freely available for download. This is a further contribution to the pre-existing ParaFEM code developed by Margetts (Margetts, 2002), available from http://code.google.com/p/parafem/. This will allow other researchers to use the software to carry out complementary research, and it will allow other users to further develop the code for other purposes, producing a self-perpetuating avenue of research.

The logical continuation of the work presented here is to investigate heterogeneous substrates, both in terms of mechanically distinct stratified layers, and in terms of randomly distributed properties within a substrate volume. Previous work in the soil mechanics literature (Paice *et al.*, 1996; Popescu *et al.*, 2005; Schweiger and Peschl, 2005) has investigated the effects of random spatial distribution of heterogeneous substrate properties beneath theoretical strip loads and noted interesting failure effects and slip lines. Such effects may have considerable consequences for track formation in which the indenter can be far more complex, leading to distinctive features associated with failure. Random distribution of substrate parameters may also alter the 'Goldilocks' effect, allowing a larger range of animals to traverse and form tracks in a substrate that appears homogenous on a large scale, but is heterogeneous on a small scale.

As noted above (section 11.2.2), PalaeoFEM has recently been modified to include a failure criterion for modelling sand. Though some of the best preserved tracks are formed in fine grained muds (e.g. many of those in the collections of Amherst College Museum of Natural History), a large number of

tracks are found in sandstones. There is considerable room then for simulation of tracks in sandy substrates: does the artificial webbing noted in Chapter 7 (Falkingham *et al.*, 2009) occur in non-cohesive substrates for instance? Is the 'Goldilocks' effect noted in Chapter 10 (Falkingham *et al.*, in prep) relevant for sandy sediments? Any continuation of this work involving more complex substrates or loading conditions will require additional validation against physical experiments. The numerical validation presented in section 6.2, and correlative physical work in Chapter 8 -is sufficient for the homogenous substrates and simple loading employed throughout this thesis, but would be insufficient for complex dynamic loading or heterogeneous substrates.

The most important direction in which to drive future research in this area is in answering more biologically orientated questions. A track is a function of both soil mechanics and biomechanics. Much of the research presented herein has examined the effects of soil mechanics on track formation. Simplifications have been made to loading and foot anatomy in order to elucidate the factors of track formation relating to the substrate. However, complex kinematic models of dinosaur locomotion are appearing in the literature (Bates *et al.*, in press; Farlow *et al.*, 2000; Gatesy, 1995; Gatesy *et al.*, 2009; Gatesy *et al.*, 1999; Hutchinson and Gatesy, 2006; Sellers and Manning, 2007; Sellers *et al.*, 2009). By using the kinematics produced by these studies to generate virtual tracks, track surfaces can be compared with fossil tracks to act as a validation for such locomotor reconstructions.

If limb kinematics do generate specific features related to locomotor mode, it may be possible to trace these features through the fossil track record and correlate them with time and geography. This may be as straightforward as

correlating the occurrence of sauropod manus only trackways with the evolution and distribution of macronarians, and other sauropod forms with a more anterior centre of mass. Tracing limb kinematics through time using tracks may be applicable to the locomotor evolution from theropods, with their tail-driven musculature, to birds (Gatesy, 1995), providing novel, direct lines of evidence applicable to wider studies of palaeobiology and evolution.

# Chapter 13 - References

Abo-Elnor, M., Hamilton, R. and Boyle, J. T., 2004. Simulation of soil-blade interaction for sandy soil using advanced 3D finite element analysis. Soil and Tillage Research, 75(1): 61-73

Agenbroad, L. D. and Mead, J. I., 1994. The Hot Springs Mammoth Site: A Decade of Field and Laboratory Research in Paleontology, Geology and Paleoecology. Fenske Printing Inc., Rapid City, S.D., 457 pp.

Alexander, R. M., 1976. Estimates of Speeds of Dinosaurs. Nature, 261(5556): 129-130

Alexander, R. M., 1989. Dynamics of Dinosaurs & other extinct giants. Columbia University Press, Chichester, 167 pp.

Alexander, R. M., 1991. Doubts and assumptions in dinosaur mechanics. Interdisciplinary Science Review, 16: 175-181

Alexander, R. M., 2006. Dinosaur biomechanics. Proceedings of the Royal Society B-Biological Sciences, 273(1596): 1849-1855

Allen, J. R. L., 1989. Fossil vertebrate tracks and indenter mechanics. Journal of the Geological Society, 146: 600-602

Allen, J. R. L., 1997. Subfossil mammalian tracks (Flandrian) in the Severn Estuary, SW Britain: Mechanics of formation, preservation and distribution. Philosophical Transactions of the Royal Society of London Series B-Biological Sciences, 352(1352): 481-518

Alonso, R., 1980. Icnites de dinosaurios (Ornithopoda, Hadrosauridae) en el Cretacio superior del norte Argentina. Acta Geologica Lilloana, 15: 55-63

Anfinson, O. A., Lockley, M. G., Kim, S. H., Kim, K. S. and Kim, J. Y., 2009. First report of the small bird track Koreanaornis from the Cretaceous of North America: implications for avian ichnotaxonomy and paleoecology. Cretaceous Research, 30(4): 885-894

Arbour, V., M. and Snively, E., 2009. Finite Element Analyses of Ankylosaurid Dinosaur Tail Club Impacts. The Anatomical Record: Advances in Integrative Anatomy and Evolutionary Biology, 292(9): 1412-1426

Bates, K. T., 2006. The application of Light Detection and Range (LIDAR) imaging to vertebrate ichnology and geoconservation (M.Phil Theses), University of Manchester, Manchester, 347 pp.

Bates, K. T., Breithaupt Brent, H., Falkingham, P. L., Matthews Neffra, A., Hodgetts, D. and Manning, P. L., 2009a. Integrated LiDAR & photogrammetric documentation of the Red Gulch Dinosaur Tracksite (Wyoming, USA). In: Foss, S.E., Cavin, J.L., Brown, T., Kirkland, J.I. and Santucci, V.L. (Editors), Proceedings of the Eighth Conference on Fossil Resources, Utah, pp. 101-103.

Bates, K. T., Falkingham, P. L., Hodgetts, D., Farlow, J. O., Breithaupt Brent, H., O'Brien, M., Matthews Neffra, A., Sellers, W. I. and Manning, P. L., 2009b. Digital imaging and public engangement in palaeontology. Geology Today, 25(4): 134-139

Bates, K. T., Manning, P. L., Margetts, L. and Sellers, W. I., in press. Sensitivity analysis in evolutionary robotic simulations of bipedal dinosaur running. Journal of Vertebrate Paleontology, 30(2)

Bates, K. T., Manning, P. L., Vila, B. and Hodgetts, D., 2008a. Three Dimensional Modelling and Analysis of Dinosaur Trackways. Palaeontology, 51(4): 999

Bates, K. T., Rarity, F., Manning, P. L., Hodgetts, D., Vila, B., Oms, O., Galobart, À. and Gawthorpe, R., 2008b. High-resolution LiDAR and photogrammetric survey of the Fumanya dinosaur tracksites (Catalonia): Implications for the conservation and interpretation of geological heritage sites. Journal of the Geological Society, London, 165(1): 115-127

Belvedere, M., 2008. Ichnological researches on the Upper Jurassic dinosaur tracks in the Iouaridène area (Demnat, cen tral High-Atlas, Morocco). Ph.D Thesis, Universitá degli Studi di Padova, Padova, Italy.

Belytschko, T. and Gracie, R., 2007. On XFEM applications to dislocations and interfaces. International Journal of Plasticity, 23(10-11): 1721-1738

Benton, M. J., 1986. Sedimentological Use of Dinosaurs. Nature, 321(6072): 732-732

Bertling, M., Braddy, S. J., Bromley, R. G., Demathieu, G. R., Genise, J., Mikulas, R., Nielsen, J. K., Nielsen, K. S. S., Rindsberg, A. K., Schlirf, M. and Uchman, A., 2006. Names for trace fossils: a uniform approach. Lethaia, 39(3): 265-286

Biewener, A. A., 2003. Animal Locomotion. Oxford University Press, Oxford, 281 pp.

Bimber, O., Gatesy, S. M., Witmer, L. M., Raskar, R. and Encarnacao, L. M., 2002. Merging fossil specimens with computer-generated information. Computer, 35(9): 25-30

Boussinesq, J., 1883. Application des potentials á l'étude de l'équilibre et du mouvement des solides élastiques. Gauthier-Villars, Paris.

Bowles, J. E., 1968. Foundation analysis and design. McGraw-Hill, New York, 659 pp.

Breithaupt, B. H., Matthews, N. and Noble, T., 2004. An Integrated Approach to Three-Dimensional Data Collection at Dinosaur Tracksites in the Rocky Mountain West. Ichnos, 11: 11-26

Breithaupt, B. H. and Matthews, N. A., 2001. Preserving paleontological resourcs using photogrammetry and geographic information systems. In: Harmon, D. (Editor), Crossing Boundaries in Park Management: Proceedings of the 11th Conference on Research and Resource Management in Parks and Public Lands. The George Wright Society, Inc.

Breithaupt, B. H., Southwell, E. H., Adams, T. and Matthews, N. A., 2001. Innovative Documentation Methodologies in the Study of the Most Extensive Dinosaur Tracksite in Wyoming. 6th Fossil Research Conference Proceedings Volume: 113-122

Breithaupt, B. H., Southwell, E. H., Adams, T. and Matthews, N. A., 2006. The Red Gulch Dinosaur Tracksite; public participation in the conservation and management of a world-class paleontological site. Bulletin New Mexico Museum of Natural History and Science, 34(10)

Brown, R., Ferguson, J., Lawrence, M. and Lees, D., 1987. Tracks and Signs of the Birds of Britain and Europe. Christopher Helm, London, 232 pp.

Burnet, D. S., 1987. Finite Element Analysis From Concepts to Applications. Addison-Wesley Publishing Company, Reading, M.A., 844 pp.

Casamiquela, R., 1968. Ichnologia. In: Casamiquela, R. and Fasola, A. (Editors), Sobre pisadas de dinosauros del Cretacio Inferior de Colchague (Chile). Universidad de Chile Publication, pp. 13-24.

Casanovas, M. L., Ezquerra, R., Fernandez, A., Perez-Lorente, F. S., J. V. and Torcida, F., 1993. Tracks of a herd of webbed ornithopods and other footprints found in the same site (Igea, la Rioja, Spain). Revue de Paleobiologie, 7: 29-36

Chen, P., Dong, Z. and Zhen, S., 1998. An exceptionally well-preserved theropod dinosaur from the Yixian formation of China. Nature, 391: 147-152

Conti, M. A., Morsilli, M., Nicosia, U., Sacchi, E., Savino, V., Wagensommer, A., Di Maggio, L. and Gianolla, P., 2005. Jurassic dinosaur footprints from southern Italy: Footprints as indicators of constraints in paleogeographic interpretation. PALAIOS, 20(6): 534-550

Coombs, W. P., 1980. Swimming Ability of Carnivorous Dinosaurs. Science, 207(4436): 1198-1200

Craig, R. F., 1997. Soil Mechanics. Chapman & Hall, London, 485 pp.

Craig, R. F., 2004. Craig's Soil Mechanics. Spon Press, Abingdon, 447 pp.

Currie, P. J., 1983. Hadrosaur Trackways from the Lower Cretaceous of Canada. Acta Palaeontologica Polonica, 28: 63-73

D'Appolonia, D. J., Poulos, H. G. and Ladd, C. C., 1971. Initial Settlement of Structures on Clay Journal of the Soil Mechanics and Foundations Division, 97(10): 1359-1377

Darwin, C. R., 1859. On the Origin of Species by Means of Natural Selection, or the Preservation of Favoured Races in the Struggle for Life. John Murray, London, 502 pp.

Day, J. J., Norman, D. B., Upchurch, P. and Powell, H. P., 2002. Biomechanics - Dinosaur locomotion from a new trackway. Nature, 415(6871): 494-495

Duncan, H., 1831. An account of the tracks and footprints of animals found impressed on sandstone in the Quarry of Corncockle Muir in Dumfries-shire. Transactions of the Royal Society of Edinburgh, 11(1830): 194-209

Duncan, K. and Holdaway, R., 1989. Footprint Pressures and Locomotion of Moas and Ungulates and Their Effects on the New-Zealand Indigenous Biota through Trampling. New Zealand Journal of Ecology, 12: 97-101

Ezquerra, R., Doublet, S., Costeur, L., Galton, P. M. and Pérez-Lorente, F., 2007. Were non-avian theropod dinosaurs able to swim? Supportive evidence from an Early Cretaceous trackway, Cameros Basin (La Rioja, Spain). Geology, 35(6): 507-510

Falkingham, P. L., Bates, K. T., Margetts, L. and Manning, P. L., in prep. The Goldilocks effect: Preservational bias in vertebrate track assemblages.

Falkingham, P. L., Bates, K. T., Margetts, L. and Manning, P. L., in review. Simulating sauropod manus only trackways.

Falkingham, P. L., Margetts, L. and Manning, P. L., in press-a. Fossil vertebrate tracks as palaeopenetrometers: Confounding effects of foot morphology. PALAIOS

Falkingham, P. L., Margetts, L., Smith, I. M. and Manning, P. L., 2009. Reinterpretation of palmate and semi-palmate (webbed) fossil tracks; insights from finite element modelling. Palaeogeography, Palaeoclimatology, Palaeoecology, 271(1-2): 69-76

Falkingham, P. L., Milàn, J. and Manning, P. L., in press-b. A Crocodilian trace from the Lance Formation (Upper Cretaceous) of Wyoming. In: Milàn, J.,

Lucas Spencer, G., Lockley, M. and Spielmann, J. (Editors), Crocodylian tracks and traces. New Mexico Museum of Natural History and Science Bulletin.

Falkingham, P. L., Thompson, K., Agenbroad, L. D. and Manning, P. L., 2010. Bird tracks at the Mammoth Site of Hot Springs, South Dakota, USA. Ichnos, 17(1): 34-39.10.1080/10420940903358669

Farlow, J. O., Gatesy, S. M., Holtz, T. R., Hutchinson, J. R. and Robinson, J. M., 2000. Theropod locomotion. American Zoologist, 40(4): 640-663

Felippa, C. A., 2004. Introduction to Finite Element Methods.

Fervers, C. W., 2004. Improved FEM simulation model for tire-soil interaction. Journal of Terramechanics, 41(2-3): 87-100

Fornos, J. J., Bromley, R. G., Clemmensen, L. B. and Rodriguez-Perea, A., 2002. Tracks and trackways of Myotragus balearicus Bate (Artiodactyla, Caprinae) in Pleistocene aeolianites from Mallorca (Balearic Islands, Western Mediterranean). Palaeogeography Palaeoclimatology Palaeoecology, 180(4): 277-313

Gatesy, S. M., 1995. Functional evolution of the hind limb and tail from basal theropods to birds. In: Thomason, J.J. (Editor), Functional vertebrate morphology in vertebrate paleontology. Cambridge University Press, Cambridge, pp. 277.

Gatesy, S. M., 2003. Direct and indirect Track Features: What Sediment Did a Dinosaur Touch? Ichnos, 10: 91-98

Gatesy, S. M., Bäker, M. and Hutchinson, J. R., 2009. Constraint-Based Exclusion of Limb Poses for Reconstructing Theropod Dinosaur

Locomotion. Journal of Vertebrate Paleontology, 29(2): 535-544.10.1671/039.029.0213

Gatesy, S. M., Middleton, K. M., Jenkins, F. A. and Shubin, N. H., 1999. Three-dimensional preservation of foot movements in Triassic theropod dinosaurs. Nature, 399(6732): 141-144

Gatesy, S. M., Shubin, N. H. and Jenkins, F. A., 2005. Anaglyph stereo imaging of dinosaur track morphology and microtopography. Palaeontologia Electronica, 8(1).10a

Artn 10a

Gauthier, J., 1986. Saurischian monophyly and the origin of birds. Memoirs of the California Academy of Sciences, 8: 1-55

Graversen, O., Milan, J. and Loope, D. B., 2007. Dinosaur Tectonics: A Structural Analysis of Theropod Undertracks with a Reconstruction of Theropod Walking Dynamics. Journal of Geology, 115: 641-654

Hambleton, J. P. and Drescher, A., 2008. Modeling wheel-induced rutting in soils: Indentation. Journal of Terramechanics, 45(6): 201-211

Harris, J. D., Johnson, K. R., Hicks, J. and Tauxe, L., 1996. Four-toed theropod footprints and a paleomagnetic age from the Whetstone Falls Member of the Harebell Formation (Upper cretaceous: Maastrichtian), northwestern Wyoming. Cretaceous Research, 17(4): 381-401

Haubold, H., 1971. Ichnia amphibiorum et reptiliorum fossilium. In: Kuhn, O. (Editor), Handbuch der Paläoherpetologie, Part 18. Gustav Fisher Verlag, Stuttgart.

Henderson, D. M., 2003. Footprints, trackways and hip heights of bipedal dinosaurs - testing hip height preictions with computer models. Ichnos, 10: 99-114

Henderson, D. M., 2006a. Burly Gaits: Centers of mass, stability, and the trackways of sauropod dinosaurs. Journal of Vertebrate Paleontology, 26(4): 907-921.doi:10.1671/0272-4634(2006)26[907:BGCOMS]2.0.CO;2

Henderson, D. M., 2006b. Simulated weathering of dinosaur tracks and the implications for their characterization. Canadian Journal of Earth Sciences, 43(6): 691-704

Hitchcock, E., 1836. Ornithichnology - description of the foot marks of birds (Ornithichnites) on New Red Sandstone in Massachusetts. American Journal of Science, 29: 307-340

Hitchcock, E., 1858. Ichnology of New England. A Report on the Sandstone of the Connecticut Valley, Especially its Fossil Footmarks. W. White, Boston, MA [reprinted 1974 by Arno Press, New York], 220 pp.

Hutchinson, J. R. and Gatesy, S. M., 2006. Dinosaur locomotion - Beyond the bones. Nature, 440(7082): 292-294

Irby, G. V., 1995. Posterolateral Markings on Dinosaur Tracks, Cameron Dinosaur Tracksite, Lower Jurassic Moenave Formation, Northeastern Arizona. Journal of Paleontology, 69(4): 779-784

Jackson, S. J., Whyte, M. A. and Romano, M., 2009. Laboratory-controlled simulations of dinosaur footprints in sand: a key to understanding vertebrate track formation and preservation. PALAIOS, 24(4): 222-238.10.2110/palo.2007.p07-070r

Karafiath, L. L. and Nowatzki, E. A., 1978. Soil Mechanics for Off-Road Vehicle Engineering. Series on Rock and Soil Mechanics. Trans Tech publications, Aedermannsdorf, 515 pp.

Karthigeyan, S., Ramakrishna, V. V. G. S. T. and Rajagopal, K., 2006. Influence of vertical load on the lateral response of piles in sand. Computers and Geotechnics, 33(2): 121-131

Kessel, A. B., Philippi, U. and Nachtigall, W., 1998. Biomechanical aspects of the insect wing: an analysis using the finite element method. Comp. Biol. Med., 28: 423-37

Larson, P. L., 2003. An important trackway site from the Lance Formation (Late Cretaceous) of Niabrara County, Wyoming, with new information on the behavior of *T.rex*. Journal of Vertebrate Paleontology, 23(70A): 72

Leach, R., 1994. Engineering properties of wetland soils. WRP technical note SG-RS-1.2, U.S. Army Engineer Research and Development Center, Vicksburg, MS.

Leonardi, G., 1984. Le impronte fossili di dinosauri, Sulle orme de dinosauri. Erizzo Editrice, Venice, pp. 165-186.

Leonardi, G., 1987. Glossary and Manual of Tetrapod Footprint Palaeoichnology. República Federativa do Brasil, Minastério das Minas e Energia, Departmento Nacional de Produção Mineral, , Brasilia.

Llompart, C., 1984. Un neuvo yacimiento de ichnitas de dinosaurios en las facies Garumniensis de la Conca de Tremp (Leida Espana). Acta Geologica Hispanica, 19: 143-147

Lockley, M., Chin, K., Houck, K., Matsukawa, M. and Kukihara, R., 2009. New interpretations of Ignotornis, the first-reported Mesozoic avian footprints:

implications for the paleoecology and behavior of an enigmatic Cretaceous bird. Cretaceous Research, 30(4): 1041-1061

Lockley, M. G., 1986. The paleobiological and paleoenvironmental importance of dinosaur footprints. PALAIOS, 1(1): 37-47

Lockley, M. G., 1987. Dinosaur Tracks Symposium Signals a Renaissance in Vertebrate Ichnology. Paleobiology, 13(2): 246-252

Lockley, M. G., 1991. Tracking Dinosaurs. Cambridge University Press, Cambridge, England., 252 pp.

Lockley, M. G., 2006. On the trail of dinosaurs. Geotimes, 51(1): 30-34

Lockley, M. G., 2007. A Tale of Two Ichnologies: The Different Goals and Potentials of Invertebrate and Vertebrate (Tetrapod) Ichnotaxonomy and How They Relate to Ichnofacies Analysis. Ichnos, 14(1): 39 - 57

Lockley, M. G. and Hunt, A. P., 1994. A track of the giant theropod dinosaur Tyrannosaurus from close to the Cretaceous/Tertiary boundary, northern New Mexico. Ichnos, 3(3): 213-218

Lockley, M. G., Lires, J., Garc, iacute, a-Ramos, J. C., Pinuela, L. and Avanzini, M., 2007. Shrinking the World's Largest Dinosaur Tracks: Observations on the Ichnotaxonomy of *Gigantosauropus asturiensis* and *Hispanosauropus hauboldi* from the Upper Jurassic of Asturias, Spain. Ichnos, 14(3): 247 - 255

Lockley, M. G., Nadon, G. and Currie, P. J., 2004. A diverse Dinosaur-Bird footprint assemblage from the Lance Formation, Upper Cretaceous, Eastern Wyoming: Implications for ichnotaxonomy. Ichnos, 11(3): 229 - 249

Lockley, M. G., Schulp, A. S., Meyer, C. A., Leonardi, G. and Kerumba Mamani, D., 2002. Titanosaurid trackways from the Upper Cretaceous of Bolivia: evidence for large manus, wide-gauge locomotion and gregarious behaviour. Cretaceous Research, 23(3): 383-400

Manning, P. L., 1999. Dinosaur track formation, preservation and interpretation: fossil and laboratory simulated dinosaur track studies. Ph.D Thesis, University of Sheffield (England).

Manning, P. L., 2004. A new approach to the analysis and interpretation of tracks: examples from the dinosauria. In: McIlroy, D. (Editor), The Application of Ichnology to Palaeoenvironmental and Stratigraphic Analysis. Special Publications, Geological Society, London, pp. 93-123.

Manning, P. L., 2008. *T.rex* speed trap. In: Carpenter, K. and Larson, P.L. (Editors), T. rex Symposium Volume. Indiana University Press., Bloomington & Indianapolis, pp. 205-231.

Manning, P. L., Margetts, L., Johnson, M. R., Withers, P. J., Sellers, W. I., Falkingham, P. L., Mummery, P. M., Barrett, P. M. and Raymont, D. R., 2009. Biomechanics of Dromaeosaurid Dinosaur Claws: Application of X-Ray Microtomography, Nanoindentation, and Finite Element Analysis. The Anatomical Record: Advances in Integrative Anatomy and Evolutionary Biology, 292(9): 1397-1405

Manning, P. L., Ott, C. and Falkingham, P. L., 2008. The First Tyrannosaurid Track from the Hell Creek Formation (Late Cretaceous), Montana, U.S.A. PALAIOS, 23: 645-647

Margetts, L., 2002. Parallel Finite Element Analysis. PhD Thesis, University of Manchester, Manchester, U.K.

Margetts, L., Smith, I. M. and Leng, J., 2005. Simulating Dinosaur Track Formation. In: Oñate, E. and Owen, D.R.J. (Editors), Extended Abstracts, VIII International Conference on Computational Plasticity (COMPLAS), CIMNE, Barcelona, pp. 4.

Margetts, L., Smith, I. M., Leng, J. and Manning, P. L., 2006. Parallel three-dimensional finite element analysis of dinosaur trackway formation. In: Schweiger, H.F. (Editor), Numerical Methods in Geotechnical Engineering. Taylor & Francis, London, pp. 743-749.

Matthews, N. A., Breithaupt, B. H., Noble, T., Titus, A. and Smith, J., 2005. A geospatial look at the morphological variation of tracks at the Twentymile Wash dinosaur tracksite, Grand Staircase-Escalante National Monument, Utah. Journal of Vertebrate Paleontology, 25(3)

Matthews, N. A., Noble, T. A. and Breithaupt, B. H., 2006. The application of photogrammetry, remote sensing and geographic information systems (GIS) to fossil resource management. Bulletin New Mexico Museum of Natural History and Science, 34: 119-131

Milàn, J., 2006. Variations in the morphology of emu (*Dromaius novaehollandiae*) tracks reflecting differences in walking pattern and substrate consistency: ichnotaxonomic implications. Palaeontology, 49: 405-420

Milàn, J. and Bromley, R. G., 2006. True tracks, undertracks and eroded tracks, experimental work with tetrapod tracks in laboratory and field. Palaeogeography Palaeoclimatology Palaeoecology, 231(3-4): 253-264

Milàn, J. and Bromley, R. G., 2008. The Impact of Sediment Consistency on Track and Undertrack Morphology: Experiments with Emu Tracks in Layered Cement. Ichnos, 15(1): 19 - 27

Milàn, J., Clemmensen, L. B. and Bonde, N., 2004. Vertical sections through dinosaur tracks (Late Triassic lake deposits, East Greenland) - undertracks and other subsurface deformation structures revealed. Lethaia, 37(3): 285-296

Milàn, J. and Loope, D. B., 2007. Preservation and Erosion of Theropod Tracks in Eolian Deposits: Examples from the Middle Jurassic Entrada Sandstone, Utah, U.S.A. The Journal of Geology, 115(3): 375-386.doi:10.1086/512758

Milner, A. R. C., Harris, J. D., Lockley, M. G., Kirkland, J. I. and Matthews, N. A., 2009. Bird-Like Anatomy, Posture, and Behavior Revealed by an Early Jurassic Theropod Dinosaur Resting Trace. PLoS ONE, 4(3): e4591

Minter, N. J., Braddy, S. J. and Davies, R. B., 2007. Between a rock and a hard place: arthropod trackways and ichnotaxonomy. Lethaia, 40(4): 365-375

Moreno, K., Carrano, M. T., Snyder, R., 2007. Morphological changes in pedal phalanges through ornithopod dinosaur evolution: A biomechanical approach. Journal of Morphology, 268(1): 50-63

Mossman, D. J., Brüning, R. and Powell, H. P., 2003. Anatomy of a Jurassic Theropod Trackway from Ardley, Oxfordshire, U.K. Ichnos, 10: 195-207

Mulungye, R. M., Owende, P. M. O. and Mellon, K., 2007. Finite element modelling of flexible pavements on soft soil subgrades. Materials & Design, 28(3): 739-756

Myers, T. S. and Fiorillo, A. R., 2009. Evidence for gregarious behavior and age segregation in sauropod dinosaurs. Palaeogeography, Palaeoclimatology, Palaeoecology, 274(1-2): 96-104

Nadon, G. C., 2001. The Impact of Sedimentology on Vertebrate Track Studies. In: Tanke, D.H. and Carpenter, K. (Editors), Mesozoic Vertebrate Life. Indiana University Press, Bloomington, pp. 395-407.

Nadon, G. C. and Issler, D. R., 1997. The compaction of floodplain sediments: Timing, magnitude, and implications. Geoscience Canada, 24(1): 37-44

Nakashima, H. and Oida, A., 2004. Algorithm and implementation of soil-tire contact analysis code based on dynamic FE-DE method. Journal of Terramechanics, 41(2-3): 127-137

Nakashima, H. and Wong, J. Y., 1993. A three-dimensional tire model by the finite element method. Journal of Terramechanics, 30(1): 21-34

Newcomb, D. E. and Birgisson, B., 1999. Measuring in situ mechanical properties of pavement subgrade soils. Transportation Research Board, 73 pp.

Nicosia, U., Petti, F. M., Perugini, G., Porchetti, S. D., rsquo, Orazi, Sacchi, E., Conti, M. A., Mariotti, N. and Zarattini, A., 2007. Dinosaur Tracks as Paleogeographic Constraints: New Scenarios for the Cretaceous Geography of the Periadriatic Region. Ichnos, 14(1): 69 - 90

Ostrom, J. H., 1972. Were some dinosaurs gregarious? Palaeogeography, Palaeoclimatology, Palaeoecology, 11(4): 287-301

Pacheco, P. S., 1997. Parallel Programming with MPI. Morgan Kaufmann, San Francisco, 418 pp.

Padian, K., 1999. Dinosaur tracks in the computer age. Nature, 399(6732): 103-104

Padian, K. and Olsen, P. E., 1984. Footprints of the Komodo Monitor and the Trackways of Fossil Reptiles. Copeia(3): 662-671

Paice, G. M., Griffiths, D. V. and Fenton, G. A., 1996. Finite Element Modeling of Settlements on Spatially Random Soil. Journal of Geotechnical Engineering, 122(9): 777-779

Pemberton, S. G. and Gingras, M. K., 2003. The Reverend Henry Duncan (1774-1846) and the Discovery of the First Fossil Footprints. Ichnos, 10: 69-75

Philippi, U. and Nachtigall, W., 1996. Functional morphology of regular echinoid tests (Echinodermata, Echinoida): a finite element study. Zoomorphology, 116: 113-35

Popescu, R., Deodatis, G. and Nobahar, A., 2005. Effects of random heterogeneity of soil properties on bearing capacity. Probabilistic Engineering Mechanics, 20(4): 324-341

Popescu, R., Prevost, J. H., Deodatis, G. and Chakrabortty, P., 2006. Dynamics of nonlinear porous media with applications to soil liquefaction. Soil Dynamics and Earthquake Engineering, 26(6-7): 648-665

Porada, H. and Bouougri, E. H., 2007. Wrinkle structures--a critical review. Earth-Science Reviews, 81(3-4): 199-215

Porro, L., 2006. Cranial biomechanics of basal ornithischians using finite-element analysis. Journal of Vertebrate Paleontology, 26: 112A

Porro, L., 2007. Feeding and Jaw Mechanism in *Heterrodontosaurus tucki* Using Finite Element Analysis. Journal of Vertebrate Paleontology, 27(3): 131A

Potts, D. M. and Zdravković, L., 1999. Finite element analysis in geotechincal engineering: Theory. Thomas Telford, London, 440 pp.

Potts, D. M. and Zdravković, L., 2001. Finite element analysis in geotechnical engineering: Application. Thomas Telford, London, 427 pp.

Raguel, M. G., Gonzalez, I. C., Diaz-Martinez, I. and Perez-Lorente, F., 2009. Fragmentos de roca con huellas de aves en el terciario de alcanadre (La Rioja). Descripcion, estructuras y problemas de identificacion. Zubia, 27: 81-158

Raikow, R. J., 1985. Locomotor System. In: King, A.S. and McLelland, J. (Editors), Form and Function in Birds. Academic Press, Londong, pp. 57-147.

Rayfield, E. J., 2004. Cranial mechanics and feeding in Tyrannosaurus rex. Proceedings of the Royal Society of London Series B-Biological Sciences, 271(1547): 1451-1459

Rayfield, E. J., 2005. Using finite-element analysis to investigate suture morphology: A case study using large carnivorous dinosaurs. Anatomical Record Part a-Discoveries in Molecular Cellular and Evolutionary Biology, 283A(2): 349-365

Rayfield, E. J., 2007. Finite Element Analysis and Understanding the Biomechanics and Evolution of Living and Fossil Organisms. Annual Review of Earth and Planetary Sciences, 35: 541-576

Rayfield, E. J., Norman, D. B., Horner, C. C., Horner, J. R., Smith, P. M., Thomason, J. J. and Upchurch, P., 2001. Cranial design and function in a large theropod dinosaur. Nature, 409(6823): 1033-1037

Reineck, H. E. and Singh, I. B., 1980. Depositional Sedimentary Environments. Springer Verlag, Berlin, 542 pp.

Richardson, L. F., 1910. The approximate arithmetical solution by finite differences of physical problems. Transactions of the Royal Society of London A, 210: 307-357

Sarjeant, W. A. S., 1974. A history and bibliography of the study of fossil vertebrate footprints in the British isles. Palaeogeography, Palaeoclimatology, Palaeoecology, 16(4): 265-378

Sarjeant, W. A. S., Delair, J. B. and Lockley, M. G., 1998. The footprints of *Iguanodon*: a history and taxonomic study. Ichnos, 6(183-202)

Scheiner, S., Pichler, B., Hellmich, C. and Eberhardsteiner, J., 2006. Loading of soil-covered oil and gas pipelines due to adverse soil settlements - Protection against thermal dilatation-induced wear, involving geosynthetics. Computers and Geotechnics, 33(8): 371-380

Schweiger, H. F. and Peschl, G. M., 2005. Reliability analysis in geotechnics with the random set finite element method. Computers and Geotechnics, 32(6): 422-435

Sellers, W. I. and Manning, P. L., 2007. Estimating maximum running speeds using evolutionary robotics. Proceedings of the Royal Society Series B., 274: 2711-2716

Sellers, W. I., Manning, P. L., Lyson, T., Stevens, K. and Margetts, L., 2009. Virtual palaeontology: gait reconstruction of extinct vertebrates using high performance computing. Palaeontologia Electronica, 12(3): 11A: 26p

Skempton, A. W., 1951. The Bearing Capacity of Clays. Proc. Building Research Congress, 1: 180-189

Smith, I. M., 2000. A general purpose system for finite element analyses in parallel. Engineering Computations, 17(1): 75-91

Smith, I. M. and Griffiths, D. V., 2004. Programming the Finite Element Method. Wiley, Chichester, 628 pp.

Smith, M. J., 1981. Soil Mechanics. George Godwin, London, 168 pp.

Song, Y., Black, R. G. and Lipps, J. H., 1994. Morphological optimization in the largest living foraminifera: implications from finite element analysis. Paleobiology, 20: 14-26

Sternberg, C. M., 1926. Dinosaur tracks from the Edmonton Formation of Alberta. Canada Museum, Bulletins geological series, 44: 85-87

Tekeste, M. Z., Tollner, E. W., Raper, R. L., Way, T. R. and Johnson, C. E., In Press. Non-linear finite element analysis of cone penetration in layered sandy loam soil - Considering precompression stress state. Journal of Terramechanics, Corrected Proof

Thomas, D. A. and Farlow, J. O., 1997. Tracking a dinosaur attack. Scientific American, 277(6): 74-79

Thulborn, R. A., 1990. Dinosaur Tracks. Chapman & Hall, London, 410 pp.

Thulborn, R. A. and Wade, M., 1989. A Footprint as a History of Movement. In: Gillette, D.D. and Lockley, M.G. (Editors), Dinosaur Tracks and Traces. Cambridge University Press, Cambridge, pp. 51-56.

Turner, M. J., Clough, R. W., Martin, H. G. and Topp, L. J., 1956. Stiffness and deflection analysis of complex structures. Journal of Aeronautical Science, 23: 805-823

Wilson, J. A., Marsicano, C. A. and Smith, R. M. H., 2009. Dynamic Locomotor Capabilities Revealed by Early Dinosaur Trackmakers from Southern Africa. PLoS ONE, 4(10): e7331

Xing, L., Harris, J. D., Deng-hai, S. and Zhao, H.-q., 2009a. The Earliest Known Deinonychosaur Tracks from the Jurassic-Cretaceous boundary in Hebei, China. Acta Palaeontologica Sinica, 48(1): 662-671

Xing, L., Harris, J. D., Feng, X. and Zhang, Z., 2009b. Theropod (Dinosauria: Saurischia) tracks from Lower Cretaceous Yixian Formation at Sihetun Village, Liaoning Province, China and possible track makers. Geological Bulletin of China, 28(6): 705-712

Xing, L., Yong, Y. E., Chunkang, S. H. U., Guangzhao, P. and Hailu, Y. O. U., 2009c. Structure, Orientation and Finite Element Analysis of the Tail Club of *Mamenchisaurus hochuanensis*. Acta Geologica Sinica - English Edition, 83(6): 1031-1040

Xu, X., Zhou, Z., Wang, X., Kuang, X., Zhang, F. and Du, X., 2003. Four-winged dinosaurs from China. Nature, 421(6921): 335-340

You, H.-l., Lamanna, M. C., Harris, J. D., Chiappe, L. M., O'Connor, J., Ji, S.-a., Lu, J.-c., Yuan, C.-x., Li, D.-q., Zhang, X., Lacovara, K. J., Dodson, P. and Ji, Q., 2006. A Nearly Modern Amphibious Bird from the Early Cretaceous of Northwestern China. Science, 312(5780): 1640-1643.10.1126/science.1126377

# Appendix

***Code for pre-processing program 'MeshGen' developed as part of this work.***

```
!PROGRAM MESHGENv5

!   ------------------------------------------------------------
!   MeshGen5.F90    2/6/10
!   Re-write of MeshGen for generating input data to PalaeoFEM
!       Generates a cuboid mesh with 2.5D foot/indenter on the
!       surface.
!   No error checking implemented yet
!       Changes: Comments standardised for ParaFEM
!   ------------------------------------------------------------

  IMPLICIT NONE

!------------------------!
!1.  Declarations:       !
!------------------------!

  INTEGER :: denseResX, denseResZ
  INTEGER :: resolutionX, resolutionZ, layers, i, x, y, z, x1, x2, x3,&
             y1, y2, y3, z1, z2, z3, random, ce, le, n1, n1b, n2, n2b
  INTEGER :: num_nodes, num_elements, nodes_per_el, xdr2, zdr, stepStages,
  loadType, old_num_els, num_load_els
  INTEGER :: num_loads, rigid_nodes, c, old_num_nodes, lightRes,
  num_nodes_x, num_nodes_y, num_nodes_z, footcount, footlayers
  INTEGER :: allonum, allonod, biggestDenseRes, smooth, num_incs,
  shallow_layers
  DOUBLE PRECISION :: cu, e, v, footThickness, elsize, mass,
  layerThickness, vari, loadperel, twelth, third, scaleFact, dist, &
                                                  mult, dummy, scaleFactY
  REAL, ALLOCATABLE :: loadedEls(:,:)
  REAL, ALLOCATABLE :: increments(:)
  CHARACTER(LEN=50),ALLOCATABLE   ::  stepFiles(:)
  CHARACTER(LEN=10) :: p3
  CHARACTER(len=50) :: job_name
  CHARACTER(LEN=50) :: ldsname
  TYPE :: node
     integer :: id
     real :: x
     real :: y
     real :: z
     integer :: freedomx
     integer :: freedomy
     integer :: freedomz
     real :: loadx
     real :: loady
     real :: loadz
  END TYPE node

!  TYPE :: element8                     !This is a stub for 8-node
hexahedral elements
!     integer :: id
!     type (node) :: node1
!     type (node) :: node2
!     type (node) :: node3
!     type (node) :: node4
!     type (node) :: node5
!     type (node) :: node6
!     type (node) :: node7
!     type (node) :: node8
!  END TYPE element8

  TYPE :: element20
     integer :: id
     type (node) :: node1
     type (node) :: node2
     type (node) :: node3
     type (node) :: node4
     type (node) :: node5
     type (node) :: node6
     type (node) :: node7
     type (node) :: node8
     type (node) :: node9
     type (node) :: node10
```

```
     type (node) :: node11
     type (node) :: node12
     type (node) :: node13
     type (node) :: node14
     type (node) :: node15
     type (node) :: node16
     type (node) :: node17
     type (node) :: node18
     type (node) :: node19
     type (node) :: node20
  END TYPE element20

!  TYPE(element8), DIMENSION(:,:,:), ALLOCATABLE :: el8
!Stub
  TYPE(element20), DIMENSION(:,:,:), ALLOCATABLE :: el20
  TYPE(node), DIMENSION(:,:,:), ALLOCATABLE :: nodes


 call GETARG(1, job_name)

!-----------------------!
!2. Read in input:              !
!-----------------------!
  OPEN(14,file=job_name)
  READ(14,*)  elSize, denseResX, denseResZ, lightRes, scaleFact,
  nodes_per_el, &
              layers, layerThickness, scaleFactY, shallow_layers, &
              footlayers, footThickness, &
              random, cu, e, v, vari
  READ(14,*)  loadType
  READ(14,*)stepStages, mass
  ALLOCATE(stepFiles(stepStages))
  READ(14,*)stepFiles
  READ(14,*)smooth
  READ(14,*)num_incs
  ALLOCATE(increments(num_incs))
  READ(14,*)increments
  CLOSE(14)

!----------------------------------------!
!2.1 Read in which elements are loaded    !
!----------------------------------------!
  OPEN(12,file=stepFiles(1)) !this will be dynamic later.
  READ(12,*)p3
  READ(12,*)denseResX,denseResZ,dummy
  ALLOCATE(loadedEls(denseResX*3,denseResZ))
  READ(12,*)loadedEls
  CLOSE(12)

  WRITE(*,*)'read denseRes X and Z from ppm: ', denseResX, denseResZ


  resolutionX = denseResX + lightRes*2
  resolutionZ = denseResZ + lightRes*2


!-------------------------------------------------!
!3.     Generate mesh
!
!   Just make mesh for 20 nodes for now.         !
!   (8-node hex elements to be implemented later)!
!-------------------------------------------------!

  allonum = -1*(footlayers-1)
  allonod = (-2*footlayers)+1

  num_nodes_x = 4*lightRes + 2*denseResX + 1
  num_nodes_y = 2*layers + 3
  num_nodes_z = 4*lightRes + 2*denseResZ + 1

  ALLOCATE(nodes(0:num_nodes_x,allonod:num_nodes_y, 0:num_nodes_z))
  ALLOCATE(el20(resolutionX, allonum:layers, resolutionZ))
```

```
  nodes = node(0,0,0,0,1,1,1,0,0,0)

  ![****Fill nodes****!]
  i = 1
  do y=1, layers*2+1, 2
     do z=1, resolutionZ*2+1, 2
        do x=1, resolutionX*2+1
           nodes(x,y,z)%id = i
           nodes(x,y,z)%x = x-1
           nodes(x,y,z)%y = -1*(y-1)
           nodes(x,y,z)%z = z-1
           i=i+1
        end do
     end do
  end do
  !  [now create half way nodes, on horizontal...]
  do y=1, layers*2+1, 2
     do z=2, resolutionZ*2+1, 2
        do x=1, resolutionX*2+1, 2
           nodes(x,y,z)%id = i
           nodes(x,y,z)%x = x-1
           nodes(x,y,z)%y = -1*(y-1)
           nodes(x,y,z)%z = z-1
           i=i+1
        end do
     end do
  end do
  ![... and vertical.]
  do y=2, layers*2+1, 2
     do z=1, resolutionZ*2+1, 2
        do x=1, resolutionX*2+1, 2
           nodes(x,y,z)%id = i
           nodes(x,y,z)%x = x-1
           nodes(x,y,z)%y = -1*(y-1)
           nodes(x,y,z)%z = z-1
           i=i+1
        end do
     end do
  end do

  num_nodes = i
  old_num_nodes = num_nodes

  ![fix nodes on edges - 0 = fixed, 1 = free]
  nodes(1,:,:)%freedomx = 0
  nodes(resolutionX*2+1,:,:)%freedomx = 0
  nodes(:,layers*2+1,:)%freedomy = 0
  nodes(:,layers*2+1,:)%freedomx = 0    !Base elements
  nodes(:,layers*2+1,:)%freedomz = 0
  nodes(:,:,1)%freedomz = 0
  nodes(:,:,resolutionZ*2+1)%freedomz = 0

  ![Fill Elements]
  i=1
  do y=1, layers
     do z = 1, resolutionZ
        do x = 1, resolutionX
           x2 = x*2
           x1 = x2-1
           x3 = x2+1
           z2 = z*2
           z1 = z2-1
           z3 = z2+1
           y2 = y*2
           y1 = y2-1
           y3 = y2+1
           el20(x,y,z)%id = i
           el20(x,y,z)%node1 = nodes(x1,y3,z1)
           el20(x,y,z)%node2 = nodes(x1,y2,z1)
           el20(x,y,z)%node3 = nodes(x1,y1,z1)
           el20(x,y,z)%node4 = nodes(x1,y1,z2)
           el20(x,y,z)%node5 = nodes(x1,y1,z3)
           el20(x,y,z)%node6 = nodes(x1,y2,z3)
```

```
            el20(x,y,z)%node7 = nodes(x1,y3,z3)
            el20(x,y,z)%node8 = nodes(x1,y3,z2)
            el20(x,y,z)%node9 = nodes(x2,y3,z1)
            el20(x,y,z)%node10 = nodes(x2,y1,z1)
            el20(x,y,z)%node11 = nodes(x2,y1,z3)
            el20(x,y,z)%node12 = nodes(x2,y3,z3)
            el20(x,y,z)%node13 = nodes(x3,y3,z1)
            el20(x,y,z)%node14 = nodes(x3,y2,z1)
            el20(x,y,z)%node15 = nodes(x3,y1,z1)
            el20(x,y,z)%node16 = nodes(x3,y1,z2)
            el20(x,y,z)%node17 = nodes(x3,y1,z3)
            el20(x,y,z)%node18 = nodes(x3,y2,z3)
            el20(x,y,z)%node19 = nodes(x3,y3,z3)
            el20(x,y,z)%node20 = nodes(x3,y3,z2)
            i = i+1
         end do
      end do
   end do
   num_elements = i
   old_num_els = num_elements



!-------------------------------------------------------!
!4. Create new elements (elements forming the indenter)!
!-------------------------------------------------------!
   if(footThickness.ne.0)then

do footcount=1, footlayers*2, 2
    x2=1
    do x=2, denseResX*3,3
       do z=1, denseResZ
          if(loadedEls(x-1,z)+loadedEls(x,z)+loadedEls(x+1,z).ne.0)then
          !this will have to become magnitude, as currently, 1+ -1 = 0
             xdr2 = x2+lightRes
             zdr = z + lightRes
             ce = footcount-1
             ce = ce/2
             ce = -1*ce
             le = ce+1
             n1 = -1*footcount
             n1b = footcount+1
             n2 = n1+1
             n2b = footcount
             el20(xdr2,ce,zdr)%id = num_elements
             num_elements = num_elements+1
             el20(xdr2,ce,zdr)%node1 = el20(xdr2,le,zdr)%node3
             el20(xdr2,ce,zdr)%node7 = el20(xdr2,le,zdr)%node5
             el20(xdr2,ce,zdr)%node8 = el20(xdr2,le,zdr)%node4
             el20(xdr2,ce,zdr)%node9 = el20(xdr2,le,zdr)%node10
             el20(xdr2,ce,zdr)%node12 = el20(xdr2,le,zdr)%node11
             el20(xdr2,ce,zdr)%node13 = el20(xdr2,le,zdr)%node15
             el20(xdr2,ce,zdr)%node19 = el20(xdr2,le,zdr)%node17
             el20(xdr2,ce,zdr)%node20 = el20(xdr2,le,zdr)%node16
             !create new nodes, layer 0

             if(nodes(xdr2*2-1, n1, zdr*2-1)%id.eq.0)then
                nodes(xdr2*2-1,n1,zdr*2-1)%id = num_nodes
                nodes(xdr2*2-1,n1,zdr*2-1)%x = nodes(xdr2*2-1,1,zdr*2-1)%x
                nodes(xdr2*2-1,n1,zdr*2-1)%y = n1b
                nodes(xdr2*2-1,n1,zdr*2-1)%z = nodes(xdr2*2-1,1,zdr*2-1)%z
                num_nodes = num_nodes+1
             end if
             el20(xdr2,ce,zdr)%node3 = nodes(xdr2*2-1,n1,zdr*2-1)

             if(nodes(xdr2*2-1, n1, zdr*2)%id.eq.0)then
                nodes(xdr2*2-1,n1,zdr*2)%id = num_nodes
                nodes(xdr2*2-1,n1,zdr*2)%x = nodes(xdr2*2-1,1,zdr*2)%x
                nodes(xdr2*2-1,n1,zdr*2)%y = n1b
                nodes(xdr2*2-1,n1,zdr*2)%z = nodes(xdr2*2-1,1,zdr*2)%z
                num_nodes = num_nodes+1
             end if
             el20(xdr2,ce,zdr)%node4 = nodes(xdr2*2-1,n1,zdr*2)
```

```
            if(nodes(xdr2*2-1,n1,  zdr*2+1)%id.eq.0)then
               nodes(xdr2*2-1,n1,zdr*2+1)%id = num_nodes
               nodes(xdr2*2-1,n1,zdr*2+1)%x = nodes(xdr2*2-1,1,zdr*2+1)%x
               nodes(xdr2*2-1,n1,zdr*2+1)%y = n1b
               nodes(xdr2*2-1,n1,zdr*2+1)%z = nodes(xdr2*2-1,1,zdr*2+1)%z
               num_nodes = num_nodes+1
            end if
            el20(xdr2,ce,zdr)%node5 = nodes(xdr2*2-1,n1,zdr*2+1)

            if(nodes(xdr2*2,n1,  zdr*2-1)%id.eq.0)then
               nodes(xdr2*2,n1,zdr*2-1)%id = num_nodes
               nodes(xdr2*2,n1,zdr*2-1)%x = nodes(xdr2*2,1,zdr*2-1)%x
               nodes(xdr2*2,n1,zdr*2-1)%y = n1b
               nodes(xdr2*2,n1,zdr*2-1)%z = nodes(xdr2*2,1,zdr*2-1)%z
               num_nodes = num_nodes+1
            end if
            el20(xdr2,ce,zdr)%node10 = nodes(xdr2*2,n1,zdr*2-1)

            if(nodes(xdr2*2,n1,  zdr*2+1)%id.eq.0)then
               nodes(xdr2*2,n1,zdr*2+1)%id = num_nodes
               nodes(xdr2*2,n1,zdr*2+1)%x = nodes(xdr2*2,1,zdr*2+1)%x
               nodes(xdr2*2,n1,zdr*2+1)%y = n1b
               nodes(xdr2*2,n1,zdr*2+1)%z = nodes(xdr2*2,1,zdr*2+1)%z
               num_nodes = num_nodes+1
            end if
            el20(xdr2,ce,zdr)%node11 = nodes(xdr2*2,n1,zdr*2+1)

            if(nodes(xdr2*2+1,n1,  zdr*2-1)%id.eq.0)then
               nodes(xdr2*2+1,n1,zdr*2-1)%id = num_nodes
               nodes(xdr2*2+1,n1,zdr*2-1)%x = nodes(xdr2*2+1,1,zdr*2-1)%x
               nodes(xdr2*2+1,n1,zdr*2-1)%y = n1b
               nodes(xdr2*2+1,n1,zdr*2-1)%z = nodes(xdr2*2+1,1,zdr*2-1)%z
               num_nodes = num_nodes+1
            end if
            el20(xdr2,ce,zdr)%node15 = nodes(xdr2*2+1,n1,zdr*2-1)

            if(nodes(xdr2*2+1,n1,  zdr*2)%id.eq.0)then
               nodes(xdr2*2+1,n1,zdr*2)%id = num_nodes
               nodes(xdr2*2+1,n1,zdr*2)%x = nodes(xdr2*2+1,1,zdr*2)%x
               nodes(xdr2*2+1,n1,zdr*2)%y = n1b
               nodes(xdr2*2+1,n1,zdr*2)%z = nodes(xdr2*2+1,1,zdr*2)%z
               num_nodes = num_nodes+1
            end if
            el20(xdr2,ce,zdr)%node16 = nodes(xdr2*2+1,n1,zdr*2)

            if(nodes(xdr2*2+1,n1,  zdr*2+1)%id.eq.0)then
               nodes(xdr2*2+1,n1,zdr*2+1)%id = num_nodes
               nodes(xdr2*2+1,n1,zdr*2+1)%x = nodes(xdr2*2+1,1,zdr*2+1)%x
               nodes(xdr2*2+1,n1,zdr*2+1)%y = n1b
               nodes(xdr2*2+1,n1,zdr*2+1)%z = nodes(xdr2*2+1,1,zdr*2+1)%z
               num_nodes = num_nodes+1
            end if
            el20(xdr2,ce,zdr)%node17 = nodes(xdr2*2+1,n1,zdr*2+1)

            if(nodes(xdr2*2-1, n2, zdr*2-1)%id.eq.0)then
               nodes(xdr2*2-1,n2,zdr*2-1)%id = num_nodes
               nodes(xdr2*2-1,n2,zdr*2-1)%x = nodes(xdr2*2-1,1,zdr*2-1)%x
               nodes(xdr2*2-1,n2,zdr*2-1)%y = n2b
               nodes(xdr2*2-1,n2,zdr*2-1)%z = nodes(xdr2*2-1,1,zdr*2-1)%z
               num_nodes = num_nodes+1
            end if
            el20(xdr2,ce,zdr)%node2 = nodes(xdr2*2-1,n2,zdr*2-1)

            if(nodes(xdr2*2-1, n2, zdr*2+1)%id.eq.0)then
               nodes(xdr2*2-1,n2,zdr*2+1)%id = num_nodes
               nodes(xdr2*2-1,n2,zdr*2+1)%x = nodes(xdr2*2-1,1,zdr*2+1)%x
               nodes(xdr2*2-1,n2,zdr*2+1)%y = n2b
               nodes(xdr2*2-1,n2,zdr*2+1)%z = nodes(xdr2*2-1,1,zdr*2+1)%z
               num_nodes = num_nodes+1
            end if
            el20(xdr2,ce,zdr)%node6 = nodes(xdr2*2-1,n2,zdr*2+1)
```

```
              if(nodes(xdr2*2+1, n2, zdr*2-1)%id.eq.0)then
                 nodes(xdr2*2+1,n2,zdr*2-1)%id = num_nodes
                 nodes(xdr2*2+1,n2,zdr*2-1)%x = nodes(xdr2*2+1,1,zdr*2-1)%x
                 nodes(xdr2*2+1,n2,zdr*2-1)%y = n2b
                 nodes(xdr2*2+1,n2,zdr*2-1)%z = nodes(xdr2*2+1,1,zdr*2-1)%z
                 num_nodes = num_nodes+1
              end if
              el20(xdr2,ce,zdr)%node14 = nodes(xdr2*2+1,n2,zdr*2-1)

              if(nodes(xdr2*2+1, n2, zdr*2+1)%id.eq.0)then
                 nodes(xdr2*2+1,n2,zdr*2+1)%id = num_nodes
                 nodes(xdr2*2+1,n2,zdr*2+1)%x = nodes(xdr2*2+1,1,zdr*2+1)%x
                 nodes(xdr2*2+1,n2,zdr*2+1)%y = n2b
                 nodes(xdr2*2+1,n2,zdr*2+1)%z = nodes(xdr2*2+1,1,zdr*2+1)%z
                 num_nodes = num_nodes+1
              end if
              el20(xdr2,ce,zdr)%node18 = nodes(xdr2*2+1,n2,zdr*2+1)
           end if
        end do
        x2 = x2+1
      end do

end do

   end if



  num_load_els = (num_elements - old_num_els)/footlayers

  do x=lightRes*2, 1, -2
        dist = (nodes(x+3,1,1)%x-nodes(x+1,1,1)%x)*scaleFact
        nodes(x,:,:)%x = nodes(x+1,:,:)%x-(0.5*dist)
        nodes(x-1,:,:)%x = nodes(x+1,:,:)%x-dist
  end do


  do z=lightRes*2, 1, -2
        dist = (nodes(1,1,z+3)%z-nodes(1,1,z+1)%z)*scaleFact
        nodes(:,:,z)%z = nodes(:,:,z+1)%z-(0.5*dist)
        nodes(:,:,z-1)%z = nodes(:,:,z+1)%z-dist
  end do

  do x=(denseResX+lightRes)*2+2, resolutionX*2+1, 2
        dist = (nodes(x-1,1,1)%x-nodes(x-3,1,1)%x)*scaleFact
        nodes(x,:,:)%x = nodes(x-1,:,:)%x+(0.5*dist)
        nodes(x+1,:,:)%x = nodes(x-1,:,:)%x+dist
  end do

  do z=(lightRes+denseResZ)*2+2, resolutionZ*2+1, 2
        dist = (nodes(1,1,z-1)%z-nodes(1,1,z-3)%z)*scaleFact
        nodes(:,:,z)%z = nodes(:,:,z-1)%z+(0.5*dist)
        nodes(:,:,z+1)%z = nodes(:,:,z-1)%z+dist
  end do

![y scaling]
if(shallow_layers<0)then

  if(denseResX.ge.denseResZ)then
    biggestDenseRes = denseResX
  else
    biggestDenseRes = denseResZ
  end if

  do y=biggestDenseRes/2+2, layers*2+1, 2 !insert here to stop foot
  expanding
        dist = (nodes(1,y-1,1)%y-nodes(1,y-3,1)%y)*scaleFactY
        nodes(:,y,:)%y = nodes(:,y-1,:)%y+(0.5*dist)
        nodes(:,y+1,:)%y = nodes(:,y-1,:)%y+dist
  end do

else
```

```
  do y=shallow_layers*2+2, layers*2+1, 2 !insert here to stop foot
  expanding
        dist = (nodes(1,y-1,1)%y-nodes(1,y-3,1)%y)*scaleFactY
        nodes(:,y,:)%y = nodes(:,y-1,:)%y+(0.5*dist)
        nodes(:,y+1,:)%y = nodes(:,y-1,:)%y+dist
  end do

end if



  mult = elSize/2
  nodes(:,:,:)%x = nodes(:,:,:)%x*mult
  nodes(:,:,:)%y = nodes(:,:,:)%y*layerthickness/2
  nodes(:,:,:)%z = nodes(:,:,:)%z*elSize/2




!-------------------------------------------------------------------------
-------!
!5. Attempt smoothing of corner els.  This is experimental! Use at your own
risk! !
!        (May cause numerical problems)
!
!-------------------------------------------------------------------------
-------!

if(smooth.eq.1)then
WRITE(*,*)'Applying smoothing algorithm...  '
write(*,*)'***WARNING*** DO NOT USE ON LOW RESOLUTION MESHES'
y = 0
do z=lightRes, lightRes+denseResZ
  do x=lightRes, lightRes+denseResX
        if(el20(x,y,z)%id.ne.0)then

          ![check upper left]
          if(el20(x-1,y,z-1)%id.eq.0)then
                if(el20(x-1,y,z)%id.eq.0)then
                  if(el20(x,y,z-1)%id.eq.0)then
                    nodes(x*2-1,:,z*2-1)%x =
                    nodes(x*2-1,:,z*2-1)%x+elSize/4
                        nodes(x*2-1,:,z*2-1)%z =
                        nodes(x*2-1,:,z*2-1)%z+elSize/4

                  end if
                end if

                if(el20(x-1,y,z)%id.ne.0)then
                  if(el20(x,y,z-1)%id.ne.0)then
                    !nodes(x*2-1,:,z*2-1)%x = nodes(x*2-1,:,z*2-1)%x-
                    elSize/4
                        !nodes(x*2-1,:,z*2-1)%z = nodes(x*2-1,:,z*2-1)%z-
                        elSize/4

                  end if
                end if

          end if

          ![check upper right]
          if(el20(x+1,y,z-1)%id.eq.0)then
                if(el20(x+1,y,z)%id.eq.0)then
                  if(el20(x,y,z-1)%id.eq.0)then
                    nodes(x*2+1,:,z*2-1)%x = nodes(x*2+1,:,z*2-1)%x-
                    elSize/4
                        nodes(x*2+1,:,z*2-1)%z =
                        nodes(x*2+1,:,z*2-1)%z+elSize/4

                  end if
                end if

                if(el20(x+1,y,z)%id.ne.0)then
```

```
                  if(el20(x,y,z-1)%id.ne.0)then
                    !nodes(x*2+1,:,z*2-1)%x =
                    nodes(x*2+1,:,z*2-1)%x+elSize/4
                        !nodes(x*2+1,:,z*2-1)%z = nodes(x*2+1,:,z*2-1)%z-
                        elSize/4

                  end if
                end if

          end if


  ![check lower left]
        if(el20(x-1,y,z)%id.eq.0)then
          if(el20(x-1,y,z+1)%id.eq.0)then
                  if(el20(x,y,z+1)%id.eq.0)then
                    nodes(x*2-1,:,z*2+1)%x =
                    nodes(x*2-1,:,z*2+1)%x+elSize/4
                        nodes(x*2-1,:,z*2+1)%z = nodes(x*2-1,:,z*2+1)%z-
                        elSize/4

                  end if
                end if
          if(el20(x-1,y,z+1)%id.ne.0)then
                if(el20(x,y,z+1)%id.ne.0)then
                    nodes(x*2-1,:,z*2+1)%x = nodes(x*2-1,:,z*2+1)%x-
                    elSize/4
                        nodes(x*2-1,:,z*2+1)%z = nodes(x*2-1,:,z*2+1)%z-
                        elSize/4

                end if

          end if

         end if


   ![check lower right]
   if(el20(x+1,y,z+1)%id.eq.0)then
        if(el20(x+1,y,z)%id.eq.0)then
          if(el20(x,y,z+1)%id.eq.0)then
            nodes(x*2+1,:,z*2+1)%x = nodes(x*2+1,:,z*2+1)%x-elSize/4
                nodes(x*2+1,:,z*2+1)%z = nodes(x*2+1,:,z*2+1)%z-elSize/4
          end if
        end if
   end if

  if(el20(x+1,y,z)%id.eq.0)then

    if(el20(x+1,y,z+1)%id.ne.0)then
    if(el20(x,y,z+1)%id.ne.0)then
        nodes(x*2+1,:,z*2+1)%x = nodes(x*2+1,:,z*2+1)%x+elSize/4
                nodes(x*2+1,:,z*2+1)%z = nodes(x*2+1,:,z*2+1)%z-elSize/4
        end if
        end if
  end if

  if(el20(x+1,y,z+1)%id.eq.0)then

    if(el20(x+1,y,z)%id.ne.0)then
    if(el20(x,y,z+1)%id.ne.0)then
        nodes(x*2+1,:,z*2+1)%x = nodes(x*2+1,:,z*2+1)%x+elSize/4
                nodes(x*2+1,:,z*2+1)%z = nodes(x*2+1,:,z*2+1)%z+elSize/4
        end if
        end if
  end if

  if(el20(x,y,z+1)%id.eq.0)then

    if(el20(x+1,y,z+1)%id.ne.0)then
    if(el20(x+1,y,z)%id.ne.0)then
        nodes(x*2+1,:,z*2+1)%x = nodes(x*2+1,:,z*2+1)%x-elSize/4
                nodes(x*2+1,:,z*2+1)%z = nodes(x*2+1,:,z*2+1)%z+elSize/4
```

```
        end if
        end if
  end if



 end if
  end do
end do
end if

! ----------------------------------------!
! end experimental section                                  !
! ----------------------------------------!



!-------------------------------------------------------!
!6.   Write *.d file and *.bnd:
!
!     Writes to file the nodes,
!
!     elements, and boundary conditions used by ParaFEM !
!-------------------------------------------------------!

  open(10,file='dino.d')
  open(11,file='dino.bnd')
  write(10,'(A18)')'*THREE_DIMENSIONAL'
  write(10,'(A6)')'*NODES'
  rigid_nodes = 0
 do y=1,layers*2+1, 2
    do z=1, resolutionZ*2+1, 2
       do x=1, resolutionX*2+1
          if(nodes(x,y,z)%id.ne.0)then
             write(10,*)nodes(x,y,z)%id,
             nodes(x,y,z)%x,nodes(x,y,z)%y,nodes(x,y,z)%z

             if(nodes(x,y,z)%freedomx+nodes(x,y,z)%freedomy+nodes(x,y,z)%fr
             eedomz.ne.3)then
                write(11,*) nodes(x,y,z)%id,
                nodes(x,y,z)%freedomx,nodes(x,y,z)%freedomy, &
                     nodes(x,y,z)%freedomz
                rigid_nodes = rigid_nodes+1
             end if
          end if
       end do
    end do
 end do
 do y=1, layers*2+1, 2
    do z=2, resolutionZ*2+1, 2
       do x=1, resolutionX*2+1, 2
          if(nodes(x,y,z)%id.ne.0)then
             write(10,*)nodes(x,y,z)%id,
             nodes(x,y,z)%x,nodes(x,y,z)%y,nodes(x,y,z)%z

             if(nodes(x,y,z)%freedomx+nodes(x,y,z)%freedomy+nodes(x,y,z)%fr
             eedomz.ne.3)then
                write(11,*) nodes(x,y,z)%id,
                nodes(x,y,z)%freedomx,nodes(x,y,z)%freedomy, &
                     nodes(x,y,z)%freedomz
                rigid_nodes = rigid_nodes+1
             end if
          end if
       end do
    end do
 end do

 do y=2,layers*2+1, 2
    do z=1, resolutionZ*2+1, 2
       do x=1, resolutionX*2+1
          if(nodes(x,y,z)%id.ne.0)then
```

```
            write(10,*)nodes(x,y,z)%id,
            nodes(x,y,z)%x,nodes(x,y,z)%y,nodes(x,y,z)%z

            if(nodes(x,y,z)%freedomx+nodes(x,y,z)%freedomy+nodes(x,y,z)%fr
            eedomz.ne.3)then
               write(11,*) nodes(x,y,z)%id,
               nodes(x,y,z)%freedomx,nodes(x,y,z)%freedomy, &
                    nodes(x,y,z)%freedomz
               rigid_nodes = rigid_nodes+1
            end if
         end if
      end do
   end do
end do
![now output indenter nodes.]
do c=old_num_nodes, num_nodes

do y=allonod,0
   do z = lightRes*2, (lightRes+denseResZ)*2+1
      do x = lightRes*2, (lightRes+denseResX)*2+1
         if(nodes(x,y,z)%id.eq.c)then
            write(10,*)nodes(x,y,z)%id,
            nodes(x,y,z)%x,nodes(x,y,z)%y,nodes(x,y,z)%z

            if(nodes(x,y,z)%freedomx+nodes(x,y,z)%freedomy+nodes(x,y,z)%fr
            eedomz.ne.3)then
               write(11,*) nodes(x,y,z)%id,
               nodes(x,y,z)%freedomx,nodes(x,y,z)%freedomy, &
                    nodes(x,y,z)%freedomz
               rigid_nodes = rigid_nodes+1
            end if
         end if
      end do
   end do
end do
end do


write(10,'(A9)')'*ELEMENTS'
do y=1,layers
   do z=1, resolutionZ
      do x=1, resolutionX
         if(el20(x,y,z)%id.ne.0)then
            write(10,*) el20(x,y,z)%id, ' 3 ', ' 20 ', ' 1 ',
            el20(x,y,z)%node1%id, &
                 el20(x,y,z)%node2%id, el20(x,y,z)%node3%id,
                 el20(x,y,z)%node4%id, &
                 el20(x,y,z)%node5%id, el20(x,y,z)%node6%id,
                 el20(x,y,z)%node7%id, &
                 el20(x,y,z)%node8%id, el20(x,y,z)%node9%id,
                 el20(x,y,z)%node10%id, &
                 el20(x,y,z)%node11%id, el20(x,y,z)%node12%id,
                 el20(x,y,z)%node13%id, &
                 el20(x,y,z)%node14%id, el20(x,y,z)%node15%id,
                 el20(x,y,z)%node16%id, &
                 el20(x,y,z)%node17%id, el20(x,y,z)%node18%id,
                 el20(x,y,z)%node19%id, &
                 el20(x,y,z)%node20%id, y
         end if
      end do
   end do
end do
![output indenter elements]
do ce=0, allonum, -1

do x=1, resolutionX
   do z=1, resolutionZ
      if(el20(x,ce,z)%id.ne.0)then
         write(10,*) el20(x,ce,z)%id, ' 3 ', ' 20 ', ' 1 ',
         el20(x,ce,z)%node1%id, &
              el20(x,ce,z)%node2%id, el20(x,ce,z)%node3%id,
              el20(x,ce,z)%node4%id, &
              el20(x,ce,z)%node5%id, el20(x,ce,z)%node6%id,
```

```
               el20(x,ce,z)%node7%id, &
               el20(x,ce,z)%node8%id, el20(x,ce,z)%node9%id,
               el20(x,ce,z)%node10%id, &
               el20(x,ce,z)%node11%id, el20(x,ce,z)%node12%id,
               el20(x,ce,z)%node13%id, &
               el20(x,ce,z)%node14%id, el20(x,ce,z)%node15%id,
               el20(x,ce,z)%node16%id, &
               el20(x,ce,z)%node17%id, el20(x,ce,z)%node18%id,
               el20(x,ce,z)%node19%id, &
               el20(x,ce,z)%node20%id, y
       end if
    end do
 end do
 end do

  close(10)
  close(11)

!------------------------------------------------------------!
!7.  Write *.mat
!
!     Writes material properties to ParaFEM format (*.mat)!
!------------------------------------------------------------!

  call writemat(footThickness, layers, cu, e, v)


!------------------------------------------------!
!8. Write *.lds (currently only vertical)                !
!   Generates loading conditions in ParaFEM format!
!   Stubs included for non-vertical loading       !
!------------------------------------------------!
  loadperel = mass/num_load_els
  third = (-1*0.333333333)*loadperel
  twelth = (0.08333333333)*loadperel

  do z=1, resolutionZ
     do x=1, resolutionX
        if(el20(x,allonum,z)%id.ne.0)then
           !nodes(x*2-1,-1,z*2-1)%loadx
           nodes(x*2-1,allonod,z*2-1)%loady     =
        nodes(x*2-1,allonod,z*2-1)%loady + twelth
           !nodes(x*2-1,-1,z*2-1)%loadz

           !nodes(x*2,-1,z*2-1)%loadx
           nodes(x*2,allonod,z*2-1)%loady       =
        nodes(x*2,allonod,z*2-1)%loady + third
           !nodes(x*2,-1,z*2-1)%loadz

           !nodes(x*2+1,-1,z*2-1)%loadx
           nodes(x*2+1,allonod,z*2-1)%loady     =
        nodes(x*2+1,allonod,z*2-1)%loady + twelth
           !nodes(x*2+1,-1,z*2-1)%loadz

           !nodes(x*2-1,-1,z*2)%loadx
           nodes(x*2-1,allonod,z*2)%loady       =
        nodes(x*2-1,allonod,z*2)%loady + third
           !nodes(x*2-1,-1,z*2)%loadz

           !nodes(x*2+1,-1,z*2)%loadx
           nodes(x*2+1,allonod,z*2)%loady       =
        nodes(x*2+1,allonod,z*2)%loady + third
           !nodes(x*2+1,-1,z*2)%loadz

           !nodes(x*2-1,-1,z*2+1)%loadx
           nodes(x*2-1,allonod,z*2+1)%loady     =
        nodes(x*2-1,allonod,z*2+1)%loady + twelth
           !nodes(x*2-1,-1,z*2+1)%loadz

           !nodes(x*2,-1,z*2+1)%loadx
           nodes(x*2,allonod,z*2+1)%loady       =
        nodes(x*2,allonod,z*2+1)%loady + third
           !nodes(x*2,-1,z*2+1)%loadz
```

```
           !nodes(x*2+1,-1,z*2+1)%loadx
           nodes(x*2+1,allonod,z*2+1)%loady     =
        nodes(x*2+1,allonod,z*2+1)%loady + twelth
           !nodes(x*2+1,-1,z*2+1)%loadz
        end if
     end do
  end do


  do c=1, num_incs

  WRITE(ldsname, '(A5,I1,A4)') "dino_", c, ".lds"

  open(13,file=ldsname)
  num_loads = 0
  do z=1, resolutionZ*2+1
     do x=1, resolutionX*2+1
        if(nodes(x,allonod,z)%id.ne.0)then
          if(nodes(x,allonod,z)%loady.ne.0)then
           WRITE(13,*)nodes(x,allonod,z)%id, increments(c)
           *nodes(x,allonod,z)%loadx, increments(c)
           *nodes(x,allonod,z)%loady, &
                                      increments(c)
                                      *nodes(x,allonod,z)%loadz
           num_loads = num_loads+1
          end if
        end if
     end do
  end do
  close(13)
  end do


!-----------------!
!9.  Write *.dat  !
!-----------------!
  open(14,file='dino.dat')
  WRITE(14,*) num_elements-1, num_nodes-1, rigid_nodes, '8'
  WRITE(14,*) '12 3 50 15000'
  WRITE(14,*) '1.e-6 1.e-7 -1.e-6 1.e-5'
  WRITE(14,*) layers, num_incs
  do c = 1, num_incs
  WRITE(14,*) '0'
  WRITE(14,*) num_loads
  end do



!------------------!
!  end of program: !
!------------------!
END PROGRAM



!--------------------------!
!10. Subroutine write *.mat:!
!--------------------------!

subroutine writemat(footThickness, layers, cu,e,v)
        DOUBLE PRECISION :: footThickness, cu, e, v
        integer :: layers, i

        open(10,file='dino.mat')
        if(footThickness.ne.0)then
                layers = layers+1
        end if
        WRITE(10,*)layers
        do i=1, layers-1
                WRITE(10,*)i, cu, e, v
        end do
```

```
        WRITE(10,*)i, cu*1000, e*1000, '0.48'
end subroutine
```